Plant Biotechnology meets Immunology

Plant-based expression of immunologically relevant proteins

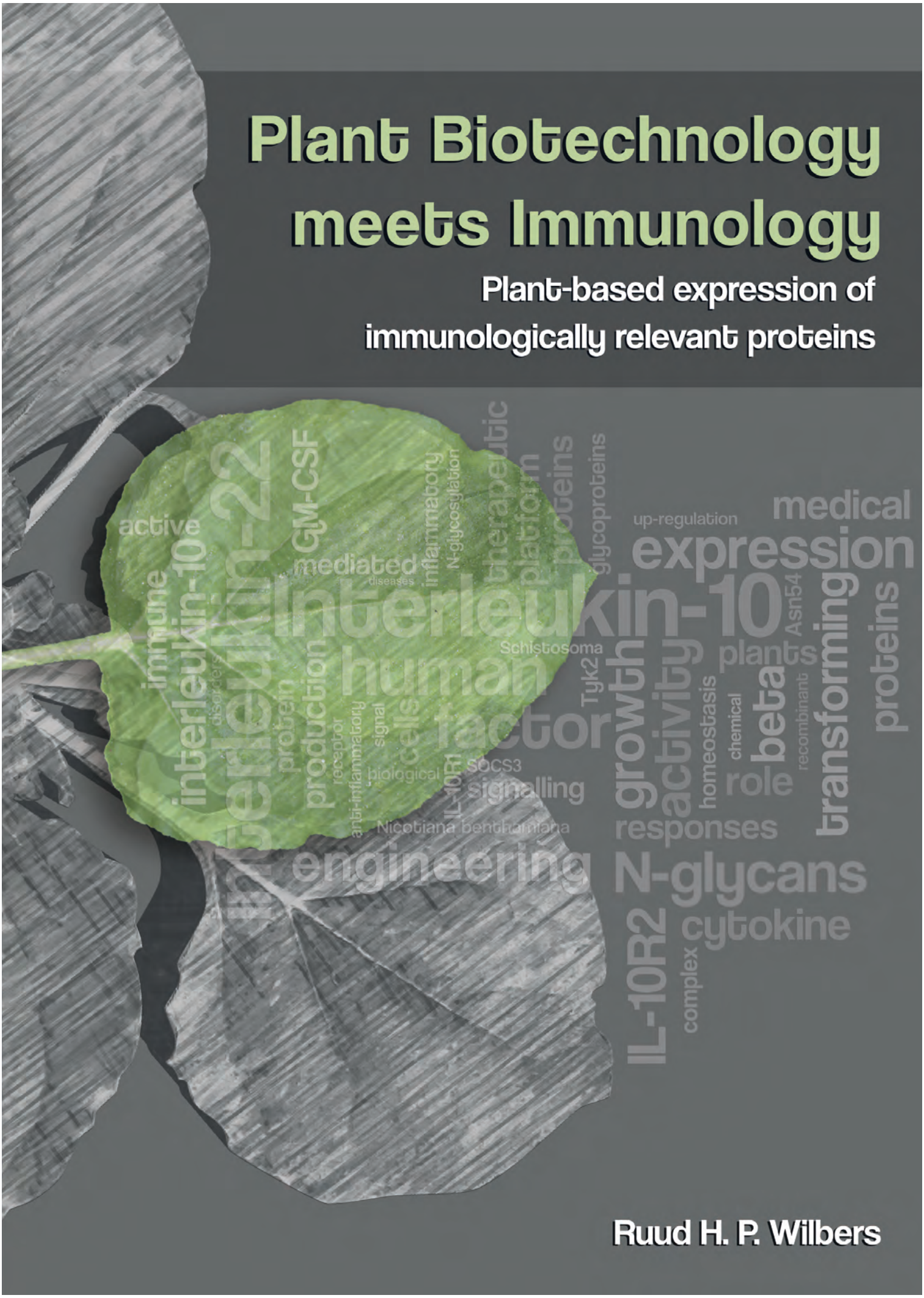

Ruud H. P. Wilbers

Plant Biotechnology meets Immunology

Plant-based expression of immunologically relevant proteins

Ruud H. P. Wilbers

Thesis committee

Promotor

Prof. Dr J. Bakker
Professor of Nematology
Wageningen University

Co-promotors

Dr A. Schots
Associate professor, Laboratory of Nematology
Wageningen University

Dr G. Smant
Assistant professor, Laboratory of Nematology
Wageningen University

Other members

Prof. Dr H.F.J. Savelkoul, Wageningen University
Prof. Dr H. Steinkellner, University of Natural Resources & Life Sciences, Vienna, Austria
Prof. Dr M. Yazdanbakhsh, Leiden University Medical Center
Prof. Dr H.J. Bosch, Utrecht University and Plant Research International, Wageningen

This research was conducted under the auspices of the Graduate School of Experimental Plant Sciences

Plant Biotechnology meets Immunology

Plant-based expression of immunologically relevant proteins

Ruud H. P. Wilbers

Thesis

submitted in fulfillment of the requirements for the degree of doctor
at Wageningen University
by the authority of the Rector Magnificus
Prof. Dr A.P.J. Mol,
in the presence of the
Thesis Committee appointed by the Academic Board
to be defended in public
on Friday 23 October 2015
at 1.30 p.m. in the Aula.

Ruud H. P. Wilbers
Plant Biotechnology meets Immunology – Plant-based expression of immunologically relevant proteins,
230 pages

PhD thesis, Wageningen University, Wageningen, NL (2015)
With references, with summaries in English and Dutch

ISBN 978-94-6257-433-5

Table of contents

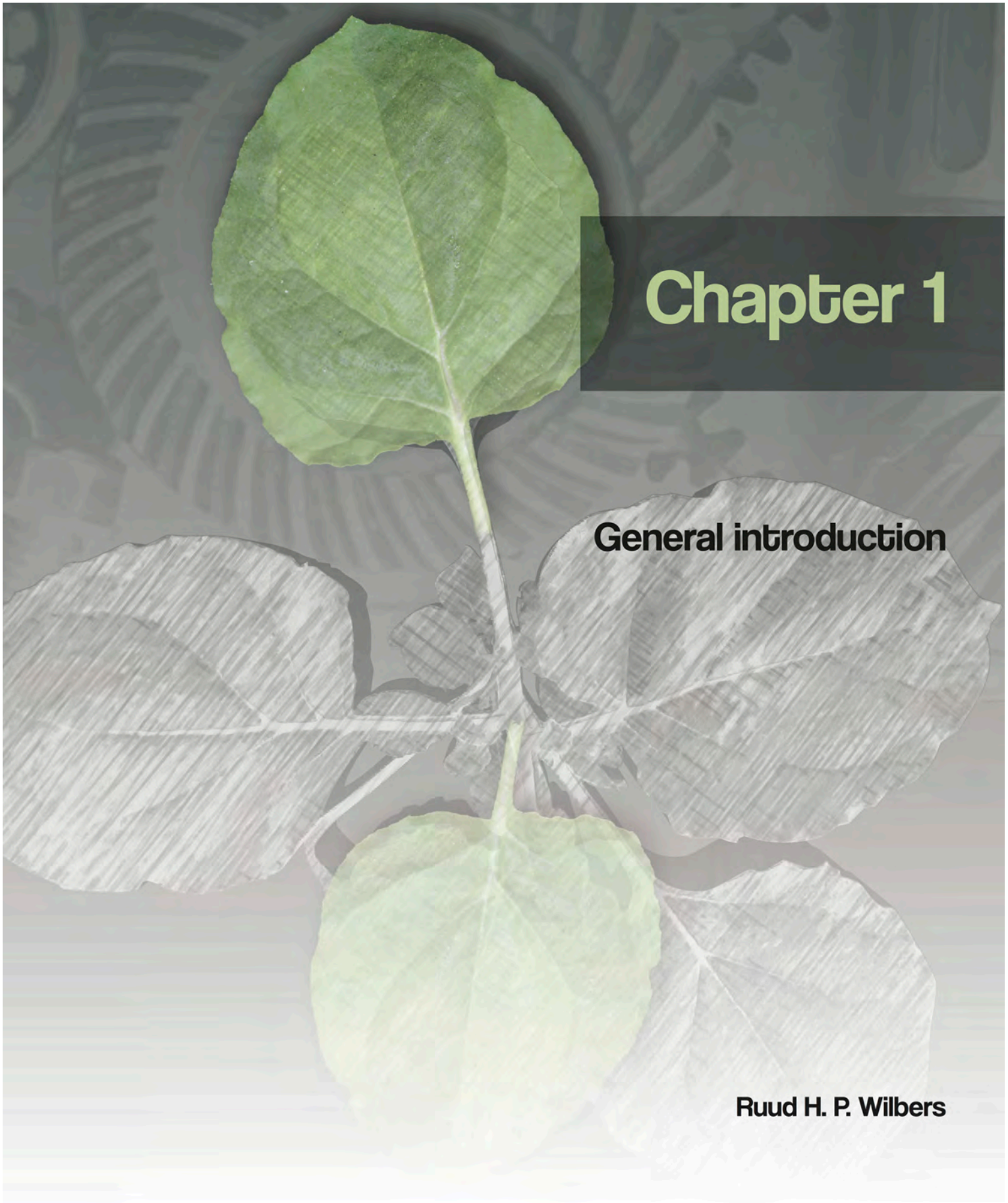

Chapter 1

General introduction

Ruud H. P. Wilbers

The human body is able to defend itself against viruses, pathogenic bacteria and fungi or multicellular parasites, such as helminthic worms. The complex set of cells that forms the immune system defends our body against pathogens and parasites. Immune cells travel throughout our body using the cardiovascular and lymphatic system. Our immune cells are specialised in the recognition of foreign (non-self) compounds and organisms, but are also capable of distinguishing different types of pathogens or parasites. Upon recognition, a specific arm of the immune system is triggered to efficiently eradicate the pathogen or parasite that is encountered. After the infection is cleared the immune system returns to its resting state. Yet, in order to function properly an intricate balance of the immune system is required as uncontrolled immune responses can result in tissue damage.

Different layers of defence

The first line of defence against invading pathogens or parasites is a layer of epithelial cells in those organs that are in direct contact with the outside world, such as skin, lungs and intestine. The epithelial layer that encounters the widest variety of non-self compounds and organisms is the intestinal epithelium (Figure 1). Intestinal epithelial cells are highly specialised cells as they serve as gatekeepers of our intestinal tract. They form a physical barrier to prevent the entry of pathogens and parasites, while these cells simultaneously facilitate the uptake of nutrients and water from our food. The protective function of the intestinal epithelium is in the first place mediated by the tight assembly of epithelial cells, which does not allow the entry of microorganisms (microbes). Secondly, specialised intestinal epithelial cells, so-called goblet cells, secrete mucins into the intestinal lumen. These mucins form a mucus layer and are another physical barrier that prevents attachment of pathogens to the epithelial cells. Finally, normal intestinal epithelial cells as well as specialised Paneth cells secrete large amounts of anti-microbial peptides that reside in the mucus layer [1].

When invading pathogens or parasites breach this first line of defence, the immune system relies on the rapid detection of these foreign compounds and organisms. Cells of the innate immune system are responsible for the early detection of such organisms and do so by recognizing specific structures shared by classes of microbes (so-called "pathogen-associated molecular patterns" or PAMP's). These structures include double stranded RNA from viruses, unmethylated DNA from bacteria or complex lipids and carbohydrates that are not found on host cells. The recognition of PAMP's is a defence response that can be found in all classes of plant and animal life. The cell types that establish innate immunity in vertebrate animal species are phagocytes (such as neutrophils, macrophages and dendritic cells) and natural killer (NK) cells. NK cells do not recognize foreign microbes, but are specialised in recognizing virus-infected cells or tumour cells. On the other hand, dendritic cells, macrophages and various other immune cells are

equipped with pattern recognition receptors (PRR's), which are proteins that are able to recognize specific PAMP's.

PRR's can be found as membrane-bound receptors on the cell surface, but also inside the cell (either cytoplasmic or membrane-bound). PRR's can be further distinguished in functionality as they function as signalling receptors or receptors that mediate uptake into the cell by a process called endocytosis (or both). Toll-like receptors (TLR's) constitute one class of membrane-bound PRR's that recognize different PAMP's and are key to activate innate immune cells upon recognition of non-self compounds. To date, over 10 mammalian TLR's have been identified and each receptor is required for the recognition of PAMP's from different classes of pathogens [2]. For instance, TLR4 can bind lipopolysaccharide (LPS) from gram-negative bacteria, whereas TLR3 is able to detect viral RNA inside the cell. Upon recognition of PAMP's by TLR's an activation signal is transduced into the cell that triggers the production of cytokines. Cytokines are signalling molecules of the immune system. They can change the activation state of immune cells or attract other immune cells to the site of infection. One cytokine commonly produced upon infection is tumour necrosis factor α (TNF-α) and is a key cytokine that drives inflammation.

C-type lectin receptors (CLR's) are another class of PRR's and are specialised in the recognition of carbohydrate structures (self and non-self), such as fungal β-glucans or complex carbohydrate structures found on helminth-secreted proteins [3-5]. Whereas TLR's have a minor role as endocytosis receptors, the main role of CLR's is to facilitate endocytosis of foreign compounds or microbes. C-type lectin receptors often collaborate with TLR's and have been shown to modulate TLR-induced signalling [3, 6]. Nevertheless, endocytosis and/or phagocytosis (internalization of large particles or microbes) are key steps in shaping the immune response against extracellular pathogens, parasites or their secreted compounds. Internalization leads to the formation of vesicles (endosomes or phagosomes) that are transported into the cell where they fuse with lysosomes. Lysosomes are intracellular vesicles that are enriched with compounds that enable the killing of microbes and degrade foreign compounds. All combined, innate immune responses function as a broad-acting mechanism by which short-term immunity can be provided against microbes. The innate immune system is often sufficient to eliminate intruders, but their responses are limited by the diversity of molecular patterns that can be recognized. Also, innate immune cells respond the same way upon repeated exposure to microbes and are not able acquire memory.

The adaptive immune system is a third layer of defence, which is only found in vertebrate species. The adaptive immune system is able to recognise a diverse array of foreign compounds in a highly specific manner, however it requires time to respond. Furthermore, the adaptive immune system also has the ability to acquire memory and

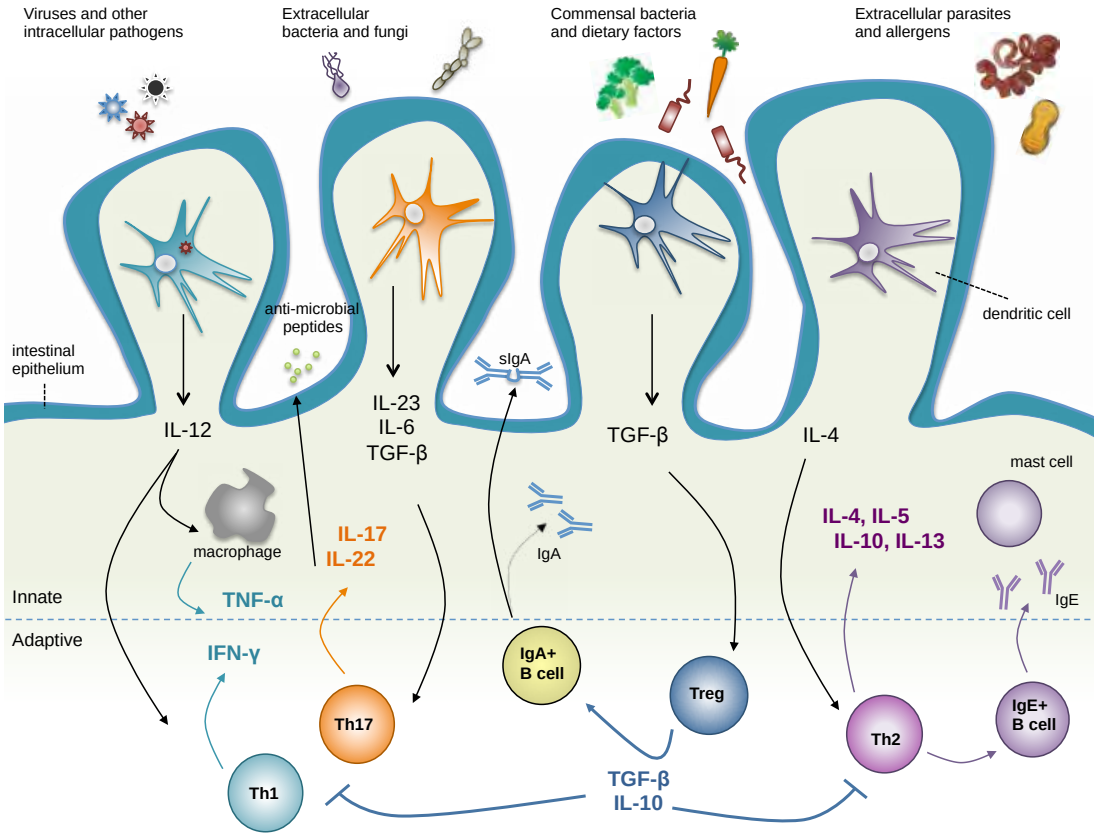

Figure 1 ◆ Innate and adaptive immune responses in the intestine. A simplified schematic overview of innate and adaptive immune responses elicited by different classes of non-self compounds, pathogens and parasites as described in the main text.

responds more vigorously upon repeated infection. Lymphocytes are the cells that provide adaptive immunity. B lymphocytes (or B cells) are responsible for the production of antibodies that can specifically target and neutralize certain intruders, like viruses and bacteria. T cells are another set of lymphocytes and provide cellular immunity. Cytotoxic T cells can recognize virus infected cells or tumour cells and are able to kill these cells. T helper (Th) cells are able to induce proliferation and differentiation of other innate and adaptive immune cells to effectively eradicate the intruding organism. T helper cells are the key cell type in shaping immune responses against different classes of non-self compounds, pathogens and parasites. The activation of T helper cells is initiated and controlled by antigen presenting cells, such as dendritic cells.

Upon infection, dendritic cells are able to internalize microbes or secreted compounds from pathogens and parasites and these so-called antigens are processed into smaller antigenic fragments. This processing step takes place in the endolysosome that forms upon internalization. Antigenic fragments are able to elicit an adaptive immune response and are most commonly of peptide origin. Dendritic cells are able to present these antigens to

T helper cells and induce their activation. The class of pathogen or parasite that is encountered determines the type of T helper cell response that is initiated (Figure 1). Viruses and other (intracellular) pathogens generally trigger the production of a cytokine called interleukin-12 (IL-12) by antigen presenting cells. IL-12 drives the polarisation of T helper cells into IFN-γ producing T cells, so-called Th1 cells. This arm of the adaptive immune system activates macrophages and neutrophils and enhances the production of antibodies by B cells, thereby facilitating efficient neutralization and killing of viruses and microbes. Another arm of the adaptive immune system is driven by the cytokine IL-4, which drives the polarization T helper cells into Th2 cells and is required to mount protective immunity against parasitic worms and allergens. IL-4 and IL-10 are secreted by Th2 cells and suppress classical macrophage activation. Furthermore, the Th2 signature cytokines IL-4, IL-5 and/or IL-13 stimulate the production of IgE-type antibodies, which in turn are used by mast cells and eosinophils (other types of granulocytes distinct from neutrophils) for optimal protective immunity. In a Th2 response induced by helminths a special type of alternatively activated macrophages is induced that have anti-inflammatory and wound healing properties. Th1 and Th2 polarized immune responses are the classic arms of cellular immunity [7], but more recently Th17 cells have been described as an arm of cellular immunity against (extracellular) pathogenic bacteria and fungi [8, 9]. Upon recognition of these pathogenic bacteria or fungi via PRR's, dendritic cells secrete pro-inflammatory cytokines such as IL-6 and IL-23. In synergy with transforming growth factor β1 (TGF-β1) these pro-inflammatory cytokines drive the polarization of Th17 cells, which secrete the signature cytokines IL-17 and IL-22. IL-17 enhances pro-inflammatory cytokine production by other immune cells and facilitates the recruitment of neutrophils to the site of infection. IL-22 on the other hand plays an important role in maintaining epithelial barrier function and induces production of anti-microbial peptides.

T helper cell subsets are able to amplify their own activation, but also suppress the activation of other subset(s). For this reason, the immune response becomes strongly polarized once it is activated along one pathway. Persistent exposure to antigens can therefore result in extreme polarization of the adaptive immune system and could thereby lead to chronic inflammation. Therefore, regulation of immune responses is of key importance and is provided by a different type of T helper cells. When naïve T helper cells (Th cells that have never encountered an antigen) are exposed to TGF-β1 alone they will differentiate into regulatory T cells [10]. These regulatory T cells secrete large amounts of the anti-inflammatory cytokines IL-10 and TGF-β1 and thereby suppress the activation of both innate and adaptive immune cells [11, 12]. TGF-β1 also drives the production of IgA antibodies, which can be transported over the intestinal epithelium as a dimeric complex. This secretory IgA is yet another component of the first line of defence that prevents entry of invading pathogens. Secretory IgA can bind to intestinal pathogens and clear them from the body by peristaltic movement. Regulatory T cells do not only play an important role in

controlling excessive immune responses against invaders, but also provide tolerance against antigens from our diet and harmless commensal bacteria.

The rise of inflammatory disorders

Over the last decennia the incidence of infectious diseases, like tuberculosis, Hepatitis A and measles has been strongly reduced in industrialized countries. Simultaneously, the incidence of autoimmune and inflammatory disorders, like multiple sclerosis, type 1 diabetes, asthma and a variety of allergies, has increased drastically. This inverse relation between the incidence of infectious diseases versus inflammatory disorders in industrialized countries is highlighted in Figure 2.

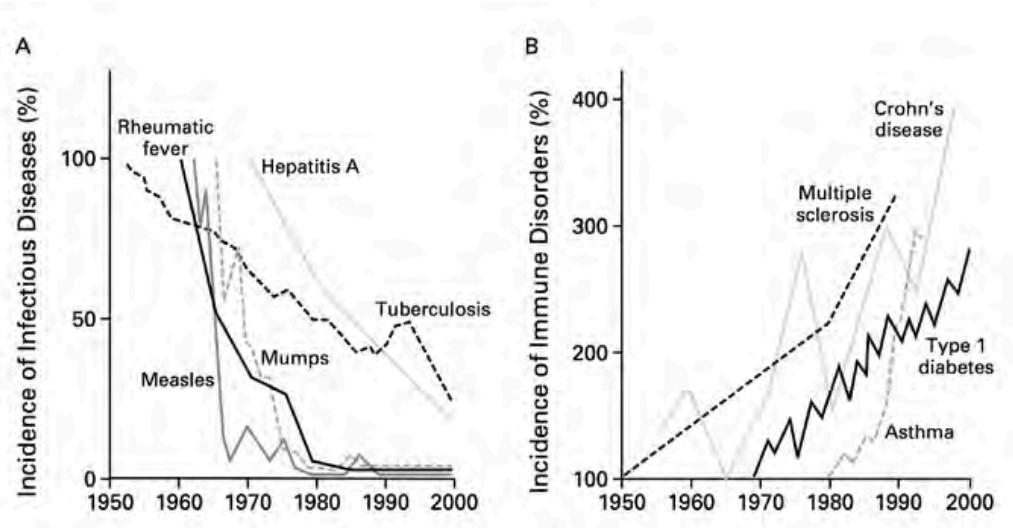

Figure 2 ◆ An inverse relation between the incidences of infectious diseases versus inflammatory disorders. Over the last couple of decades the incidence of infectious diseases, like Hepatitis A or tuberculosis, has been reduced dramatically in industrialized countries (A), whereas inflammatory disorders such as Crohn's disease and multiple sclerosis have become more prevalent (B). Reproduced with permission from Bach 2002 [13], Copyright Massachusetts Medical Society.

Several research groups have described this inverse relation between infectious diseases and inflammatory disorders. Strachan was the first to postulate that early-life exposure to common childhood infections protected younger siblings in larger families from developing allergies, such as hay fever [14, 15]. These and other observations have led to the formulation of the 'hygiene hypothesis'. Nowadays, the decreased incidence of infectious diseases is believed to be a result from a change in life-style in industrialized countries where common infections are almost eradicated by the use of vaccines, increased sanitation and better socio-economic conditions [13].

The immunological mechanism underlying the 'hygiene hypothesis' was first thought to be an imbalance of Th1 versus Th2 immune responses. Th1-promoting viral and bacterial infections would thereby educate the immune system of infants and prevent from the development of excessive and allergy-promoting Th2 responses [16]. Still, this could only explain the rise of Th2-mediated inflammatory disorders, like allergies and asthma, whereas other 'modern' inflammatory diseases, like multiple sclerosis, type 1 diabetes, rheumatoid arthritis and Crohn's disease are generally driven by excessive Th1- and/or Th17-mediated immune responses. The prevalence of helminth infections in non-industrialized countries sheds a new perspective on the original 'hygiene hypothesis' as it is also inversely correlated with the incidence of inflammatory disorders. Helminth infections in children in developing countries can also lower the risk of allergic reactions [16], which is remarkable as both helminths and allergens elicit Th2-mediated immune responses. In the case of *Schistosoma haematobium*, infected children were shown to produce high levels of the anti-inflammatory cytokine IL-10 upon stimulation with parasite antigens [17]. IL-10 is an anti-inflammatory cytokine just like TGF-β1 and both are secreted by regulatory T cells. Furthermore, IL-10 and TGF-β1 are able to control both Th2-mediated allergies as well as Th1/Th17-mediated inflammatory disorders [18-20]. This lead to an updated version of the 'hygiene hypothesis' where infections, and infection experience, are believed to be key in maintaining the balance between regulatory T cells, on one side, and active Th1, Th2 and Th17 cells on the other [16].

Strategies to treat inflammatory disorders

Treatment of inflammatory disorders relies on the intervention of exacerbated immune responses to re-establish immunological homeostasis. Classical therapeutic approaches are based on the administration of chemical drugs to suppress the immune system. Corticosteroids for example have broad anti-inflammatory properties and are typically used to treat allergies. Furthermore, cytostatics (e.g. methotrexate or azathioprine) are molecules that inhibit cell division and are successfully used to treat inflammatory disorders, like rheumatoid arthritis and inflammatory bowel disease [21, 22]. However, up to one-third of inflammatory bowel disease patients do not respond to treatment with classical immunosuppressive drugs [22]. An alternative approach to treat patients with inflammatory disorders was made possible when in 1982 the Food and Drug Administration (FDA) approved the first biopharmaceutical for medicinal use in humans in the United States of America (Humulin; recombinant human insulin; Eli Lilly, Indianapolis). Biopharmaceuticals are medicinal products, which can be extracted from or manufactured in biological sources. Biopharmaceuticals include monoclonal antibodies, hormones, cytokines, enzymes, vaccines and other blood-related proteins. Since 2000, the therapeutic market for monoclonal antibodies has grown exponentially and the

majority of antibodies (and antibody-like products) target inflammatory and/or autoimmune conditions [23]. Monoclonal antibodies can be used to specifically bind and neutralize cytokines or immune receptors, thereby intervening with inflammatory immune responses. For instance, the top-selling monoclonal antibodies target the pro-inflammatory cytokine TNF-α (e.g. adalimumab and infliximab) already generate a turnover of $30.5 billion in 2013, which is ~21% of total market value of biopharmaceuticals [23].

Like with chemical immunosuppressive drugs not all patients respond to therapy with biopharmaceuticals as is seen for anti-TNF-α therapy in patients with rheumatoid arthritis, inflammatory bowel disease or psoriasis [22, 24]. Similarly, blockade of TNF-α might be beneficial for treating rheumatoid arthritis, Crohn's disease and psoriasis, but it is not effective in multiple sclerosis [24]. So, even though TNF-α, and several other cytokines, are common targets for treating a wide range of inflammatory disorders, a single therapy is not sufficient to treat all inflammatory disorders. This also emphasizes the problem that many inflammatory disorders are categorized based on the symptoms they have in common, but not on the actual underlying cause. Inflammatory bowel diseases for instance are a wide range of diseases with varying causes that ultimately result in similar symptoms among patients. Furthermore, conventional treatment is aimed on treating symptoms or on strong immunosuppression. The consequence of the latter strategy is that broad immune suppression can also enhance the risk of interference with other processes in the patient and thereby cause adverse side effects. The way forward would be to have more in-depth knowledge on the underlying cause of inflammatory disorders. But as patients have their own unique genetic variation that underlies disease, personalized medicine might also be required in the future to treat these inflammatory disorders.

For personalized medicine, biopharmaceuticals are probably most convenient as they are more specific than chemical immunosuppressive drugs. However, more knowledge is required on the genetic variation that predisposes patients to the development of inflammatory disorders, and how this variation contributes to altered immunological processes. Furthermore, the arsenal of biopharmaceuticals needs to be increased to have a wide variety of drugs to intervene with specific immunological responses. Every year new monoclonal antibodies are approved for medicinal use in humans and the variety in molecules that can be targeted increases as well [23]. But even though antibodies dominate the therapeutic market, alternative approaches might be required as well. For instance, the natural signaling molecules of the immune system (cytokines) can possibly be used to specifically manipulate immune responses [25]. Looking back at the hygiene hypothesis, re-establishing the balance between regulatory T cells and other T helper cell subsets might be of great potential in treating inflammatory disorders. The use of immune-regulatory cytokines that drive regulatory T cell development or are secreted by these cells (e.g. IL-10, TGF-β1 and the recently discovered IL-35 [26]) might therefore be an interesting therapeutic approach for the future. Systemic administration of recombinant

human IL-10 produced in *Escherichia coli* has been used in the clinic to treat patients with Crohn's disease. IL-10 treatment is well tolerated [27], but patients do not all respond to IL-10 treatment [28]. The reason why IL-10 treatment has not been a successful therapy is therefore of great interest.

Alternative therapeutic approaches can also be deducted from the hygiene hypothesis. The inverse relation between the incidences of inflammatory disorders and helminth infections indicate that these parasitic worms are somehow capable of regulating their host's immune system. Helminth therapy has been applied in patients suffering from inflammatory bowel diseases. Treatment with eggs of the parasitic nematode *Trichuris suis* was shown to be safe and effective [29, 30]. The protective effect of helminth infection against immune-mediated diseases was tested in several animal models for human diseases [31]. For instance, *Schistosoma mansoni* was shown to protect mice against TNBS-induced colitis [32], allergen-induced airway hyperreactivity [33], autoimmune encephalitis [33, 34] and autoimmune diabetes [35, 36]. Protection against immune-mediated diseases was associated with the down-regulation of Th1-type cytokines (IFN-γ and IL-12) and increased expression of regulatory and Th2-type cytokines (IL-4, IL-10 and/or IL-13). However, more information is required to better understand how helminths modulate their host's immune system. Knowledge on helminth-secreted proteins that play a key role in immunomodulation could ultimately lead to the identification of novel therapeutic targets for the treatment of several immune-mediated diseases.

Production of pharmaceutical proteins and the importance of N-glycosylation

Biopharmaceuticals are of great interest, but these medicinal proteins cannot be extracted in large quantities from biological sources, such as human blood or helminth secretions. Nowadays, production of most biopharmaceutical proteins relies on recombinant DNA technology. This technology allows the introduction of a gene of interest into a host organism that can be easily cultured, for example the bacterium *Escherichia coli*. Expression of the gene in such a host enables the production of proteins by heterologous ('from one species to another') expression. Therefore recombinant DNA technology has revolutionized the production and application of pharmaceutical proteins.

Several heterologous expression systems exist. The majority of biopharmaceuticals approved for medicinal use in humans are produced in the bacterium *E. coli*, the yeast *Saccharomyces cerevisiae* or mammalian cell lines, like Chinese hamster ovarian (CHO) cells or murine myeloma (SP2/0) cells [23]. Yet, care has to be taken with regard to the choice of the expression host for the production of pharmaceutical proteins. *E. coli* allows the most cost effective production of biopharmaceuticals, but as a prokaryote it is not able to produce complex proteins. The formation of inclusion bodies (large aggregates) is a common feature when proteins are expressed in *E. coli* and these proteins require

chemical refolding to become biologically active. Furthermore, *E. coli* is naturally not able to perform complex post-translational processes, like N-glycosylation.

N-glycosylation is the attachment of sugar molecules (or N-glycans) to a protein backbone in eukaryotes. The type of N-glycan found on glycoproteins varies between classes of eukaryotic species. One of the major roles of N-glycosylation in eukaryotes is that N-glycans aid in protein folding and quality control after folding. Furthermore, N-glycans can alter the biochemical properties of a protein and can thereby influence protein stability and solubility [37]. As a large number of biopharmaceutical proteins are N-glycosylated (glycoproteins), a eukaryotic expression host is often preferred. Like bacteria, yeasts are also easy and cheap to culture and they are capable of producing glycoproteins. However, yeasts mainly produce mannose-enriched N-glycans and have the tendency to hyper-glycosylate [38]. Mannose-enriched N-glycans can be a target for antigen presenting cells by binding to the mannose receptor [39]. Engagement of the mannose receptor can result in quick clearance of the protein from the blood stream, thereby strongly reducing its half-life [40]. Mannose-enriched N-glycans are therefore mostly not preferred on pharmaceutical glycoproteins.

An additional function of N-glycosylation in more complex organisms is the role of N-glycans in cell-to-cell communication, glycoprotein targeting and modulation of glycoprotein activity [37]. For instance, antibodies, the largest group of biopharmaceutical proteins, rely on their N-glycosylation for their activity [41-43]. N-glycans on antibodies are required for optimal binding to Fc-receptors and subsequent effector functions [41]. N-glycan composition can thereby affect pharmacokinetics and biological activity and is therefore crucial to obtain optimal efficacy. Mammalian cell lines are the most common production platform for pharmaceutical glycoproteins as they are able to synthesize these glycoproteins with their native N-glycans. However, a major disadvantage of mammalian cell lines is that the N-glycan composition on a therapeutic glycoprotein is heterogeneous and affects batch-to-batch reproducibility [44]. Furthermore, engineering of N-glycosylation in mammalian cells is complicated by the complex endogenous glycome.

Over the last three decades, plants have emerged as a good alternative production platform for biopharmaceuticals [45-48]. Like mammals, plants are higher eukaryotes and are able to correctly fold complex proteins, assemble heteromultimeric protein complexes [49], and perform post-translational modifications, such as N-glycosylation. In contrast to mammalian cells, plants depend only on water, energy from the sun and basic nutrients and are therefore much cheaper to maintain. Furthermore, plants can also be regarded as more safe, because they have a low risk for contamination with human pathogens. This is especially relevant when a production platform is used for the expression of immunomodulating proteins. One major limitation for the acceptance of plants as a production platform for pharmaceutical glycoproteins is the addition of typical plant N-glycans that can be immunogenic [50]. However, engineering of the N-glycosylation

machinery in plants has been investigated intensively. Plants are now able to synthesize human glycoproteins with a homogeneous human-like N-glycan composition.

Engineering of the plant N-glycosylation pathway

N-glycosylation is initiated in the endoplasmic reticulum by the oligosaccharyl transferase complex. This complex attaches a common oligosaccharide precursor ($Glc_3Man_9GlcNAc_2$) to the asparagine residue within the N-glycosylation consensus sequence Asn-X-Ser/Thr (where X can be any amino acid, except proline). This common precursor is then trimmed down to $Man_8GlcNAc_2$ (Man8) and the glycoprotein is subsequently transported to the Golgi-system. These first steps in the N-glycosylation pathway are conserved within all eukaryotes, but from this point onwards the N-glycosylation pathways diverge. Within the Golgi system of yeast this common Man8 structure is further extended with mannose residues and results in the formation of mannose-enriched N-glycans (Figure 3). In higher eukaryotes, the Man8 structure is first trimmed down by mannosidases and then further extended by the addition of GlcNAc, galactose, sialic acid, fucose and/or xylose. In plants the typical complex N-glycan structure terminates with GlcNAc residues and carries typical plant core α1,3-fucose and β1,2-xylose residues as depicted in figure 3. Mammalian N-glycans also carry core fucose, but in contrast to plants this fucose is α1,6-linked. Furthermore, the terminal GlcNAc residues can be further extended with galactose and/or sialic acid residues and additional branching can occur (Figure 3).

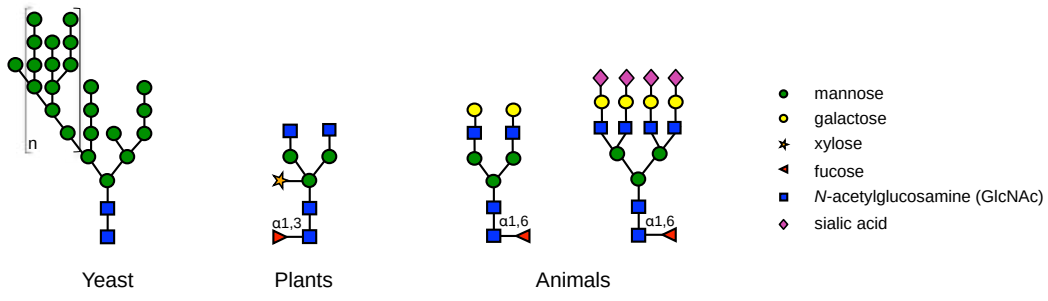

Figure 3 ◆ Schematic representation of typical N-glycans found in yeast, plants and animals.

Engineering of the N-glycosylation pathway in different expression hosts has gained much attention, as the N-glycan composition of therapeutic proteins is crucial to their efficacy. Engineering of the N-glycosylation pathway is enabled by co-expression of desired glycosyltransferases or down-regulation of undesired host glycosyltransferases. The engineering of the N-glycosylation in different non-mammalian host species is

extensively reviewed by Loos and Steinkellner [51]. Here we will further focus on the glyco-engineering in plants. Over the last two decades plants have demonstrated to possess a high degree of tolerance towards changes in their glycosylation pathway. This tolerance allows the modification of recombinant glycoproteins in a specific and controlled manner [52]. The first attempts to humanise N-glycans in plants were made by stably expressing human β1,4-galactosyltransferase in BY-2 cells or *Nicotiana tabacum* plants [53-55]. The efficiency of galactosylation in plants was proven to be a challenge as expression of human β1,4-galactosyltransferase resulted in the formation of incompletely processed N-glycans, mainly lacking typical plant β1,2-xylose and/or α1,3-fucose or a single β1,4-galactose [54]. A major breakthrough in humanizing the N-glycans of plants was made in 2008 by Strasser and co-workers. They generated transgenic *Nicotiana benthamiana* plants in which the expression of the α1,3-fucosyltransferase and β1,2-xylosyltransferase genes were down-regulated [56]. These transgenic ΔXT/FT plants enabled the expression of monoclonal antibodies with homogeneous galactosylation of their N-glycans upon co-expression of a *trans*-Golgi targeted human β1,4-galactosyltransferase [57]. This study also revealed that the N-glycan composition of a monoclonal antibody from glyco-engineered plants was strikingly homogeneous, notably when compared to the CHO cell-derived antibody.

Further steps in humanizing N-glycosylation in plants were made by transiently co-expressing human α1,6-fucosyltransferase 8 along with monoclonal antibodies in ΔXT/FT plants [58]. Again this study revealed the ability of plants to synthesize human-like N-glycans carrying core α1,6-fucose to great homogeneity. Furthermore, the synthesis of more complex bisected or branched N-glycans has been explored as well by co-expressing the human *N*-acetyl-glucosaminyltransferases GnTIII, GnTIV and/or GnTV [58-60]. Finally, a remarkable achievement in making sialylated N-glycans in plants has been made by Castilho and co-workers [61]. Transient co-expression of all the required enzymes for the synthesis of the CMP-Neu5Ac substrate, its transport into the Golgi and galactosyl- and sialyltransferase enabled the synthesis of sialylated N-glycans on a monoclonal antibody expressed in plants.

All these achievements reveal that plants are an excellent production platform for recombinant proteins with a tailored N-glycan composition. Yet, almost all efforts in engineering the N-glycosylation pathway of plants have been directed towards humanization of its N-glycans. The ability of plants to synthesize tailored N-glycans with great homogeneity and their extreme tolerance towards changes in the N-glycosylation pathway make them an interesting research tool to further explore the potential of engineering virtually any type of N-glycan structures. For instance, immunogenic N-glycan structures found on helminth-secreted proteins (see figure 4) could potentially be used to target subunit vaccines to specific C-type lectin receptors on antigen presenting cells and thereby improve their efficacy [62]. Plants offer a great starting point for

engineering helminth-like N-glycans as the typical plant sugar residues β1,2-xylose and/or α1,3-fucose are also found on helminth N-glycans. The ability of plants to synthesize helminth-like N-glycans would also allow the functional characterization of helminth-secreted glycoproteins, but would also allow investigation into the role that N-glycans play on the immunomodulatory properties of these helminth-secreted glycoproteins. Ultimately, this could lead to the identification of novel therapeutic strategies for vaccination as wells as treatment of inflammatory disorders.

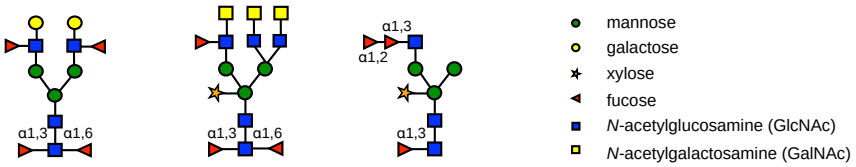

Figure 4 ◆ Schematic representation of N-glycan structures found on helminth glycoproteins.

Outline of this thesis

This thesis describes the plant-based expression and investigation of immunologically relevant proteins. Immunologically relevant in this case relates to the potential therapeutic use of these proteins to treat inflammatory disorders. In **Chapter 2** we describe the plant-based expression of the immune-regulatory cytokine human transforming growth factor β1 (TGF-β1). By co-expressing human furin with latent TGF-β1 we were able to engineer the post-translational proteolytic processing of TGF-β1, which enabled the production of biologically active TGF-β1. In **Chapter 3** we reveal that aggregation is a major production bottleneck for the anti-inflammatory cytokine interleukin-10 (IL-10). By protein engineering we were able to prevent aggregation and created a biologically active fusion protein of IL-10. In **Chapter 4** we express biologically active IL-22 in plants. We reveal that, in contrast to current literature, its activity is independent of the presence of N-glycans or their composition. This chapter further reveals that plants offer a powerful tool to allow investigation into the role of N-glycans in protein folding and biological activity of glycoproteins. In **Chapter 5** we further explore the potential of glyco-engineering in plants by engineering helminth-like N-glycans. We produce large quantities of two major egg antigens from *Schistosoma mansoni* and successfully engineer Lewis X, LDN and LDNF N-glycan structures. These plant biotechnological research lines are a showcase for the potential of engineering proteins as well as post-translational modifications in plants with special emphasis on N-glycan engineering.

In parallel to the plant biotechnological research lines, we further investigated the biological activity of IL-10. We studied IL-10-mediated signalling to possibly obtain clues on why IL-10 therapy has not been as effective as previously anticipated. In **Chapter 6** we have set-up biological activity assays based on bone marrow-derived cells and reveal that IL-10 activity is dependent on both IL-10R1 and IL-10R2, but not IL-10R2-associated signalling via Tyk2. We also show that interactions between IL-10R1 and IL-10R2 (both intracellular and extracellular) reduce cellular binding of IL-10, but are crucial to initiate IL-10 mediated signalling. Furthermore, we observed that macrophages and dendritic cells respond differently to IL-10. This was further investigated in **Chapter 7** where we reveal that GM-CSF (the cytokine used to differentiate dendritic cells) is responsible for negatively regulating early IL-10-mediated responses. Strikingly, GM-CSF does not strongly affect the IL-10-induced activation of the transcription factor STAT3. Instead, GM-CSF induces strong constitutive phosphorylation of GSK-3β, a signalling component downstream of the PI3K/Akt pathway. These immunological chapters give novel insights on the mechanism of initiating IL-10-induced signalling and on the possible integration of signal transduction pathways elicited by different cytokines. Ultimately this knowledge could provide us with new therapeutic strategies to treat inflammatory disorders.

References

1. Maynard CL, Elson CO, Hatton RD and Weaver CT (2012) Reciprocal interactions of the intestinal microbiota and immune system. Nature 489: 231-241.
2. Lee CC, Avalos AM and Ploegh HL (2012) Accessory molecules for Toll-like receptors and their function. Nature Reviews Immunology 12: 168-179.
3. Geijtenbeek TB and Gringhuis SI (2009) Signalling through C-type lectin receptors: shaping immune responses. Nature Reviews Immunology 9: 465-479.
4. Meevissen MHJ, Driessen NN, Smits HH, Versteegh R, van Vliet SJ, et al. (2012) Specific glycan elements determine differential binding of individual egg glycoproteins of the human parasite Schistosoma mansoni by host C-type lectin receptors. International Journal of Parasitology 42: 269-277.
5. Meevissen MHJ, Yazdanbakhsh M and Hokke CH (2012) Schistosoma mansoni egg glycoproteins and C-type lectins of host immune cells: Molecular partners that shape immune responses. Experimental Parasitology 132: 14-21.
6. Gringhuis SI, den Dunnen J, Litjens M, van Het Hof B, van Kooyk Y, et al. (2007) C-type lectin DC-SIGN modulates Toll-like receptor signaling via Raf-1 kinase-dependent acetylation of transcription factor NF-kappaB. Immunity 26: 605-616.
7. Mosmann TR and Coffman RL (1989) TH1 and TH2 cells: different patterns of lymphokine secretion lead to different functional properties. Annual Reviews Immunology 7: 145-173.
8. Veldhoen M, Hocking RJ, Atkins CJ, Locksley RM and Stockinger B (2006) TGF beta in the context of an inflammatory cytokine milieu supports de novo differentiation of IL-17-producing T cells. Immunity 24: 179-189.
9. Bettelli E, Oukka M and Kuchroo VK (2007) T(H)-17 cells in the circle of immunity and autoimmunity. Nature Immunology 8: 345-350.
10. Chen WJ, Jin WW, Hardegen N, Lei KJ, Li L, et al. (2003) Conversion of peripheral CD4(+)CD25(-) naive T cells to CD4(+)CD25(+) regulatory T cells by TGF-beta induction of transcription factor Foxp3. Journal of Experimental Medicine 198: 1875-1886.
11. Moore KW, de Waal Malefyt R, Coffman RL and O'Garra A (2001) Interleukin-10 and the interleukin-10 receptor. Annual Reviews Immunology 19: 683-765.
12. Li MO and Flavell RA (2008) TGF-beta: a master of all T cell trades. Cell 134: 392-404.
13. Bach JF (2002) The effect of infections on susceptibility to autoimmune and allergic diseases. The New England Journal of Medicine 347: 911-920.
14. Strachan DP (1989) Hay fever, hygiene, and household size. BMJ 299: 1259-1260.

15. Strachan DP (2000) Family size, infection and atopy: the first decade of the "hygiene hypothesis". Thorax 55 (Supplement 1): S2-10.

16. Maizels RM, McSorley HJ and Smyth DJ (2014) Helminths in the hygiene hypothesis: sooner or later? Clinical and Experimental Immunology 177: 38-46.

17. van den Biggelaar AH, van Ree R, Rodrigues LC, Lell B, Deelder AM, et al. (2000) Decreased atopy in children infected with Schistosoma haematobium: a role for parasite-induced interleukin-10. Lancet 356: 1723-1727.

18. Akdis M, Verhagen J, Taylor A, Karamloo F, Karagiannidis C, et al. (2004) Immune responses in healthy and allergic individuals are characterized by a fine balance between allergen-specific T regulatory 1 and T helper 2 cells. Journal of Experimental Medicine 199: 1567-1575.

19. Hawrylowicz CM and O'Garra A (2005) Potential role of interleukin-10-secreting regulatory T cells in allergy and asthma. Nature Reviews Immunology 5: 271-283.

20. Kim JM, Rasmussen JP and Rudensky AY (2007) Regulatory T cells prevent catastrophic autoimmunity throughout the lifespan of mice. Nature Immunology 8: 191-197.

21. Favalli EG, Biggioggero M and Meroni PL (2014) Methotrexate for the treatment of rheumatoid arthritis in the biologic era: still an "anchor" drug? Autoimmunity Reviews 13: 1102-1108.

22. Ng SC, Chan FK and Sung JJ (2011) Review article: the role of non-biological drugs in refractory inflammatory bowel disease. Alimentary & Pharmacology & Therapeutics 33: 417-427.

23. Walsh G (2014) Biopharmaceutical benchmarks 2014. Nature Biotechnology 32: 992-1000.

24. Steinman L, Merrill JT, McInnes IB and Peakman M (2012) Optimization of current and future therapy for autoimmune diseases. Nature Medicine 18: 59-65.

25. McLean MH, Neurath MF and Durum SK (2014) Targeting Interleukins for the Treatment of Inflammatory Bowel Disease-What Lies Beyond Anti-TNF Therapy? Inflammatory Bowel Disease 20: 389-397.

26. Collison LW, Workman CJ, Kuo TT, Boyd K, Wang Y, et al. (2007) The inhibitory cytokine IL-35 contributes to regulatory T-cell function. Nature 450: 566-569.

27. van Deventer SJ, Elson CO and Fedorak RN (1997) Multiple doses of intravenous interleukin 10 in steroid-refractory Crohn's disease. Crohn's Disease Study Group. Gastroenterology 113: 383-389.

28. Schreiber S, Fedorak RN, Nielsen OH, Wild G, Williams CN, et al. (2000) Safety and efficacy of recombinant human interleukin 10 in chronic active Crohn's disease. Crohn's Disease IL-10 Cooperative Study Group. Gastroenterology 119: 1461-1472.

29. Summers RW, Elliott DE, Urban JF, Jr., Thompson R and Weinstock JV (2005) Trichuris suis therapy in Crohn's disease. Gut 54: 87-90.

30. Summers RW, Elliott DE, Urban JF, Jr., Thompson RA and Weinstock JV (2005) Trichuris suis therapy for active ulcerative colitis: a randomized controlled trial. Gastroenterology 128: 825-832.

31. Finlay CM, Walsh KP and Mills KHG (2014) Induction of regulatory cells by helminth parasites: exploitation for the treatment of inflammatory diseases. Immunological Reviews 259: 206-230.

32. Elliott DE, Li J, Blum A, Metwali A, Qadir K, et al. (2003) Exposure to schistosome eggs protects mice from TNBS-induced colitis. American Journal of Physiology - Gastrointestinal and Liver Physiology 284: G385-391.

33. Mangan NE, van Rooijen N, McKenzie AN and Fallon PG (2006) Helminth-modified pulmonary immune response protects mice from allergen-induced airway hyperresponsiveness. Journal of Immunology 176: 138-147.

34. Sewell D, Qing Z, Reinke E, Elliot D, Weinstock J, et al. (2003) Immunomodulation of experimental autoimmune encephalomyelitis by helminth ova immunization. International Immunology 15: 59-69.

35. Cooke A, Tonks P, Jones FM, O'Shea H, Hutchings P, et al. (1999) Infection with Schistosoma mansoni prevents insulin dependent diabetes mellitus in non-obese diabetic mice. Parasite Immunology 21: 169-176.

36. Zaccone P, Fehervari Z, Jones FM, Sidobre S, Kronenberg M, et al. (2003) Schistosoma mansoni antigens modulate the activity of the innate immune response and prevent onset of type 1 diabetes. European Journal of Immunology 33: 1439-1449.

37. Schwarz F and Aebi M (2011) Mechanisms and principles of N-linked protein glycosylation. Current Opinion in Structural Biology 21: 576-582.

38. Gemmill TR and Trimble RB (1999) Overview of N- and O-linked oligosaccharide structures found in various yeast species. Biochimica et Biophysica Acta 1426: 227-237.

39. Taylor ME, Bezouska K and Drickamer K (1992) Contribution to ligand binding by multiple carbohydrate-recognition domains in the macrophage mannose receptor. Journal of Biological Chemistry 267: 1719-1726.

40. Lee SJ, Evers S, Roeder D, Parlow AF, Risteli J, et al. (2002) Mannose receptor-mediated regulation of serum glycoprotein homeostasis. Science 295: 1898-1901.

41. Jefferis R (2009) Recombinant antibody therapeutics: the impact of glycosylation on mechanisms of action. Trends in Pharmacological Sciences 30: 356-362.

42. Jefferis R and Lund J (2002) Interaction sites on human IgG-Fc for FcgammaR: current models. Immunology Letters 82: 57-65.

43. Shields RL, Lai J, Keck R, O'Connell LY, Hong K, et al. (2002) Lack of fucose on human IgG1 N-linked oligosaccharide improves binding to human Fcgamma RIII and antibody-dependent cellular toxicity. Journal of Biological Chemistry 277: 26733-26740.

44. Meuris L, Santens F, Elson G, Festjens N, Boone M, et al. (2014) GlycoDelete engineering of mammalian cells simplifies N-glycosylation of recombinant proteins. Nature Biotechnology 32: 485-489.

45. Daniell H, Streatfield SJ and Wycoff K (2001) Medical molecular farming: production of antibodies, biopharmaceuticals and edible vaccines in plants. Trends in Plant Science 6: 219-226.

46. Giddings G, Allison G, Brooks D and Carter A (2000) Transgenic plants as factories for biopharmaceuticals. Nature Biotechnology 18: 1151-1155.

47. Goldstein DA and Thomas JA (2004) Biopharmaceuticals derived from genetically modified plants. QJM : monthly journal of the Association of Physicians 97: 705-716.

48. Warzecha H (2008) Biopharmaceuticals from plants: a multitude of options for posttranslational modifications. Biotechnology & Genetic Engineering Reviews 25: 315-330.

49. Ma JK, Hiatt A, Hein M, Vine ND, Wang F, et al. (1995) Generation and assembly of secretory antibodies in plants. Science 268: 716-719.

50. Bardor M, Faveeuw C, Fitchette AC, Gilbert D, Galas L, et al. (2003) Immunoreactivity in mammals of two typical plant glyco-epitopes, core alpha(1,3)-fucose and core xylose. Glycobiology 13: 427-434.

51. Loos A and Steinkellner H (2012) IgG-Fc glycoengineering in non-mammalian expression hosts. Archives of Biochemistry and Biophysics 526: 167-173.

52. Bosch D, Castilho A, Loos A, Schots A and Steinkellner H (2013) N-Glycosylation of Plant-produced Recombinant Proteins. Current Pharmaceutical Design 19: 5503-5512.

53. Palacpac NQ, Yoshida S, Sakai H, Kimura Y, Fujiyama K, et al. (1999) Stable expression of human β1,4-galactosyltransferase in plant cells modifies N-linked glycosylation patterns. Proceedings of the National Academy of Sciences of the United States of America 96: 4692-4697.

54. Bakker H, Bardor M, Molthoff JW, Gomord V, Elbers I, et al. (2001) Galactose-extended glycans of antibodies produced by transgenic plants. Proceedings of the National Academy of Sciences of the United States of America 98: 2899-2904.

55. Bakker H, Rouwendal GJA, Karnoup AS, Florack DEA, Stoopen GM, et al. (2006) An antibody produced in tobacco expressing a hybrid beta-1,4-galactosyltransferase is essentially devoid of plant carbohydrate epitopes. Proceedings of the National Academy of Sciences of the United States of America 103: 7577-7582.

56. Strasser R, Stadlmann J, Schahs M, Stiegler G, Quendler H, et al. (2008) Generation of glyco-engineered Nicotiana benthamiana for the production of monoclonal antibodies with a homogeneous human-like N-glycan structure. Plant Biotechnology Journal 6: 392-402.

57. Strasser R, Castilho A, Stadlmann J, Kunert R, Quendler H, et al. (2009) Improved virus neutralization by plant-produced anti-HIV antibodies with a homogeneous beta1,4-galactosylated N-glycan profile. Journal of Biological Chemistry 284: 20479-20485.

58. Castilho A, Bohorova N, Grass J, Bohorov O, Zeitlin L, et al. (2011) Rapid High Yield Production of Different Glycoforms of Ebola Virus Monoclonal Antibody. Plos One 6(10): e26040.

59. Rouwendal GJ, Wuhrer M, Florack DE, Koeleman CA, Deelder AM, et al. (2007) Efficient introduction of a bisecting GlcNAc residue in tobacco N-glycans by expression of the gene encoding human N-acetylglucosaminyltransferase III. Glycobiology 17: 334-344.

60. Castilho A, Gattinger P, Grass J, Jez J, Pabst M, et al. (2011) N-glycosylation engineering of plants for the biosynthesis of glycoproteins with bisected and branched complex N-glycans. Glycobiology 21: 813-823.

61. Castilho A, Strasser R, Stadlmann J, Grass J, Jez J, et al. (2010) In planta protein sialylation through overexpression of the respective mammalian pathway. Journal of Biological Chemistry 285: 15923-15930.

62. Bosch D and Schots A (2010) Plant glycans: friend or foe in vaccine development? Expert Reviews Vaccines 9: 835-842.

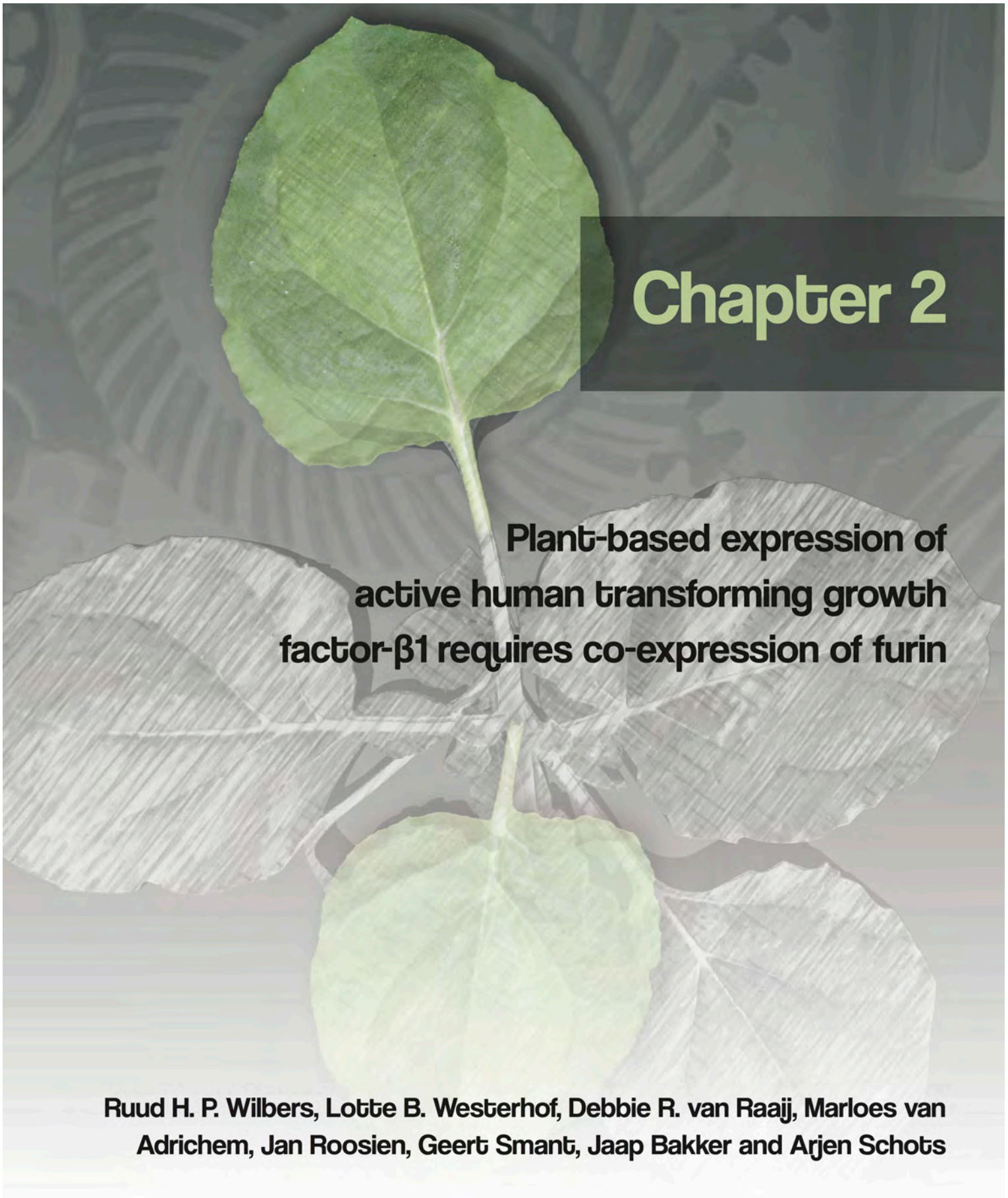

Chapter 2

Plant-based expression of active human transforming growth factor-β1 requires co-expression of furin

Ruud H. P. Wilbers, Lotte B. Westerhof, Debbie R. van Raaij, Marloes van Adrichem, Jan Roosien, Geert Smant, Jaap Bakker and Arjen Schots

Abstract

Transforming growth factor beta (TGF-β) is a signaling molecule that plays a key role in regulating developmental processes and the immune system. Three TGF-β isoforms exist in humans and each isoform has putative therapeutic applications. For the production of large quantities of recombinant TGF-β a suitable expression platform is required. Plants offer a platform for the production of recombinant proteins that is cheap and easy to scale-up and has a low risk for contamination with human pathogens. TGF-β3 has been produced in plants before using a chloroplast expression system. However, this strategy required chemical refolding to obtain a biologically active protein. In this study we investigated the possibility to transiently express active human TGF-β1 in *Nicotiana benthamiana* plants. We were able to show that processing of latent LAP-TGF-β1 by a furin-like enzyme does not occur *in planta*. Expression of mature TGF-β1 in the absence of LAP was successful when an *Arabidopsis* chitinase signal peptide was used, however the obtained protein was inactive. The same chitinase signal peptide enhanced the expression of LAP-TGF-β1 and co-expression of human furin enabled the expression of biologically active TGF-β1. Our data demonstrate that plants can be a suitable platform for the production of active TGF-β1 without the need for chemical refolding.

Introduction

Transforming growth factor beta (TGF-β) is a signaling molecule with crucial roles during early development and the regulation of immune responses. TGF-β controls cellular processes, including cell proliferation, recognition, differentiation and apoptosis [1, 2]. Three different TGF-β isoforms (TGF-β1, TGF-β2 and TGF-β3) exist in humans, which are all encoded by a different gene [3]. The TGF-β genes encode prepro-TGF-β that consists of the signal peptide, latency associated peptide (LAP) and the mature TGF-β protein. The signal peptide targets the protein to the endoplasmic reticulum (ER) where it is cleaved off. Pro-TGF-β then forms homodimers and is further processed in the trans-Golgi by a furin convertase. Proteolytic cleavage by this enzyme separates mature TGF-β from LAP, but they stay non-covalently associated [4]. This dimeric complex is called the small latency complex (SLC) and keeps mature TGF-β in an inactive form. Upon secretion of the SLC, LAP binds to latent transforming growth factor binding protein (LTBP) in the extracellular matrix, resulting in a membrane-bound complex known as the large latency complex (LLC) [5]. TGF-β is activated by either proteolytic degradation of LAP, reactive oxygen species (ROS), an acidic environment or interaction with integrin receptors [5]. Active TGF-β is a dimeric protein of ~25 kDa wherein a disulphide bridge connects the two monomers. Each monomer also has 4 internal disulphide bridges that create a cysteine knot structure [6-9].

The three TGF-β isoforms share high homology on amino acid level (70-80%, considering mature TGF-β) and bind to the same receptors (TβRI and TβRII). However, the three isoforms have distinct functions. It is unclear if the differences in function are due to the difference in receptor binding affinity or because the isoforms are further regulated by controlled expression in time, place or cell type. Another possibility is that activity can be controlled by differences in activation mechanisms. For instance, TGF-β1 and TGF-β3 can be activated via the interaction with integrin receptors, while TGF-β2 cannot [10]. TGF-β1 is best known for its potent immunoregulatory functions, whereas TGF-β2 and TGF-β3 play key roles during early embryonic development.

From a pharmaceutical point of view, all three TGF-β isoforms have potential therapeutic applications. TGF-β1 maintains immune homeostasis by controlling lymphocyte proliferation, differentiation and survival, but also inhibits the maturation and activation of antigen presenting cells [11, 12]. Also, TGF-β1 plays a key role in the differentiation of regulatory T cells (Tregs), a population of T cells that strongly suppresses immune responses [13]. Thus, TGF-β1 might be used as a remedy for patients with (chronic) inflammatory diseases, like arthritis, inflammatory bowel disease and multiple sclerosis. However, in the presence of the proinflammatory cytokines IL-4 or IL-6, TGF-β1 gives rise to populations of T helper cells that can promote inflammation (Th9 and Th17 cells respectively) [14-16]. TGF-β2 also plays a role in controlling the immune system by

inducing oral tolerance and suppressing immune responses. Next to that, TGF-β2 inhibits growth of intestinal epithelial cells and promotes their differentiation. Therefore TGF-β2 might be effective in treating inflammatory bowel diseases [17]. A disadvantage of TGF-β1 and TGF-β2 is the strong fibrotic response they can elicit. TGF-β3 on the other hand does not induce fibrosis and therefore has a therapeutic application in scar-free wound healing [18].

For large-scale production of recombinant TGF-β a suitable expression system is required. TGF-β has been heterologously expressed in bacterial, insect and mammalian expression systems, however, expression of TGF-β in large quantities seems difficult. TGF-β is improperly folded when using bacterial expression systems and requires chemical refolding. Mammalian expression systems have a low yield and require multi-step purification procedures [19]. In the last two decades, plants have emerged as an alternative expression system for the production of recombinant proteins. As eukaryotes, plants are capable of correctly folding complex proteins and perform post-translational modifications, like N-glycosylation. Plants are relatively cheap compared to other expression systems and are easy to scale-up. One additional advantage for the production of immunoregulatory proteins in plants is that plants do not harbor human pathogens and therefore could be regarded as more safe. Recently, TGF-β3 has been produced in *Nicotiana tabacum* by using a chloroplast expression strategy [20]. A synthetic gene was used for chloroplast transformation and yielded up to 3 mg TGF-β3 per 80 grams of tobacco leaves (37.5 µg/gram leaf). However, because TGF-β3 was expressed in chloroplasts the protein was not folded correctly, as could be expected due to the many cysteine bridges required for the cysteine knot structure in TGF-β. Plant produced TGF-β3 had to be chemically refolded upon purification, thereby loosing the plants economical advantage over bacterial expression systems.

In this study we investigated the possibility of expressing TGF-β1 in *Nicotiana benthamiana* plants that is active without the need for chemical refolding. We show that a furin-like cleavage, which is required for the release of mature TGF-β1, does not occur *in planta*. Mature TGF-β1 could be expressed in plants, but unfortunately this protein lacked activity. Accumulation of LAP-TGF-β1 was enhanced to 140 ng/mg total soluble protein (~2.7 µg/gram leaf) by replacing the signal peptide and co-expression of human furin. Co-expression of LAP-TGF-β1 and furin optimized the post-translational processing of LAP-TGF-β1, enabling the production of biologically active TGF-β1 in plants.

Results

Furin cleavage does not occur in *Nicotiana benthamiana*

As it has been suggested that LAP plays a role in folding of mature TGF-β we first expressed the complete open reading frame of human TGF-β1 in plants. Expression was achieved by agroinfiltration of leaves of *Nicotiana benthamiana* plants and the yield in crude extracts was determined on 2-5 dpi using a sandwich ELISA (Fig. 1a). Crude extracts were analysed with and without acid activation, but this did not influence the obtained yield. Maximum yield was found on 3 dpi, reaching 20 ng TGF-β1/mg TSP.

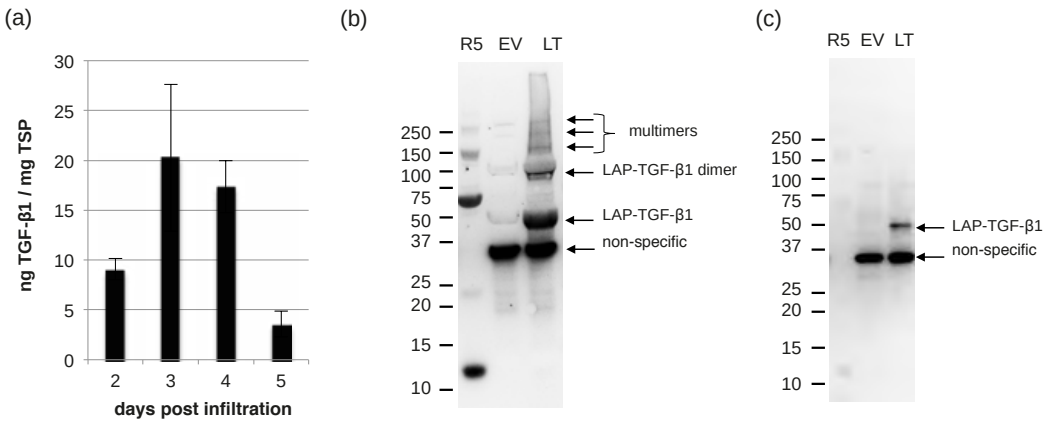

Figure 1 ◆ Analysis of LAP-TGF-β1 expression in *Nicotiana benthamiana*. Native human LAP-TGF-β1 is expressed in *Nicotiana benthamiana* leaves, but proteolytic cleavage between the latency-associated peptide (LAP) and TGF-β1 by a furin-like protease does not occur in plants. (a) Yield of human LAP-TGF-β1 in crude extracts at 2 to 5 days post infiltration (dpi) as determined by ELISA after acid activation (*n*=3, error bars indicate standard error). (b/c) Mature TGF-β specific western blot analysis under reducing conditions of plant produced human LAP-TGF-β1 (LT). As controls, empty vector plant extract (EV) or 5 ng recombinant hTGF-β1 (R5) was used. A molecular weight marker indicates protein size in kDa. Extracts were prepared under neutral pH (b) and at a pH of 3 for acid activation (c).

To investigate the conformation of LAP-TGF-β1 western blot analysis was performed to detect mature TGF-β1. Leaf extracts were prepared under neutral pH conditions or low pH conditions (pH=3) for acid activation of the latent TGF-β1 complex (Figure 1b/c). LAP-TGF-β1 migrated at the expected size for latent LAP-TGF-β1, just below 50 kDa. When extracted under neutral conditions also bands at 100, 150 and several bands >150 kDa were detected, which most likely represent dimers and multimers of LAP-TGF-β1. These multimers were not observed when LAP-TGF-β1 was extracted under acid conditions, which may be due to protein precipitation of large proteins under these conditions. Also a band just below 37 kDa was detected, but this band was also deteced in the empty vector (EV) sample and must therefore be the result of cross-reaction of the TGF-β antibody with

a plant protein. Most importantly, under both neutral and acid conditions mature TGF-β1 with an expected size of ~12.5 kDa was not detected. This indicates that a furin-type cleavage between LAP and TGF-β1 does not occur *in planta*.

Mature TGF-β1 can be expressed without LAP, but results in necrosis

As a furin-like cleavage did not occur *in planta*, TGF-β1 was expressed in the absence of the LAP sequence. A construct was created whereby mature TGF-β1 was fused in frame with its native signal peptide (SP). To investigate whether the signal peptide resulted in adequate uptake into the endoplasmic reticulum (ER), we fused GFP C-terminally to SP-TGF-β1 and followed expression by confocal imaging (Fig. 2a). Plants expressing SP-TGF-β1-GFP at 3 dpi showed fluorescence in the nuclear envelope and the endoplasmic reticulum (ER), indicating that the signal peptide was recognized and that the fusion protein was translocated in the ER.

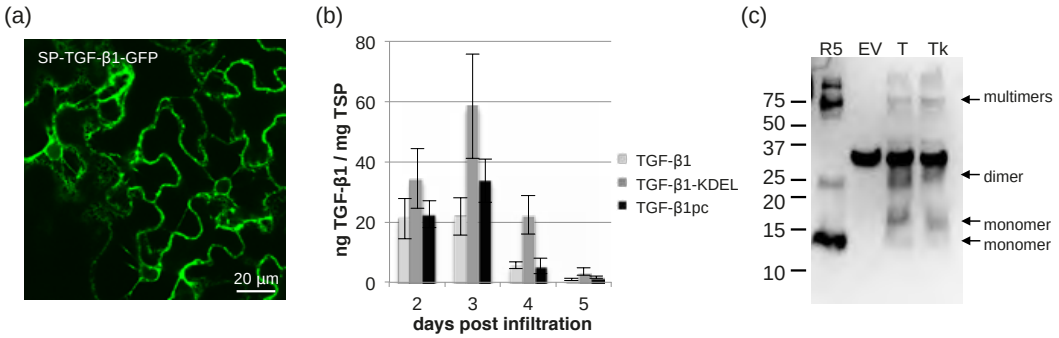

Figure 2 ◆ Analysis of mature TGF-β1 expression in *Nicotiana benthamiana*. (a) Whole mount confocal microscopy output of GFP fused C-terminally to TGF-β1 excluding LAP, but including its native signal peptide (SP). (b) Yield of SP-TGF-β1 with/without C-terminal KDEL sequence and plant codon optimised SP-TGF-β1 in crude extracts at 2 to 5 dpi as determined by ELISA (*n*=3, error bars indicate standard error). (c) Mature TGF-β specific western blot analysis under reducing conditions of plant produced TGF-β1 with/without KDEL (T/Tk). As controls, empty vector plant extract (EV) and 5 ng recombinant hTGF-β1 (R5) were used. A molecular weight marker is indicating size in kDa.

Next, we assessed the effect of different strategies to boost the yield of mature TGF-β1 in plant leaves. Thereto, a C-terminal KDEL sequence to facilitate ER retention was added or codon use was optimized. The yield of mature TGF-β1 constructs in crude extracts was determined on 2-5 dpi using a sandwich ELISA (Fig. 2b). Eventhough the maximum yield of ER-retained TGF-β1 seems slightly higher (up to ~60 ng/mg TSP), no significant differences in maximum yield was observed between TGF-β1 constructs or between mature TGF-β1 constructs and LAP-TGF-β1. The yield of mature TGF-β1 quickly drops after 3 dpi, which could be explained by the observation that mature TGF-β1 induces necrosis in plant leaves (see Figure 3a). Necrosis appeared as early as 3 dpi for the codon

optimised TGF-β1 and reached its maximum for all constructs at 5 dpi. Necrosis was never observed upon expression of LAP-TGF-β1.

When analysing plant extracts by western blot, several bands were detected for mature TGF-β1 with and without KDEL. The bands of 12.5, 25 and >75 corresponded with the bands detected in the sample with recombinant human TGF-β1 (Fig. 2c) and most likely represent monomers, dimers and multimers of TGF-β1. However, a band at 16 kDa was also detected and may represent TGF-β1 with its signal peptide still attached. This would mean that although the signal peptide is recognized and enables protein uptake into the ER, it is not cleaved off upon translocation to the ER.

Fcα-fusion of TGF-β1 enhances yield and prevents necrosis

To increase yield and circumvent improper signal peptide processing we fused TGF-β1 to the C-terminus of a stable partner. The Fc portion of immunoglobulin alpha 1 (Fcα), a natural dimer, was used as a fusion partner allowing dimerization of TGF-β1. This strategy was previously used to express human interleukin-10, which is also active as a dimer [21]. In contrast to mature TGF-β1 constructs, expression of Fcα-TGF-β1 did not result in necrosis in leaves (Figure 3a), even though TGF-β1 yield increased significantly as analyzed in crude extracts at 2-5 dpi (Fig. 3b). Fcα-TGF-β1 yield was ~16-fold higher compared to mature TGF-β1, reaching up to 338 ng TGF-β1/mg TSP on 3 dpi.

Finally, biological activity of Fcα-TGF-β1 in crude plant extracts was assessed in a cell-based assay using mink lung epithelial cells carrying a TGF-β responsive luciferase reporter gene that is activated upon binding to the TGF-β receptor. Unfortunately, Fcα-TGF-β1 was not able to induce luciferase expression in the reporter cell line (Figure 3c). We therefore conclude that Fcα fusion of TGF-β1 aids in stability of the protein, but the fusion protein lacks activity.

Improper signal peptide cleavage of TGF-β1 induces necrosis

To investigate if an alternative signal peptide would improve signal peptide processing and yield, a construct was created where mature TGF-β1 was fused in frame with the signal peptide of an *Arabidopsis thaliana* chitinase gene. The cSP-TGF-β1 construct was used for agroinfiltration and analysed by western blot (Figure 4a). In extracts of transformed leaves with cSP-TGF-β1 a band was detected around ~12.5 kDa corresponding with the size of recombinant TGF-β1. The band of ~16 kDa, which resembles TGF-β1 still harbouring its SP, was not detected We therefore conclude that the *Arabidopsis thaliana* chitinase signal peptide ensures proper processing of mature TGF-β1. Besides the band for monomeric recombinant TGF-β1.

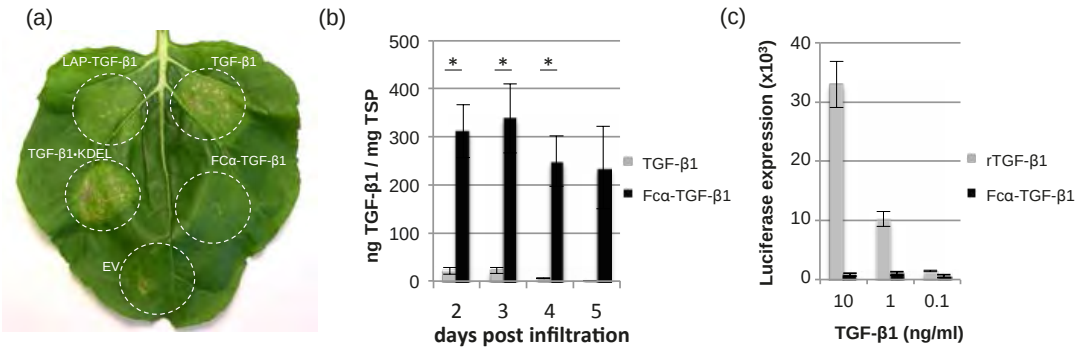

Figure 3 ◆ Analysis of the effect of Fcα-fusion on expression and activity. Necrosis is induced in *Nicotiana benthamiana* leaves upon expression of SP-TGF-β1 and SP-TGF-β1-KDEL, but not when fused to LAP or Fcα. (a) Leaf necrosis on 5 days post infiltration of several TGF-β1 constructs. (b) Yield of SP-TGF-β1 and Fcα-TGF-β1 in crude extracts at 2 to 5 dpi as determined by ELISA (n=3, error bars indicate standard error). Significant differences as determined by a Welch's t-test ($P<0.05$) between samples are indicated with an asterisk. (c) Biological activity of Fcα-TGF-β1 was determined by using MLEC cells containing a TGF-β1-inducible luciferase reporter construct. Cells were treated with recombinant TGF-β1 (rTGF-β1) from mammalian cells or plant-produced Fcα-TGF-β1 and luciferase expression was measured after overnight incubation.

The band of ~16 kDa, which resembles TGF-β1 still harbouring its SP, was not detected We therefore conclude that the *Arabidopsis thaliana* chitinase signal peptide ensures proper processing of mature TGF-β1. Besides the band for monomeric TGF-β1 several other bands representing dimeric and multimeric TGF-β1 were detected as well, whereas bands for recombinant TGF-β1 and TGF-β1pc are very faint. Next to that, cSP-TGF-β1 does not induce necrosis in *Nicotiana benthamiana* leaves from 3 dpi onwards (Figure 4b). We therefore also conclude that the improper processing of the signal peptide was responsible for the necrotic symptoms.

As the cSP-TGF-β1 construct does not induce necrosis we used the silencing inhibitor p19 to further boost TGF-β1 expression. Therefore, the yield of cSP-TGF-β1 was determined in crude extracts at 5 dpi by sandwich ELISA. Figure 4c reveals that the yield of cSP-TGF-β1 can be enhanced significantly by p19 when compared to mature TGF-β1 (P=0.004). This is most likely explained by the lack of necrosis due to replacement of the signal peptide. However, the maximum yield of ~50 ng TGF-β1/mg TSP was not significantly higher as native mature TGF-β1-KDEL at dpi 3 as shown in Figure 2. With a yield of 50 ng/mg TSP only 2.5 ng of TGF-β1 was loaded on gel for western blot analysis, however, the band intensity of cSP-TGF-β1 is much stronger than the 5 ng recombinant TGF-β1. Plant-expressed mature TGF-β1 could be folded incorrectly, thereby explaining the difference in detection between ELISA and western blot.

To test whether plant-produced mature TGF-β1 is active, crude extracts containing TGF-β1 were applied in the TGF-β responsive luciferase reporter assay (Figure 4d). Mature

TGF-β1 from plants was not able to induce luciferase expression in the reporter cell line, whereas recombinant human TGF-β1 was, even in the presence of plant proteins. Thus, replacing the signal peptide of TGF-β1 can prevent leaf necrosis, but this form of plant-produced mature TGF-β1 still lacks biological activity. It is therefore likely that mature TGF-β1 is not folded correctly in plants and might require LAP for proper folding.

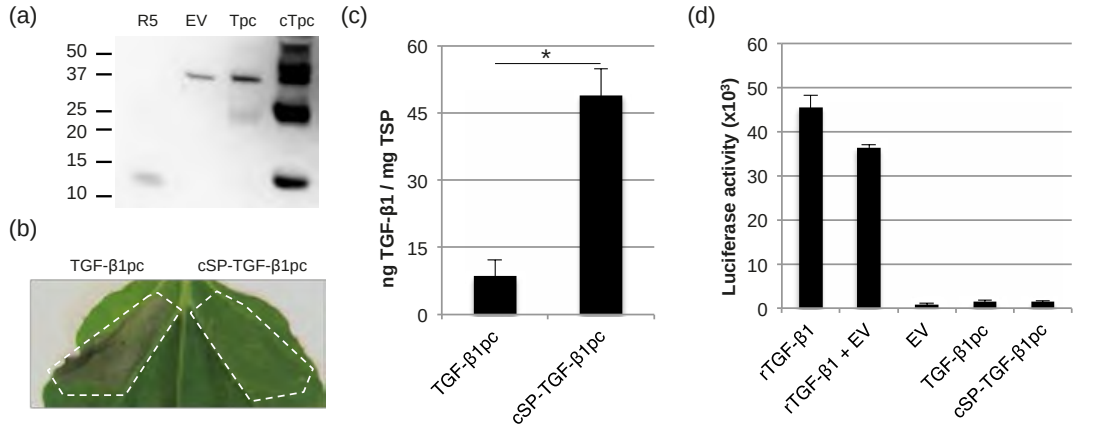

Figure 4 ◆ Analysis of the effect of a plant signal peptide on necrosis. Improper signal peptide cleavage results in necrosis. (a) Mature TGF-β1 specific western blot analysis under reducing conditions of plant produced TGF-β1pc (Tpc) and cSP-TGF-β1pc (cTpc). A molecular weight marker indicates protein size in kDa. As controls, empty vector plant extract (EV) and 5 ng recombinant hTGF-β1 (R5) were used. (b) Leaf necrosis on 5 days post infiltration (dpi) of TGF-β1pc and cSP-TGF-β1pc. (c) Yield of TGF-β1 and cSP-TGF-β1 in crude extracts at 5 dpi upon co-expression of p19 as determined by ELISA (n=3, error bars indicate standard error). (d) Biological activity of recombinant (r)TGF-β1 and plant–produced TGF-β1 constructs (10 ng/ml) as determined by the induction of luciferase expression in MLEC reporter cells.

Expression of biologically active TGF-β1 requires co-expression of furin

As mature TGF-β1 from plants lacks biological activity we further investigated whether furin is required for producing biologically active TGF-β1 in plants. We first replaced the native signal peptide of LAP-TGF-β1 with the *Arabidopsis* chitinase signal peptide (cSP) and analysed the yield of LAP-TGF-β1 at 3, 5 and 7 dpi while co-expressing the p19 silencing suppressor. The expression profile for both LAP-TGF-β1 constructs is given in figure 5a. Replacing the native signal peptide with the chitinase signal peptide significantly increased LAP-TGF-β1 yield 4.5-fold (P=0.002). Next, we investigated the effect of co-expression of human furin. Figure 5b shows that co-expression of furin enhances the yield of both LAP-TGF-β1 constructs. Maximum yield of cSP-LAP-TGF-β1 was ~140 ng TGF-β1/mg TSP, which is 2.7-fold (P=0.084) higher than without co-expression of furin.

Next, we performed a mature TGF-β1 specifc and LAP specific western blot to analyse the post-translational processing of LAP-TGF-β1 by furin. Under non-reducing conditions LAP-TGF-β1 is detected as a band just above 100 kDa with both antibodies, which is the

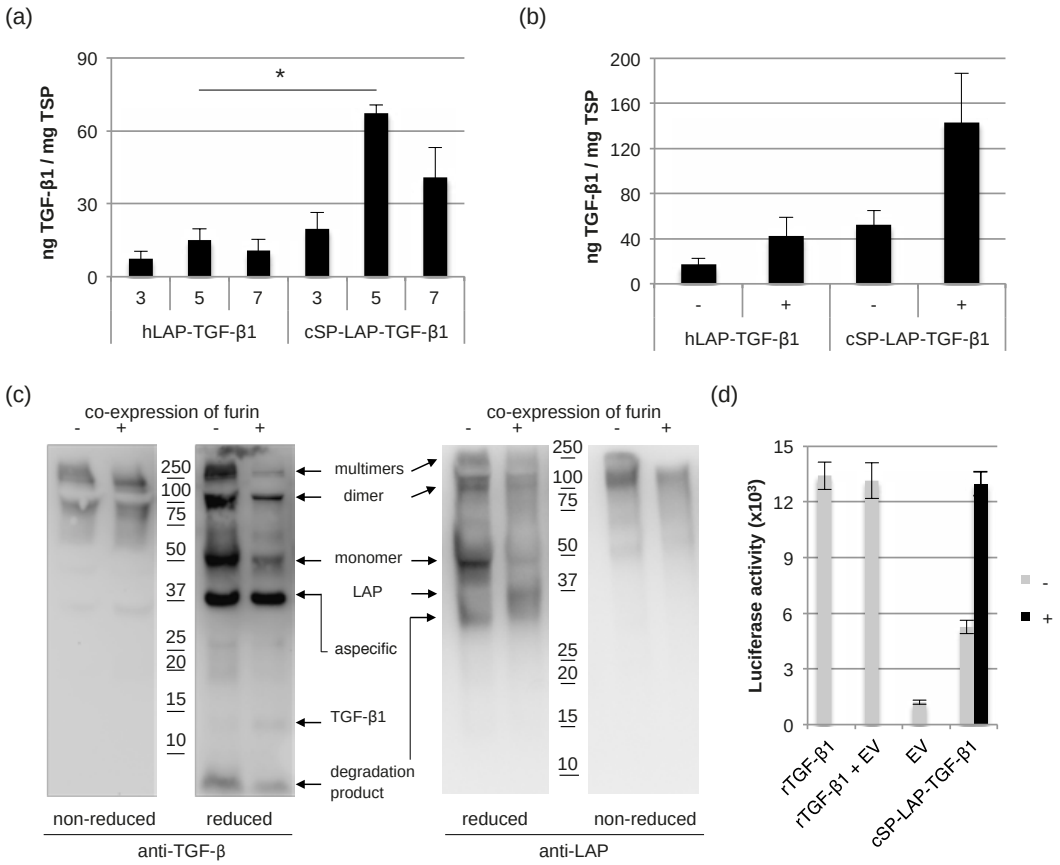

Figure 5 ◆ Expression of biologically active TGF-β1 requires co-expression of furin. (a) Yield of LAP-TGF-β1 and cSP-LAP-TGF-β1 in crude extracts at 3, 5 and 7 days post infiltration (dpi) upon co-expression of p19 as determined by ELISA after acid activation (*n*=3, error bars indicate standard error). (b) Yield of LAP-TGF-β1 constructs in crude extracts at 5 dpi upon co-expression of furin (*n*=3, error bars indicate standard error, +: furin co-expression). Significant differences between samples as determined by a Welch's t-test ($P<0.05$) are indicated with an asterisk. (c) Mature TGF-β1 and LAP specific western blot analysis under non-reducing and reducing conditions of LAP-TGF-β1. (d) Biological activity of recombinant (r)TGF-β1 and acid activated plant–produced LAP-TGF-β1 constructs (5 ng/ml) as determined by the induction of luciferase expression in MLEC reporter cells (+: furin co-expression).

expected size for the latent LAP-TGF-β1 homodimer (Figure 5c; first and fourth panel, respectively)). Multimers were detected as well, but no differences were observed upon co-expression of furin. Under reducing conditions LAP-TGF-β1 was detected as a monomeric band of approximately 50 kDa with the TGF-β antibody (Figure 5c, second

panel). However, the intensity of this band is strongly reduced upon co-expression of furin. The western blot probed with anti-LAP also shows this reduction in intensity for the LAP-TGF-β1 monomer (Figure 5c, third panel). Also, a band around 12,5 kDa, the size of monomeric TGF-β1 appears upon co-expression of furin (Figure 5c, second panel). These facts suggest that LAP-TGF-β1 is processed correctly by co-expressed furin. Properly processed LAP is approximately 37 kDa and a band of this size was detected under reducing conditions. However, the anti-LAP blot also reveals a degradation product of LAP of approximately 30 kDa in both samples. Therefore, LAP-TGF-β1 seems to be processed by endogenous proteases in plants as well.

To evaluate the biological activity of LAP-TGF-β1 we applied acid activated crude extracts to mink lung epithelial cells carrying the TGF-β1-responsive luciferase reporter construct. Figure 5d shows that some active TGF-β1 can be extracted from leaves without co-expression of furin. This is most likely due to the proteolytic processing by endogenous plant proteases. However, activity of LAP-TGF-β1 is comparable to recombinant TGF-β1 only when furin is co-expressed. Co-expression of furin is therefore required to produce fully active TGF-β1 in plants without the need for chemical refolding.

Discussion

Here we show that expression of biologically active TGF-β without the requirement of chemical refolding is feasible in plants. Previously, TGF-β3 was successfully produced in *Nicotiana tabacum* plants by targeting expression to the chloroplasts [20] and yielded considerable amounts of TGF-β3 (37.5 µg/gFW and 80% purity). This strategy, however, required chemical refolding of purified TGF-β3 to obtain biological activity. Therefore chloroplast expression, as a plant-based expression system, looses one of its advantages over bacterial expression systems, namely cost-effectiveness. When we studied the transient expression of the whole open reading frame of the TGF-β1 gene in *Nicotiana benthamiana* plants the obtained yield of TGF-β1 was ~20 ng/mg TSP. This yield was considerably lower compared to many other proteins heterologously expressed in plants, like antibodies or other cytokines [21, 22]. More importantly, we revealed that a furin-like cleavage between LAP and TGF-β1 does not occur in *Nicotiana benthamiana* plants. This furin-like cleavage is required to release active TGF-β1 from the latent complex. Furin is a mammalian subtilisin/kex2p-like endoprotease. Although a kex2p-like pathway was shown to exist in *N. tabacum* [23], no furin cleavage of LAP-TGF-β1 was observed in our expression system. Hence, it is likely that a protease with the right specificity does not exist in *N. benthamiana*. The lack of furin cleavage might be a crucial factor that limits the yield of TGF-β1 in plants.

To circumvent the posttranslational processing of LAP-TGF-β1 we expressed mature TGF-β1 as an in frame fusion with its native signal peptide. We confirmed that the signal peptide of TGF-β1 is functional by monitoring localization of a GFP fusion protein with confocal imaging, as TGF-β1 is taken up into the secretory pathway. However, after translocation into the ER, the signal peptide is not completely removed from the mature protein. When the signal peptide stays attached to mature TGF-β1 it could compromise the function of the plant ER. The unprocessed signal peptide could act as membrane anchor [24], thereby facilitating accumulation of unprocessed TGF-β1 in the ER. On the other hand, the signal peptide could also affect the folding of TGF-β1 and trigger the unfolded protein response. Disturbance of ER function could ultimately lead to necrosis [25]. This disturbance of ER function may explain the necrosis that we observed upon expression of mature TGF-β1.

Replacing the signal peptide with an *Arabidopsis thaliana* chitinase signal peptide circumvents improper processing of the TGF-β1 signal peptide, prevented the induction of necrosis and increased yield of mature TGF-β1. Surprisingly, signal peptide replacement with the chitinase signal peptide also significantly increased the yield of LAP-TGF-β1. The chitinase signal peptide may also influence expression by changing the mRNA secondary structure at the 5′-end. The secondary structure of the 5′ UTR sequence containing the *Alfalfa mosaic virus* RNA 4 (AlMV) leader and the first 40 nucleotides of LAP-TGF-β1 was predicted by the Vienna RNA fold software [26]. In Figure S1 drawings of the minimum free energy predictions for both LAP-TGF-β1 genes are given. This prediction reveals that the combination of the AIMV leader with the chitinase signal peptide increases the minimal free folding energy 6.5-fold, making the secondary structure less stable. Furthermore, strong GC-rich secondary structures are present downstream of the start codon in the native signal peptide. As low minimal free folding energy has been suggested to enhance translation initiation [27, 28] these observed differences could explain differences in yield.

Even though the yield was improved, a major bottleneck for accumulation of mature TGF-β1 seems to be low stability or misfolding of the protein. Fusion of TGF-β1with a stable partner, like Fcα, increased the yield 16-fold. Although the fusion with Fcα increased yield it still did not result in active TGF-β1. The observation that plant-produced mature TGF-β1 or Fcα-TGF-β1 are inactive, is therefore most likely explained by misfolding of TGF-β1 in the absence of LAP. This idea is further supported by the fact that we observed a strong difference in detection of mature TGF-β1 by ELISA and western blot. Misfolded TGF-β1 is likely not detected properly in a sandwich ELISA, but might be detected by western blot under reducing conditions as continuous epitopes become available. This could also explain why we did not obtain a higher yield for mature TGF-β1 upon co-expression of p19. Proper folding of biologically active TGF-β1 likely requires expression of the full LAP-TGF-β1 gene.

Post-translational modification of LAP-TGF-β1 is a complex process, which is controlled at multiple levels. The secretion of biologically active TGF-β1 dimers first of all requires the dimerization of the LAP-TGF-β1 proprotein, which occurs in the endoplasmic reticulum [29]. LAP-TGF-β1 is N-glycosylated at three residues (82, 136 and 176) of which the first two N-glycans contain mannose-6-phosphate [30]. Furthermore, the presence and early stage remodeling of the N-glycans on residues Asn82 and Asn136 were shown to be required for proper secretion of LAP-TGF-β1 [31, 32]. Yet, secretion of latent TGF-β1 is a slow process as LAP-TGF-β1 is retained within the *cis*-Golgi in an Endo H-sensitive form [33]. *Cis*-Golgi retention of LAP-TGF-β1 is presumed to be caused by its capture by a sequestering protein, such as the chaperone GRP78 [34]. Retention of LAP-TGF-β1 in the ER/cis-Golgi is the limiting step for secretion and furin processing [34]. Only properly glycosylated LAP-TGF-β1 is transported to the *trans*-Golgi where it is processed by a furin convertase [4]. Within our study we co-expressed human furin with LAP-TGF-β1 to investigate the proper proteolytic processing of LAP and TGF-β1 in plants. First of all, we observed that co-expression of furin increased the yield of LAP-TGF-β1 by 2.7-fold. We also observed that the majority of extracted LAP-TGF-β1 is processed by co-expressed furin. Furthermore, we analyzed oligomannose enrichment of the N-glycans on LAP-TGF-β1 and only observed a small fraction of Endo H-sensitive LAP-TGF-β1 (data not shown). This would explain why not all LAP-TGF-β1 is processed by furin in the *trans*-Golgi, because oligomannose-enriched LAP-TGF-β1 is retained in the ER or *cis*-Golgi. Nevertheless, engineering the post-translational pathways by co-expressing furin enabled the production of biologically active TGF-β1 in plants.

Our study demonstrates that the production of biologically active TGF-β1 in plants is feasible without the need for chemical refolding. Thereby we avoid difficult and expensive chemical refolding steps, which are required upon bacterial or chloroplast expression. We also show that the post-translational machinery of plants can be engineered to allow proteolytic processing of heterologous expressed mammalian proteins. Therefore, this study highlights the fact that plants are a suitable expression platform for the production of complex glycoproteins, like TGF-β1, that rely on correct cellular targeting and post-translational processing for biological activity.

Experimental procedures

Construct design

The complete native open reading frame (ORF) of human (h)LAP-TGF-β1 and furin were amplified from the MegaMan™ Human Transcriptome cDNA library (Stratagene) Similarly, mouse LAP-TGF-β1 was amplified from the FirstChoice™ PCR-Ready Mouse Spleen cDNA library (Ambion). To remove LAP from the mature ORF, mature hTGF-β1 was reamplified whereby a SacII restriction site was introduced at the 5′ end. This SacII was used to clone mature human TGF-β1 in frame with the mouse signal peptide, as SacII was uniquely present in the mouse (and not human) LAP-TGF-β1 signal peptide. Thereafter, SP-TGF-β1 was reamplified to introduce the ER retention signal KDEL at the 3′ end of the gene.

To create a GFP fusion of hTGF-β1, the enhanced green fluorescent protein (eGFP) gene was re-amplified and used to replace the mature hIL-10 sequence in the previously published Fcα-IL-10 construct [21] using SpeI/KpnI. Similarly, hTGF-β1 was reamplified and used to replace Fcα in the same Fcα-hIL-10 construct using NcoI/SacI. In this way, a SP-TGF-β1-GFP construct was created where a glycine-serine linker separated hTGF-β1 and GFP. To create a Fcα-fusion of hTGF-β1, mature hTGF-β1 (SpeI/KpnI) was reamplified and used to replace the mature hIL-10 sequence in the previously mentioned Fcα-IL-10 construct.

The mature TGF-β1 sequence was codon optimized using an in-house optimization procedure and ordered at GeneArt (Invitrogen). The codon optimized TGF-β1 gene was cloned in frame with the *Arabidopsis* chitinase signal peptide (cSP) by means of overlap-extension PCR. Similarly, the mature sequence for native LAP-TGF-β1 sequence was cloned in frame with cSP.

All construct sequences were confirmed by sequencing (Macrogen) in the expression vector pHYG [21]. In pHYG, expression is controlled by the 35S promoter of the *Cauliflower mosaic virus* with duplicated enhancer (d35S) and the *Agrobacterium tumefaciens* nopaline synthase transcription terminator (Tnos). A 5′ leader sequence of the *Alfalfa mosaic virus* RNA 4 (AlMV) is included between the promoter and construct to boost translation. The expression vectors were subsequently transformed to *Agrobacterium tumefaciens* strain MOG101 for plant expression. In some experiments the silencing suppressor p19 from tomato bushy stunt virus was co-infilitrated to enhance heterologous expression. The vector pBIN61-p19 was obtained from Dr. D. Baulcombe [35].

Agroinfiltration of *Nicotiana benthamiana*

Agrobacterium tumefaciens clones were cultured for 16 hours at 28°C/250 rpm in LB medium (10g/l pepton140, 5g/l yeast extract, 10g/l NaCl with pH=7.0) containing 50 µg/ml kanamycin, 20 µg/ml rifampicin and 20µM acetosyringone. The bacteria were resuspended in MMA infiltration medium (20g/l sucrose, 5g/l MS-salts, 1.95g/l MES, pH5.6) containing 200 µM acetosyringone to obtain an OD of 1. For co-infiltration experiments a final OD of 0.5 of each individual culture was used. After 1-2 hours incubation at room temperature, the two youngest fully expanded leaves of 5-6 weeks old *Nicotiana benthamiana* plants were infiltrated completely.

Total soluble protein extraction

Leaves were immediately snap-frozen upon harvesting and homogenized in liquid nitrogen. Homogenized plant material was ground in ice-cold extraction buffer (50mM phosphate-buffered saline (PBS) pH=7.4, 100 mM NaCl, 0.1% v/v Tween-20 and 2% w/v immobilized polyvinylpolypyrrolidone (PVPP)) using 2ml/g fresh weight. For extraction at low pH a 30 mM sodium citrate buffer (30 mM sodium citrate buffer pH=3, 100 mM NaCl, 0.1% v/v Tween-20 and 2% w/v PVPP) was used. Crude extracts were clarified by centrifugation at 16.000 rpm for 5 min at 4°C and supernatants were directly used in an ELISA and BCA protein assay. For biological activity assays, above-mentioned protein extraction would be followed by desalting using a G25 Sephadex column and filter sterilization (0.22 µm; Millipore Corporation).

Quantification of human TGF-β1 protein levels

TGF-β1 protein concentration in crude plant extracts was determined by ELISA. Samples containing LAP-TGF-β1 were activated by the addition of 1M hydrochloric acid (10 µl acid/50 µl sample) and subsequently neutralized after 10 min by adding the same volume of 1M sodium hydroxide. Human TGF-β1 Ready-SET-Go!® ELISA kits (eBioscience) were used according to suppliers protocol. For sample comparison the total soluble protein (TSP) content was determined by the BCA method (Pierce) according to supplier's protocol using bovine serum albumin (BSA) as a standard.

Protein analysis by western blot

Soluble plant proteins (50 µg) were separated under reducing or non-reducing conditions by SDS-PAGE on a 12% Bis-Tris gel. Recombinant human TGF-β1 (R&D Systems) was used as a control. Proteins were transferred to a PVDF membrane (Invitrogen) by a wet blotting procedure. Thereafter the membrane was blocked in PBST-BL (PBS containing 0.1% v/v Tween-20 and 5% w/v non-fat dry milk powder) for 1 hour at room temperature, followed by overnight incubation with a rabbit anti-TGF-β monoclonal antibody (Cell Signaling Technology) or a goat anti-LAP polyclonal antibody (R&D Systems) in PBST

(including 0.1% w/v bovine serum albumin) at 4°C. HRP conjugated secondary antibodies (Jackson ImmunoResearch) were used for visualization. Finally, the SuperSignal West Femto substrate (Pierce) was used to detect the HRP-conjugated antibodies.

Confocal microscopy

Plants were agroinfiltrated with *A. tumefaciens* harbouring the pHYG vector containing the expression cassette encoding N-terminal fusions of human TGF-β1 to GFP as described previously. Leaves were taken from the plant at 3 days post infiltration and small sections were examined from the abaxial side using a Zeiss LSM510 confocal laser-scanning microscope in combination with an argon ion laser supplying a 488 nm wavelength.

Biological activity assay

The mink lung epithelial cell line with TGF-β inducible luciferase reporter construct [36] was kindly provided by Dr. C. Arancibia (Oxford University). MLEC cells were maintained at 37°C with 5% CO_2 in RPMI-1640 medium containing 4 mM L-glutamine, 25 mM HEPES and supplemented with 10% fetal calf serum, 50 U/ml penicillin, 50 µg/ml streptomycin and 200 µg/ml G418. MLEC cells were harvested by trypsinisation and seeded at a density of $1.5x10^6$ cells/ml in 96 well plates and were allowed to rest for 4 hours in medium without G418 prior to bioassays. For bioassays cells were treated with 0.1-10 ng/ml plant produced TGF-β1 (acid activated) or recombinant human TGF-β1 expressed in Chinese hamster ovary cells (R&D Systems). Recombinant TGF-β1 was supplemented with EV plant extract to keep plant protein levels equal. After overnight incubation luciferase expression was analysed using the Bright-Glo™ Luciferase assay system (Promega) according to the supplier's protocol.

Data analysis

All expression data shown in the figures indicate the average of at least three biological replicates (*n*). In the figure legends *n* is indicated and error bars indicate standard error. Significant differences between samples were calculated using the Welch's t-test and regarded as significant when $P<0.05$. Significant differences are indicated in the figures by an asterisk (*).

Acknowledgements

This study was financially supported in part by Synthon (Nijmegen, The Netherlands). We would like to thank Gerry Ariaans for all helpful discussions and Mohamed Abdi Hassan, Sophie van Gorkom, Kelly Heckman, Tram Hong, Xandra Schrama, Koen Verhees, Tineke Vliek and Michelle Yang for their input in the practical work of this study.

Supplemental figure

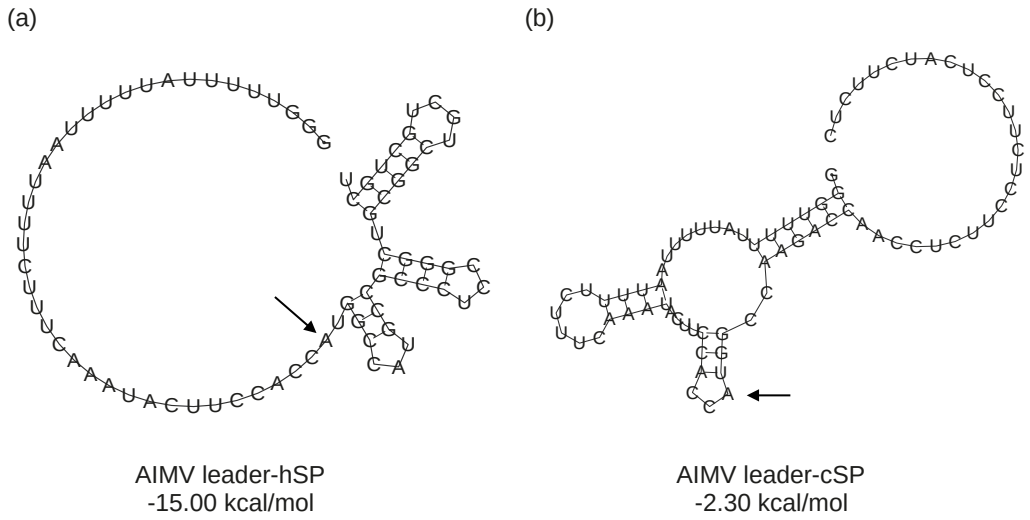

Figure S1 ◆ mRNA structure prediction of the 5′ end of LAP-TGF-β1 genes. Secondary mRNA structure prediction of the 5′ UTR sequence containing the *Alfalfa mosaic virus* RNA 4 (AlMV) leader and the first 40 nucleotides of the LAP-TGF-β1 genes by the Vienna RNA fold software. Drawings of the minimum free energy prediction and the free energy are given for the signal peptides of native LAP-TGF-β1 (a) and cSP-LAP-TGF-β1 (b) where the native signal peptide was replaced with the signal peptide of the *Arabidopsis* chitinase gene (cSP). Arrows indicate the adenine nucleotide of the ATG start codon.

References

1. Blobe GC, Schiemann WP and Lodish HF (2000) Mechanisms of disease: Role of transforming growth factor beta in human disease. New England Journal of Medicine 342: 1350-1358.

2. Li MO, Wan YY, Sanjabi S, Robertson AKL and Flavell RA (2006) Transforming growth factor-beta regulation of immune responses. Annual Review of Immunology 24: 99-146.

3. Govinden R and Bhoola KD (2003) Genealogy, expression, and cellular function of transforming growth factor-beta. Pharmacology and Therapeutics 98: 257-265.

4. Dubois CM, Laprise MH, Blanchette F, Gentry LE and Leduc R (1995) Processing of Transforming Growth-Factor-Beta-1 Precursor by Human Furin Convertase. Journal of Biological Chemistry 270: 10618-10624.

5. Annes JP, Munger JS and Rifkin DB (2003) Making sense of latent TGFbeta activation. Journal of Cell Science 116: 217-224.

6. Archer SJ, Bax A, Roberts AB, Sporn MB, Ogawa Y, et al. (1993) Transforming Growth Factor-Beta-1 - Secondary Structure as Determined by Heteronuclear Magnetic-Resonance Spectroscopy. Biochemistry-Us 32: 1164-1171.

7. Daopin S, Piez KA, Ogawa Y and Davies DR (1992) Crystal-Structure of Transforming Growth-Factor-Beta-2 - an Unusual Fold for the Superfamily. Science 257: 369-373.

8. Schlunegger MP and Grutter MG (1992) An Unusual Feature Revealed by the Crystal-Structure at 2.2-Angstrom Resolution of Human Transforming Growth-Factor-Beta-2. Nature 358: 430-434.

9. Lin SJ, Lerch TF, Cook RW, Jardetzky TS and Woodruff TK (2006) The structural basis of TGF-beta, bone morphogenetic protein, and activin ligand binding. Reproduction 132: 179-190.

10. Ludbrook SB, Barry ST, Delves CJ and Horgan CMT (2003) The integrin alpha(v)beta(3) is a receptor for the latency-associated peptides of transforming growth factors beta(1) and beta(3). Biochemistry Journal 369: 311-318.

11. Takeuchi M, Alard P and Streilein JW (1998) TGF-beta promotes immune deviation by altering accessory signals of antigen-presenting cells. Journal of Immunology 160: 1589-1597.

12. Geissmann F, Revy P, Regnault A, Lepelletier Y, Dy M, et al. (1999) TGF-beta 1 prevents the noncognate maturation of human dendritic Langerhans cells. Journal of Immunology 162: 4567-4575.

13. Chen WJ, Jin WW, Hardegen N, Lei KJ, Li L, et al. (2003) Conversion of peripheral CD4(+)CD25(-) naive T cells to CD4(+)CD25(+) regulatory T cells by TGF-beta induction of transcription factor Foxp3. Journal of Experimental Medicine 198: 1875-1886.

14. Veldhoen M, Hocking RJ, Atkins CJ, Locksley RM and Stockinger B (2006) TGF beta in the context of an inflammatory cytokine milieu supports de novo differentiation of IL-17-producing T cells. Immunity 24: 179-189.

15. Veldhoen M, Uyttenhove C, van Snick J, Helmby H, Westendorf A, et al. (2008) Transforming growth factor-beta 'reprograms' the differentiation of T helper 2 cells and promotes an interleukin 9-producing subset. Nature Immunology 9: 1341-1346.

16. Dardalhon V, Awasthi A, Kwon H, Galileos G, Gao W, et al. (2008) IL-4 inhibits TGF-beta-induced Foxp3(+) T cells and, together with TGF-beta, generates IL-9(+) IL-10(+) Foxp3(-) effector T cells. Nature Immunology 9: 1347-1355.

17. Oz HS, Ray M, Chen TS and McClain CJ (2004) Efficacy of a transforming growth factor 82 containing nutritional support formula in a murine model of inflammatory bowel disease. The Journal of the American College Nutrition 23: 220-226.

18. O'Kane S and Ferguson MWJ (1997) Transforming Growth Factor beta s and wound healing. International Journal of Biochemistry and Cell Biology 29: 63-78.

19. Zou ZC and Sun PD (2006) An improved recombinant mammalian cell expression system for human transforming growth factor-beta 2 and -beta 3 preparations. Protein Expression and Purification 50: 9-17.

20. Gisby MF, Mellors P, Madesis P, Ellin M, Laverty H, et al. (2011) A synthetic gene increases TGF beta 3 accumulation by 75-fold in tobacco chloroplasts enabling rapid purification and folding into a biologically active molecule. Plant Biotechnology Journal 9: 618-628.

21. Westerhof LB, Wilbers RHP, Roosien J, van de Velde J, Goverse A, et al. (2012) 3D Domain Swapping Causes Extensive Multimerisation of Human Interleukin-10 When Expressed In Planta. Plos One 7 (10): e46460.

22. Westerhof LB, Wilbers RHP, van Raaij DR, Nguyen DL, Goverse A, et al. (2014) Monomeric IgA can be produced in planta as efficient as IgG, yet receives different N-glycans. Plant Biotechnology Journal.

23. Kinal H, Park CM, Berry JO, Koltin Y and Bruenn JA (1995) Processing and Secretion of a Virally Encoded Antifungal Toxin in Transgenic Tobacco Plants - Evidence for a Kex2p Pathway in Plants. Plant Cell 7: 677-688.

24. High S and Dobberstein B (1992) Mechanisms that determine the transmembrane disposition of proteins. Current Opinion in Cell Biology 4: 581-586.

25. Ye CM, Dickman MB, Whitham SA, Payton M and Verchot J (2011) The Unfolded Protein Response Is Triggered by a Plant Viral Movement Protein. Plant Physiology 156: 741-755.

26. Lorenz R, Bernhart SH, Honer Zu Siederdissen C, Tafer H, Flamm C, et al. (2011) ViennaRNA Package 2.0. Algorithms for molecular biology : AMB 6: 26.

27. Tuller T, Waldman YY, Kupiec M and Ruppin E (2010) Translation efficiency is determined by both codon bias and folding energy. Proceedings of the National Academy of Sciences 107: 3645-3650.

28. Hall MN, Gabay J, Debarbouille M and Schwartz M (1982) A role for mRNA secondary structure in the control of translation initiation. Nature 295: 616-618.

29. Gray AM and Mason AJ (1990) Requirement for Activin-a and Transforming Growth Factor-Beta-1 Pro-Regions in Homodimer Assembly. Science 247: 1328-1330.

30. Purchio AF, Cooper JA, Brunner AM, Lioubin MN, Gentry LE, et al. (1988) Identification of Mannose 6-Phosphate in 2 Asparagine-Linked Sugar Chains of Recombinant Transforming Growth Factor-Beta-1 Precursor. Journal of Biological Chemistry 263: 14211-14215.

31. Brunner AM, Lioubin MN, Marquardt H, Malacko AR, Wang WC, et al. (1992) Site-Directed Mutagenesis of Glycosylation Sites in the Transforming Growth Factor-Beta-1 (Tgf-Beta-1) and Tgf-Beta-2 (414) Precursors and of Cysteine Residues within Mature Tgf-Beta-1 - Effects on Secretion and Bioactivity. Molecular Endocrinology 6: 1691-1700.

32. Sha X, Brunner AM, Purchio AF and Gentry LE (1989) Transforming Growth-Factor Beta-1 - Importance of Glycosylation and Acidic Proteases for Processing and Secretion. Molecular Endocrinology 3: 1090-1098.

33. Miyazono K, Thyberg J and Heldin CH (1992) Retention of the transforming growth factor-beta 1 precursor in the Golgi complex in a latent endoglycosidase H-sensitive form. Journal of Biological Chemistry 267: 5668-5675.

34. Oida T and Weiner HL (2010) Overexpression of TGF-beta(1) Gene Induces Cell Surface Localized Glucose-Regulated Protein 78-Associated Latency-Associated Peptide/TGF-beta. Journal of Immunology 185: 3529-3535.

35. Voinnet O, Rivas S, Mestre P and Baulcombe D (2003) An enhanced transient expression system in plants based on suppression of gene silencing by the p19 protein of tomato bushy stunt virus. Plant Journal 33: 949-956.

36. Abe M, Harpel JG, Metz CN, Nunes I, Loskutoff DJ, et al. (1994) An Assay for Transforming Growth-Factor-Beta Using Cells Transfected with a Plasminogen-Activator Inhibitor-1 Promoter Luciferase Construct. Analytical Biochemistry 216: 276-284.

Chapter 3

3D domain swapping causes extensive multimerisation of human interleukin-10 when expressed *in planta*

Lotte B. Westerhof*, Ruud H. P. Wilbers*, Jan Roosien, Jan van de Velde, Aska Goverse, Jaap Bakker and Arjen Schots

* Equal contribution

This work has been published in:
PlosOne 7 (10), 2012; doi:10.1371/journal.pone.0046460

Abstract

Heterologous expression platforms of biopharmaceutical proteins have been significantly improved over the last decade. Further improvement can be established by examining the intrinsic properties of proteins. Interleukin-10 (IL-10) is an anti-inflammatory cytokine with a short half-life that plays an important role in re-establishing immune homeostasis. This homodimeric protein of 36 kDa has significant therapeutic potential to treat inflammatory and autoimmune diseases. In this study we show that the major production bottleneck of human IL-10 is not protein instability as previously suggested, but extensive multimerisation due to its intrinsic 3D domain swapping characteristic. Extensive multimerisation of human IL-10 could be visualised as granules *in planta*. On the other hand, mouse IL-10 hardly multimerised, which could be largely attributed to its N-glycosylation. By introducing a short glycine-serine-linker between the fourth and fifth alpha helix of human IL-10 a stable monomeric form of IL-10 (hIL-10^{mono}) was created that no longer multimerised and increased yield up to 20-fold. However, hIL-10^{mono} no longer had the ability to reduce pro-inflammatory cytokine secretion from lipopolysaccharide-stimulated macrophages. Forcing dimerisation restored biological activity. This was achieved by fusing human IL-10^{mono} to the C-terminal end of constant domains 2 and 3 of human immunoglobulin A (Fcα), a natural dimer. Stable dimeric forms of IL-10, like Fcα-IL-10, may not only be a better format for improved production, but also a more suitable format for medical application.

Introduction

Recombinant DNA technology has revolutionised the production and application of pharmaceutical proteins. Current heterologous production hosts include bacteria, yeasts, insect and mammalian cells, and, more recently, plants. Most expression systems have been rapidly improved in terms of yield and cost efficiency in the last decades. However, these advances have mainly been achieved with antibodies and hormones, which are relatively stable proteins. Recently more attention in optimising the production of biopharmaceutical proteins is directed to their intrinsic properties that result of post-translational modifications and folding processes. Improved insight in these processes may increase the yield of still poorly expressed proteins.

Many cytokines have a promising therapeutic potential. However, several cytokine families show a short half-life *in vivo* and are poorly expressed in heterologous hosts. Human interleukin-10 (IL-10) is such a cytokine that may be used for treatment of many inflammatory and autoimmune diseases due to its immunosuppressive properties [1,2]. Generally, IL-10 facilitates the return of the immune system to homeostasis after clearance of antigen and plays an important role in conferring oral tolerance. It exerts its function through reduction of the activity of macrophages, inhibition of antigen presentation by dendritic cells and inhibition of the production of pro-inflammatory cytokines by antigen presenting cells and T lymphocytes [3-6]. The human IL-10 gene encodes a 178 amino acid protein including a N-terminal signal peptide for secretion. An IL-10 monomer consists of six alpha helices (A-F) with two internal disulphide bridges (Cys30-Cys126 and Cys80-Cys132). Two monomers are stabilised into a biologically active dimer by exchanging their C-terminal domains composed of the helices E and F, a process called 3D domain swapping [7-9].

Human interleukin-10 has previously been produced in bacterial systems for medical purposes [10,11], and in insect and mammalian cells for research purposes. The use of plants as a production platform for IL-10 provides a cheap alternative compared to bacterial, insect and mammalian expression systems. As plants are eukaryotes they can correctly fold and assemble proteins, and are able to perform complex post-translational processes, such as N-glycosylation. Plants as production hosts for IL-10 offer an extra advantage as they have a low risk of contamination with human pathogens, especially relevant when producing immunosuppressive molecules for medical application. Human IL-10 was produced for the first time *in planta* by stable transformation of a low-alkaloid *Nicotiana tabacum* variety [12]. High transcript levels were contrasted by low protein levels with a maximum of 0.000069% of total soluble protein (TSP). Biological activity of plant-derived human IL-10 was shown *in vitro* and *in vivo* without the need for purification [12,13]. Yield could be increased to 0.55% of TSP by transient expression of human IL-10 fused to an elastin-like polypeptide combined with retention in the

endoplasmic reticulum (ER), but biological activity was not confirmed [14]. From these experiments it was concluded that protein instability is a major bottleneck for human IL-10 production.

We show that 3D domain swapping is an important bottleneck for human IL-10 production in *Nicotiana benthamiana*. Human IL-10 multimerises extensively as was visualised *in situ* using GFP fusions. Domain swapping could be prevented by engineering a stable monomer [15] that regained biological activity through fusion to the Fc portion of IgA, a natural dimer. Identification of this expression bottleneck enabled us to increase yield considerably to levels that approach the economic threshold.

Results

Yield of mouse IL-10 is significantly higher compared to human IL-10

To determine the maximum yield of human (h) and mouse (m) IL-10 in a transient expression system, leaves of 5-6 weeks-old *Nicotiana benthamiana* plants were agro-infiltrated. The expression vector contained the complete native coding sequence of the human or mouse IL-10 gene with or without a 3' tag coding for a thrombin cleavage site, a 6xHis-tag and the ER retention sequence KDEL (thk) (Figure 1a). Adequate transcription of the constructs was confirmed two and three days post infiltration (dpi) through determination of mRNA levels by means of quantitative PCR. Similar relative transcription levels (around 1000 transcripts of IL-10 per β-actin transcript) were found for all four constructs on both days (Figure 1b). Human and mouse IL-10 yield was determined on 1-6 dpi using a sandwich ELISA (Figure 1c and 1d). Maximum human and mouse IL-10 yield was obtained between 2-4 dpi. Although maximum yields were similar for native and ER-retained IL-10, expression levels of ER-retained IL-10 remained higher over time. Considering average yields from 2 to 5 dpi showed that ER-retained IL-10 resulted in 11 and 10-fold more protein for human and mouse IL-10 respectively. More striking was the observation that even though mRNA transcript levels were comparable, mouse IL-10 yield was significantly higher when compared to human IL-10 (P=0.043), regardless of ER-retention (P=0.003). The average yield of mIL-10 was 19 and 17-fold higher for secreted and ER-retained IL-10 respectively. Retention of a protein in the ER can lead to increased yield due to the presence of chaperones that assist protein folding and the absence of many proteases explaining reduced degradation over time [16]. However, as the difference in expression level between human and mouse IL-10 was significant despite ER-retention another factor than protein degradation supposedly influences yield.

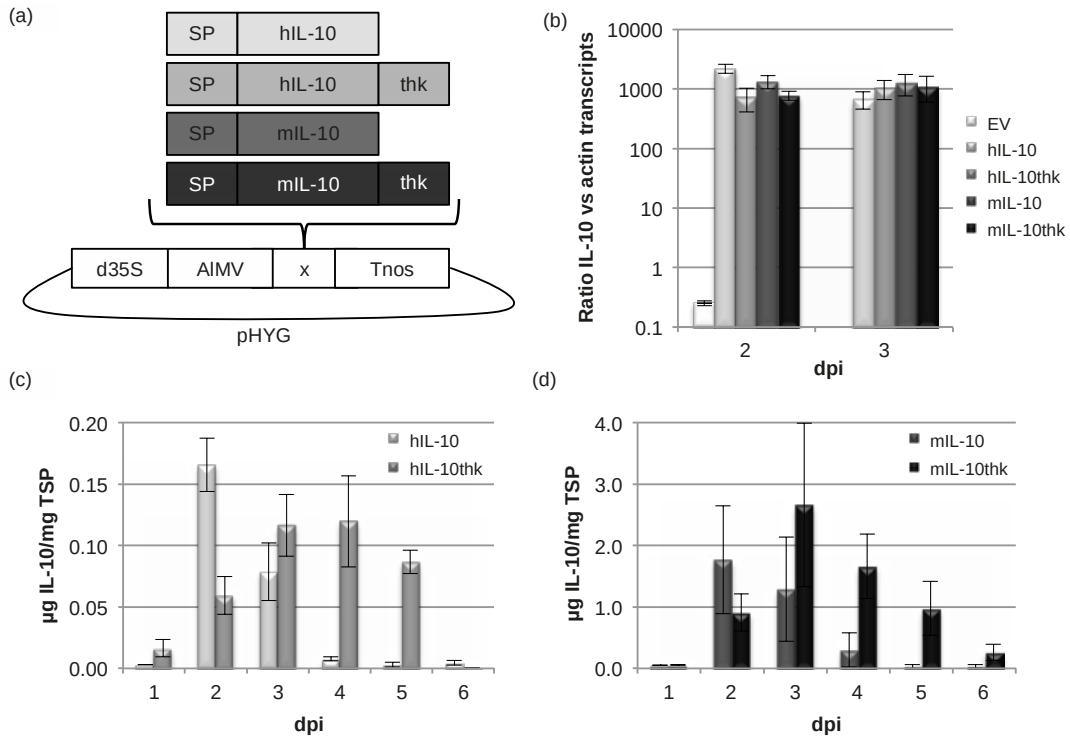

Figure 1 ◆ Expression data of human and mouse IL-10 in transiently transformed *Nicotiana benthamiana* leaves. Use of the thk-tag gives an increasing boost in yield for both human and mouse IL-10 from 2 days post infiltration (dpi). Strikingly, mouse IL-10 yield was significantly higher compared to human IL-10, regardless of ER-retention. Differences in yield could not be explained by differences in mRNA transcript levels. (a) Schematic representation of expression cassettes and vector used. Expressed genes include the native coding sequence of the human (h) or mouse (m) IL-10 gene including signal peptide for secretion (SP) with or without a 3' tag coding for a thrombin cleavage site, a 6xHis-tag and the ER retention sequence KDEL (thk). All expression cassettes include the 35S promoter of the *Cauliflower mosaic virus* with duplicated enhancer (d35S), 5' leader sequence of the *Alfalfa mosaic virus* RNA 4 (AlMV) and *Agrobacterium tumefaciens* nopaline synthase transcription terminator (Tnos). (b) Relative transcript levels of IL-10 versus actin as determined by Q-PCR on 2 and 3 dpi (n=3, error bars indicate standard error). (c/d) Human and mouse IL-10 yield in crude extracts (1 to 6 dpi) in µg per mg total soluble protein (TSP) as determined by ELISA (n=3, error bars indicate standard error).

Human IL-10 accumulates in granules

To investigate the cellular fate of human and mouse IL-10 *in planta*, GFP was fused C- and N-terminally to both proteins and expression was monitored by confocal microscopy. Plants expressing hIL-10-GFP showed fluorescent globular structures up to 5 µm in size (Figure 2b). These granules resembled Golgi-bodies and were, regardless of their size, highly mobile as they travelled along ER strands. In contrast, mIL-10-GFP showed no or negligible signs of this phenomenon (Figure 2c). For both proteins, fluorescence was observed in the nuclear envelope, the ER and, putatively, the apoplast as expected for a secretory protein (Figure 2a). The results of C-terminal GFP fusions harbouring the native

IL-10 signal peptides, like the un-fused variants, are shown. N-terminal GFP fusions gave similar results (data not shown). Formation of granules may be caused by aggregation of folding intermediates or extensive multimerisation of human IL-10. Since mouse IL-10 did not show granules as observed for human IL-10, we assumed that formation of granules hinders yield of biologically active IL-10.

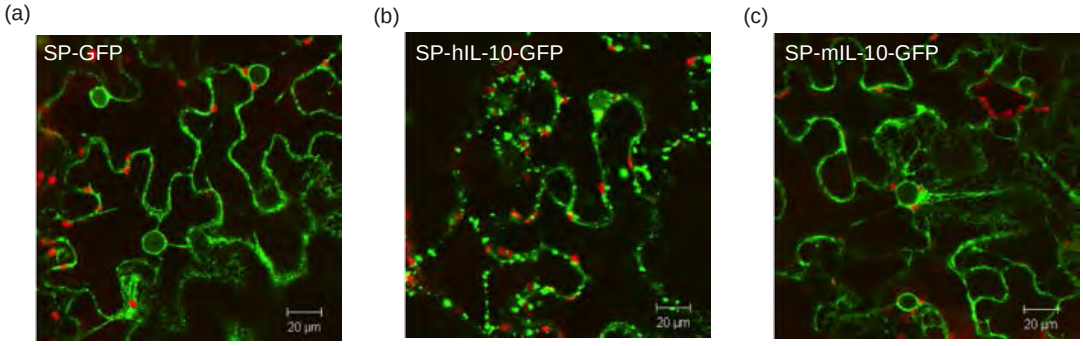

Figure 2 ◆ Whole mount confocal microscopy output of leaves expressing human or mouse IL-10 fused to GFP. Highly mobile globular granules of up to 5µm in size were observed traveling along cytoplasmic and/or ER strands for SP-hIL-10-GFP only. (a) GFP preceded by the *Arabidopsis thaliana* chitinase signal peptide for secretion (SP-GFP). (b/c) The native open reading frame of human (h) and mouse (m) IL-10 including the native signal peptide (SP) with GFP fused C-terminally.

Glycosylation of IL-10 hinders granulation

Human and mouse IL-10 have a homology of 73% at amino acid level. The most apparent difference between human and mouse IL-10 during post-translational processing is the glycosylation of mouse IL-10. Both proteins have one potential N-glycosylation site (Asn116) that is not glycosylated, while mouse IL-10 has yet another site that is glycosylated (Asn11). As N-glycosylation can stabilize a protein and influence protein folding by mediating interaction with chaperones, it may explain the difference in protein processing between human and mouse IL-10. To investigate the influence of N-glycosylation of IL-10 on granulation, the glycosylation site of mouse IL-10 was introduced in human IL-10 and removed from mouse IL-10. In both cases this was done by a single nucleotide mutation causing the serine of human IL-10 on position 11 of the mature protein to change into an asparagine and vice versa (hIL-10^{S11N} and mIL-10^{N11S}). Figures 3a and 3d show a micrograph of GFP fused C-terminally to hIL-10^{S11N} and mIL-10^{N11S}, respectively. Granulation of hIL-10^{S11N}-GFP was greatly reduced, however, never completely absent. For mIL-10^{N11S}-GFP granulation was induced, however, never reached the same extent as seen for hIL-10-GFP.

To confirm the presence of a N-glycan on hIL-10^{S11N} and the absence on mIL-10^{N11S}, all non-GFP fused variants were analysed by western blot (Figure 3b and 3e). *E. coli*

produced human and mouse IL-10, hence non-glycosylated, had the same molecular mass of 18 kDa when compared to plant-produced hIL-10 and mIL-10^{N11S}. The molecular weight of mIL-10 and hIL-10^{S11N} was, as expected upon single N-glycosylation, approximately 1.5 kDa higher. Both mIL-10 and hIL-10^{S11N} samples also showed a small proportion of non-glycosylated IL-10.

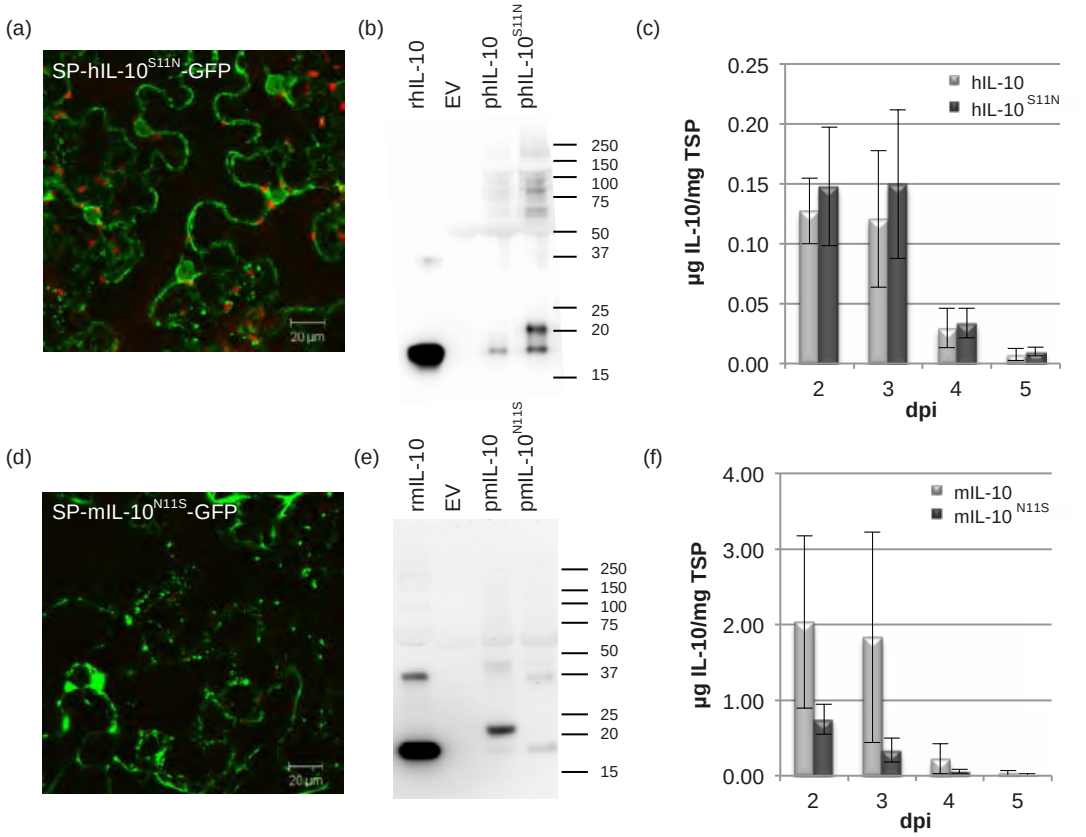

Figure 3 ◆ Analysis of the effect of N-glycosylation at Asn11 on granulation. N-glycosylation of IL-10 plays a role in preventing granulation. (a/d) Whole mount confocal microscopy output of leaves expressing GFP fused C-terminally to human (h) and mouse (m) IL-10 including native signal peptide (SP) and with introduced (S11N) or removed (N11S) glycosylation site, respectively. (b/e) Western blot analysis under reducing conditions of plant produced (p) hIL-10 and mIL-10 with and without glycosylation site. As controls, empty vector (EV) and 50 ng recombinant (r) *E. coli* produced hL-10 and mIL-10 were used. A molecular weight marker is indicated in kDa. (c/f) Yield of hIL-10 and mIL-10 with and without glycosylation site in crude extracts 2 to 5 days post infiltration (dpi) as determined by ELISA (n=4, error bars indicate standard error).

The effect of glycosylation on human and mouse IL-10 yield was compared. ELISA indicated that removal of the glycosylation of mouse IL-10 decreased yield on average 4-fold, however, this was found not to be significant (Figure 3c). Introducing a glycosylation site in human IL-10 did not lead to a yield increase (Figure 3f), however, for hIL-10 the band intensities on western blot (Figure 3b) showed that an increased amount of

glycosylated hIL-10 was extracted. This discrepancy might be explained by interference of the glycan on Asn-11 of hIL-10^{S11N} with the binding of the monoclonal antibodies used in ELISA.

Glycosylation does not influence biological activity

The possible effects of N-glycosylation on the biological activity of plant-produced human and mouse IL-10 was next assessed. The capacity of the different IL-10 variants to reduce tumour necrosis factor-alpha (TNF-α) expression by human (THP-1) and mouse (RAW264.7) macrophages upon stimulation by lipopolysaccharide from *E. coli* was determined. Figure 4 shows the percentage inhibition of TNF-α secretion by macrophages when compared to the empty vector control. As expected, glycosylated as well as non-glycosylated mouse IL-10 suppressed the secretion of pro-inflammatory TNF-α from mouse macrophages, confirming

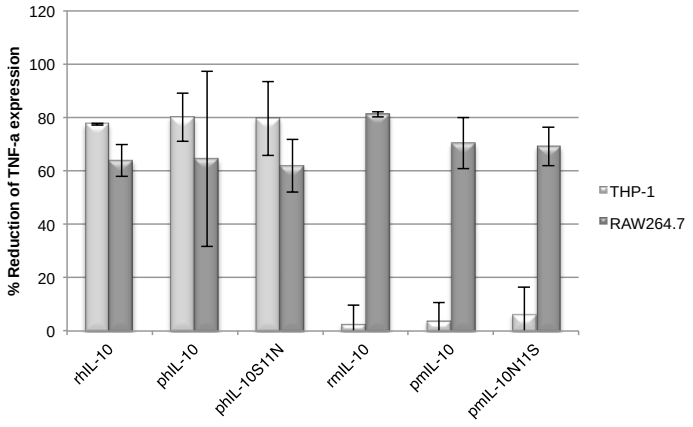

Figure 4 ◆ Biological activity of human and mouse IL-10 variants on human and mouse macrophages. Plant produced (p) and recombinant (r) *E. coli* produced human (h) or mouse (m) IL-10 were calibrated to contain the same amount of IL-10 as well as total soluble protein by using the empty vector control. Human (THP-1) and mouse (RAW264.7) macrophages were then pre-treated with 10 ng/ml hIL-10 or mIL-10 for 20 min and subsequently stimulated with 1 µg/ml *E. coli* lipopolysaccharide. Tumour necrosis factor-alpha (TNF-α) expression was determined by ELISA and IL-10 activity is indicated as the percentage of inhibition of TNF-α expression as compared to the empty vector control (n=3, error bars indicate standard error).

that N-glycosylation is not necessary for mouse IL-10 activity [3]. Strikingly, our data show that glycosylated human IL-10 is as active as its native non-glycosylated form on both human and mouse cells. Apparently, the structure of human IL-10 is not negatively influenced by the glycosylation event. Neither non-glycosylated nor glycosylated mouse IL-10 was active on human cells.

Granulation of human IL-10 is caused by extensive multimerisation

Literature describes IL-10 to be a 3D domain swapping protein, a term used to describe a process wherein two or more protein chains exchange identical structural elements or "domains" [9,17]. Two IL-10 monomers dimerise by exchanging their E-F helices. However, when the concentration of a potentially 3D domain swapping protein is high, swapping of domains does not have to be limited to two partners [18]. For example, IL-10 can provide its A-D helices to one partner, while giving its E-F helices to another partner. This can create a chain reaction that can, in theory, continue until a stable form is reached. To determine if human IL-10 granulation was triggered by extensive multimerisation, a flexible linker was introduced between α-helices D and E of human IL-10. This allows helices E-F of one human IL-10 molecule to fold into its own A-D α-helices, creating a stable monomer (hIL-10^{mono}) as designed by Josephson and co-workers [15]. Figure 5a shows three cartoons of the expected human IL-10 (I) dimer, (II) monomer and (III) stable monomer conformations.

When the monomeric form of hIL-10 was fused to GFP no signs of granulation was observed (Figure 5b). hIL-10^{mono}-GFP was detected in the ER and, putatively, the apoplast. Unlike hIL-10-GFP and mIL-10-GFP, fluorescence was also observed in the cytoplasm and nucleoplasm. This may be indicative of partial failure of the protein to be taken up into the secretory pathway. However, on western blot a band of 21 kDa, the expected size for hIL-10^{mono} with signal peptide, was never observed. Therefore, hIL-10^{mono}-GFP must be expelled from the secretory pathway and enter the nucleoplasm by either diffusion or active transport. Active transport into the nucleus after expulsion from the ER was demonstrated with a secretory GFP fusion with the P-domain of the chaperone calreticulin [19].

Western blot analysis demonstrated that hIL-10^{mono} was indeed present as a monomer, whereas plant and *E. coli* produced hIL-10 also revealed bands corresponding to dimeric (36 kDa) and multimeric hIL-10 (Figure 5c). In repetitive experiments a small proportion of dimeric hIL-10^{mono} was observed occasionally, but never larger multimers. Analysing average yields of hIL-10 and hIL-10^{mono} by ELISA revealed that the hIL-10^{mono} protein level was significantly higher (P=0.048) resulting in 16-fold more protein. Maximum yield obtained with hIL-10^{mono} was 3,2 µg IL-10/mg (0.32%) TSP at 3 dpi (Figure 5d). However, when hIL-10^{mono} was tested for biological activity by assessing its ability to suppress TNF-α expression by LPS stimulated macrophages, it appeared not to be functional (Figure 6a), which was expected as IL-10 receptor binding studies suggest that the dimeric form of IL-10 confers biological activity [20]. This experiment was repeated several times and on some occasion slight activity of the hIL-10^{mono} was observed, however, always less than E. coli produced hIL-10. It appeared that the biological activity coincided with the proportion of dimeric hIL-10^{mono} seen on western blot. It is likely that the extent of

dimerisation and multimerisation of IL-10 is dependent on sample treatment such as freeze-thaw cycles, temperature and pH of the solution after extraction.

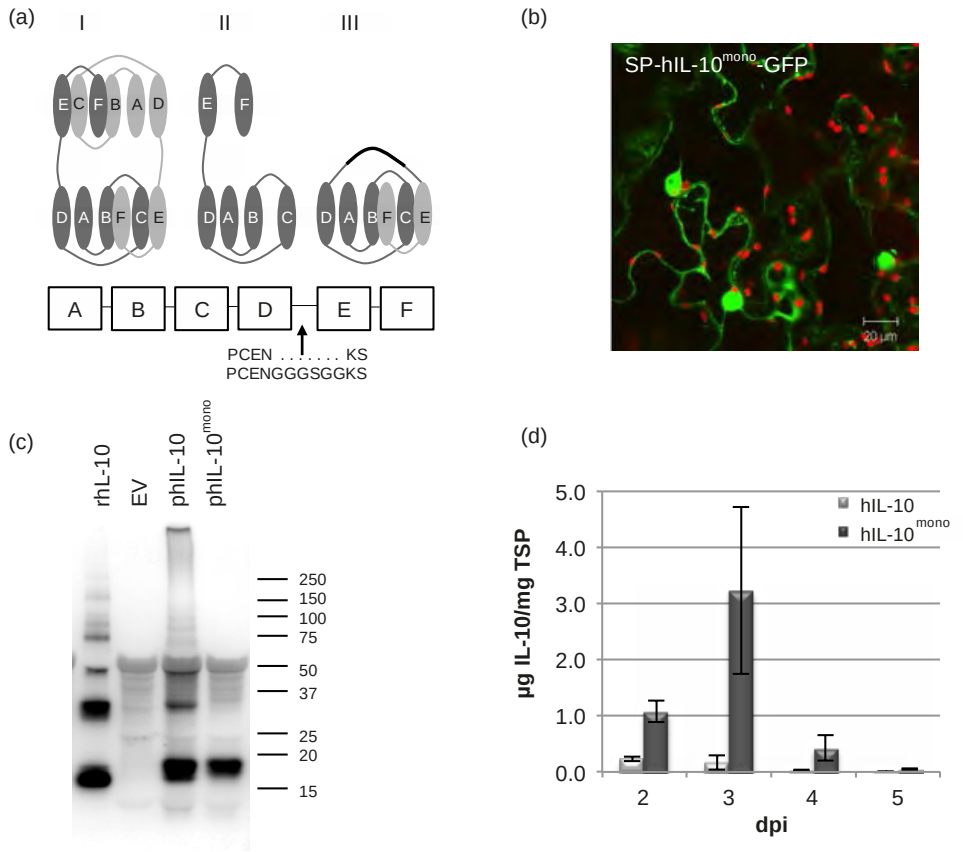

Figure 5 ◆ Analysis of expression of a stable monomeric form of human IL-10. A stable monomeric form of human IL-10 (hIL-10^{mono}) does not granulate and yield increases 30-fold. (a) Three cartoons illustrating the human IL-10 (I) dimer, (II) monomer and (III) stable monomer structure, as well as a schematic representation of the human (h) IL-10 alpha helices A-F. Helices are represented by ovals, whereby a fragment of the amino acid sequence and the location of insertion of the small GS-linker is indicated. (b) Whole mount confocal microscopy output of GFP fused C-terminally to hIL-10^{mono} including native signal peptide (SP). (c) Western blot analysis under non-reducing conditions of plant produced hIL-10 and hIL-10^{mono}. As controls, empty vector (EV) and 50 ng recombinant (r) *E. coli* produced hL-10 were used. A molecular weight marker is indicated in kDa. (d) Yield of hIL-10 and hIL-10^{mono} in crude extracts 2 to 5 days post infiltration as determined by ELISA (n=3, error bars indicate standard error). Average yield of hIL-10^{mono} was significantly higher compared to hIL-10.

Biological activity of hIL-10^{mono} was restored by fusion to Fcα

To re-establish biological activity, dimerisation of hIL-10^{mono} was forced by fusion to the C-terminus of constant domains 2 and 3 of human immunoglobulin A2m1 (Fcα). As a reference, a construct with unmodified hIL-10 fused to Fcα was also made. Figure 6a shows the percentage inhibition of TNF-α secretion by macrophages when compared to the empty vector control. As mentioned before, hIL-10^{mono} had reduced biologically

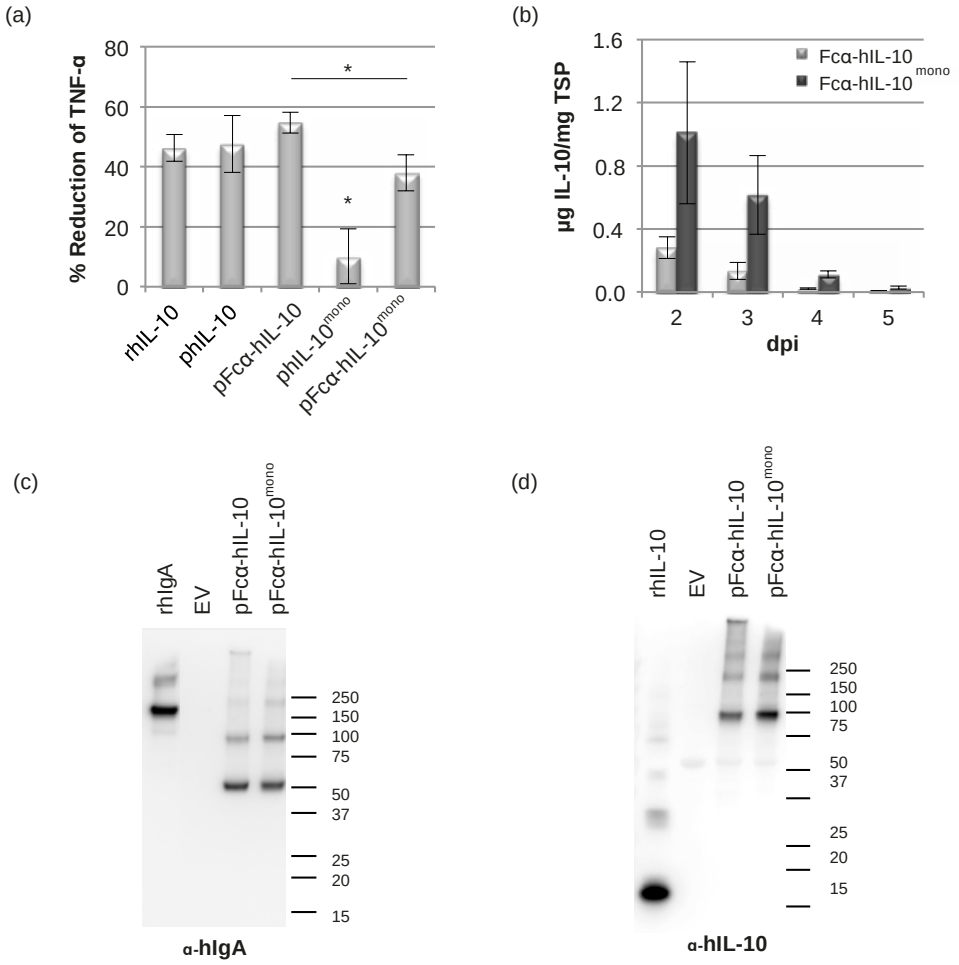

Figure 6. ◆ Analysis of expression and biological activity of IL-10 fused to Fcα. (a) Bioactivity assay of hIL-10^{mono} and Fcα-hIL-10 fusion proteins on mouse macrophages (RAW267.4) as described before. Tumour necrosis factor-alpha (TNF-α) expression was determined by ELISA and IL-10 activity is indicated as the percentage of inhibition of TNF-α expression as compared to the empty vector control (n=4, error bars indicate standard error). Significant difference (P<0.05) between samples is indicated with an asterisk, where biological activity of hIL-10^{mono} was significantly lower as all other samples. (b) Yield of human (h) IL-10 in crude extracts 2 to 5 days post infiltration as determined by ELISA (n=3, error bars indicate standard error). (c/d) Western blot analysis under non-reducing conditions of plant produced (p) Fcα-hIL10 and Fcα-hIL-10^{mono} using an antibody raised against human IL-10 and human IgA for visualisation, respectively. As controls, empty vector (EV), 50 ng recombinant (r) *E. coli* produced hIL-10 and 10 ng purified hIgA were used. A molecular weight marker is indicated in kDa.

activity, but by fusion to Fcα we were able to restore its biological activity (*P*=0.0230). Also, fusion of native hIL-10 to Fcα slightly increased biological activity, but not significant. While the activity of the monomeric IL-10 Fcα fusion had no significant difference with *E. coli* or plant produced native hIL-10, a significant difference was found with the native IL-10 Fcα fusion (*P*=0.0375).

Both fusion proteins showed similar accumulation patterns as observed for the un-fused variants of IL-10. However, yield of Fcα-hIL-10^{mono} was slightly lower compared to the un-fused variant on dpi 3, but was found not to be significant (Figure 6b). This indicates that fusion with a stable fusion partner does not ensure increase in yield of IL-10, as was the case with fusion to elastin-like polypeptides [14,21].

Western blot analysis using antibodies raised against hIL-10 showed that the largest proportion had the expected size of dimeric Fcα-hIL-10 (95 kDa) for both hIL-10 and hIL-10^{mono} fusions, but also bands at 200 kDa and 300 kDa were observed, which could again indicate the presence of multimers of these fusion proteins (Figure 6c). Using antibodies raised against IgA revealed, in addition to all bands corresponding with the IL-10 blot, an extra band around 50 kDa (Figure 6d). Because this band does not appear on the IL-10 blot, it is probably a cleavage product whereby IL-10 is removed.

Discussion

Here we show that extensive multimerisation of human IL-10 is the most important factor limiting yield and not protein instability. Human IL-10 has previously been expressed in plants [12,14,21-23]. The highest yield of 0.55% of TSP was obtained by transient expression of human IL-10 fused to an elastin-like polypeptide while retained in the ER. It was suggested that retention in the protein friendly environment of the ER protects the protein against degradation and that elastin-like polypeptides might prevent aspecific aggregation by association with chaperones [12,14]. These data suggested a role for protein instability or inefficient post-translational processing as a limiting factor for production of human IL-10. Protein instability as a bottleneck for production of IL-10 would not be surprising, as cytokines are known for their short half-life *in vivo*.

When we studied the cellular fate of human and mouse IL-10 *in planta* using GFP fusions, we revealed that human IL-10 accumulates in granules, while mouse IL-10 does not. The most evident difference between human and mouse IL-10 is the N-glycosylation of mouse IL-10. Both proteins have one potential N-glycosylation site (Asn116) that is not glycosylated, while mouse IL-10 has yet another site that is glycosylated (Asn11). Removal of the Asn11 glycosylation site resulted in increased granulation of mouse IL-10, whereas introduction of this glycosylation site in human IL-10 prevented granulation to a large extent. As N-glycosylation can aid in protein folding and stabilisation, we hypothesised that the granules were in fact very large aggregates, potentially compartmentalised as a cell protective mechanism.

Aggregation can be due to protein instability and/or misfolding resulting in random hydrophobic patch interaction or, in the case of IL-10, due to extensive multimerisation. Literature describes IL-10 to be a 3D domain swapping protein, a term used to describe a process wherein two or more protein chains exchange identical structural elements or "domains" [9, 17]. IL-10 monomers form biologically active dimers by exchanging their E-F helices. However, at high concentrations of IL-10 it would be possible that the domain swapping of IL-10 is not limited to two partners and causes a chain reaction that, in theory, could go on unlimited until a stable form is reached. To determine whether human IL-10 granulation was due to protein instability or due to 3D domain swapping, the behaviour of a previously developed stable monomeric form of human IL-10 [15] was studied *in planta*. This stable monomeric form of human IL-10 has a short glycine-serine (GS)-linker between helices D and E allowing the helices E-F to fold back into its own hydrophobic core created by the A-D helices (human IL-10^{mono}). No granulation was observed when human IL-10^{mono} was fused with GFP. Multimeric or high molecular weight bands of human IL-10^{mono} were also not detected by western blot. Furthermore, yield was increased on average 16-fold by this minor modification of the human IL-10 protein. This expression level was comparable to the highest yield obtained for human IL-10 so far, however,

without retention in the ER or fusion with a stable protein partner. Taken together, we show that not protein instability, but extensive multimerisation of human IL-10, due to its intrinsic 3D domain swapping characteristic, is the major limiting factor for yield.

Bennett and colleagues introduced the term 3D domain swapping [17] and up to date almost 300 proteins have been reported with 3D domain swapping ability [24]. Besides IL-10, the cytokines Granulocyte Macrophage Colony-Stimulating Factor (GM-CSF), Interleukin-5 (IL-5) and Interfernon-beta (IFN-β) are also described as 3D domain swapping proteins [9] and have been heterologously expressed in several platforms. Upon expression in *E. coli* the formation of inclusion bodies were described for these four cytokines [25-28]. Although formation of inclusion bodies could be indicative of multimerisation, they are a relatively common feature when expressing eukaryotic proteins in *E. coli* due to aggregation of folding intermediates. However, in the case of IFN-β and IL-5, experiments also demonstrated the need for slow removal of denaturing agents to prevent aggregation to reoccur after solubilisation of inclusion bodies [25,26]. To our knowledge, IL-5 has not been produced in plants before and expression of human IFN-β in lettuce leaves resulted in poor yields [29]. On the other hand, many research groups have produced human GM-CSF *in planta*. Interestingly, human GM-CSF secreted by a tobacco cell culture could be stabilised in the growth medium by addition of bovine serum albumin, gelatin or salt, all methods that could inhibit protein aggregation [30,31]. Next to that, when produced in rice seeds a morphological change in both plant protein body type I and the ER were observed together with high molecular weight variants of human GM-CSF from 50 to 120 kDa [32,33]. Menassa and colleagues also described a 200 kDa weight variant of human IL-10 when expressed stably in a tobacco species [12]. For both human IL-10 and human GM-CSF yield from rice seeds was relatively high compared to the leaf-based and cell culture systems, however, extraction from rice seeds was only efficient using reducing agents [23,34]. Unfortunately, use of reducing agents during extraction would increase production costs again, as the protein would need to be chemically refolded. There are many indications that extensive multimerisation has also hampered the production of other 3D domain swapping cytokines, and may represent a more common mechanism affecting yield than thus far anticipated. In addition, it is unclear how 3D domain swapping influences biopharmaceutical proteins during formulation, storage and administration.

Although we could increase the yield of human IL-10 significantly by expression of a stable monomeric form of IL-10, this form was not biologically active, as determined by its ability to reduce TNF-α secretion by lipopolysaccharide-stimulated macrophages. Even though human IL-10^{mono} has all the receptor binding sites, the affinity may be reduced. Josephson and co-workers did show biological activity of human IL-10^{mono}based on its ability to induce proliferation of a B cell line, however, a 10-fold higher amount of human IL-10^{mono} was needed to obtain the same effect as recombinant human IL-10 [15]. Stable

monomeric forms of IL-5 were also created and shown to have reduced receptor affinity. Nevertheless, they did show biological activity with concentration dependence close to that of the wild type [35]. Such stabilised biologically active forms of 3D domain swapping cytokines will ensure that the protein stays in its biologically active conformation, which may have great benefit for formulation and administration to patients.

To mimic the natural dimerisation of IL-10 while still preventing multimerisation, human IL-10^{mono} was fused to the naturally dimerising Fc portion of IgA2m1 (Fcα), which restored the ability to suppress TNF-α in stimulated macrophages. As well as ensuring dimeric conformation, it is likely that fusion with Fcα increases *in vivo* half-live of IL-10, which could be beneficial for efficacy. Our construct is comparable to that of mouse IL-10 fused to the N-terminus of a non-cytolytic version of the Fc portion of mouse IgG2a, which was shown to be functional *in vivo* with a prolonged efficacy due to its increased circulating half-life [36]. However, an increased half-life of IL-10 could also lead to unwanted systemic side effects, such as a compromised immune system. By using complete antibodies it may be possible to circumvent these side effects. Through the antigen binding capacity of an antibody with IL-10 fused C-terminally, specific cells or tissues can be targeted enabling IL-10 therapy for a variety of diseases, as was already demonstrated by Schwager and co-workers [37]. In disease therapy, use of a human fusion protein is desired to limit the chance of an immune response against the therapeutic agent. Also, in inflammatory disease therapy the use of IgA may be preferred over other antibody isotypes, as it does not activate the classical complement pathway. Thus, a stable molecule that ensures a biologically active conformation and targeting, such as Fcα-IL-10, may be a more suitable format for medical applications and may prove effective in therapy of inflammatory diseases.

Experimental procedures

Construction of expression cassettes and vector

The complete native open reading frames of human and mouse IL-10 were amplified from the MegaMan™ Human Transcriptome cDNA library (Stratagene) and FirstChoice™ PCR-Ready Mouse Spleen cDNA library (Ambion), respectively, using oligonucleotides indicated in Table 1. Sense and antisense oligonucleotides included NcoI and KpnI restriction sequences, respectively, for subsequent cloning steps. Introduction of the NcoI restriction site resulted in the addition of two extra amino acids to the signal peptide at the N-terminus. All oligonucleotides used for subsequent reamplification, mutagenesis and insertion can be found in Table 1.

To create hIL-10thk and mIL-10thk, both hIL-10 and mIL-10 ORFs were reamplified, resulting in the removal of the stop codon and replacement of the KpnI by a NotI restrictrion site. The thk coding DNA fragment could be added in frame. To remove and introduce the glycosylation site of mouse and human IL-10 respectively, the QuickChange XL kit (Stratagene) was used. For insertion of the 6 amino acid glycine-serine spacer overlap extension PCR was performed in combination with original hIL-10 oligonucleotides.

The DNA fragment encoding the enhanced green fluorescent protein (eGFP) was reamplified from gateway vector pK7FWG2 [38]. Constructs with eGFP fused C-terminally to IL-10 were composed of the IL-10 fragments ending with NotI (as described for the h/mIL-10thk constructs) the "NotI-NcoI" oligo and the eGFP fragment.

The constant domains 2 and 3 of human immunoglobulin A2m1 heavy chain including a N-terminal IgA signal peptide and a C-terminal linker sequence was synthetically constructed by GeneArt and fused N-terminally to reamplified SpeI-hIL-10 and SpeI-hIL-10mono fragments.

All constructs were placed under the control of the 35S promoter of the *Cauliflower mosaic virus* with duplicated enhancer (d35S) and the *Agrobacterium tumefaciens* nopaline synthase transcription terminator (Tnos). A 5′ leader sequence of the *Alfalfa mosaic virus* RNA 4 (AlMV) was included between the promoter and construct to boost translation. All elements were present in pRAP35 (or pUCAP35S [39]) from which expression cassettes were digested with AscI and PacI and ligated into a modified version of the expression vector pMDC32 [40], renamed pHYG. The pHYG vector resulted upon removal of the Gateway recombination sequences by digestion with EcoRI and HindIII and replacement with a DNA fragment (oligos "pHYG adaptor") including AscI and PacI restriction sites for insertion of the expression cassettes.

All construct sequences were confirmed by sequencing (BaseClear) at the expression vector stage. The expression vectors were subsequently transformed to *Agrobacterium tumefacien*s strain MOG101 for plant expression.

Table 1 Oligonucleotides used for construct re-amplification, mutagenesis and insertion.

Gene fragment	Function	5' --> 3' Sense oligonucleotides	5' --> 3' Antisense oligonucleotides
hIL-10	Isolation hIL-10 NcoI/KpnI	ccatgggcATGCACAGCTCAG CACTGCTCT	cggtaccTCAGTTTCGTATCTT CATTGTCA
mIL-10	Isolation mIL-10 NcoI/KpnI	ccatggccATGCCTGGCTCAG CACTGCTAT	ccggtaccTTAGCTTTTCATTT TGATCATC
pHYG adaptor	MCS including AscI/PacI	aattcggcgcgcctacgcgtaaggacg agctctgaggtacctctagattaattaaa	agcttttaattaatctagaggtacctcag agctcgtccttacgcgtaggcgcgccg
hIL-10-NotI	Removal stop codon, addition NotI	ccatgggcATGCACAGCTCAG CACTGCTCT	ggcggccgcGTTTCGTATCTTC ATTGTCATG
mIL-10-NotI	Removal stop codon, addition NotI	ccatggccATGCCTGGCTCAG CACTGCTAT	ggcggccgcGCTTTTCATTTTG ATCATCATG
thk	Thrombin, 6xHIS, KDEL	ggccgcattagttcctcgtggttctgcta gccatcaccatcaccatcacaaagatg agctatgacgtacgggtac	ccgtacgtcatagctcatctttgtgatggt gatggtgatggctagcagaaccacgag gaactaatgc
eGFP	Isolation GFP NcoI/KpnI	gtcgacggatccATGGTGAGCA AGGGCGAGGAGCTGTTC	aggtaccTTAGCTCATGACTG ACTTGTAGAGCTCGTCCAT GCCGAGAG
NotI-NcoI	Linker C-terminal GFP fusion	ggccgctgcagtcgacggatc	catggatccgtcgactgcagc
mIL-10^{N11S}	Removal glycosylation site	GCCGGGAAGACAATAgCT GCACCCACTTCCC	GGGAAGTGGGTGCAGcTA TTGTCTTCCCGGC
hIL-10^{S11N}	Introduction glycosylation site	CCCAGTCTGAGAACAaCTG CACCCACTTCCCAG	CTGGGAAGTGGGTGCAGt TGTTCTCAGACTGGG
hIL-10^{mono}	Insertion GGGSGG-linker	AAACggtggcggatctgggggtAA GAGCAAGGCCGTGGAGC AGGTGAA	CTTacccccagatccgccaccGTT TTCACAGGGAAGAAATCG ATGA
SpeI-hIL-10	Removal SP, addition SpeI	accatggactagtAGCCCAGGC CAGGGCAC	cggtaccTCAGTTTCGTATCTT CATTGTCA
h/m IL-10	Q-PCR analysis	ATGATCCAGTTTTACCTGG	AGAAATCGATGACAGCG
Nb β-actin	Q-PCR analysis	CCAGGTATTGCCGATAGA ATG	GAGGGAAGCCAAGATAG AGC

Native sequences in capitals, added/mutated sequences in small and restriction sites are underlined. h; human, IL-10; interleukin-10, MCS; multiple cloning site, m; mouse, Nb; *Nicotiana benthamiana*, SP; signal peptide for secretion, thk; thrombin-6xHIS-KDEL tag.

Agrobacterium tumefaciens transient transformation assay

Agrobacterium tumefaciens clones were cultured overnight (o/n) at 28°C in LB medium (10g/l pepton140, 5g/l yeast extract, 10g/l NaCl with pH 7.0) containing 50 µg/ml kanamycin and 20 µg/ml rifampicin. The optical density (OD) of the o/n cultures was measured at 600 nm and used to inoculate 50 ml of LB medium containing 200 µM acetosyringone and 50 µg/ml kanamycin with x µl of culture using the following formula: x = 80000/(1028*OD). OD was measured again after 16 hours and the bacterial cultures were centrifuged for 15 min at 2800 x*g*. The bacteria were resuspended in MMA infiltration medium (20g/l sucrose, 5g/l MS-salts, 1.95g/l MES, pH5.6) containing 200 µM acetosyringone till an OD of 1 was reached. After 1-2 hours incubation at room temperature, the two youngest fully expanded leaves of 5-6 weeks old Nicotiana benthamiana plants were infiltrated completely. Infiltration was performed by injecting the *Agrobacterium* suspension into a *Nicotiana benthamiana* leaf at the abaxial side using a 1 ml syringe. Infiltrated plants were maintained in a controlled greenhouse compartment (UNIFARM, Wageningen) and infiltrated leaves were harvested at selected time points.

Total soluble protein extraction

Leaves were immediately snap-frozen upon harvesting, homogenised in liquid nitrogen and stored at -20°C until use. Homogenised plant material was ground in ice-cold extraction buffer (50mM phosphate-buffered saline (PBS) pH=7.4, 100 mM NaCl, 10 mM ethylenediaminetetraacetic acid (EDTA), 0.1% v/v Tween-20, 2% w/v immobilised polyvinylpolypyrrolidone (PVPP)) using 2 ml/g fresh weight. Crude extract was clarified by centrifugation at 16.000 x*g* for 5min at 4°C and supernatant was directly used in an ELISA and BCA protein assay. For western blotting and biological activity assays, above-mentioned protein extraction would be followed by desalting using a G25 Sephadex column and filter sterilisation (0.22 µm; Millipore Corporation).

Quantification of human and mouse IL-10 mRNA levels

mRNA was isolated from homogenised plant material using the RNAeasy Plant Mini Kit (Qiagen) according to supplier's protocol. A Turbo DNaseI (Ambion) treatment was included to remove any residual DNA. cDNA was synthesised using the SuperScript®III First-Strand Synthesis System (Invitrogen) according to supplier's protocol. Samples were analysed by quantitative PCR in triplo using ABsolute SYBR Green Fluorescein mix (Thermo Scientific). *Nicotiana benthamiana* β-actin was used as a reference gene. Oligonucleotides used can be found in Table 1. Relative transcript levels of IL-10 versus actin were determined by the Pfaffl method [41].

Quantification of human and mouse IL-10 protein levels

IL-10 protein concentration in crude plant extract was determined by ELISA. Human and mouse IL-10 ELISA Ready-SET-Go!® kits (eBioscience) were used according to supplier's protocol using the model 680 plate reader (BioRad) to measure the OD at 450 nm with correction filter of 690 nm. For sample comparison the total soluble protein (TSP) concentration was determined by the BCA method (Pierce) according to supplier's protocol using bovine serum albumin (BSA) as a standard.

Protein analysis by western blot

Soluble plant proteins were separated under reducing or non-reducing conditions by SDS-PAGE on a NuPAGE® 12% Bis-Tris gel (Invitrogen). Recombinant *E. coli* produced human or mouse IL-10 (R&D Systems) or IgA1 (Invivogen) was used as a control. Proteins were transferred to an Invitrolon™ PVDF membrane (Invitrogen) by semi-dry blotting procedure. Thereafter the membrane was blocked in PBST-BL (PBS containing 0.1% v/v Tween-20 and 5% w/v non-fat dry milk powder) for 1 hour at room temperature, followed by overnight incubation with hIL-10 specific goat polyclonal antibody (R&D systems), mIL-10 specific rat monoclonal antibody (BioLegend) or IgA specific HRP conjugated goat polyclonal antibody (Sigma) in PBST at 4°C. The membrane was washed 5 times with 5 min intervals in PBST. For h/mIL-10 specific western blots the procedure was continued with a 1 hour incubation at room temperature with HRP conjugated secondary antibodies (Jackson ImmunoResearch) in PBST and washed again as described before. Finally, the SuperSignal West Femto substrate (Pierce) was used to detect HRP-conjugated antibodies.

Confocal microscopy

Plants were agro-infiltrated with expression cassettes encoding C-terminal fusions of GFP to human and mouse IL-10 as described previously. Leaves were taken from the plant and small sections were examined from the abaxial side using a Zeiss LSM510 confocal laser-scanning microscope in combination with an argon ion laser supplying a 488 nm wavelength.

Biological activity assay

The monocyte THP-1 and monocyte/macrophage RAW264.7 cell lines were purchased from the American Type Culture Collection and cells were maintained at 37°C with 5% CO_2. THP-1 cells were cultured in RPMI-1640 medium containing containing 4 mM L-glutamine, 25 mM HEPES and supplemented with 10% fetal calf serum, 50 U/ml penicillin and 50 µg/ml streptomycin. THP-1 monocytes were differentiated into macrophages for 4 days using 30 ng/ml PMA at a density of $3x10^5$ cells/ml in 96 well plates. Cells were allowed to rest for 2-3 days in medium without PMA prior to bioassays. RAW264.7 cells were cultured in DMEM containing 4 mM L-glutamine, 25 mM HEPES

and supplemented with 10% fetal calf serum, 50 U/ml penicillin and 50 µg/ml streptomycin. Cells were sub-cultured every 2-3 days, whereby the cells were harvested by gently disrupting the monolayer with a cell scraper. For cell-based assays cells were seeded in 96 well plates at a density of $5x10^4$ cells/well and allowed to rest overnight. For bioassays cells were pre-treated with 10-50 ng/ml plant produced or recombinant *E. coli* produced human or mouse IL-10 (R&D Systems) in plant extract for 20 min, and subsequently stimulated with 1 µg/ml of lipopolysaccharide (Sigma). After overnight incubation supernatants were analysed with the mouse TNF-α ELISA Ready-Set-Go! ® Kit (eBioscience) according to the supplier's protocol.

Data analysis

All data shown in the figures indicate the average of at least three biological replicates (n) that were determined by at least three technical replicates. Significant differences between samples were calculated using the student's *t*-test and regarded as significant when $P<0.05$. Significant differences in expression levels between constructs were calculated by using the whole data set from dpi 2 to 5 and are indicated in the main text as well as the figure legends. When comparing biological activity between proteins significant differences are indicated in the figure by asterisks.

Acknowledgements

This study was financially supported in part by Synthon (Nijmegen, The Netherlands). The authors declare no conflict of interest. We would like to thank Gerry Ariaans for all helpful discussions and Kevin van der Eijken, Francisco Marques, Bart Nijland, Debbie van Raaij, Sonja Warmerdam and Edgar Wils for their input in the practical work of this study.

References

1. Asadullah K, Sterry W, Volk HD (2003) Interleukin-10 Therapy - Review of a New Approach. Pharmacological Reviews 55: 241-269.
2. O'Garra A, Barrat FJ, Castro AG, Vicari A, Hawrylowicz C (2008) Strategies for use of IL-10 or its antagonists in human disease. Immunological Reviews 223: 114-131.
3. Moore KW, O'Garra A, de Waal Malefyt R, Vieira P, Mosmann TR (1993) Interleukin-10. Annual Reviews Immunology 11: 165-190.
4. Moore KW, de Waal Malefyt R, Coffman RL, O'Garra A (2001) Interleukin-10 and the interleukin-10 receptor. Annual Reviews Immunology 19: 683-765.
5. Mocellin S, Marincola F, Rossi CR, Nitti D, Lise M (2004) The multifaceted relationship between IL-10 and adaptive immunity: putting together the pieces of a puzzle. Cytokine & Growth Factor Reviews 15: 61-76.
6. Saraiva M, O'Garra A (2010) The regulation of IL-10 production by immune cells. Nature Reviews Immunology 10: 170-181.
7. Walter MR, Nagabhushan TL (1995) Crystal-Structure of Interleukin-10 Reveals an Interferon Gamma-Like Fold. Biochemistry 34: 12118-12125.
8. Zdanov A, Schalk-Hihi C, Gustchina A, Tsang M, Weatherbee J, *et al*. (1995) Crystal structure of interleukin-10 reveals the functional dimer with an unexpected topological similarity to interferon gamma. Structure 3: 591-601.
9. Liu Y, Eisenberg D (2002) 3D domain swapping: As domains continue to swap. Protein Science 11: 1285-1299.
10. Colombel JF, Rutgeerts P, Malchow H, Jacyna M, Nielsen OH, *et al*. (2001) Interleukin 10 (Tenovil) in the prevention of postoperative recurrence of Crohn's disease. Gut 49: 42-46.
11. Steidler L, Neirynck S, Huyghebaert N, Snoeck V, Vermeire A, *et al*. (2003) Biological containment of genetically modified *Lactococcus lactis* for intestinal delivery of human interleukin 10. Nature Biotechnology 21: 785-789.
12. Menassa R, Nguyen V, Jevnikar A, Brandle J (2001) A self-contained system for the field production of plant recombinant interleukin-10. Molecular Breeding 8: 177-185.
13. Menassa R, Du C, Yin ZQ, Ma S, Poussier P, *et al*. (2007) Therapeutic effectiveness of orally administered transgenic low-alkaloid tobacco expressing human interleukin-10 in a mouse model of colitis. Plant Biotechnology Journal 5: 50-59.
14. Patel J, Zhu H, Menassa R, Gyenis L, Richman A, *et al*. (2007) Elastin-like polypeptide fusions enhance the accumulation of recombinant proteins in tobacco leaves. Transgenic Research 16: 239-249.

15. Josephson K, DiGiacomo R, Indelicato SR, Ayo AH, Nagabhushan TL, *et al*. (2000) Design and Analysis of an Engineered Human Interleukin-10 Monomer. Journal of Biological Chemistry 275: 13552-13557.

16. Schouten A, Roosien J, van Engelen FA, de Jong GAM, Borst-Vrenssen AWM, *et al*. (1996) The C-terminal KDEL sequence increases the expression level of a single-chain antibody designed to be targeted to both the cytosol and the secretory pathway in transgenic tobacco. Plant Molecular Biology 30: 781-793.

17. Bennett MJ, Schlunegger MP, Eisenberg D (1995) 3D domain swapping: A mechanism for oligomer assembly. Protein Science 4: 2455-2468.

18. Yang S, Levine H, Onuchic JN (2005) Protein Oligomerization Through Domain Swapping: Role of Inter-molecular Interactions and Protein Concentration. Journal of Molecular Biology 352: 202-211.

19. Brandizzi F, Hanton S, daSilva LLP, Boevink P, Evans D, *et al*. (2003) ER quality control can lead to retrograde transport from the ER lumen to the cytosol and the nucleoplasm in plants. The Plant Journal 34: 269-281.

20. Josephson K, Logsdon NJ, Walter MR (2001) Crystal Structure of the IL-10/IL-10R1 Complex Reveals a Shared Receptor Binding Site. Immunity 15: 35-46.

21. Conley AJ, Joensuu JJ, Jevnikar AM, Rima Menassa R, Brandle JE (2009) Optimization of elastin-like polypeptide fusions for expression and purification of recombinant proteins in plants. Biotechnology and Bioengineering 103(3): 562-573

22. Menassa R, Kennette W, Nguyen V, Rymerson R, Jevnikar A, *et al*. (2004) Subcellular targeting of human interleukin-10 in plants. Journal of Biotechnology 108: 179-183.

23. Fujiwara Y, Aiki Y, Yang L, Takaiwa F, Kosaka A, *et al*. (2010) Extraction and purification of human interleukin-10 from transgenic rice seeds. Protein Expression and Purification 72: 125-130.

24. Shameer K, Pugalenthi G, Kandaswamy KK, Sowdhamini R (2011) 3dswap-pred: prediction of 3D domain swapping from protein sequence using Random Forest approach. Protein & Peptide Letters 18: 1010-1020.

25. Rao DV, Ramu CT, Rao JV, Narasu ML, Rao AK (2009) Cloning, high expression and purification of recombinant human intereferon-beta-1b in *Escherichia coli*. Applied Biochemistry and Biotechnology 158: 140-154.

26. Proudfoot AE, Fattah D, Kawashima EH, Bernard A, Wingfield PT (1990) Preparation and characterization of human interleukin-5 expressed in recombinant *Escherichia coli*. Biochemistry Journal 270: 357-361.

27. Schwanke RC, Renard G, Chies JM, Campos MM, Batista EL Jr., *et al*. (2009) Molecular cloning, expression in *Escherichia coli* and production of bioactive homogeneous recombinant human granulocyte and macrophage colony stimulating factor. International Journal of Biological Macromolecules 45: 97-102.

28. Sun J, Li BA, Qi Y, Zhou JW, Zhu L, *et al*. (2007) Cloning, expression and identification of human interleukin-10 gene. Xi Bao Yu Fen Zi Mian Yi Xue Za Zhi 23: 220-222.

29. Li J, Chen M, Liu X-W, Zhang H-C, Shen FF, *et al*. (2007) Transient expression of an active interferon-beta in lettuce. Scientia Horticulturae 112: 258-265.

30. James EA, Wang C, Wang Z, Reeves R, Shin JH, *et al*. (2000) Production and characterization of biologically active human GM-CSF secreted by genetically modified plant cells. Protein Expression and Purification 19: 131-138.

31. Lee JH, Kim NS, Kwon TH, Jang YS, Yang MS (2002) Increased production of human granulocyte-macrophage colony stimulating factor (hGM-CSF) by the addition of stabilizing polymer in plant suspension cultures. Journal of Biotechnology 96: 205-211.

32. Luo J, Ning T, Sun Y, Zhu J, Zhu Y, *et al*. (2008) Proteomic Analysis of Rice Endosperm Cells in Response to Expression of hGM-CSF. Journal of Proteome Research 8: 829-837.

33. Ning T, Xie T, Qiu Q, Yang W, Zhou S, *et al*. (2008) Oral administration of recombinant human granulocyte-macrophage colony stimulating factor expressed in rice endosperm can increase leukocytes in mice. Biotechnology Letters 30: 1679-1686.

34. Sardana R, Dudani AK, Tackaberry E, Alli Z, Porter S, *et al*. (2007) Biologically active human GM-CSF produced in the seeds of transgenic rice plants. Transgenic Research 16: 713-721.

35. Li J, Cook R, Doyle ML, Hensley P, McNulty DE, *et al*. (1997) Monomeric isomers of human interleukin 5 show that 1:1 receptor recruitment is sufficient for function. Proceedings of the National Academy of Science USA 94: 6694-6699.

36. Zheng XX, Steele AW, Nickerson PW, Steurer W, Steiger J, *et al*. (1995) Administration of noncytolytic IL-10/Fc in murine models of lipopolysaccharide-induced septic shock and allogeneic islet transplantation. Journal of Immunology 154: 5590-5600.

37. Schwager K, Kaspar M, Bootz F, Marcolongo R, Paresce E, *et al*. (2009) Preclinical characterization of DEKAVIL (F8-IL10), a novel clinical-stage immunocytokine which inhibits the progression of collagen-induced arthritis. Arthritis Research & Therapy 11: R142.

38. Karimi M, Inzé D, Depicker A (2002) GATEWAY™ vectors for *Agrobacterium*-mediated plant transformation. Trends in Plant Science 7: 193-195.

39. van Engelen FA, Schouten A, Molthoff JW, Roosien J, Salinas J, *et al.* (1994) Coordinate expression of antibody subunit genes yields high levels of functional antibodies in roots of transgenic tobacco. Plant Molecular Biology 26: 1701-1710.

40. Curtis MD, Grossniklaus U (2003) A Gateway Cloning Vector Set for High-Throughput Functional Analysis of Genes *in Planta*. Plant Physiology 133: 462-469.

41. Pfaffl MW (2001) A new mathematical model for relative quantification in real-time RT-PCR. Nucleic Acids Research 29: e45.

Chapter 4

The N-glycan on Asn54 affects the atypical N-glycan composition of plant-produced interleukin-22, but does not influence its activity

Ruud H. P. Wilbers, Lotte B. Westerhof, Lauri J. Reuter, Alexandra Castilho, Debbie R. van Raaij, Dieu-Linh Nguyen, Jose L. Lozano-Torres, Geert Smant, Cornelis H. Hokke, Jaap Bakker and Arjen Schots

This work has been accepted for publication in:
Plant Biotechnology Journal

Abstract

Human interleukin-22 (IL-22) is a member of the IL-10 cytokine family that has recently been shown to have major therapeutic potential. IL-22 is an unusual cytokine as it does not act directly on immune cells. Instead, IL-22 controls the differentiation, proliferation and anti-microbial protein expression of epithelial cells, thereby maintaining epithelial barrier function. In this study we transiently expressed human IL-22 in *Nicotiana benthamiana* plants and investigated the role of N-glycosylation on protein folding and biological activity. Expression levels of IL-22 were up to 5.4 µg/mg TSP and N-glycan analysis revealed the presence of the atypical Lewis A structure. Surprisingly, upon engineering of human-like N-glycans on IL-22 by co-expressing mouse FUT8 in ΔXT/FT plants a strong reduction in Lewis A was observed. Also, core α1,6-fucoylation did not improve the biological activity of IL-22. The combination of site-directed mutagenesis of Asn54 and *in vivo* deglycosylation with PNGase F also revealed that N-glycosylation at this position is not required for proper protein folding. However, we do show that the presence of a N-glycan on Asn54 contributes to the atypical N-glycan composition of plant-produced IL-22 and influences the N-glycan composition of N-glycans on other positions. Altogether, our data demonstrate that plants offer an excellent tool to investigate the role of N-glycosylation on folding and activity of recombinant glycoproteins, such as IL-22.

Introduction

Interleukin-22 (IL-22) is a peculiar cytokine that belongs to the IL-10 cytokine family, which does not act directly on immune cells, but mainly exerts its functions on epithelial cells [1, 2]. IL-22 induces the expression of antimicrobial proteins in colonic and lung epithelial cells as well as acute phase response proteins in hepatocytes [3-5]. These observations demonstrate the crucial role of IL-22 in controlling early defence responses against bacterial pathogens. Furthermore, IL-22 promotes hepatocyte survival and induces differentiation and proliferation of epithelial cells in the lung and intestine, thereby providing protection against injury and maintaining mucosal barrier function [5, 6]. Therapeutic application of IL-22 is currently being investigated for disorders where increased antimicrobial defence, protection against tissue injury and tissue regeneration is most likely beneficial. Therefore, IL-22 has been considered for treatment of ulcerative colitis, tissue damage and/or inflammation of liver and pancreas, graft-versus-host disease, and may be used short-term after transplantation of lung, pancreas and kidney [1].

The biologically active form of IL-22 is thought to be a monomer that is mainly secreted by T cells. IL-22 only shares ~23% amino acid similarity with IL-10, however, structurally these two cytokines are very similar [7, 8]. Both cytokines consist of 6 α-helices (helices A to F) that form a bundle-like structure, which is further stabilised by two intramolecular disulphide bridges. In contrast to IL-10, which is not glycosylated, IL-22 has three potential N-glycosylation sites. When expressed in insect cells the majority of IL-22 is N-glycosylated at all three sites. The predominant form of these N-glycans consisted of two core *N*-acetylglucosamines (GlcNAc's), three mannoses and one core α1,6-linked fucose [9]. Comparison of the crystal structure of IL-22 expressed in insect cells with IL-22 from *Escherichia coli* revealed minor structural differences due to N-glycosylation [10, 11].

IL-22 exerts its activity by binding the hetero-dimeric receptor complex IL-22R1/IL-10R2 on the surface of its target cells. Engagement of the IL-22R1/IL-10R2 complex triggers the activation of Janus kinases Jak1 and Tyk2, which in turn activate the transcription factor STAT3. IL-22 initially binds to IL-22R1 with high affinity, thereby inducing conformational changes in the helices pre-A and A as well as the AB-loop [12, 13]. These structural changes enable binding of the low-affinity receptor subunit IL-10R2, which is a component of the receptor complexes of both IL-22 and IL-10. Interestingly, the IL-22 binding hotspot for IL-10R2 includes asparagine 54. N-glycosylation of asparagine residue 54 (Asn54), and more specifically the core GlcNAc with α1,6-linked fucose, was shown to be crucial for the binding to IL-10R2 [14]. However, the contribution of this sugar residue on the activity of IL-22 remains to be elucidated.

In the last two decades, plants have emerged as a valuable expression system for the production of recombinant proteins. As eukaryotes, plants enable the production of correctly folded complex proteins including post-translational modifications, like N-

glycosylation. Engineering of the N-glycosylation machinery in plants has further advanced research on the humanization of N-glycans. Transgenic plants lacking plant specific α1,3-fucose and β1,2-xylose sugar residues (ΔXT/FT plants) have been generated and mammalian core α1,6-fucose can be engineered in plants [15, 16]. Furthermore, plant-based production of recombinant proteins is relatively cheap and easy to scale-up compared to other expression systems. One additional advantage for the production of immunoregulatory proteins in plants is that plants have a low contamination risk with human pathogens and therefore can be regarded as safe.

To our knowledge, IL-22 has not been expressed in plants before, but several reports exist on the plant-based expression of the closely related cytokine IL-10 [17-19]. We have recently reported on a major bottleneck for expression of biologically active human IL-10 in plants [20]. IL-10 is also a member of the IL-10 cytokine family, which in contrast to monomeric IL-22 forms dimers. Extensive multimerisation of recombinant IL-10 results in aggregation of this cytokine, which leads to granule formation upon transient expression *in planta*. Here we describe that biologically active IL-22 can be efficiently produced in plants as it does not aggregate and that its activity is neither dependent on the presence of N-glycans nor their composition. Surprisingly, the N-glycan on Asn54 influences the N-glycan composition of N-glycans on other positions and contributes to the atypical N-glycan composition of plant-produced IL-22. Altogether our study shows the potential of using plants as a toolbox to study the role of N-glycans on the folding and activity of heterologous expressed glycoproteins

Results

IL-22 does not aggregate *in planta*

IL-22 naturally occurs as a monomer, in contrast to dimeric IL-10. We have previously shown that human IL-10 expression in plants is hampered by granule formation as a consequence of aggregation [20]. Granule formation prevented extraction of soluble IL-10 from plant leaves thereby significantly lowering the yield of the recombinant protein. To investigate whether IL-22 aggregates and forms granules *in planta* we monitored the expression of a N-terminal GFP-fusion of IL-22 in plant leaves by confocal microscopy. At 3 dpi fluorescence was observed in the nuclear envelope, the ER and, putatively, the apoplast as expected for a secretory protein, but we did not observe fluorescent aggregates (Figure 1a). Apparently IL-22 does not aggregate and therefore we expected human IL-22 to reach a higher soluble yield in plants than human IL-10. To test this hypothesis, we transiently expressed both cytokines by agroinfiltration in *Nicotiana benthamiana* plants. IL-10 and IL-22 yield was determined at 3, 5 and 7 days post infiltration (dpi) using sandwich ELISA's (Figure 1b). A maximum yield of 5.4 µg IL-22/mg total soluble protein (0.54% TSP) was obtained at 5 dpi, which was significantly higher when compared to IL-10 (P=0.003). Overall yield of soluble IL-22 was approximately 10-fold higher than the yield of IL-10.

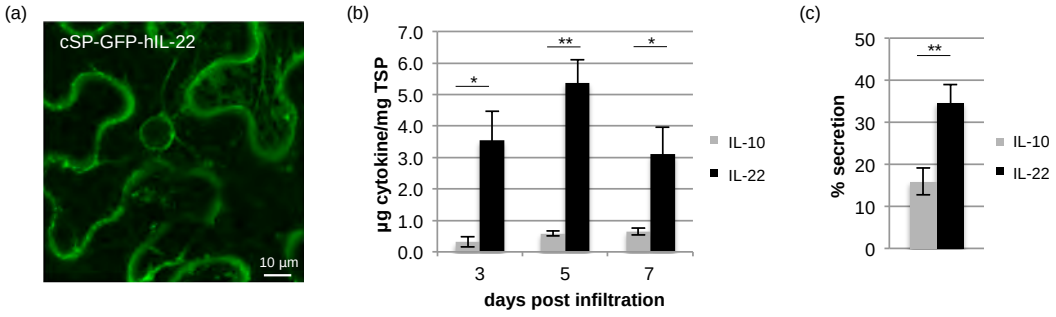

Figure 1 ◆ Analysis of IL-22 expression in agroinfiltrated *Nicotiana benthamiana* leaves. (a) Whole mount confocal microscopy output of secreted IL-22 with N-terminally fused GFP. (b) Yield of human IL-10 and IL-22 in crude extracts at 3, 5 and 7 days post infiltration (dpi) as determined by ELISA (n=4, error bars indicate standard error). (c) Percentage of secretion of IL-10 and IL-22 by determining the amount of cytokine in apoplast fluids versus crude extracts (n=4, error bars indicate standard error). (cSP: *Arabidopsis thaliana* chitinase signal peptide; TSP: total soluble protein). Asterisk(s) indicate significant differences as determined by a Welch's t-test (*P<0.05; ** P<0.005).

Aggregation can prevent secretion of recombinant proteins into the apoplast. Therefore, we determined the level of secretion for both cytokines at 5 dpi. As expected, IL-22 is secreted more efficiently into the apoplast than IL-10 (P=0.003). Up to 35% of the produced IL-22 could be isolated from the apoplast, whereas 16% of IL-10 was secreted.

Altogether we conclude that recombinant IL-22 does not aggregate *in planta,* which in turn explains the significantly higher yield of IL-22 compared to IL-10.

Secreted IL-22 is biologically active

To enable purification of IL-22 we replaced the native signal peptide with the signal peptide of the *Arabidopsis thaliana* chitinase gene (cSP) followed by a N-terminal 6x histidine tag and FLAG tag (H6F). cSP-H6F-IL-22 was expressed and purified from the leaf apoplast at 5 dpi. Apoplast purification ensures that the N-glycan composition is as homogenous as possible, since all proteins have passed the entire secretory pathway. Up to 200 µg IL-22 was purified from collected apoplast fluid of 12 agroinfiltrated plants, and analysed by SDS-PAGE and Oriole fluorescent gel staining to check purity. IL-22 produced in *E. coli* and HEK293 cells were taken along for comparison. Purified plant-produced IL-22 migrated as different proteins ranging from ~20-32 kDa in size (Figure 2a). The theoretical molecular weight of H6F-IL-22 without N-glycans is 19.3 kDa and therefore the lowest band (~20kDa) most likely represents non-glycosylated H6F-IL-22. The higher molecular weight bands most likely represent H6F-IL-22 with different numbers of N-glycans. Recombinant IL-22 from *E. coli* migrated as a single band just above 15 kDa, which resembles the molecular weight of unglycosylated IL-22. HEK293 cell produced IL-22 migrated as different proteins ranging from ~20-32 kDa in size, just like plant-produced IL-22. Western blot analysis with a goat polyclonal anti-IL-22 antibody almost gave an identical picture as the Oriole stained gel (Figure 2b). However, the prominent band for plant-produced IL-22 at ~20 kDa is hardly detected by this antibody. The band therefore does likely not only resemble non-glycosylated IL-22, but also a contaminating plant protein.

To evaluate N-glycan maturity of plant-expressed IL-22 we treated purified IL-22 with PNGase F *in vitro*. PNGase F releases all N-glycan types from a protein backbone except for N-glycans that are core α1,3-fucosylated. Four bands were detected for H6F-IL-22 by anti-FLAG western blot and all 4 bands were almost completely deglycosylated by PNGase F treatment (Figure 2c). Plant-produced IL-22 most likely exists as four differentially glycosylated proteins, either containing 0, 1, 2 or 3 N-glycans of which the most prominent form harbours 3 N-glycans. Furthermore, these results also reveal that the majority of the N-glycans on plant-produced IL-22 do not contain core α1,3-linked fucose.

PNGase F was therefore used to release the N-glycans from IL-22 produced in plants or HEK293 cells and the released N-glycans were subjected to MALDI-TOF-MS analysis. The N-glycan profile for plant-produced IL-22 consists of ~50% of typical plant complex N-glycans (Figure 2d). Biantennary N-glycans with terminal GlcNAc residues or

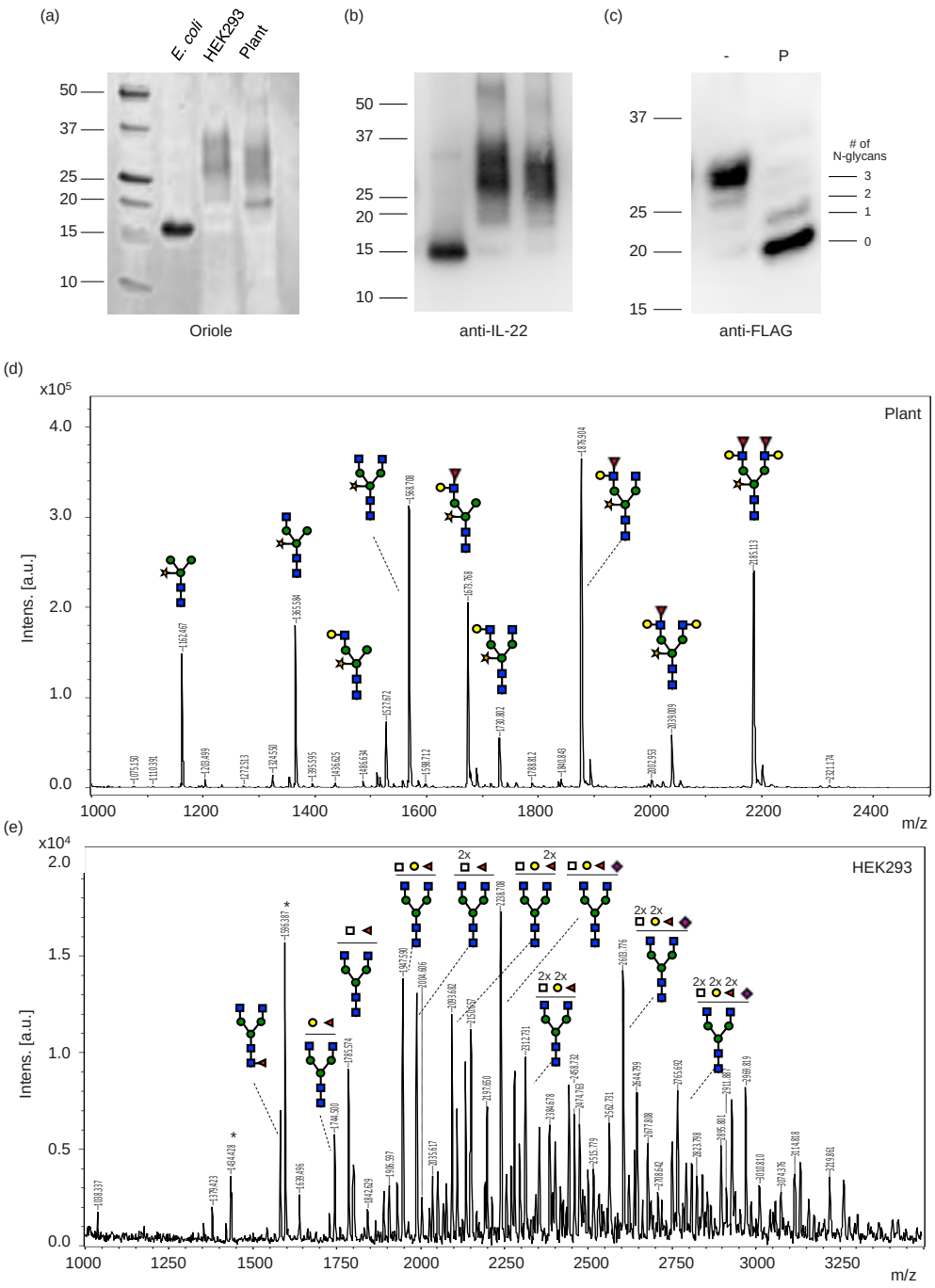

Figure 2 ◆ Purification and biological activity of plant-produced IL-22. (a) SDS-PAGE analysis under reducing conditions followed by Oriole fluorescent gel staining of apoplast purified IL-22 (500 ng). As controls, 500 ng of recombinant human IL-22 from *E. coli* or HEK293 cells was used. (b) Anti-IL-22 western blot analysis under reducing conditions of 100 ng IL-22 from *E. coli*, HEK293 cells or purified from the plant apoplast. (c) Anti-FLAG western blot analysis under reducing conditions of 100 ng apoplast purified IL-22 upon *in vitro* treatment with PNGase F (P). Next to the figure, the bands are indicated for H6F-IL-22 that most likely contain 0, 1, 2 or 3 N-glycans. N-glycan composition was analysed using MALDI-TOF-MS analysis upon PNGase F release. N-glycan profiles are given for IL-22 purified from *N. benthamiana* leaf apoplast fluid (d) and for IL-22 from HEK293 cells (e). Asterisk (*) indicates peaks in the N-glycan profile that do no resemble N-glycans.

paucimannosidic type N-glycans were found, which all contained β1,2-xylose ((GnGnX, MGnX and MMX). Interestingly, the remaining 50% of the N-glycan types contained the Lewis A structure (for enzymatic confirmation of the Lewis A structure see Figure S1), which is atypical for heterologous plant expressed glycoproteins. However, the N-glycan profile does not completely reflect the native N-glycan profile as a minor fraction of core α1,3-fucose containing N-glycans was excluded from analysis by the use of PNGase F. The N-glycan profile for HEK293 cell produced IL-22 is given in figure 2e and shows a heterogeneous mixture of complex N-glycans with 2 or 3 branches that terminate in either GlcNAc, GalNAc, galactose, sialic acid and/or (sialyl-)Lewis X. Furthermore, fucose residues are also found on the N-glycans of human cell-produced IL-22 and enzymatic digestion with α(1-3,4)-fucosidase reveals that the N-glycans that harbour only one fucose residue are hardly affected by this treatment. Therefore, the majority of HEK293 cell-produced IL-22 is core α1,6-fucosylated (Figure S2).

To test whether plant-produced IL-22 is biologically active, we investigated the ability of plant-produced IL-22 to induce IL-10 expression in the human colon carcinoma cell line Colo-205 [21]. Colo-205 cells were treated overnight with plant-produced IL-22 or recombinant IL-22 from *E. coli* or HEK293 cells and IL-10 expression was determined in culture supernatants by ELISA. We did not find significant differences in activity between IL-22 produced in plants, *E. coli* or HEK293 cells (Figure S3a). Plants are therefore a suitable platform for the expression of biologically active human IL-22.

The N-glycan on Asn54 influences the composition of another N-glycan

Since unglycosylated IL-22 from *E. coli* is as active as N-glycosylated IL-22 from plants and human cells, we questioned whether N-glycosylation is indeed required for IL-22 activity as has been suggested in literature [14]. As N-glycans can also play a role in protein folding, it is possible that the N-glycan on Asn54 contributes to the folding of IL-22 *in vivo* and/or to the folding of the region of IL-22 that is involved in IL-10R2 binding. To investigate the role for N-glycosylation of Asn54 on IL-22 folding we transiently expressed an IL-22^{N54S} glycan mutant in *N. benthamiana*. We also co-expressed IL-22 with ER-retained PNGase F to deglycosylate IL-22 *in planta* as reported previously [22].

Misfolding can result in ER retention [23], which consequently leads to reduced secretion and enrichment of oligomannose type N-glycans. Therefore, we determined the percentage of secretion into the apoplast upon expression of IL-22, IL-22^{N54S} and IL-22 with PNGase F. Secretion efficiency increased to 50% for all three N-glycan variants upon use of the chitinase signal peptide (Figure 3a). Co-expression of PNGase F did not influence IL-22 yield, whereas mutagenesis of Asn54 increased yield by ~2-fold (data not shown). A role for N-glycosylation on Asn54 in preventing misfolding is unlikely as IL-22, IL-22^{N54S} and deglycosylated IL-22 are equally well expressed and secreted.

The three IL-22 N-glycan variants were purified from the apoplast and then deglycosylated *in vitro* with PNGase F or Endo H. Anti-FLAG western blot was performed to resolve their N-glycosylation pattern (Figure 3b). Western blot analysis revealed that apoplast purified IL-22 is indeed completely deglycosylated upon co-expression of ER-retained PNGase F *in planta* (Figure 3b, right panel). In contrast to the other IL-22 variants, PNGase F co-expression resulted in the formation of dimers (~38 kDa) and multimers (data not shown). This could indicate misfolding or aggregation of IL-22 in the complete absence of N-glycans, which is possible when PNGase F removes the N-glycans before proper folding can occur.

As expected, IL-22^{N54S} migrates through the gel as three protein bands instead of four and the band with the highest mass observed for IL-22 is absent. This confirms that the N-glycan on Asn54 is absent (Figure 3b, middle panel). Endo H treatment of apoplast purified IL-22 revealed that no oligomannose type N-glycans were present on any of the purified IL-22 N-glycan variants. This indicates that secreted IL-22 and IL-22^{N54S} fold correctly. Figure S4 gives a similar overview of glycosidase treatments of intracellular IL-22 and IL-22^{N54S} or when isolated from the apoplast. Intracellular IL-22 and IL-22^{N54S} are almost completely sensitive towards Endo H digestion, which indicates that intracellular IL-22 carries N-glycans of the oligomannose type. Purification of apoplastic IL-22 is therefore favoured to study the role of complex N-glycans on biological activity.
Strikingly, IL-22^{N54S} was only partially sensitive to PNGase F digestion, because this treatment did not increase the band intensity of the smallest band on western blot (Figure 3b, middle panel). Therefore, one of the two remaining N-glycans on IL-22^{N54S} contains typical plant core α1,3-fucose, which is different when compared to the heterologous expressed native IL-22. Mutation of Asn54 therefore seems to influence core α1,3-fucosylation of the N-glycan on Asn68 or Asn97. To confirm this difference in N-glycan composition we released the N-glycans from IL-22 and IL-22^{N54S} by PNGase A digestion and subjected them to MALDI-TOF-MS analysis. The N-glycan profile for IL-22 reveals only minor peaks for core α1,3-fucosylated N-glycans and confirms that the N-glycans hardly carry this typical plant sugar residue as was shown with PNGase F digestion (Figure 3c). In contrast, the majority of the N-glycans of IL-22^{N54S} carried typical plant core α1,3-fucose, while the amount of Lewis A was strongly reduced (Figure 3d). The presence of a N-glycan on position Asn54 therefore seem to influence the composition of another N-glycan on IL-22.

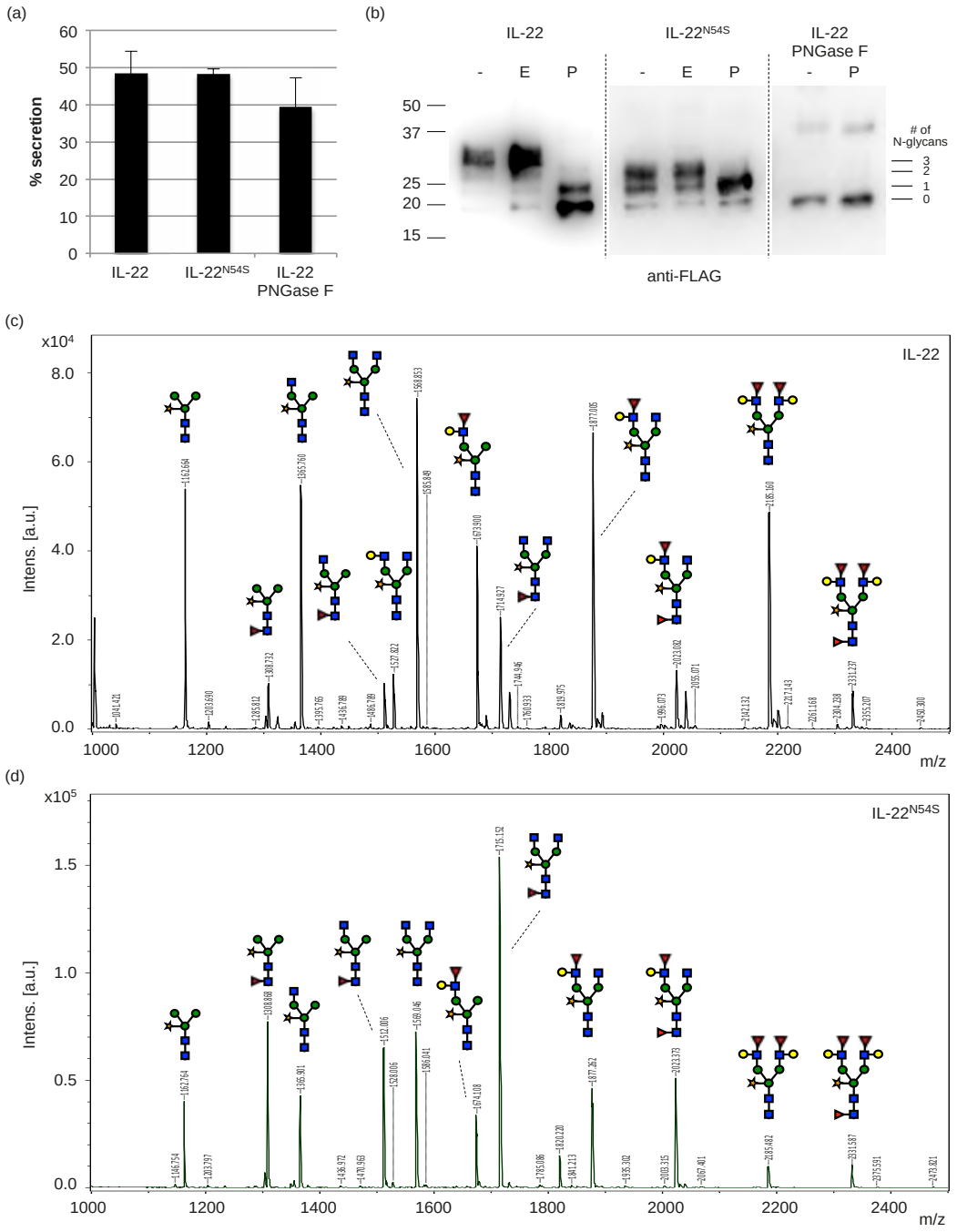

Figure 3 ◆ N-glycosylation of Asn54 on IL-22 influences the composition of another N-glycan. (a) Percentage of secretion of IL-22, IL-22^{N54S} and *in vivo* deglycosylated IL-22 (with co-expression of PNGase F) by determining the amount of IL-22 in apoplast fluids versus crude extracts (n=4, error bars indicate standard error). (b) Anti-FLAG western blot analysis under reducing conditions of 100 ng purified IL-22 or glycan variants upon *in vitro* treatment with PNGase F (P) or Endo H (E). N-glycan composition was analysed using MALDI-TOF-MS analysis upon PNGase A release. N-glycan profiles are given for IL-22 (c) and IL-22^{N54S} (d) purified from *N. benthamiana* leaf apoplast fluid.

N-glycosylation of Asn54 is not required for activity

In order to test the role of N-glycosylation on IL-22 biological activity, purified IL-22, IL-22^{N54S} and IL-22 co-expressed with ER-retained PNGase F were tested for their biological activity using Colo-205 cells. We did not find any significant difference in the induction of IL-10 expression in Colo-205 cells by the three glycan variants (Figure S3b). Surprisingly, IL-22^{N54S} was found to be active. Logsdon and co-workers previously reported IL-22^{N54A} and IL-22^{N54Q} mutants that completely lacked activity [14]. Therefore we also expressed the IL-22^{N54Q} mutant in plants and tested it for activity. IL-22^{N54Q} did not completely lack activity, but was significantly less active compared to IL-22 and IL-22^{N54S} (Figure S3c). We therefore conclude that IL-22 activity is not dependent on the presence of a N-glycan on Asn54, but is dependent on the amino acid situated at this position.

Engineering human-like N-glycans on IL-22

To exploit the possibility of engineering human-type N-glycosylation in plants, we continued to investigate the effect of core α1,6-fucosylation on IL-22 activity. Thereto, we expressed IL-22 in ΔXT/FT transgenic *Nicotiana benthamiana* plants together with mouse α1,6-fucosyltransferase with the CTS domain (C, cytoplasmic tail; T, transmembrane domain; S, stem region) of *Arabidopsis thaliana* FUT11 (mFUT8). In ΔXT/FT transgenic *Nicotiana benthamiana* plants the α1,3-fucosyltransferase and β1,2-xylosyltransferase genes are down-regulated [15]. IL-22 was again purified from the apoplast, but this time at 3 dpi as IL-22 expression peaks at this time point when the silencing suppressor p19 is not included. SDS-PAGE and western blot analysis revealed that engineered IL-22 also involves four differentially N-glycosylated proteins, which were all sensitive to *in vitro* PNGase F treatment (Figure 4a). This confirms the complete lack of core α1,3-fucose on the N-glycans of engineered IL-22.

To confirm the presence of core α1,6-fucose on IL-22 we used a fucose binding lectin from *Aleuria aurantia* [24]. In an ELISA-based assay it was shown that *A. aurantia* lectin strongly binds to engineered IL-22 (Figure 4b). *A. aurantia* lectin did not bind to IL-22 expressed in wild-type or in ΔXT/FT transgenic plants in the absence of mFUT8. Furthermore, we also used *A. aurantia* lectin on western blots to show that the lectin strongly binds to the IL-22 variants containing 2 or 3 N-glycans (Figure 4c). The N-glycan composition of IL-22 from ΔXT/FT plants was then analysed by MALDI-TOF-MS analysis (Figure 4d/e). To exclude differences between mammalian and insect cell FUT8 specificities we included an engineering strategy where we co-expressed FUT8 from *Drosophila melanogaster* (dFUT8). Figure S5 shows *A. aurantia* lectin binding and MALDI-TOF-MS analysis of IL-22 upon co-expression of dFUT8. The presence of Lewis A on the N-glycans of IL-22 is strongly reduced when IL-22 is expressed in ΔXT/FT plants.

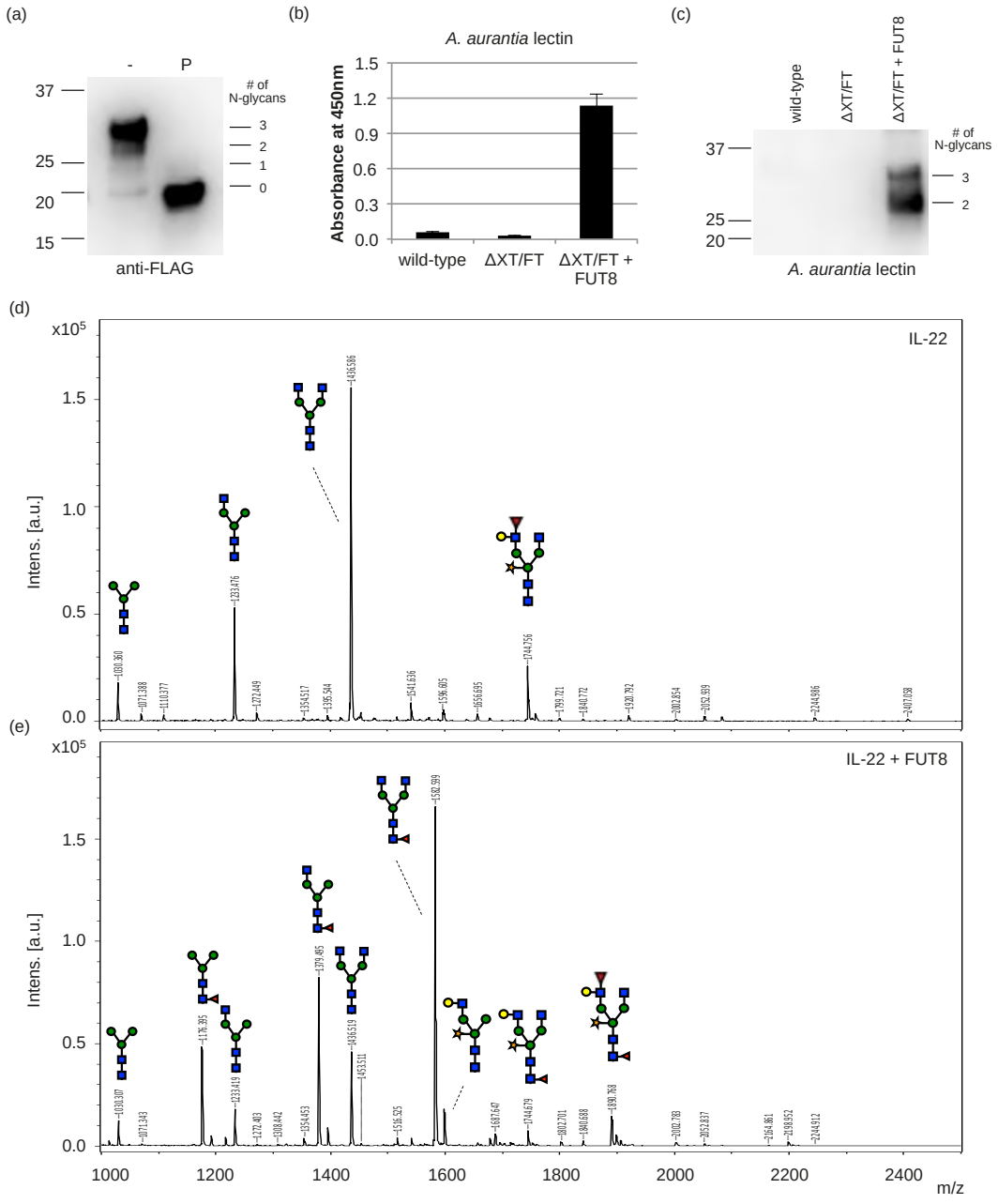

Figure 4 ◆ The effect of core α1,6-fucosylation on the activity of plant-produced IL-22. (a) Anti-FLAG western blot analysis under reducing conditions of 100 ng purified IL-22 expressed in ΔXT/FT plants together with mFUT8. Engineered IL-22 was treated with PNGase F (P) and analysed by anti-FLAG Western blot to confirm complete absence of core α1,3-fucose. (b) Binding of *Aleuria aurantia* lectin to purified IL-22 produced in wild-type and ΔXT/FT plants as determined by ELISA. (c) Western blot analysis under reducing conditions with *A. aurantia* lectin to confirm core α1,6-fucosylation of plant-produced IL-22 when expressed in ΔXT/FT together with mFUT8. N-glycan composition was analysed using MALDI-TOF-MS analysis upon PNGase A release and N-glycan profiles are given for IL-22 from ΔXT/FT plants with/without co-expression of mFUT8 (d/e).

Upon co-expression of FUT8 (both mouse and *Drosophila*) approximately 60-65% of the N-glycans on IL-22 carry core α1,6-fucose. As Asn54 carries one of the two surface exposed N-glycans of IL-22 we expect core α1,6-fucosylation of this N-glycan to occur.

Glyco-engineering of IL-22 has no effect on activity

To investigate whether core α1,6-fucosylation contributes to the biological activity of IL-22 we tested core α1,6-fucosylated IL-22 and IL-22 from wild-type plants for their ability to induce IL-10 expression in Colo-205 cells. We did not find significant differences between the activity of these two glycan variants of IL-22 (Figure 5a). Biological activity of IL-22 was also not altered when FUT8 from *Drosophila melanogaster* was used for engineering of core α1,6-fucose (Figure S5b). Finally, we also analysed the activation of the transcription factor STAT3 by IL-22 in Colo-205 cells. Lysates of IL-22 treated Colo-205 cells were subjected to western blotting with antibodies specific for STAT3 or phosphorylated STAT3 at tyrosine 705 (Y705) (Figure 5b). IL-22 expressed in *E. coli*, wild-type plants and ΔXT/FT transgenic plants together with mFUT8 were identical in their ability to activate the STAT3 signalling pathway. Together these data indicate that IL-22 activity is independent of core α1,6-fucosylation of its N-glycans.

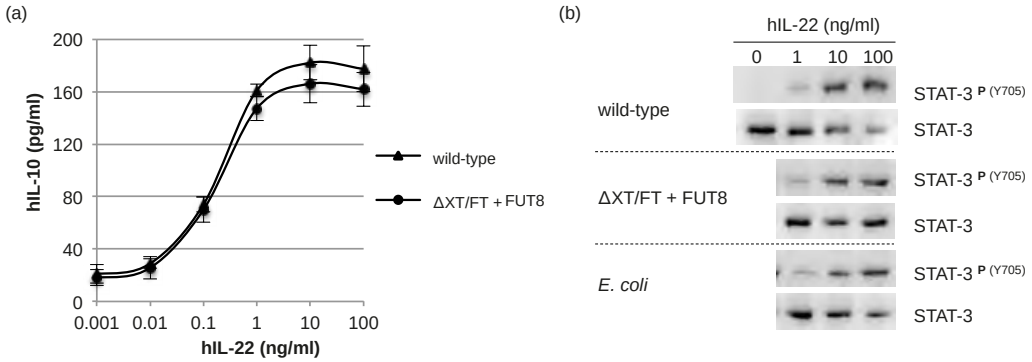

Figure 5 ◆ Core α1,6-fucose does not contribute to activity (a) Biological activity of engineered IL-22 as determined by the induction of IL-10 expression by Colo-205 cells after overnight treatment with IL-22 (*n*=4, error bars indicate standard error). (b) Western blot analysis under reducing conditions of intracellular STAT3 of Colo-205 cells treated with 0, 1, 10 or 100 ng/ml IL-22. Total STAT3 and phosphorylated STAT3 at tyrosine 705 (Y705) were analysed for IL-22 from wild-type plants, glyco-engineered IL-22 from plants and *E. coli* produced IL-22.

Discussion

Interleukin-22 (IL-22) has only recently been recognized as a signalling molecule of the human immune system with major therapeutic potential. Yet, when producing IL-22 for pharmaceutical purposes care has to be taken with regard to the choice of the expression host, notably because IL-22 activity was thought to depend on N-glycosylation [14]. A eukaryotic expression host is therefore preferred for the production of IL-22. In this study we evaluated the plant-based expression of IL-22 and exploited the possibility to synthesise human-like N-glycans in plants for optimal activity. We expressed IL-22 transiently in *Nicotiana benthamiana* by agroinfiltration and compared its yield to human IL-10. IL-10 is structurally similar to IL-22 and we reported previously that extensive multimerisation of IL-10 is a major expression bottleneck for this cytokine [20]. Extensive multimerisation of IL-10 results in the formation of large insoluble granules, but was not observed for IL-22 in this study. The lack of aggregation may explain why IL-22 yield in plants is ~10-fold higher than IL-10. The maximum yield obtained for IL-22 was 5.4 µg/mg TSP (0.54%), which is relatively high for leaf-based expression of cytokines [25]. Furthermore, up to 50% of the produced IL-22 could be isolated from the apoplastic fluid, which enabled easy purification and ensures enrichment of mature N-glycans. Plants are therefore a suitable expression platform for human IL-22.

The first striking observation was that IL-22 produced in wild-type plants carries a large proportion of N-glycans with terminal Lewis A motifs (Galβ1,3(Fucα1,4)GlcNAc). Lewis A was first described as a human blood group determinant, but has also been reported to exist in plants [26, 27]. Lewis A harbouring glycoproteins are widely distributed among plant species and mainly localize at the surface of the plant cell. Lewis A was also detected on a murine monoclonal antibody expressed in *Nicotiana tabacum* and on human erythropoietin expressed in either *Nicotiana benthamiana* or moss [28-30]. However, the presence of Lewis A on the majority of N-glycans of a heterologously produced glycoprotein is to our knowledge a rare observation. Lewis A synthesis in plants is still poorly understood. It requires β1,3-galactosyltransferase and this enzyme was only recently identified in *Arabidopsis thaliana* [31]. Sourrouille and co-workers did show that over-expression of human β1,4-galactosyltransferase in alfalfa inhibits not only β1,2-xylosyltransferase and α1,3-fucosyltransferase, but also completely blocks the synthesis of Lewis A in plants [32]. When we expressed IL-22 in ΔXT/FT plants, the Lewis A motif was almost completely absent. This observation, combined with the fact that our human IL-22 almost completely lacks core α1,3-fucose, suggests that the enzymes that synthesize Lewis A in plants require the presence of β1,2-xylose. Alternatively, the silencing construct used to target plant core α1,3-fucosyltransferase in ΔXT/FT plants also down-regulates the expression of the fucosyltransferase responsible for synthesizing the Lewis A structure. IL-

22 would be an ideal candidate to further investigate the processes of Lewis A synthesis in plants.

In this study we also analysed the N-glycan composition of IL-22 produced by HEK293 cells. IL-22 from HEK293 cells carries a heterogeneous mixture of complex N-glycans with 2 or 3 branches that either terminate with GlcNAc, GalNAc, galactose, sialic acid and/or (sialyl-)Lewis X. Similarly, plant-produced IL-22 carries highly complex plant N-glycans terminating in Lewis A structures. However, the majority of the N-glycans of IL-22 from HEK293 cells carry the core α1,6-fucose suggested to be indispensible for biological activity. Regardless of the differences in N-glycan composition, we did show that plant-produced IL-22 retained its biological activity and that there was no difference between IL-22 expressed in plants, bacteria or human cells. This addressed the question whether N-glycosylation indeed plays a role in IL-22-mediated responses as reported previously by Logsdon and co-workers [14].

Besides the difference in N-glycosylation there is another major difference between *E. coli* expressed IL-22 and IL-22 from eukaryotic cells, which is the need for chemical refolding after production in *E. coli*. Chemical refolding results in biologically active IL-22, which is structurally very similar to insect cell produced IL-22 [10, 11]. However, during *in vivo* protein folding in eukaryotic cells N-glycans can aid in the correct folding of a protein and provide additional stability. This may explain the need for N-glycosylation of IL-22 when produced in eukaryotic cells. Therefore we evaluated whether N-glycosylation plays a role in the correct folding of IL-22 by site-directed mutagenesis of Asn54 or co-expression of PNGase F *in planta*. This strategy allows investigation of the role of N-glycosylation on IL-22 folding, as misfolding may result in ER-retention and/or enrichment of oligomannose type N-glycans. The addition of an N-glycan on Asn54 is completely abolished by mutagenesis of the N-glycosylation site and therefore cannot contribute to protein folding. But, when co-expressing ER-retained PNGase F, N-glycans are initially attached to the glycoprotein and can assist the folding process before being removed by PNGase F. In case of IL-22, removal of the N-glycan on Asn54 by mutagenesis (IL-22^{N54S}) or complete deglycosylation with PNGase F did not result in reduced secretion, enrichment of oligomannose type N-glycans, nor did it alter the biological activity of IL-22. But what we did observe for IL-22^{N54S} is a difference in core α1,3-fucosylation of another N-glycan, most likely the N-glycan on surface exposed Asn68. The fact that mutation of Asn54 influences core α1,3-fucosylation of other N-glycans could indicate that N-glycosylation of Asn54 influences local folding of IL-22, making one of the other N-glycans more accessible for α1,3-fucosyltransferase.

Another advantage of PNGase F is that it deaminates asparagine to aspartic acid [25]. PNGase F therefore has the same result as site-directed mutagenesis by turning all N-X-S/T N-glycosylation signals into D-X-S/T sites. So, in our study we have mutated IL-22 in both IL-22^{N54S} and, effectively, IL-22^{N54D} without loosing biological activity. This is in contrast

to observations with the IL-22^{N54A} and IL-22^{N54Q} mutants, which lack both IL-10R2 binding and biological activity [14]. We also mutated Asn54 to a glutamine (IL-22^{N54Q}) and in our assay on Colo-205 cells the activity of the mutant was indeed significantly reduced, but not completely abolished. We therefore conclude that the amino acid situated on position 54 is important for biological activity and not the presence of a N-glycan.

From the assays described above we concluded that core α1,6-fucose does not contribute to IL-22 activity. Yet, the N-glycan composition of human cell produced IL-22 is very heterogeneous and does not resemble the N-glycan composition of previously reported insect cell produced IL-22 [9]. Therefore we used ΔXT/FT plants combined with the co-expression of α1,6-fucosyltransferase (FUT8) to engineer a more homogeneous human-like N-glycan on IL-22 [15, 16]. As IL-22 has previously been produced in *Drosophila* S2 cells, we used FUT8 from both mouse and *Drosophila* to exclude differences in enzyme specificity. The N-glycan profiles for IL-22 obtained with these two glycosyltransferases were almost identical as revealed by MALDI-TOF-MS analysis. Therefore, we can conclude that the specificity of these two FUT8 enzymes is not significantly different. In both cases we obtained N-glycans of which ~60-65% (two out of three N-glycans) carried core α1,6-fucose. This is in line with the observation by Xu and co-workers who found that there is always at least one out of three N-glycans without a core α1,6-fucose [9]. As both Asn54 and Asn68 carry a surface exposed N-glycan it is most likely that the N-glycan on Asn97 is not core fucosylated. Furthermore, the N-glycosylation signal of Asn97 contains the hydrophobic amino acid phenylalanine on position X. This is in line with our previous hypothesis that hydrophobic amino acids (like leucine and valine) within the N-X-S/T signals of human IgA inhibit core-altering fucosyltransferases [33]. Yet, when IL-22 is produced in ΔXT/FT plants core α1,6-fucosylation of IL-22 is efficient. The amount of Lewis A was strongly reduced when IL-22 was expressed in ΔXT/FT plants, but also when Asn54 was mutated into a serine. We therefore speculate that the presence of Lewis A might prevent the addition of core α1,3-fucose in wild-type plants. The core modifying α1,3-fucosyltransferase and α1,4-fucosyltransferase might compete for the N-glycans on IL-22 as a donor substrate. Most important was the observation that even though we were able to engineer homogeneous human-like N-glycans carrying core α1,6-fucose on IL-22, we did not observe significant differences in activity between core α1,6-fucosylated IL-22 and IL-22 produced in ΔXT/FT plants without co-expression of FUT8.

An important question that also needs to be addressed for pharmaceutical purposes is whether the human-like N-glycans engineered in this study actually resemble the native N-glycans found on human IL-22. To our knowledge, the native N-glycan composition on serum IL-22 has not been reported. Analysing the N-glycan composition of serum cytokines is difficult as serum cytokine levels are typically in the picogram range [34]. Nevertheless, a homogeneous N-glycan composition of IL-22 is preferred for

pharmaceutical purposes. Unlike HEK293 cell produced IL-22, a homogeneous human-like N-glycan composition can be obtained when producing IL-22 in plants as shown in this study. Additionally, the N-glycans on plant-produced IL-22 carry terminal GlcNAc residues, which is in contrast to insect cell produced IL-22 [9]. The presence of terminal GlcNAc can protect IL-22 from internalization by antigen presenting cells via the mannose receptor, which binds terminal mannose containing glycans [35]. This indicates that plants might be a preferred platform for the production of IL-22.

Our study demonstrates that plants are a suitable platform for the production of biologically active human IL-22. Furthermore, we show that plants can be used to study the role of N-glycans on protein folding and that plants are versatile in the type of N-glycans they can synthesize. This, combined with the speed of transient expression by means of agroinfiltration, makes *Nicotiana benthamiana* an excellent tool for studying the role of N-glycans on glycoproteins.

Experimental procedures

Construction of expression vectors

The complete open reading frame of human IL-22 was synthetically constructed by GeneArt (Life Technologies, Bleiswijk, the Netherlands). The IL-22 sequence was flanked by NcoI and KpnI restriction sequences at 5' and 3' ends respectively. The sequence encoding the last two amino acids of the signal peptide where modified to a NheI restricition site without changing the amino acid sequence. The IL-22 sequence was inserted into the pHYG plant expression vector by NcoI/KpnI [20].

To create a GFP fusion of IL-22 an AscI/SacI 35S promoter-cSP-GFP fragment was isolated from pHYG-cSP-GFP and used to replace the 35S-Fcα sequence in pHYG-hFcα-IL-10 (both vectors were previously published, [20]). The sequence for hIL-10 was then removed by SpeI/KpnI and replaced by a NheI-KpnI fragment of IL-22. This creates a cSP-GFP-IL-22 construct where IL-22 and GFP are separated by a glycine-serine linker.

To create a tagged version of IL-22 for purification purposes, the *Arabidopsis* chitinase signal peptide (cSP) followed by a 6x histidine and FLAG tag were synthetically constructed by GeneArt (Life Technologies). The cSP-H6F fragment was used to replace the native IL-22 signal peptide in the pHYG expression vector (cSP-H6F-IL-22) using NcoI/NheI restriction sites. cSP-H6F-IL-22^{N54S} and cSP-H6F-IL-22^{N54Q} were created by means of overlap extension PCR.

PNGase F from *Flavobacterium meningosepticum* with a N-terminal chitinase signal peptide (cSP) and a C-terminal FLAG tag and KDEL ER-retention signal was codon optimized and the full gene was synthesized by GeneArt (Life Technologies) and subsequently cloned into pBINPLUS [36].

Fucosyltransferase 8 from *Drosophila melanogaster* (dFUT8) was amplified from cDNA (kindly provided Christina May from the Genetics department at Wageningen University). Subsequently, dFUT8 was cloned into the pBINPLUS expression vector.

Expression of all genes was driven by the 35S promoter of the *Cauliflower mosaic virus* with duplicated enhancer (d35S) and the *Agrobacterium tumefaciens* nopaline synthase transcription terminator (Tnos). In most experiments the silencing suppressor p19 from tomato bushy stunt virus in pBIN61 was co-infiltrated to prevent yield loss after 3 dpi [37]. For glyco-engineering of IL-22 an expression vector for mouse α1,6-fucosyltransferase 8 fused to the CTS region of the *Arabidopsis thaliana* FUT11 gene (mFUT8) and ΔXT/FT *Nicotiana benthamiana* plants were used [15, 16]. P19 was never co-expressed with IL-22 in ΔXT/FT plants to avoid possible loss of silencing of xylosyltransferase and fucosyltransferase.

Agroinfiltration of *Nicotiana benthamiana*

Agrobacterium tumefaciens clones were cultured for 16 hours at 28°C/250 rpm in LB medium containing 50 µg/ml kanamycin, 20 µg/ml rifampicin and 20µM acetosyringone. The bacteria were resuspended in MMA infiltration medium (20g/l sucrose, 5g/l MS-salts, 1.95g/l MES, pH5.6) containing 200µM acetosyringone to an optical density (OD) of 0.5-1. For co-infiltration experiments with *Agrobacterium* harbouring the mFUT8 expression vector or PNGase F expression vector a final OD of 0.1 was used. After 1-2 hours incubation at room temperature leaves of 5-6 weeks old *Nicotiana benthamiana* plants were infiltrated.

Confocal microscopy

Plants were agroinfiltrated with *A. tumefaciens* harbouring the expression vector encoding a N-terminal fusion of GFP to IL-22 as described above. Leaves were harvested 3 days post infiltration and were examined from the abaxial side using a Zeiss LSM510 confocal laser-scanning microscope in combination with an argon ion laser supplying a 488 nm wavelength.

Total soluble protein extraction

Leaves were snap-frozen upon harvesting and homogenized in liquid nitrogen. Homogenized plant material was ground in ice-cold extraction buffer (50mM phosphate-buffered saline (pH=8), 100 mM NaCl, 0.1% v/v Tween-20 and 2% w/v immobilized polyvinylpolypyrrolidone (PVPP)) using 2 ml buffer per gram fresh leaf weight. Crude extracts were clarified by centrifugation at 16.000x*g* at 4°C.

Isolation of apoplast fluid

Leaves were vacuum infiltrated with ice-cold extraction buffer (50mM phosphate-buffered saline (pH=8), 100 mM NaCl and 0.1% v/v Tween-20). Leaves were centrifuged for 20 min. at 2000xg to isolate apoplast fluid. Apoplast fluids were clarified by centrifugation at 16.000x*g* at 4°C. To determine the percentage of secretion, the remaining leaf material was processed as described above.

Quantification of cytokine yield

IL-10 and IL-22 protein concentrations in crude plant extract or apoplast fluids were determined by ELISA. Human IL-10 or IL-22 Ready-SET-Go!® ELISA kits (eBioscience; Vienna, Austria) were used according to supplier's protocol. For sample comparison the total soluble protein (TSP) content was determined by the BCA method (Life Technologies) according to supplier’s protocol using bovine serum albumin (BSA) as a standard.

Purification of IL-22

Plant-produced IL-22 was purified from apoplast fluids using Ni-NTA Sepharose (Westburg B.V., Leusden, The Netherlands). Apoplast fluid was transferred over G25 Sephadex columns to exchange for Ni-NTA binding buffer (50 mM phosphate buffered saline (pH 8) containing 100 mM NaCl). Ni-NTA Sepharose was incubated with the apoplast fluid for 30 minutes, followed by 3 washing steps with binding buffer. IL-22 was eluted from the Ni-NTA Sepharose using binding buffer supplemented with 0.5M imidazole. Finally, purified IL-22 was dialysed against PBS.

Protein analysis and western blot

Purified IL-22 was separated under reducing conditions by SDS-PAGE on a 12% Bis-Tris gel. To analyse purity of the proteins, the gel was stained with Oriole Fluorescent Gel Stain (Bio-Rad). Recombinant human IL-22 from *E. coli* (R&D Systems; Abingdon, UK) or HEK293 cells (Bioké; Leiden, The Netherlands) were used as controls. For western blotting, proteins were transferred to a PVDF membrane. For visualisation HRP conjugated anti-FLAG M2 antibody (Sigma-Aldrich; Zwijndrecht, the Netherlands) or a goat polyclonal antibody directed against human IL-22 (R&D Systems) followed by incubation with a HRP-conjugated secondary antibody (Jackson ImmunoResearch, Suffolk, UK) were used. SuperSignal West Femto or Dura substrate (Thermo Fisher Scientific; Etten-Leur, the Netherlands) was used to detect HRP-conjugated antibodies in the G:BOX Chemi System (Syngene; Cambridge, UK).

N-glycan analysis of IL-22

IL-22 was deglycosylated with PNGase F or Endo H (both from Bioké) to screen for the presence of plant-specific α1,3-fucose or oligomannose sugars, respectively. Deglycosylated IL-22 was then detected by western blot. Biotinylated *Aleuria aurantia* lectin (Brunschwig Chemie; Amsterdam, The Netherlands) was used to confirm the presence of α1,6-fucose on engineered IL-22. A 96 wells plate was used to coat IL-22 overnight at a concentration of 100 ng/ml. The plate was then blocked with 1% w/v BSA in PBST and all subsequent steps were performed in blocking buffer. Biotinylated lectin (2 µg/ml) was loaded onto the ELISA plate and the procedure was continued according to the IL-22 ELISA (eBioscience). Biotinylated *Aleuria aurantia* lectin was also used to detect α1,6-fucose on 100 ng IL-22 upon blotting using the same conditions as in the ELISA.

For N-glycan analysis, glycans were released from 5-10 µg IL-22 by PNGase F digestion (Bioké). Alternatively, IL-22 was digested with trypsin (Sigma-Aldrich) followed by N-glycan release with 0.5 mU PNGase A (Roche, Woerden, the Netherlands). Released N-glycans were purified over C18 Baker-bond™ SPE cartridges (VWR, Amsterdam, the Netherlands) and subsequent Extract Clean™ Carbo SPE columns (Grace, Breda, the Netherlands). N-glycans were labelled with anthranilic acid (AA) (Sigma-Aldrich), desalted

over Biogel P10 (BioRad). MALDI-TOF-MS analysis and fucosidase treatment was performed as previously described [38]. Illustrations of different glycoforms and sugar residues are given in Figure S6 to complement the N-glycan profiles.

Biological activity assay

Human Colo-205 colon epithelial cells (CLS Cell Lines Service GmbH; Eppelheim, Germany) were maintained at 37°C with 5% CO_2 in RPMI-1640 medium containing 4 mM L-glutamine, 25 mM HEPES and supplemented with 10% fetal calf serum, 50 µM β-mercaptoethanol, 50 U/ml penicillin and 50 µg/ml streptomycin. Colo-205 cells were harvested by trypsinisation and seeded at a density of $3.0x10^5$ cells/ml in 96 well plates and were allowed to rest overnight. For bioassays cells were treated with 0.001-10 ng/ml plant produced IL-22 or recombinant IL-22 from *E. coli* (R&D Systems) or HEK293 cells (Bioké). After overnight incubation, expression of human IL-10 was analysed using the Human IL-10 Ready-Set-Go!® ELISA kit (eBioscience) according to the supplier's protocol.

STAT3 activation

$3x10^6$ Colo-205 cells were treated for 20 min. with IL-22 (0, 1, 10 or 100 ng/ml). Cells were then washed with PBS and lysed using 1x Cell Lysis Buffer (Bioké). Total soluble protein content in the lysates was determined by the BCA method (Life Technologies) and 10 µg total protein was separated on 12% Bis-Tris gels. Monoclonal antibodies specific for STAT3, and phospho-$STAT3^{Y705}$ (both from Bioké) and HRP-conjugated secondary antibody (Jackson ImmunoResearch) were used for western blotting as described above. All antibodies were diluted in PBST containing 1% w/v BSA.

Data analysis

All data shown in the figures indicate the average of at least three biological replicates (*n*), which is indicated in the figure legends. Significant differences were calculated with a Welch's t-test and regarded significant when $P<0.05$. Significant differences are indicated in the figures by an asterisk(s) ($P<0.05$ = * and $P<0.005$ = **).

Acknowledgements

We thank Dr. Hertha Steinkellner for providing our lab with the mFUT8 expression construct as well as the ΔXT/FT *Nicotiana benthamiana* plants. We also thank Lizeth G. Meza Guzman and Sandra de Jongh for their input in the practical work of this study.

Supplemental Figures

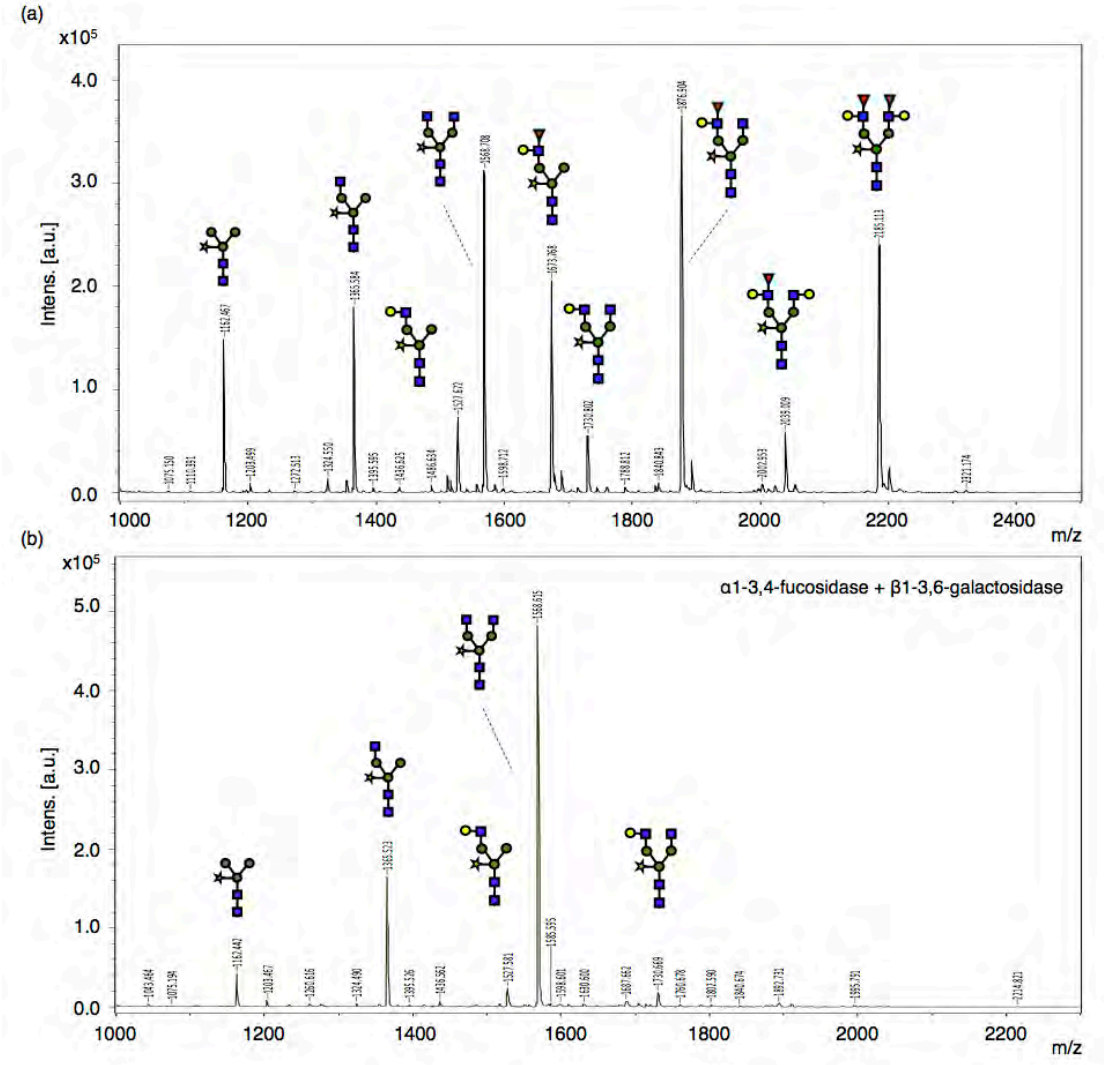

Figure S1 ◆ Enzymatic confirmation of the presence of Lewis A structures on IL-22. N-glycans from purified IL-22 were analysed by MALDI-TOF-MS upon PNGase F release of N-glycans. (a) N-glycan profile for purified IL-22 from wild-type *N. benthamiana* plants. (b) Profile of the same N-glycans upon treatment with β(1-3,6)-galactosidase and α(1-3,4)-fucosidase both from *Xanthomonas manihotis*.

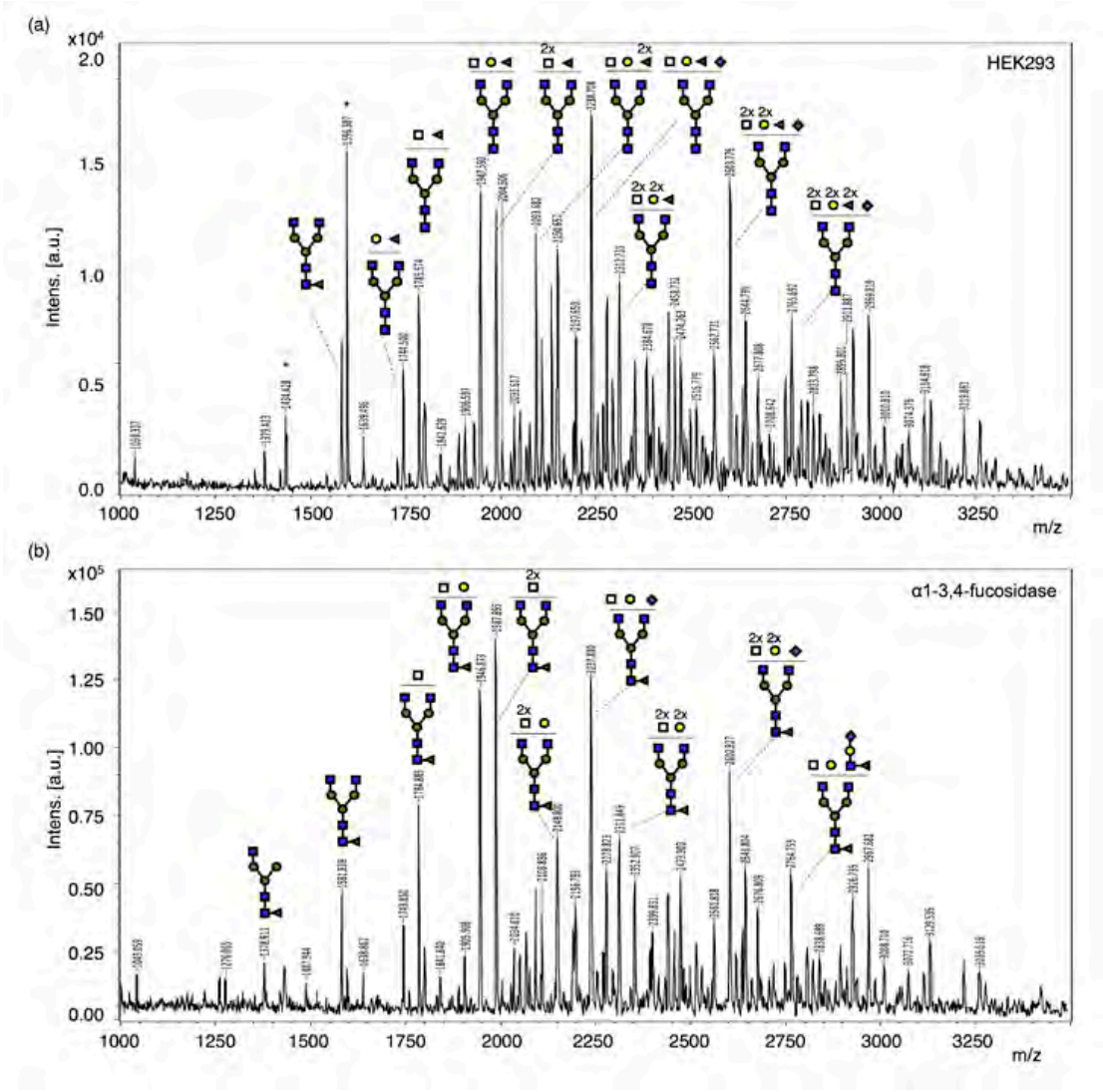

Figure S2 ◆ Enzymatic confirmation of the presence of core α1,6-fucose on IL-22. N-glycans from purified IL-22 were analysed by MALDI-TOF-MS upon PNGase F release of N-glycans. (a) N-glycan profile for IL-22 from HEK293 cells. (b) Profile of the same N-glycans upon treatment with α(1-3,4)-fucosidase both from *Xanthomonas manihotis*.

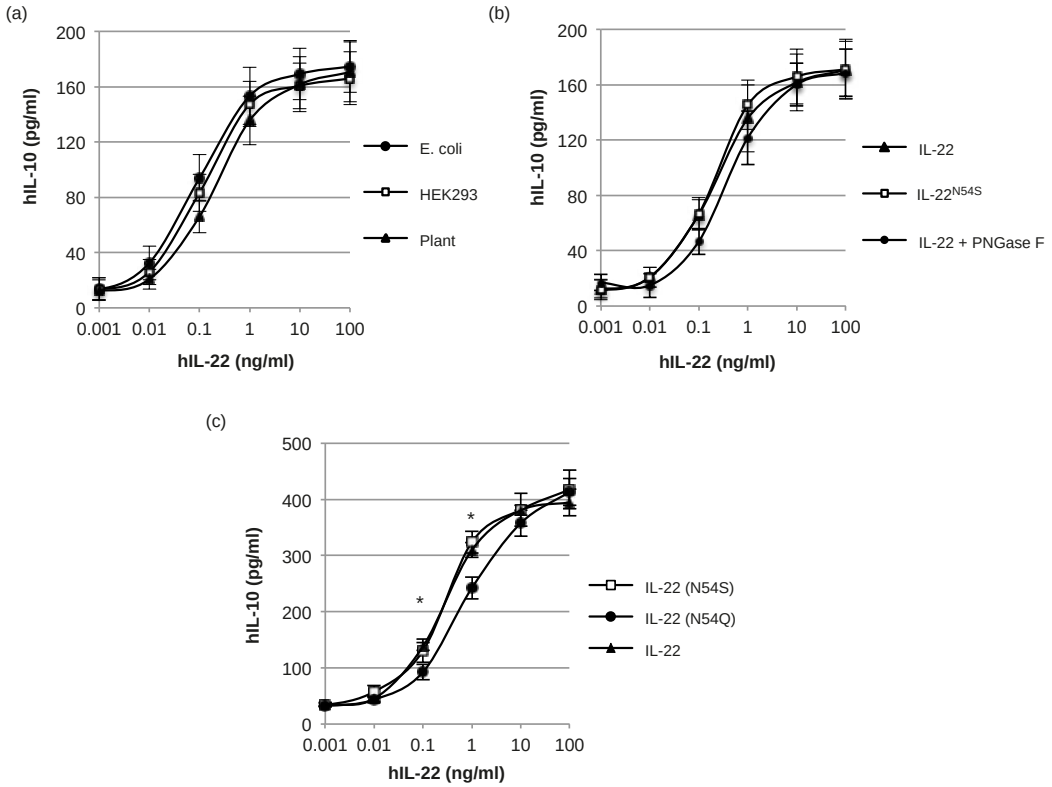

Figure S3 ◆ Biological activity of recombinant *E. coli*, HEK293 and plant-produced IL-22 variants. Biological activity of IL-22 as determined by the induction of IL-10 expression by Colo-205 colon carcinoma cells after overnight treatment with IL-22. As controls, recombinant human IL-22 from *E. coli* or HEK293 cells were used (*n*=4, error bars indicate standard error). Asterisk (*) indicate *P*<0.05.

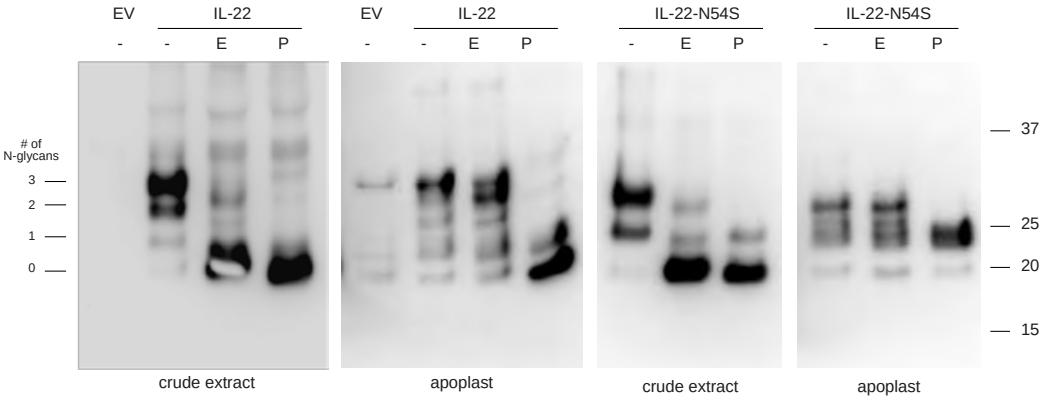

Figure S4 ◆ Comparison of N-glycan maturity of intracellular and apoplastic IL-22. Anti-FLAG western blot analysis of 100 ng IL-22 under reducing conditions. IL-22 and IL-22^{N54S} were isolated from the apoplast, followed by crude extraction to obtain intracellular fractions of IL-22. N-glycan maturity was assessed by *in vitro* treatment with PNGase F (P) or Endo H (E).

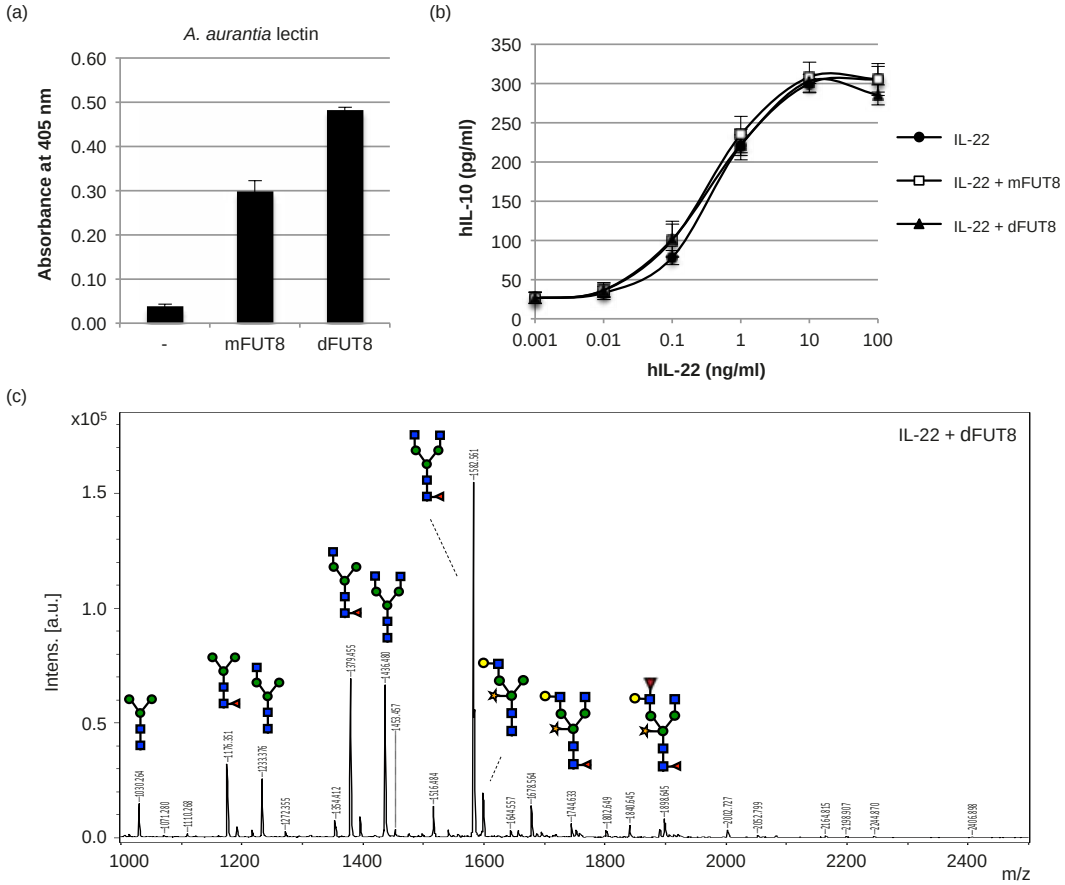

Figure S5 ◆ Comparison of core α1,6-fucosylation of IL-22 by FUT8 from mice and *Drosophila*. (a) Binding of *Aleuria aurantia* lectin to purified IL-22 produced in ΔXT/FT plants upon co-expression of mFUT8 or dFUT8. PNGase F deglycosylated anti-IL-22 antibody was used to capture plant-produced IL-22, followed by detection with *A. aurantia* lectin. (b) Biological activity of engineered IL-22 as determined by the induction of IL-10 expression in Colo-205 cells after overnight treatment with IL-22 (*n*=3, error bars indicate standard error). (c) N-glycan profile for IL-22 from ΔXT/FT plants upon co-expression of dFUT8.

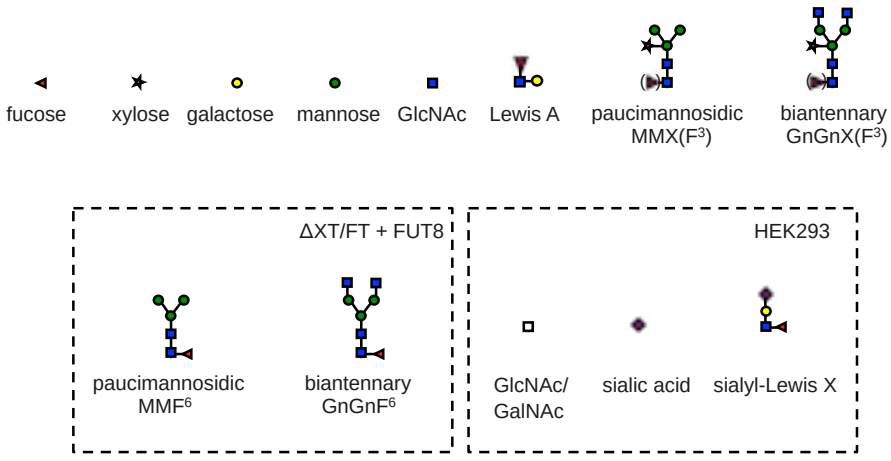

Figure S6 ◆ Illustrations of different glycoforms and sugar residues described in this study.

References

1. Sabat R, Ouyang W and Wolk K (2014) Therapeutic opportunities of the IL-22-IL-22R1 system. Nature Reviews Drug Discovery 13: 21-38.
2. Dumoutier L, Louahed J and Renauld JC (2000) Cloning and characterization of IL-10-related T cell-derived inducible factor (IL-TIF), a novel cytokine structurally related to IL-10 and inducible by IL-9. Journal of Immunology 164: 1814-1819.
3. Dumoutier L, Van Roost E, Colau D and Renauld JC (2000) Human interleukin-10-related T cell-derived inducible factor: molecular cloning and functional characterization as an hepatocyte-stimulating factor. Proceedings of the National Academy of Sciences of the United States of America 97: 10144-10149.
4. Wolk K, Kunz S, Witte E, Friedrich M, Asadullah K, et al. (2004) IL-22 increases the innate immunity of tissues. Immunity 21: 241-254.
5. Zheng Y, Valdez PA, Danilenko DM, Hu Y, Sa SM, et al. (2008) Interleukin-22 mediates early host defense against attaching and effacing bacterial pathogens. Nature Medicine 14: 282-289.
6. Aujla SJ, Chan YR, Zheng M, Fei M, Askew DJ, et al. (2008) IL-22 mediates mucosal host defense against Gram-negative bacterial pneumonia. Nature Medicine 14: 275-281.
7. Xie MH, Aggarwal S, Ho WH, Foster J, Zhang ZM, et al. (2000) Interleukin (IL)-22, a novel human cytokine that signals through the interferon receptor-related proteins CRF2-4 and IL-22R. Journal of Biological Chemistry 275: 31335-31339.
8. Logsdon NJ, Jones BC, Josephson K, Cook J and Walter MR (2002) Comparison of interleukin-22 and interleukin-10 soluble receptor complexes. Journal of Interferon & Cytokine Research 22: 1099-1112.
9. Xu T, Logsdon NJ and Walter MR (2004) Crystallization and X-ray diffraction analysis of insect-cell-derived IL-22. Acta Crystallographica D 60: 1295-1298.
10. Xu T, Logsdon NJ and Walter MR (2005) Structure of insect-cell-derived IL-22. Acta Crystallographica D 61: 942-950.
11. Nagem RAP, Colau D, Dumoutier L, Renauld JC, Ogata C, et al. (2002) Crystal structure of recombinant human interleukin-22. Structure 10: 1051-1062.
12. Kotenko SV, Izotova LS, Mirochnitchenko OV, Esterova E, Dickensheets H, et al. (2001) Identification of the functional interleukin-22 (IL-22) receptor complex - The IL-10R2 chain (IL-10R beta) is a common chain of both the IL-10 and IL-22 (IL-10-related T cell-derived inducible factor, IL-TIF) receptor complexes. Journal of Biological Chemistry 276: 2725-2732.
13. Bleicher L, de Moura PR, Watanabe L, Colau D, Dumoutier L, et al. (2008) Crystal structure of the IL-22/IL-22R1 complex and its implications for the IL-22 signaling mechanism. FEBS Letters 582: 2985-2992.

14. Logsdon NJ, Jones BC, Allman JC, Izotova L, Schwartz B, et al. (2004) The IL-10R2 binding hot spot on IL-22 is located on the n-terminal helix and is dependent on N-linked glycosylation. Journal of Molecular Biology 342: 503-514.

15. Strasser R, Stadlmann J, Schahs M, Stiegler G, Quendler H, et al. (2008) Generation of glyco-engineered Nicotiana benthamiana for the production of monoclonal antibodies with a homogeneous human-like N-glycan structure. Plant Biotechnology Journal 6: 392-402.

16. Castilho A, Bohorova N, Grass J, Bohorov O, Zeitlin L, et al. (2011) Rapid High Yield Production of Different Glycoforms of Ebola Virus Monoclonal Antibody. Plos One 6(10): e26040.

17. Menassa R, Kennette W, Nguyen V, Rymerson R, Jevnikar A, et al. (2004) Subcellular targeting of human interleukin-10 in plants. Journal of Biotechnology 108: 179-183.

18. Menassa R, Nguyen V, Jevnikar A and Brandle J (2001) A self-contained system for the field production of plant recombinant interleukin-10. Molecular Breeding 8: 177-185.

19. Bortesi L, Rossato M, Schuster F, Raven N, Stadlmann J, et al. (2009) Viral and murine interleukin-10 are correctly processed and retain their biological activity when produced in tobacco. BMC Biotechnology 9: 22.

20. Westerhof LB, Wilbers RHP, Roosien J, van de Velde J, Goverse A, et al. (2012) 3D Domain Swapping Causes Extensive Multimerisation of Human Interleukin-10 When Expressed In Planta. Plos One 7(10): e46460.

21. Nagalakshmi ML, Rascle A, Zurawski S, Menon S and de Waal Malefyt R (2004) Interleukin-22 activates STAT3 and induces IL-10 by colon epithelial cells. International Immunopharmacology 4: 679-691.

22. Mamedov T, Ghosh A, Jones RM, Mett V, Farrance CE, et al. (2012) Production of non-glycosylated recombinant proteins in Nicotiana benthamiana plants by co-expressing bacterial PNGase F. Plant Biotechnology Journal 10: 773-782.

23. Vitale A and Ceriotti A (2004) Protein quality control mechanisms and protein storage in the endoplasmic reticulum. A conflict of interests? Plant Physiology 136: 3420-3426.

24. Debray H and Montreuil J (1989) Aleuria aurantia agglutinin. A new isolation procedure and further study of its specificity towards various glycopeptides and oligosaccharides. Carbohydrate Research 185: 15-26.

25. Gora-Sochacka A, Redkiewicz P, Napiorkowska B and Sirko A (2009) [Plant-based production of recombinant cytokines]. Postepy Biochemii 55: 85-94.

26. Fitchette-Laine AC, Gomord V, Cabanes M, Michalski JC, Saint Macary M, et al. (1997) N-glycans harboring the Lewis a epitope are expressed at the surface of plant cells. Plant Journal 12: 1411-1417.

27. Wilson IB, Zeleny R, Kolarich D, Staudacher E, Stroop CJ, et al. (2001) Analysis of Asn-linked glycans from vegetable foodstuffs: widespread occurrence of Lewis a, core alpha1,3-linked fucose and xylose substitutions. Glycobiology 11: 261-274.

28. Petruccelli S, Otegui MS, Lareu F, Tran Dinh O, Fitchette AC, et al. (2006) A KDEL-tagged monoclonal antibody is efficiently retained in the endoplasmic reticulum in leaves, but is both partially secreted and sorted to protein storage vacuoles in seeds. Plant Biotechnology Journal 4: 511-527.

29. Parsons J, Altmann F, Arrenberg CK, Koprivova A, Beike AK, et al. (2012) Moss-based production of asialo-erythropoietin devoid of Lewis A and other plant-typical carbohydrate determinants. Plant Biotechnology Journal 10: 851-861.

30. Castilho A, Neumann L, Gattinger P, Strasser R, Vorauer-Uhl K, et al. (2013) Generation of biologically active multi-sialylated recombinant human EPOFc in plants. Plos One 8(1): e54836.

31. Strasser R, Bondili JS, Vavra U, Schoberer J, Svoboda B, et al. (2007) A unique beta1,3-galactosyltransferase is indispensable for the biosynthesis of N-glycans containing Lewis a structures in Arabidopsis thaliana. Plant Cell 19: 2278-2292.

32. Sourrouille C, Marquet-Blouin E, D'Aoust MA, Kiefer-Meyer MC, Seveno M, et al. (2008) Down-regulated expression of plant-specific glycoepitopes in alfalfa. Plant Biotechnology Journal 6: 702-721.

33. Westerhof LB, Wilbers RHP, van Raaij DR, Nguyen DL, Goverse A, et al. (2014) Monomeric IgA can be produced in planta as efficient as IgG, yet receives different N-glycans. Plant Biotechnology Journal.

34. Biancotto A, Wank A, Perl S, Cook W, Olnes MJ, et al. (2013) Baseline levels and temporal stability of 27 multiplexed serum cytokine concentrations in healthy subjects. Plos One 8(12): e76091.

35. Taylor ME, Bezouska K and Drickamer K (1992) Contribution to ligand binding by multiple carbohydrate-recognition domains in the macrophage mannose receptor. Journal of Biological Chemistry 267: 1719-1726.

36. van Engelen FA, Molthoff JW, Conner AJ, Nap JP, Pereira A, et al. (1995) pBINPLUS: an improved plant transformation vector based on pBIN19. Transgenic Research 4: 288-290.

37. Voinnet O, Rivas S, Mestre P and Baulcombe D (2003) An enhanced transient expression system in plants based on suppression of gene silencing by the p19 protein of tomato bushy stunt virus. Plant Journal 33: 949-956.

38. Meevissen MH, Balog CI, Koeleman CA, Doenhoff MJ, Schramm G, et al. (2011) Targeted glycoproteomic analysis reveals that kappa-5 is a major, uniquely glycosylated component of Schistosoma mansoni egg antigens. Molecular & Cellular Proteomics 10: M110 005710.

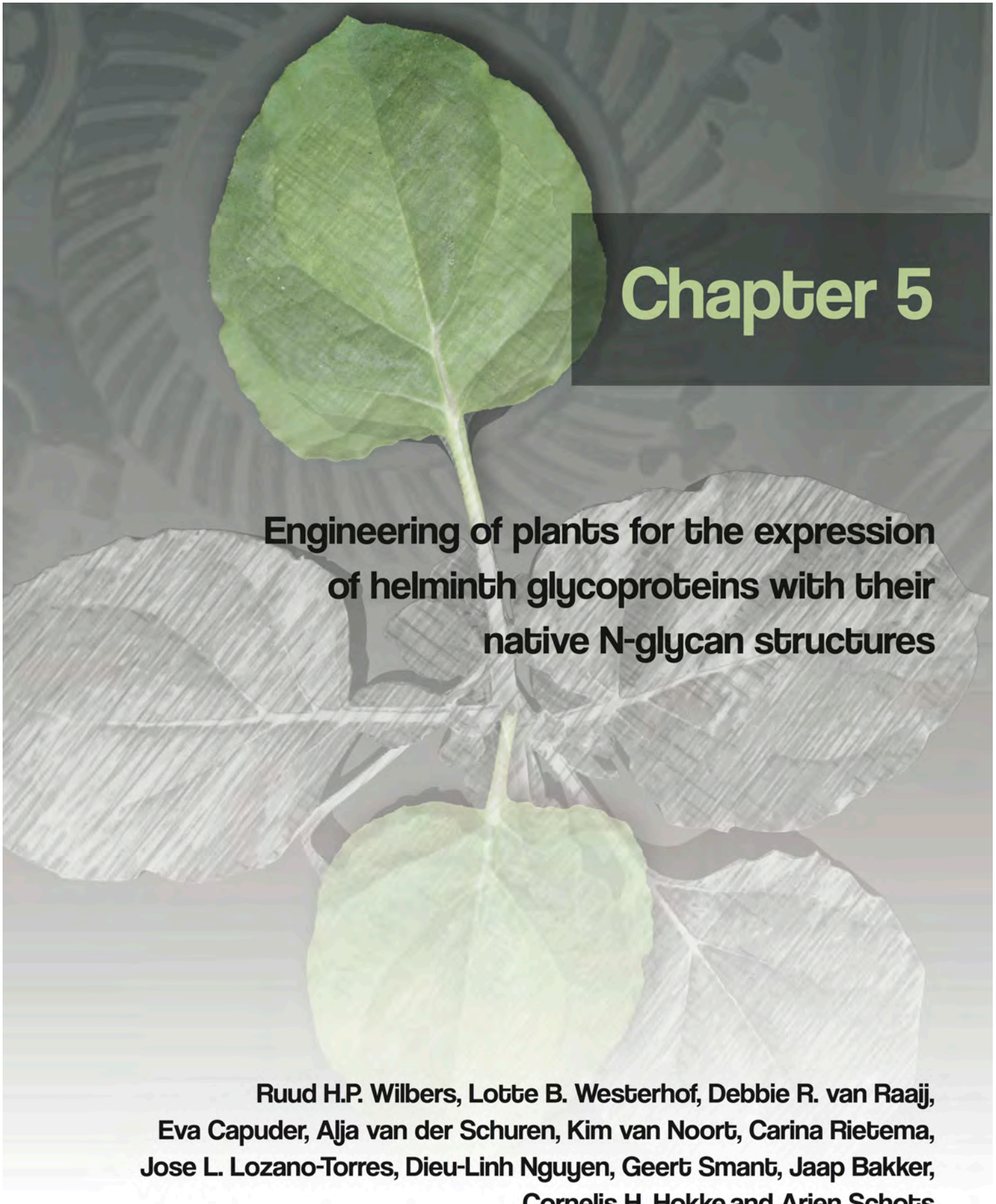

Chapter 5

Engineering of plants for the expression of helminth glycoproteins with their native N-glycan structures

Ruud H.P. Wilbers, Lotte B. Westerhof, Debbie R. van Raaij, Eva Capuder, Alja van der Schuren, Kim van Noort, Carina Rietema, Jose L. Lozano-Torres, Dieu-Linh Nguyen, Geert Smant, Jaap Bakker, Cornelis H. Hokke and Arjen Schots

Abstract

Schistosoma mansoni is a parasitic trematode that, like other helminths, secretes immunomodulatory proteins. These secreted proteins are main topics of research as they are possible vaccine candidates or may have therapeutic potential to treat inflammatory disorders. Many helminth secretory proteins carry complex N-glycans, but the exact role of these N-glycans on immunomodulatory properties remains to be elucidated. As the purification of a single glycoprotein from *S. mansoni* is inefficient and unsustainable, a platform is required that enables production of such glycoproteins. Here we show that *S. mansoni*-derived glycoproteins can be efficiently produced in plants. Furthermore, we have engineered the plant glycosylation machinery to synthesise N-glycans carrying structures like Lewis X or LDNF. Altogether, our results demonstrate that plants are an excellent platform for the expression of helminth glycoproteins with their native N-glycans. This opens up a new field of research and might lead to the identification of novel therapeutic targets.

Introduction

Over the last few decades the incidence of immune-mediated diseases, like inflammatory bowel disease, various allergies, asthma, multiple sclerosis and autoimmune (type 1) diabetes, has strongly increased in industrialised countries. Interestingly, there is an inverse correlation between the occurrences of these immune-mediated diseases with parasitic helminth infections. Helminths are complex multicellular organisms that upon infection of their host are masters in modulating their host's immune system. The trematode *Schistosoma mansoni* is one of the best-studied helminths and the ability of *S. mansoni* eggs to induce strong Th2 responses in humans and experimental animal models is well documented [1, 2]. The protective effect of infection with *S. mansoni* against immune-mediated disease was tested in several animal models for human diseases. For instance, *S. mansoni* was shown to protect mice against TNBS-induced colitis [3], allergen-induced airway hyperreactivity [4], autoimmune encephalitis [4, 5] and autoimmune diabetes [6, 7]. Protection against immune-mediated diseases was associated with the down-regulation of Th1-type cytokines (IFN-γ and IL-12) and increased expression of regulatory and Th2-type cytokines (IL-4, IL-10 and/or IL-13). However, more information is required to better understand how helminths, like *S. mansoni*, modulate their host's immune system. Knowledge on helminth-secreted proteins that play a key role in immunomodulation could ultimately lead to the identification of new therapeutic targets for the treatment of several immune-mediated diseases.

Immune modulation during helminth infection is mediated by a variety of proteins that are secreted by the cercariae (larvae), worms and/or their eggs [8]. The mix of soluble egg antigens from *S. mansoni* (SEA) is well known for its capacity to promote Th2 responses, however, *S. mansoni* eggs secrete several proteins and not all these proteins are functionally characterised [9, 10]. The purification and functional characterisation of a single protein from SEA is difficult, because only limited amounts can be obtained. Therefore, an expression platform is required that enables the production of helminth secreted proteins in large quantities.

Recently omega-1 was identified as the major component in *S. mansoni* eggs that is responsible for conditioning dendritic cells (DC's) for Th2 polarisation [11-13]. Omega-1 is a glycoprotein secreted by the eggs of *S. mansoni* and has T2 ribonuclease activity. Site-directed mutagenesis of the catalytic domain or the two potential N-glycosylation sites of omega-1 demonstrated that the priming of Th2 responses by omega-1 treated DC's was dependent on its RNase activity as well as its N-glycosylation [14]. The major N-glycans identified on *S. mansoni*-derived omega-1 are core-difucosylated diantennary N-glycans with one or two terminal Lewis X structures [15]. Omega-1 was shown to bind to several C-type lectin receptors, but the mannose receptor (CD206) was shown to be crucial for internalisation into DC's and subsequent polarisation of Th2 cells [14]. Another major

antigen found in SEA is kappa-5. Kappa-5 is a glycoprotein with unknown function, but harbours N-glycans distinct from omega-1 [16, 17]. Kappa-5 carries triantennary N-glycans with terminal LDN structures, and to a lesser extent LDNF, thereby targeting the C-type lectin receptor macrophage galactose lectin (MGL) [16].

Besides omega-1 and kappa-5 several SEA components have been shown to interact with antigen presenting cells via a range of C-type lectin receptors and in many cases this interaction is thought to be important for shaping immune responses during schistosomiasis [18]. As the interaction with distinct C-type lectin receptors can influence the outcome of the immune response that is initiated by a certain SEA protein, it is crucial for the functional characterisation of these proteins that they carry appropriate N-glycan structures. Therefore, an expression platform is required that not only enables high expression of helminth glycoproteins, but should also be capable to synthesize native helminth N-glycan structures.

In the last two decades, plants have emerged as a promising expression platform for the production of recombinant proteins. An added value of plants as expression platform is the possibility to engineer the N-glycosylation machinery. This has been surprisingly successful because plants have demonstrated a high degree of tolerance towards changes in the glycosylation pathway. Thus the modification of recombinant glycoproteins in a specific and controlled manner is enabled [19]. Notably research on humanising N-glycans in plants has advanced over the last couple of years. Transgenic plants lacking non-human α1,3-fucose and β1,2-xylose sugar residues on their N-glycans have been generated (ΔXT/FT plants) and typical mammalian core α1,6-fucose can be engineered in plants as well [20, 21]. Lewis X structures have been synthesised before in *Nicotiana tabacum* by stably expressing a hybrid β1,4-galactosyltransferase and a hybrid α1,3-fucosyltransferase IXa that were targeted to the medial-Golgi compartment [22]. However, these N-glycans were of a hybrid type as they only contained one antenna with a Lewis X structure and another antenna containing mannoses. The formation of hybrid N-glycans was attributed to the incorrect targeting of the glycosyltransferases. In contrast, targeting human β1,4-galactosyltransferase to the *trans*-Golgi compartment in ΔXT/FT plants allowed the generation of monoclonal antibodies with diantennary N-glycans containing two terminal galactose residues [23]. Engineering plants to synthesize N-glycans with terminal N-acetylgalactosamine residues (GalNAc or LDN) has to our knowledge never been reported. On the other hand, GalNAc containing O-glycans have been synthesized successfully in plants [24-26].

In this study we investigated the suitability of plants as expression platform for *S. mansoni*-derived glycoproteins and the possibility to engineer the N-glycosylation machinery such that diantennary N-glycans can be synthesized that carry either Lewis X or LDN(F) structures. Our work demonstrates that plants are able to produce helminth glycoproteins in large quantities and due to their efficient secretion can be easily purified from the apoplast. We also show that both Lewis X and LDN(F) structures can be efficiently engineered in wild-type plants.

Results

Plants are an excellent expression host for *S. mansoni*-derived glycoproteins

In order to achieve high expression for *Schistosoma mansoni*-derived glycoproteins we applied in-house codon optimization to the native omega-1 and kappa-5 genes. Codon optimisation was applied as the GC-content of the native omega-1 and kappa-5 genes are ~40% and plants generally prefer a higher GC-content in their highly expressed genes [27]. The mature protein sequences were preceded by the *Arabidopsis thaliana* chitinase signal peptide for secretion followed by a N-terminal 6x histidine-tag and FLAG-tag (H6F). Expression was achieved by agroinfiltration of *Nicotiana benthamiana* plants, while co-expressing the p19 silencing suppressor of tomato bushy stunt virus.

Expression of omega-1 and kappa-5 was analysed in crude plant extracts at 3, 5 and 7 days post infiltration (dpi) using anti-FLAG western blots. Omega-1 migrated as two bands between 25 and 37 kDa, which were detected at all three time points with greatest band intensity at dpi 5 (Figure 1a). The theoretical molecular weight of omega-1 is ~27 kDa, but omega-1 harbours two N-glycosylation sites. Thus, the two bands most likely represent intact omega-1, but with a different number of N-glycans. Kappa-5 was detected as a dominant band between 37 and 50 kDa and, like omega-1, its accumulation peaks at 5 dpi (Figure 1e). The theoretical molecular weight of kappa-5 is ~35 kDa, but kappa-5 harbours four N-glycosylation sites. Therefore, the dominant band most likely represents intact kappa-5 with at least 3 N-glycans. Furthermore, a weaker band was detected as well above 75 kDa and this band most likely represents dimeric kappa-5.

Next we tested whether omega-1 and kappa-5 are efficiently secreted from plant cells into the apoplast. At 5 dpi we isolated apoplast fluids from infiltrated leaves and used the remaining leaf material to prepare crude extracts. Samples containing either omega-1 or kappa-5 were analysed by SDS-PAGE and Coomassie staining (Figure 1b and f, respectively). Strikingly, the majority of both plant-produced helminth glycoproteins (>90%) was recovered from the apoplast. This means that both omega-1 and kappa-5 are secreted with high efficiency. Only few endogenous proteins are present in the apoplast fluids and upon expression of omega-1 or kappa-5, they became the predominant protein constituting >50% of total soluble protein.

Since omega-1 was characterised as a T2 ribonuclease (RNase), purified omega-1 was analysed for its RNase activity. Purified omega-1 was used in a RNA break down assay using total RNA from mouse bone marrow-derived dendritic cells. A mutant of omega-1, which should lack RNase activity (omega-1^{H58F}) [14], was also expressed in plants, purified, and tested for activity. Figure 1d shows that purified omega-1 from plants is able to break down total RNA from mouse dendritic cells, whereas the omega-1^{H58F} mutant did not.

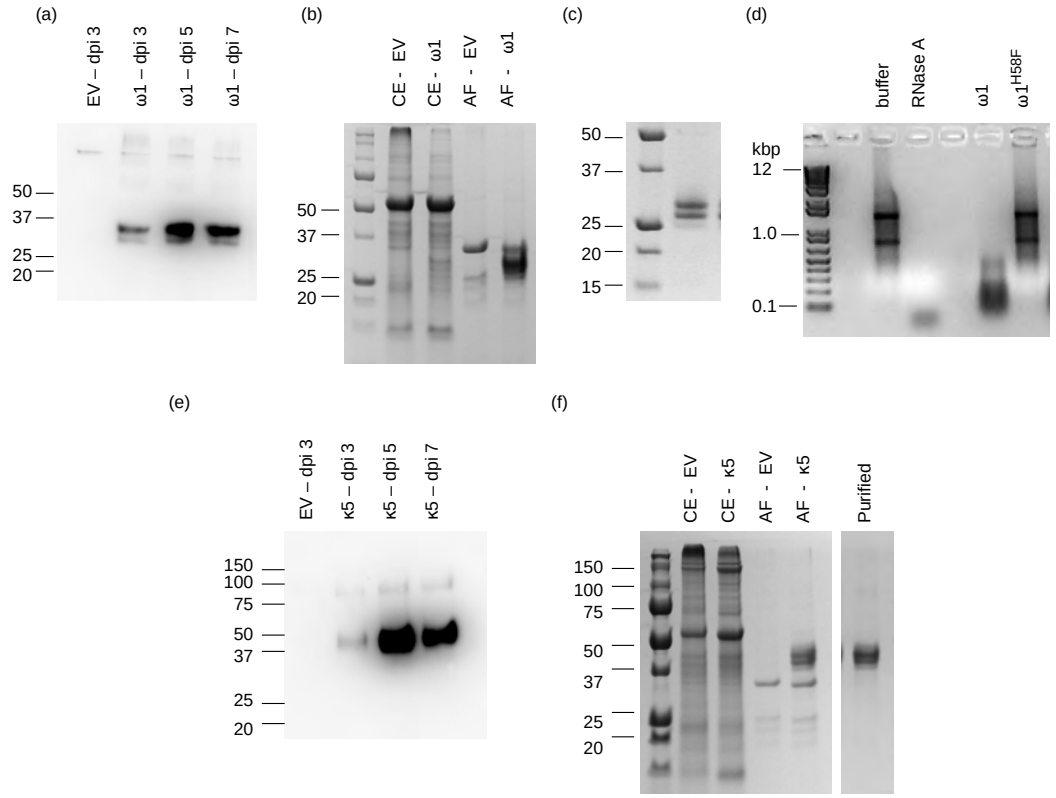

Figure 1 ◆ Analysis of omega-1 and kappa-5 expressed in *N. benthamiana* plants. (a) Anti-FLAG western blot analysis under reducing conditions of 1 µg total protein from crude plant extracts for omega-1 or (ω1) empty vector (EV) infiltrated plants 3, 5 and 7 days post infiltration (dpi). (b). SDS-PAGE analysis under reducing conditions and Coomassie staining of 2.5 µl of crude extract (CE) or apoplast fluid (AF) from omega-1 or EV infiltrated plants. (c) SDS-PAGE analysis under reducing conditions and Coomassie staining of 2 µg purified omega-1. (d) RNase breakdown assay of total RNA from mouse bone marrow-derived dendritic cells using 500 ng purified omega-1 and omega-1^{H58F}. RNase A was used a positive control. (e) Anti-FLAG western blot analysis under reducing conditions of 1 µg total soluble proteins from crude plant extracts for kappa-5 (κ5) or empty vector (EV) infiltrated plants 3, 5 and 7 days post infiltration (dpi). (f). SDS-PAGE analysis under reducing conditions and Coomassie staining of 2.5 µl of crude extract (CE) or apoplast fluid (AF) from kappa-5 or EV infiltrated plants or 2 µg of purified kappa-5.

This indicates that plant-produced omega-1 has RNase activity. Taken together our data show that plants offer an excellent expression platform for the production of large quantities of *S. mansoni*-derived glycoproteins. Furthermore, both omega-1 and kappa-5 are secreted into the apoplast with high efficiency, thereby enabling easy purification of these helminth glycoproteins.

Omega-1 and kappa-5 are differentially N-glycosylated

To assess the N-glycan composition of both omega-1 and kappa-5 from wild-type plants we performed N-glycan analysis. Tryptic peptides were prepared from purified omega-1 and kappa-5 and N-glycans were released by PNGase A digestion. The N-glycosylation profile was determined by matrix assisted laser desorption/ionisation time-of-flight mass spectrometry (MALDI-TOF-MS). A representative N-glycan profile for omega-1 isolated from apoplast fluid is shown in Figure 2a. The predominant N-glycan type found on omega-1 is a typical plant complex N-glycan for secreted proteins with β1,2-xylose and core α1,3-fucose. Yet, the N-glycans of omega-1 lack terminal GlcNAc residues putatively due to β-hexosaminidase activity in the apoplast (paucimannosidic type N-glycan; MMXF[3]). For apoplastic kappa-5 a representative N-glycan profile is shown in Figure 2b.

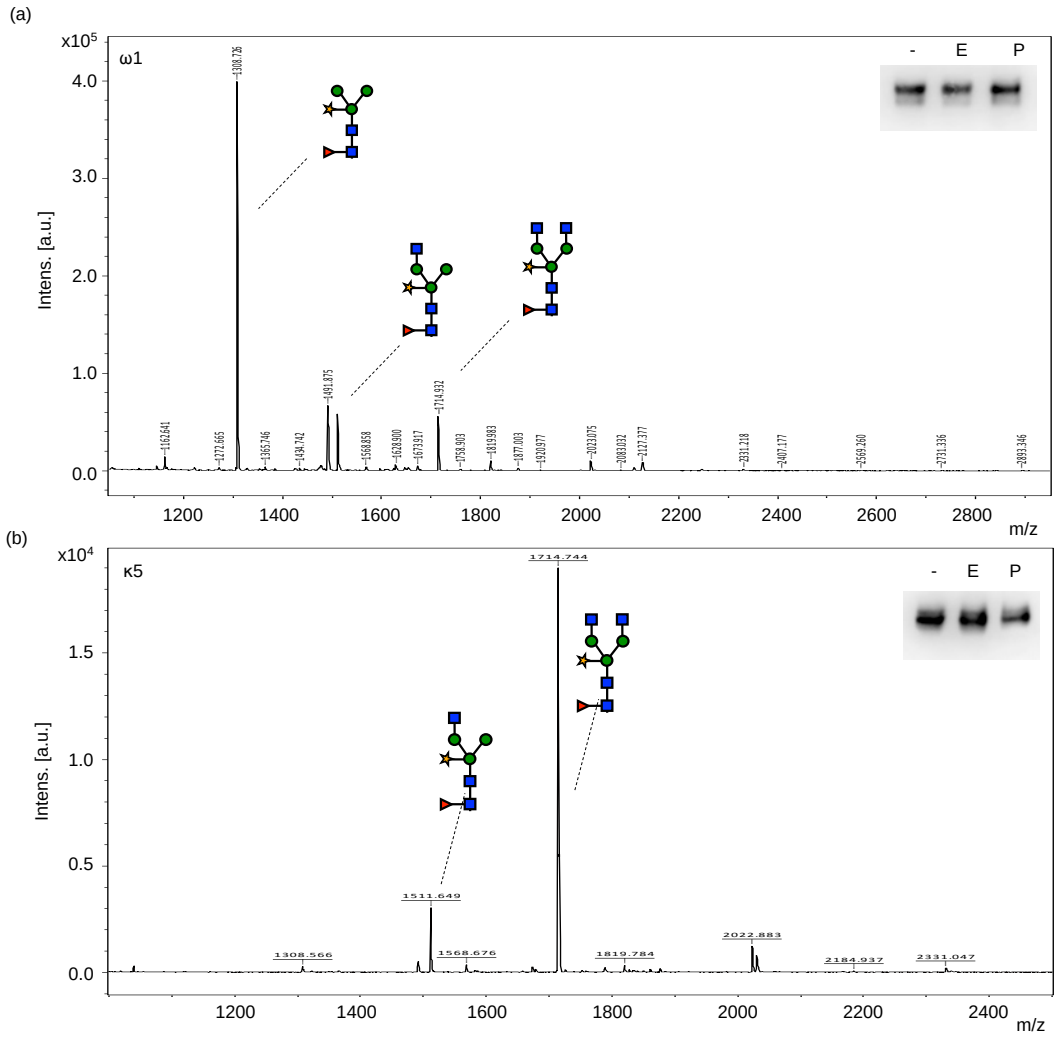

Figure 2 ◆ N-glycan profiles for omega-1 and kappa-5 expressed in *N. benthamiana* plants. N-glycans were analysed using MALDI-TOF-MS analysis upon tryptic digestion and PNGase A release of N-glycans. N-glycan profiles are given for omega-1 (a) and kappa-5 (b), which were purified from the apoplast of wild-type *N. benthamiana* plants. Each N-glycan profile is accompanied by an image of *in vitro* digestion with PNGase F (P) and Endo H (E) as analysed by anti-FLAG western blotting.

The predominant N-glycan type found on kappa-5 is also a typical plant complex N-glycan for secreted proteins with β1,2-xylose and core α1,3-fucose (GnGnXF). However, in contrast to omega-1, the N-glycans on kappa-5 do not lack terminal GlcNAc residues. So, even though omega-1 and kappa-5 are both isolated and purified from the apoplast, their N-glycans seem to reveal differences in sensitivity towards β-hexosaminidase activity.

Glyco-engineering of omega-1 results in hybrid Lewis X-type N-glycans

A major fraction of *S. mansoni*-derived omega-1 harbours diantennary N-glycans that carry Lewis X structures. We set out to engineer Lewis X type N-glycans in wild-type *N. benthamiana* plants. Lewis X carrying N-glycans were previously synthesised in *N. tabacum*, but resulted in the formation of hybrid Lewis X-type N-glycans due to medial-Golgi targeting [22]. In our study we used α1,3-fucosyltransferase IXa from pufferfish and β1,4-galactosyltransferase 1 from zebrafish. Both genes were genetically fused with the CTS domain (C, cytoplasmic tail; T, transmembrane domain; S, stem region) of rat α2,6-sialyltransferase for *trans*-Golgi targeting and from here forward named sialFucT and sialGalT, respectively. We co-expressed both glycosyltransferases together with omega-1 and the p19 silencing suppressor in plants. Omega-1 was purified from the apoplast and N-glycan composition was analysed as described in the previous section. A representative N-glycan profile is shown in Figure 3a. The major N-glycan found on omega-1 upon co-expression of sialFucT and sialGalT consisted of one antenna carrying Lewis X, while the other antenna carried two additional mannoses (hybrid Lewis X). Furthermore, plant specific β1,2-xylose and core α1,3-fucose were absent. Besides the hybrid Lewis X-type N-glycan we also observed a smaller fraction of mannose-enriched N-glycans (Man5). To complement the N-glycan profile, omega-1 was deglycosylated with PNGase F and Endo H to confirm the presence or absence of core α1,3-fucose or oligomannose/hybrid type N-glycans, respectively. In the upper right corner of the N-glycan profile, the deglycosylation of omega-1 is shown upon anti-FLAG western blotting. Deglycosylation with PNGase F or Endo H coincides with the obtained N-glycan profile. N-glycans carrying Lewis X structures are formed upon co-expression of sialFucT and sialGalT, but surprisingly are still of the hybrid Lewis X-type as reported by Rouwendal and co-workers [22].

Over-expression of sialGalT results in hybrid Lewis X-type N-glycans

Over-expression of a glycosyltransferase might result in overflow of the glycosyltransferase into other Golgi sub-compartments. In our case, our glycosyltransferases might therefore not be restricted to the *trans*-Golgi only. Activity of β1,4-galactosyltransferase in the medial-Golgi may interfere with α-mannosidase II activity in this compartment resulting in

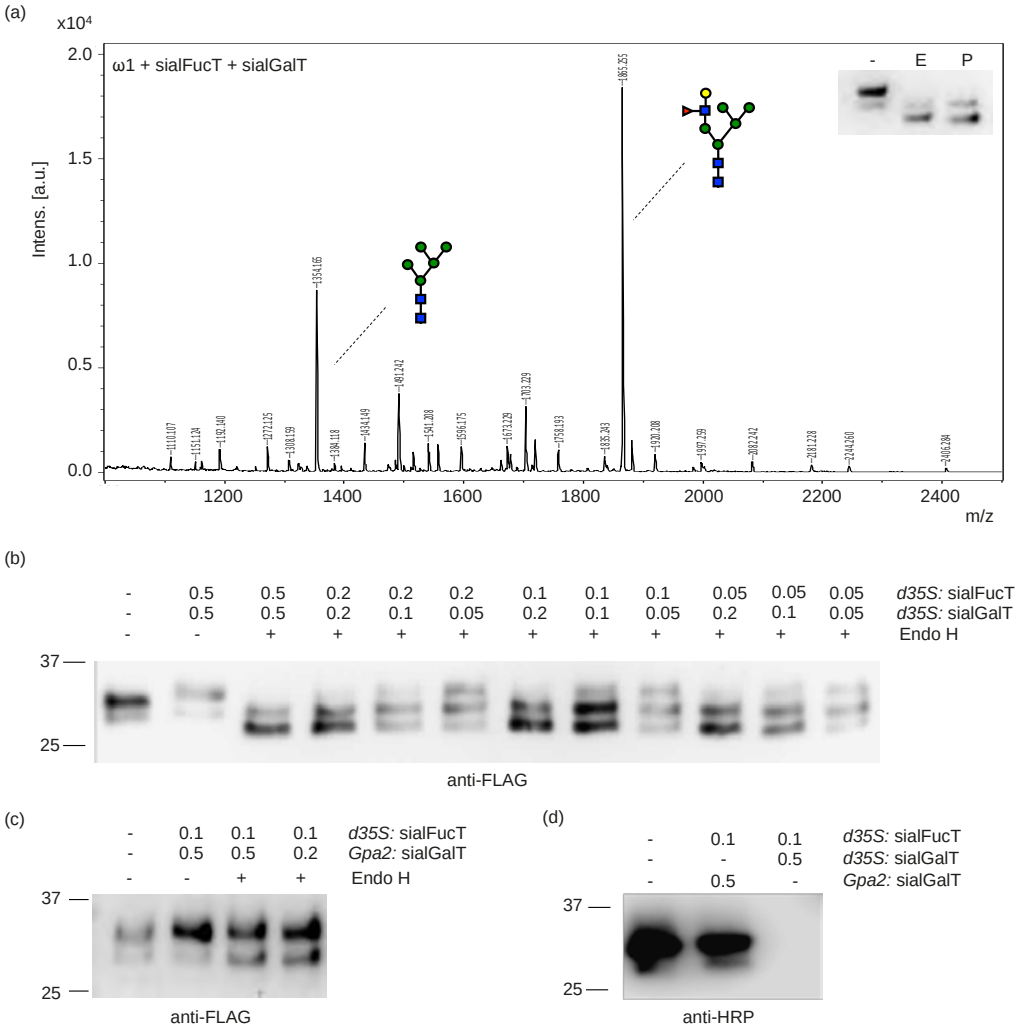

Figure 3 ◆ Screening for hybrid Lewis X-type N-glycans. (a) N-glycan profile for omega-1 upon co-expression of sialFucT and sialGalT. N-glycans were analysed using MALDI-TOF-MS analysis upon tryptic digestion and PNGase A release of N-glycans. The N-glycan profile is accompanied by an image of *in vitro* digestion with PNGase F (P) and Endo H (E) as analysed by anti-FLAG western blotting. (b) Anti-FLAG western blot analysis of Endo H treated apoplast fluids for omega-1 expressed in wild-type plants while co-expressing *35S:*sialFucT and *35S:*sialGalT at different ratios of *Agrobacterium* cultures. Optical densities (OD) of 0.5-0.05 were used. (c) Anti-FLAG western blot analysis of Endo H treated apoplast fluids for omega-1 expressed in wild-type plants while co-expressing *35S:*sialFucT and *Gpa2:*sialGalT (using an OD of 0.5-0.1) to lower sialGalT expression. (d) Anti-HRP western blot analysis of purified omega-1 expressed in wild-type plants or engineered omega-1 while co-expressing *35S:*sialFucT (OD=0.1) with either *d35S:*sialGalT or *Gpa2:*sialGalT (using an OD of 0.5).

the formation hybrid N-glycans [28]. As Endo H was capable of cleaving off hybrid Lewis X-type N-glycans, we employed Endo H digestion to investigate if over-expression of β1,4-galactosyltransferase causes the formation of these hybrid N-glycans. We co-expressed omega-1 with sialFucT and sialGalT, but used different ratio's for the *Agrobacterium*

cultures of these two glycosyltransferases. By scaling down optical densities of *Agrobacterium* cultures (testing an OD-range from 0.5 to 0.05) we assume the expression of either sialFucT or sialGalT can be reduced. Apoplast fluids were harvested at 5 dpi and were treated with Endo H. The cleavage of hybrid N-glycans by Endo H was analysed using anti-FLAG western blots (Figure 3b). When using an optical density of 0.5 for both glycosyltransferases, omega-1 migrates slightly higher in the SDS-PAGE gel than omega-1 expressed without co-expression of both glycosyltransferases, indicating a higher N-glycan mass. Upon treatment with Endo H the majority of omega-1 is deglycosylated, which confirms the presence of oligomannose- and/or hybrid-type N-glycans. When the optical density for sialGalT was lowered to 0.1 or 0.05, Endo H was only capable of cleaving a part of the N-glycans from omega-1. Lowering the expression of sialFucT did not have this effect. This observation supports the hypothesis that the over-expression of sialGalT, but not sialFucT, is linked to the formation of hybrid Lewis X N-glycans.

We also tested whether controlled expression of sialGalT by using a weaker promoter could prevent the formation of hybrid N-glycans completely. We chose the promoter region of the potato resistance gene *Gpa2* to control the expression of sialGalT, because resistance genes are constitutively expressed at a low level. Co-expression of omega-1 with sialFucT and sialGalT, the latter being controlled by the *Gpa2* promoter region, resulted in the production of omega-1 that was hardly sensitive to Endo H (Figure 3c). Next, western blot analysis with a rabbit anti-HRP antibody, which specifically binds to plant β1,2-xylose and core α1,3-fucose, was performed as hybrid glycans do not carry these typical plant sugar residues (Figure 3d). As expected the anti-HRP antibody bound strongly to omega-1 from wild-type plants, but not to omega-1 co-expressed with the *d35S*:sialGalT construct. When the *Gpa2*:sialGalT construct was used, the N-glycans on omega-1 were insensitive towards Endo H digestion and carried typical plant sugars again. We therefore conclude that by co-expressing the *Gpa2*:sialGalT construct omega-1 does not receive hybrid-type N-glycans. However, the question is whether sialGalT expression controlled by the *Gpa2* promoter is still high enough to facilitate efficient galactosylation.

Controlled expression of sialGalT enables synthesis of non-hybrid Lewis X

To investigate if omega-1 carries diantennary N-glycans with terminal Lewis X structures upon co-expression with *35S:*sialFucT and *Gpa2:*sialGalT we analysed the N-glycan composition. N-glycans were prepared as described above and a representative N-glycan profile is shown in Figure 4a. The predominant N-glycan type found on omega-1 upon Lewis X engineering is still the typical plant paucimannosidic N-glycan. However, by using this engineering strategy a significant proportion of diantennary N-glycans carrying Lewis X structures was also found. On top of that, several intermediate N-glycans containing antennae with a single Lewis X structure and/or a terminal galactose residue

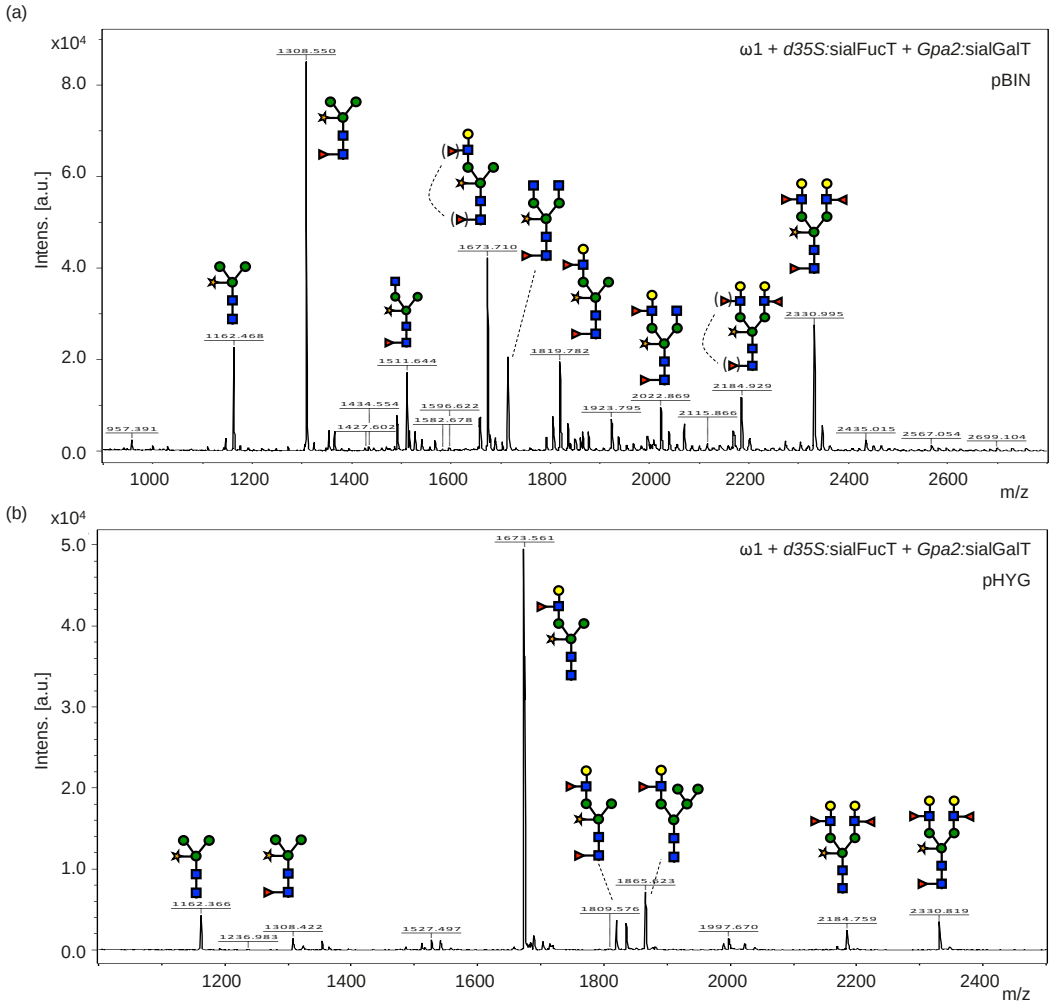

Figure 4 ◆ N-glycan profiles for omega-1 (ω1) carrying Lewis X structures. N-glycans from purified omega-1 were analysed by MALDI-TOF-MS upon tryptic digestion and PNGase A release of N-glycans. (a) N-glycan profile for omega-1 from wild-type *N. benthamiana* plants upon co-expression of *d35S:*sialFucT (OD=0.1) and *Gpa2:*sialGalT (OD=0.5). Sugar residues for which the position is not completely clear are placed between brackets. (b) N-glycan profile for omega-1 from wild-type *N. benthamiana* plants upon co-expression of *d35S:*sialFucT (OD=0.1) and *Gpa2:*sialGalT (OD=0.5), but the latter being expressed using the pHYG vector.

were found as well. Strikingly, all N-glycan structures contained typical plant β1,2-xylose. None of them were of the hybrid type carrying additional mannose residues on the α1,6-mannosyl branch. The most likely reason for the presence of mainly plant wild-type N-glycans on omega-1 when co-expressing *35S:*sialFucT and *Gpa2*:sialGalT in pBIN is low galactosylation efficiency. We therefore attempted to increase the expression level by transferring the *Gpa2*:sialGalT expression cassette from the pBIN to pHYG expression vector. The pHYG expression vector generally gives more mRNA transcript levels for a heterologously expressed gene due to its smaller size and higher copy number in bacteria

(unpublished data). N-glycans were prepared as described before and a representative N-glycan profile is shown in Figure 4b. The predominant N-glycan found on omega1 with this strategy is a complex N-glycan with β1,2-xylose and carrying a single Lewis X structure, but lacking a second terminal GlcNAc and core α1,3-fucose. Only marginal fractions of paucimannosidic N-glycans, hybrid Lewis X-type N-glycans and N-glycans carrying two Lewis X structures were detected. Treatment with β(1-4,6)-galactosidase from jack bean confirmed that ≥95% of the N-glycans indeed carried Lewis X (Figure S1). Altogether, we conclude that synthesis of non-hybrid N-glycans carrying Lewis X structures can be achieved in wild-type *N. benthamiana* plants, but depends on the tightly controlled expression of β1,4-galactosyltransferase.

Engineering of LDN(F) carrying N-glycans in plants

S. mansoni-derived kappa-5 mainly harbours N-glycans that carry terminal LDN and LDNF structures [16]. The synthesis of GalNAc containing O-glycans was performed previously in plants by several groups [24-26], but the enzymes that are required remain a matter of debate. To engineer GalNAc containing N-glycans we investigated the requirement of a C4 epimerase (converts UDP-GlcNAc into UDP-GalNAc in the cytosol) and Golgi-transporters for the UDP-GalNAc substrate. Furthermore, we investigated the effect of a CTS domain for *trans*-Golgi targeting. We co-expressed kappa-5 with different combinations of the following enzymes: native β1,4-*N*-acetylgalactosaminyltransferase (GalNAcT) from *C. elegans*, *trans*-Golgi targeted GalNAcT (sialGalNAcT), UDP-GalNAc transporters (nstp-4, nstp-5 and sqv-7) from *C. elegans*, and/or a codon optimised C4 epimerase from *Pseudomonas aeruginosa* (WbpP) [26]. Total soluble proteins were isolated from the leaf apoplast and coated on 96 well ELISA plates. Biotinylated agglutinin from soybean (SBA) was used to screen for the presence of terminal LDN structures. Figure 5a shows that SBA bound specifically to the N-glycans of apoplastic plant proteins upon co-expression of GalNAcT. However, the use of a *trans*-Golgi targeting CTS domain for GalNAcT (sialGalNAcT) did not result in the synthesis of LDN. Furthermore, we can conclude that co-expression of a C4 epimerase increased the binding of SBA. Co-expression of a C4 epimerase could therefore increase the efficiency of LDN synthesis by raising the cellular pool of the UDP-GalNAc substrate. On the other hand, co-expression of different GalNAc transporters only influenced SBA binding in a negative way depending on the transporter used. Co-expression of GalNAcT along with kappa-5 would therefore be sufficient to synthesize LDN carrying N-glycans, but whether co-expression of a C4 epimerase is required, needs further investigation.

Next, kappa-5 was purified from the apoplast and SBA was used to check for the presence of LDN structures on the N-glycans of purified kappa-5 (Figure 5b). SBA bound strongly to the N-glycans of kappa-5 upon co-expression of GalNAcT as was observed for total apoplast proteins containing kappa-5. Co-expression of a C4 epimerase hardly

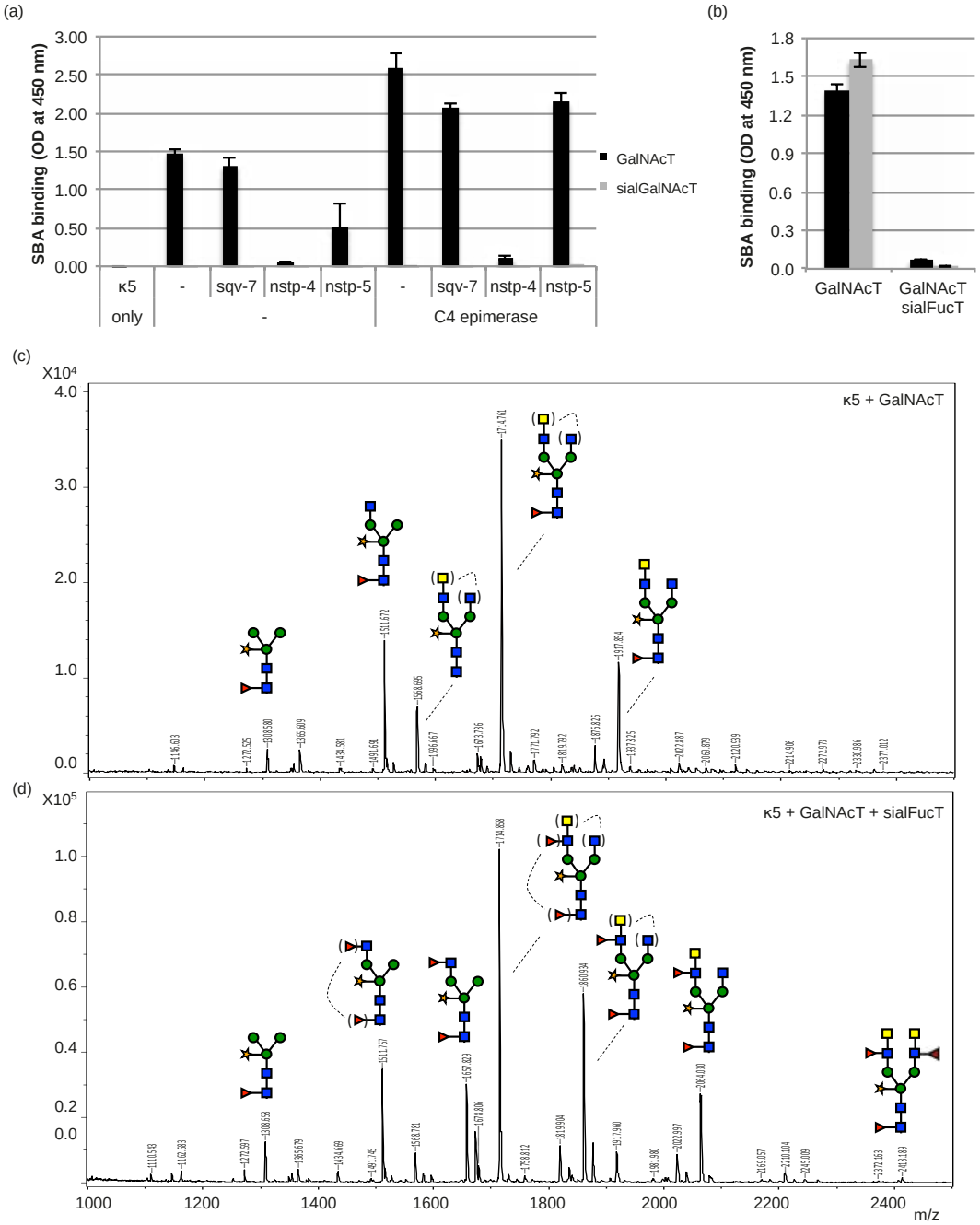

Figure 5 ◆ Engineering of LDN(F) carrying N-glycans in plants. (a) Soybean agglutinin (SBA) binding assay on total soluble proteins from apoplast fluid (1 µg/ml) to determine which enzymes are required for the synthesis of LDN carrying N-glycans. Apoplast proteins were treated with 5 µg/ml biotinylated SBA. (b) SBA binding to purified kappa-5 upon co-expression of sialFucT and/or GalNAcT (black bars), as well as C4 epimerase (grey bars). N-glycan profiles obtained upon MALDI-TOF-MS analysis are given for purified kappa-5 from wild-type *N. benthamiana* plants upon co-expression of GalNAcT (c) or GalNAcT and sialFucT (d). Sugar residues for which the position is not completely clear are placed between brackets.

influenced the binding of SBA to the N-glycans of purified kappa-5 (Figure 5b, grey versus black bars). In order to synthesise LDNF structures, we also co-expressed sialFucT. Co-expression of sialFucT blocked the binding of SBA to the N-glycans of kappa-5. This would suggest that α1,3-fucosylation of LDN occurs and blocks the binding of SBA.

To confirm the presence of LDN or LDNF structures on the N-glycans of kappa-5, N-glycans were prepared for MALDI-TOF-MS analysis as described in the previous sections. Representative N-glycan profiles are given for kappa-5 isolated from wild-type *N. benthamiana* plants upon co-expression of sialFucT and/or GalNAcT (Figure 5d and 5c, respectively). Co-expression of a C4 epimerase did not change these profiles (data not shown). In figure 5c it is shown that GalNAc containing N-glycans can be engineered in plants upon co-expression of GalNAcT. However, the percentage of GalNAc carrying N-glycans is difficult to determine. The major peak in the profile can resemble complex wild-type plant N-glycans carrying terminal GlcNAc's ($GnGnXF^3$), but also LDN carrying N-glycans of which one branch terminates in a single mannose residue. Treatment of these N-glycans with β-glucosaminidase from *Xanthomonas manihotis* or β-hexosaminidase from *Streptomyces plicatus* reveals that there is indeed a mix of $GnGnXF^3$ glycans as well as LDN carrying N-glycans (Figure S2). Furthermore, the specific cleavage of terminal GlcNAc residues with β-glucosaminidase shows that approximately 30% of the N-glycans carries terminal GalNAc.

Engineering of LDNF in plants was also successful upon co-expression of both GalNAcT and sialFucT as shown in figure 5d. Again a major peak was observed that could resemble the $GnGnXF^3$ glycan as well as a complex type N-glycans carrying the LDNF structure. However, in the latter case core α1,3-fucose would then be absent. Furthermore, difucosylated N-glycans carrying one terminal LDNF structure were also detected. Upon treatment with β-hexosaminidase or β-glucosaminidase we observed that approximately 50% of the N-glycans carries the LDNF structure (Figure S3). This indicates that fucosylation of LDN makes the structure more stable and could protect against plant β-hexosaminidase activity. Fucosylation of the LDN structure also completely protects against cleavage by β-hexosaminidase from *Streptomyces*. N-glycan structures with a fucosylated terminal GlcNAc residue that lack GalNAc where also observed. This indicates that GalNAc residues must have been present on these N-glycans, but are most likely removed by plant β-hexosaminidases. This would also infer that plant β-hexosaminidases could remove terminal GalNAc in the presence of fucose.

Discussion

Schistosoma mansoni soluble egg antigens (SEA) play a crucial role in immune modulation during helminth infection and more detailed knowledge on the activity of its individual components can ultimately lead to the identification of new therapeutic targets for treatment of inflammatory disorders. Functional studies on individual components from this egg antigen mixture are challenged by the limited amount of SEA proteins that can be isolated. In our study we investigated the possibility to use *Nicotiana benthamiana* plants as a production platform for large quantities of the biologically active *S. mansoni*-derived egg antigens omega-1 and kappa-5. Furthermore, we investigated whether the *N*-glycosylation machinery of plants could be engineered to synthesise diantennary N-glycans carrying terminal Lewis X or LDN(F) structures, which naturally occur on omega-1 or kappa-5, respectively. Both omega-1 and kappa-5 were highly expressed and, most remarkable, >90% was secreted into the apoplast. The efficient secretion of omega-1 and kappa-5 enabled easy purification as only few endogenous proteins reside in this extracellular compartment. In addition, purification from the apoplast fluid ensures that all the proteins have passed through the entire secretory pathway and most likely results in a more homogeneous N-glycan composition.

N-glycan analysis revealed that omega-1 expressed in wild-type *N. benthamiana* plants predominantly carries paucimannosidic N-glycans containing the plant specific sugar residues β1,2-xylose and core α1,3-fucose (MMXF^3). The lack of terminal GlcNAc residues on the α1,3- and α1,6-mannosyl branches of N-glycans of plant proteins can be attributed to β-hexosaminidase activity in the apoplast as postulated by Strasser and co-workers [29]. They identified three β-hexosaminidases (HEXO1-3) in *Arabidopsis thaliana,* which localised in either the vacuole (HEXO1) or the apoplast (HEXO2 and HEXO3) that were able to remove terminal GlcNAc residues from N-glycans. Especially HEXO3 seemed responsible for the formation of paucimannosidic N-glycans in leaves of *A. thaliana* [30]. Up to 7 genes with high similarity to β-hexosaminidases from *Arabidopsis* can be identified within the genome of *N. benthamiana*, but their function and localisation are unknown. Surprisingly, kappa-5 predominantly carries N-glycans of the GnGnXF^3 type, even though kappa-5 is purified from the leaf apoplast, like omega-1. This would imply that these two proteins are differently affected by β-hexosaminidases.

In a first attempt to engineer terminal Lewis X structures, a hybrid β1,4-galactosyltransferase from *Danio rerio* (zebrafish) and a hybrid α1,3-fucosyltransferase IXa from *Tetraodon nigriviridus* (pufferfish) were co-expressed with omega-1. The CTS domain of rat α2,6-sialyltransferase was used for *trans*-Golgi targeting as it was previously shown to enable efficient galactosylation [23]. Our approach differed from previous reports wherein medial-Golgi targeting of galactosyltransferase with the CTS domain of *Arabidopsis* β1,2-xylosyltransferase (XylT) resulted in the formation of hybrid N-glycans

[22, 31]. These authors suggested that hybrid N-glycans are formed when early galactosylation in the medial-Golgi prevents trimming of mannose residues on the α1,6-mannosyl branch of a N-glycan by α-mannosidase-II (Man-II). In our experiments, co-expression of *trans*-Golgi targeted glycosyltransferases surprisingly resulted in the formation of Lewis X hybrid N-glycans as well. Like previously observed, our hybrid Lewis X N-glycans are also devoid of plant specific β1,2-xylose and core α1,3-fucose. The lack of β1,2-xylose on hybrid Lewis X-type N-glycans would be in line with the suggestion that XylT only adds xylose after removal of the two mannoses on the α1,6-mannosyl branch, but before the addition of galactose to terminal GlcNAc residues [32]. This coincides with the fact that XylT from *Arabidopsis thaliana* is inhibited by mannoses on the α1,6-mannosyl branch or terminal galactose on the α1,3-mannosyl branch [33]. Thus, early galactosylation in the medial-Golgi of plants blocks the addition of β1,2-xylose, but may also inhibit Man-II activity leading to hybrid N-glycans. This would infer that within our experiments the use of a *trans*-Golgi targeting CTS domain is not sufficient to retain zebrafish galactosyltransferase within the *trans*-Golgi compartment of plants. Over-expression of zebrafish galactosyltransferase may cause overflow of the *trans*-Golgi compartment, resulting in medial-Golgi localised galactosyltransferase.

In order to lower the transient expression of sialGalT we used the *Gpa2* promoter region. This controlled fashion of expressing *Gpa2*:sialGalT with the pBIN expression vector resulted in the complete lack of hybrid Lewis X-type N-glycans. This engineering strategy is also the first to enable the synthesis of diantennary N-glycans carrying two Lewis X structures. Furthermore, our findings demonstrate another layer of complexity to glyco-engineering, as it is not sufficient to only choose a proper CTS domain for targeting of a glycosyltransferase. Controlled expression of the glycosyltransferase is also important to obtain the correct localization in the Golgi.

Besides complex N-glycans carrying two Lewis X structures, several intermediate N-glycans containing antennae with a single Lewis X structure and/or terminal galactose residues were found upon controlled expression of sialGalT. However, a major fraction of the N-glycans is still paucimannosidic. This indicates that perhaps the efficiency of galactosylation is not yet optimal. As the majority of the N-glycans, including some of the Lewis X intermediate N-glycans, lack terminal GlcNAc residues, it might be that omega-1 is still sensitive to β-hexosaminidases in the leaf apoplast. This could be caused by inefficient galactosylation, as galactose would prevent GlcNAc removal by β-hexosaminidase. In order to fine-tune the expression of sialGalT we transferred the expression cassette for *Gpa2*:sialGalT to the pHYG expression vector. This strategy resulted in a non-hyrbid N-glycan that carried β1,2-xylose and a single Lewis X structure, but lacked a second terminal GlcNAc and core α1,3-fucose. This suggests that when galactosylation is efficient that there is still interference with plant endogenous glycosyltransferases, like α1,3-fucosyltransferase (FucT) and N-acetylglucosaminyl-

transferase II (GnTII). Golgi localization of many plant glycosyltransferases has recently been reported [34], but the localization of GnTII was not investigated. Furthermore, several pathways for N-glycosylation in plants have been suggested, but the exact localization of GnTII is still unclear [33, 35]. The observation that in our study both hybrid Lewis X-type and single Lewis X-type N-glycans are devoid of core α1,3-fucose as well as a second GlcNAc supports the novel N-glycosylation pathway that was postulated by Kajiura and co-workers [33]. In this pathway GnTII acts on N-glycans that have already been modified by ManII and XylT, which positions GnTII to the end of the medial-Golgi or trans-Golgi compartment. Further investigation on the re-localization of GnTII to earlier Golgi compartments or co-expression of a GnTII of animal origin might therefore enable the synthesis of N-glycans carrying two Lewis X structures in wild-type plants in the future.

In addition to the synthesis of Lewis X, our study is the first to describe the synthesis of N-glycans in plants that carry terminal GalNAc residues (LDN). GalNAc containing O-glycans were previously synthesized on recombinant MUC1 in tobacco and required the co-expression of human GalNAc-T2 in combination with a UDP-GlcNAc C4-epimerase and a UDP-GalNAc transporter [25]. Yet, more recent reports showed that it is possible to synthesize GalNAc containing O-glycans on several recombinant proteins in the absence of a transporter and/or epimerase [24, 26]. To find out which enzymes are required for the synthesis of the LDN structure on N-glycans, we transiently co-expressed kappa-5 with different combinations of GalNAcT from *C. elegans*, *trans*-Golgi targeted GalNAcT (sialGalNAcT), a C4 epimerase from *P. aeruginosa* and/or different GalNAc transporters from *C. elegans*. Our results demonstrate that LDN synthesis in plants only requires the co-expression of the native GalNAcT from *C. elegans*. This suggests that plants have all the required proteins for the production of the UDP-GalNAc substrate and transport of this substrate into the Golgi. This idea is further supported by the recent identification of the first UDP-GlcNAc/UDP-GalNAc transporter in *Arabidopsis thaliana* [36].

Like for Lewis X engineering, the synthesis of LDN and LDNF structures in plants only results in complex N-glycans that carry a single LDN or LDNF structure. So in both engineering strategies there might be the same underlying problem. Co-expression of glycosyltransferases of animal origin interferes with the activity of plant endogenous enzymes. However, there seem to be differences between co-expression of sialGalT or GalNAcT. The majority of the LDN(F) carrying N-glycans still contain core α1,3-fucose, which is in contrast to the complete lack of core α1,3-fucose upon controlled expression of sialGalT. Still it is possible that the addition of either galactose or GalNAc to the α1,3-mannosyl branch would interfere with the activity of endogenous GnTII. This idea is further supported by the observation that kappa-5 from wild-type plants mainly carries N-glycans from the $GnGnXF^3$-type, but upon co-expression of GalNAcT one of the terminal GlcNac residues is lost. This is most likely explained by the fact that plant GnTII is not able to use LDN carrying N-glycans as a substrate. Co-expression of a GnTII of animal

origin would therefore be an interesting strategy to improve the synthesis of complex N-glycans carrying multiple Lewis X or LDN(F) structures.

Another bottleneck for the synthesis of LDN(F) structures in plants is the enzymatic activity of endogenous β-hexosaminidases in *Nicotiana benthamiana*. Our N-glycan profiles reveal that the synthesis of LDN is most likely counteracted by β-hexosaminidases, since the amount of GalNAc containing N-glycans increases by the addition of α1,3-linked fucose to create LDNF. This suggests that the fucose residue protects against the removal of terminal GalNAc. This protection is only partial as we also observe N-glycans with fucosylated terminal GlcNAc residues, which arise after removal of terminal GalNAc. This indicates that plant β-hexosaminidases are able to remove terminal GalNAc from the LDNF structure. This is in line with the previous observation that β-hexosaminidase from jack bean is able to remove terminal GalNAc residues from the LDNF structure on kappa-5 [16]. Strategies to reduce β-hexosaminidase activity would therefore be of interest and might be required for the engineering of N-glycans with multiple LDN(F) structures.

From our study we can conclude that glyco-engineering of helminth-like N-glycans makes it possible to synthesize N-glycans containing Lewis X, LDN or LDNF in plants. Yet, the N-glycans naturally found on *S. mansoni*-derived glycoproteins are not homogenous [15, 16]. For instance, the majority of the N-glycans of *S. mansoni*-derived omega-1 carry terminal Lewis X, but the N-glycans on omega-1 can also carry terminal galactose and/or mannose, LDN or LDNF, difucosylated terminal structures or tandem Lewis X structures. The ability of plants to synthesize different N-glycans homogenously enables more detailed studies on the exact contribution of a specific N-glycan structure on glycoprotein function. Plants are therefore an excellent platform for the production of *S. mansoni*-derived glycoproteins carrying engineered N-glycans. Plant-based expression of uncharacterised helminth glycoproteins enables their functional characterisation and glyco-engineering in plants would allow investigation on the role of helminth-like N-glycans on immunomodulatory properties. The use of plants as a production platform for native helminth glycoproteins therefore opens up a new field of research and might ultimately lead to the identification of new therapeutic targets for treatment of inflammatory disorders.

Experimental procedures

Construction of expression vectors

The complete sequence encoding mature *Schistosoma mansoni* omega-1 and kappa-5 proteins was codon optimised according to an in-house optimisation procedure based on codons frequently used in highly expressed genes in plants. The mature protein sequence was preceded by a signal peptide from the *Arabidopsis thaliana* chitinase gene (cSP) and a N-terminal 6x histidine-FLAG tag (H6F). The amino acid sequence VEDAS was placed in-between the signal peptide and tags to ensure proper signal peptide cleavage and to prevent cleavage of the N-terminal histidine tag. The full sequences were flanked by NcoI and KpnI restriction sequences at 5' and 3' ends respectively and synthetically constructed by GeneArt (Life Technologies; Bleiswijk, the Netherlands). The H58F mutation in the catalytic site of omega-1 to remove RNase activity was introduced by means of overlap extension PCR. Omega-1, omega-1^{H58F} and kappa-5 were cloned into the pHYG expression vector using NcoI/KpnI [37].

Expression vectors for hybrid α1,3-fucosyltransferase IXa (Fut9a) from *Tetraodon nigriviridus* (pufferfish) and hybrid β1,4-galactosyltransferase (GalT) from *Danio rerio* (zebrafish) to engineer N-glycans carrying terminal Lewis X structures were used [22, 38]. The N-terminal domain of *Arabidopsis thaliana* β1,2-xylosyltransferase in the Fut9a hybrid gene was replaced by the CTS domain (C, cytoplasmic tail; T, transmembrane domain; S, stem region) of rat α2,6-sialyltransferase enabling *trans*-Golgi targeting (from now on referred to as sialFucT). The GalT gene already contained this CTS domain for *trans*-Golgi targeting (referred to as sialGalT). Expression cassettes for sialFucT and sialGalT were then transferred to the plant expression vector pBINPLUS [39]. For controlled expression of sialGalT the full gene was reamplified to introduce NcoI/KpnI restriction at the 5' and 3' ends respectively. SialGalT was then used to replace YFP in the pRAP-pGPAII::Gpa2-3'UTR-YFP vector, thereby placing the expression of sialGalT under the control of the promoter region of the *Gpa2* gene [40]. The entire *Gpa2:*sialGalT expression cassette was then transferred to pBINPLUS with AscI/PacI. A synthetic hybrid construct of *Arabidopsis thaliana* GnTII (amino acids 72-430) with the CTS domain of *Arabidopsis thaliana* β1,2-xylosyltransferase was ordered at GeneArt (Life Technologies) and transferred to the pBIN expression vector.

To engineer N-glycans carrying terminal GalNAc (LDN) we cloned the β1,4-*N*-acetylgalactosaminyltransferase (bre-4, GalNAcT) and the UDP-GalNAc transporters nstp-4, nstp-5 and sqv-7 from *Caenorhabditis elegans* cDNA. A hybrid form of the *C. elegans* GalNAcT was cloned by replacing the native CTS domain with the CTS domain of rat α2,6-sialyltransferase enabling *trans*-Golgi targeting (from now on referred to as sialGalNAcT). A codon optimised C4 epimerase from *Pseudomonas aeruginosa* (WbpP) [26] was synthetically constructed at GeneArt and all genes were cloned into the pBIN

expression vector. To add α1,3-linked fucose to the LDN structure (LDNF) we used the previously described hybrid α1,3-fucosyltransferase IXa from pufferfish (sialFucT).

Expression of all constructs (unless stated differently) was driven by the 35S promoter of the *Cauliflower mosaic virus* with duplicated enhancer (d35S) and the *Agrobacterium tumefaciens* nopaline synthase transcription terminator (Tnos). A 5′ leader sequence of the Alfalfa mosaic virus RNA 4 (AlMV) was included between the promoter and construct to boost translation. In all experiments the silencing suppressor p19 from tomato bushy stunt virus in pBIN61 was co-infiltrated to enhance expression [41].

Agroinfiltration of *Nicotiana benthamiana*

Agrobacterium tumefaciens clones were cultured for 16 hours at 28°C/250 rpm in LB medium (10g/l pepton140, 5g/l yeast extract, 10g/l NaCl with pH=7.0) containing 50 µg/ml kanamycin, 20 µg/ml rifampicin and 20µM acetosyringone. The bacteria were suspended in MMA infiltration medium (20g/l sucrose, 5g/l MS-salts, 1.95g/l MES, pH5.6) containing 200 µM acetosyringone till a final OD of 0.5 was reached. For co-infiltration experiments with *Agrobacterium* harbouring the expression vectors for glycosyltransferases OD's of 0.05-0.5 were used. After 1-2 hours incubation at room temperature, the two youngest fully expanded leaves of 5-6 weeks old *Nicotiana benthamiana* plants were infiltrated completely. Infiltration was performed by injecting the *Agrobacterium* suspension into a *Nicotiana benthamiana* leaf at the abaxial side using a 1 ml syringe. *Nicotiana benthamiana* plants were maintained in a controlled greenhouse compartment (UNIFARM, Wageningen) and infiltrated leaves were harvested at selected time points.

Total soluble protein extraction

Leaves were immediately snap-frozen upon harvesting, homogenized in liquid nitrogen and stored at -20°C until use. Homogenized plant material was ground in ice-cold extraction buffer (50mM phosphate-buffered saline (pH=8), 100 mM NaCl, 0.1% v/v Tween-20 and 2% w/v immobilized polyvinylpolypyrrolidone (PVPP)) using 2 ml/g fresh weight. Crude extracts were clarified by centrifugation at 16.000 rpm for 5 min at 4°C and supernatants were directly analysed for total protein content by a BCA protein assay (Life Technologies).

Apoplast wash

Leaves were submerged in ice-cold extraction buffer (50mM phosphate-buffered saline (pH=8), 100 mM NaCl and 0.1% v/v Tween-20) after which vacuum was applied for 10min. Vacuum was released slowly to ensure infiltration of the apoplastic space. Leaves were placed in 10-ml syringes and centrifuged for 20 min. at 2000*xg*. Apoplast washes were clarified by centrifugation at 16.000 rpm for 5 min at 4°C and supernatants were stored at -80°C.

Purification from the apoplast fluid

Plant produced omega-1 and kappa-5 were purified from apoplast fluids using Ni-NTA Sepharose (IBA GmbH; Goettingen, Germany). Apoplast fluid was transferred over G25 Sephadex columns to exchange for Ni-NTA binding buffer (50 mM phosphate buffered saline (pH 8) containing 100 mM NaCl). Ni-NTA Sepharose was incubated with the apoplast fluid for 30 min. followed by 3 washing steps with binding buffer. Omega-1 was eluted from the Ni-NTA Sepharose with 0.5M imidazole (in binding buffer). Finally, purified omega-1 was dialysed against PBS.

Protein analysis by western blot

Total soluble plant proteins and purified omega-1 or kappa-5 were separated under reducing conditions by SDS-PAGE on a 12% Bis-Tris gel. To analyse purity of the proteins the gel was stained with Coomassie brilliant blue staining. For western blotting proteins were transferred to a PVDF membrane by a wet blotting procedure. Thereafter the membrane was blocked in PBST-BL (PBS containing 0.1% v/v Tween-20 and 5% w/v non-fat dry milk powder) for 1 hour at room temperature, followed by overnight incubation with a HRP conjugated anti-FLAG M2 antibody (Sigma-Aldrich; Zwijndrecht, the Netherlands) in PBST at 4°C. The membrane was washed 5 times with 5 min intervals in PBST. Finally, the SuperSignal West Femto substrate (Thermo Fisher Scientific; Etten-Leur, the Netherlands) was used to detect HRP-conjugated antibodies in the G:BOX Chemi System (Syngene; Cambridge, UK).

Characterisation of N-glycan composition

Omega-1 or kappa-5 (100 ng) were deglycosylated with PNGase F or Endo H (both from Bioké; Leiden, the Netherlands) to screen for the presence of plant-specific α1,3-fucose or oligomannose/hybrid-type N-glycans respectively. Deglycosylated omega-1 was then analysed by anti-FLAG western blot. The synthesis of LDN structures on plant proteins or kappa-5 was analysed by ELISA with biotinylated agglutinin from soybean (SBA) (Bio-Connect; Huissen, The Netherlands). For this 1 µg/ml of total soluble apoplast proteins or purified kappa-5 was coated overnight at 4°C on ELISA plates. Plates were blocked with PBST containing 1% w/v BSA and all subsequent steps were performed in blocking buffer. Plates were then incubated with biotinylated lectin (5 µg/ml) and subsequently avidin-HRP (eBioscience; Vienna, Austria). TMB substrate (eBioscience) was used for detection.

For MALDI-TOF-MS analysis, 1-2 µg of purified omega-1 or kappa-5 were reduced for 10 min at 95°C in PBS containing 1.3% w/v SDS and 0.1% v/v β-mercaptoethanol. SDS was neutralized with NP-40 prior to overnight digestion at 37°C with trypsin (Sigma-Aldrich) immobilized to NHS-activated Sepharose (GE Healthcare; Zwolle, The Netherlands). Trypsin-beads were removed from the digestion mix by centrifugation and the pH of the mix was adjusted to 5 using 1M sodium acetate. 0.5 mU of PNGase A

(Roche; Woerden, The Netherlands) was used to release N-glycans from omega-1 while incubating overnight at 37°C. Released N-glycans were purified by C18 Bakerbond™ SPE cartridges (VWR; Amsterdam, The Netherlands) and subsequent Extract Clean™ Carbo SPE columns (Grace; Breda, the Netherlands). N-glycans were labeled with anthranilic acid (Sigma) and desalted over Biogel P10 (BioRad; Veenendaal, The Netherlands). To confirm the presence of Lewis X, purified N-glycans were treated with Jack bean β(1-4,6)-galactosidase (Prozyme; Hayward, CA, USA) according to the suppliers protocol. Samples in 75% acetonitrile were mixed with 1 µl of matrix solution (20 mg/ml 2,5-dihydroxybenzoic acid in 50% acetonitrile, 0.1% TFA) and were dried under a stream of warm air. Matrix-assisted laser desorption/ionization (MALDI) time-of-flight (TOF) mass spectra (MS) were obtained using an Ultraflex II mass spectrometer (Bruker Daltonics; Wormer, The Netherlands) as previously described [16].

RNase activity assay

Total RNA was isolated from $5.0x10^6$ bone marrow-derived dendritic cells using the RNeasy Mini Kit (Qiagen; Venlo, The Netherlands) as described by the supplier's protocol. 1 µg of total RNA was incubated with 500 ng purified omega-1 for 1 hour at 37°C using PBS as buffer. PBS only was used as negative control and 500 ng RNase A as positive control. RNA breakdown was then analysed on a 1.5% agarose gel and visualised with UV light.

Acknowledgements

We would like to thank Tam Nguyen and Simone Oostindie for their input in the practical work of this study.

Supplemental Figures

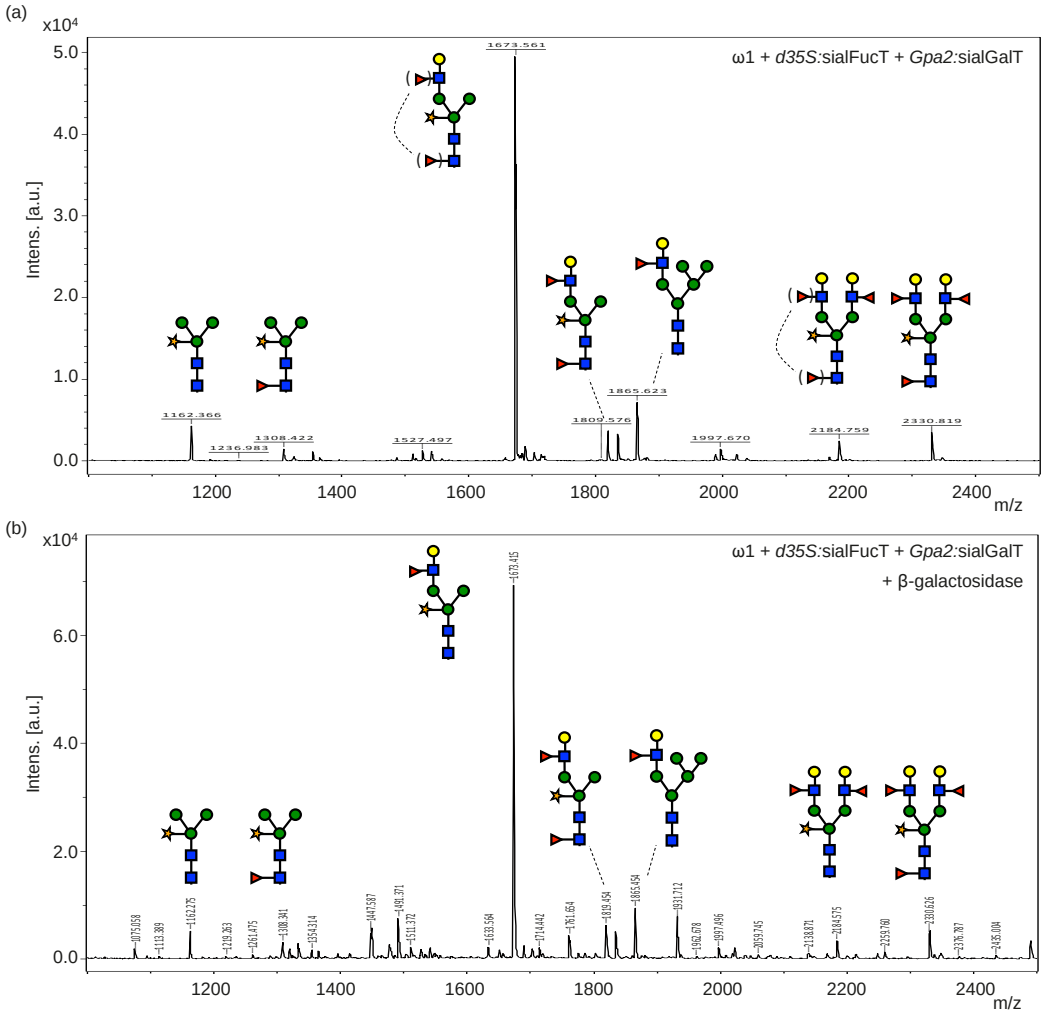

Figure S1 ◆ Confirmation of the presence of Lewis X structures. N-glycans from purified omega-1 were analysed by MALDI-TOF-MS upon tryptic digestion and PNGase A release of N-glycans. (a) N-glycan profile for omega-1 from wild-type *N. benthamiana* plants upon co-expression of *d35S:*sialFucT (OD=0.1) and *Gpa2:*sialGalT (OD=0.5), but the latter being expressed with the pHYG vector. Sugar residues for which the position is not completely clear are placed between brackets. (b) Profile of the same N-glycans upon treatment with β(1-4,6)-galactosidase from Jack bean.

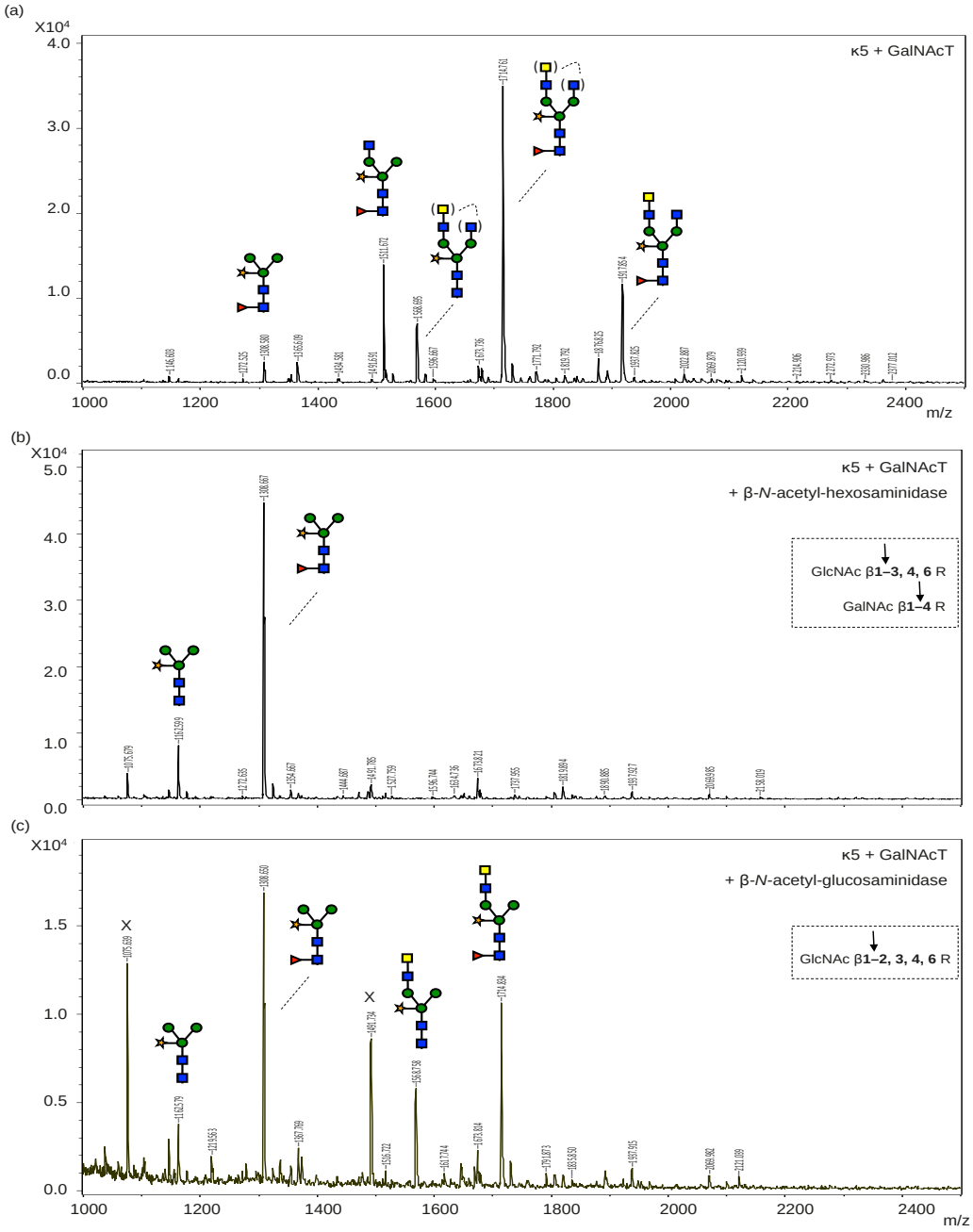

Figure S2 ◆ Confirmation of the presence of LDN structures. N-glycans from purified kappa-5 were analysed by MALDI-TOF-MS upon tryptic digestion and PNGase A release of N-glycans. (a) N-glycan profile for kappa-5 from wild-type *N. benthamiana* plants upon co-expression of GalNAcT. Sugar residues for which the position is not completely clear are placed between brackets. (b) Profile of the same N-glycans upon treatment with β-*N*-acetyl-hexosaminidase from *Streptomyces plicatus*. (c) Profile of the same N-glycans upon treatment with β-*N*-acetyl-glucosaminidase from *Xanthomonas manihotis*. For both enzymatic digestions the substrate specificity is indicated in the dashed box.

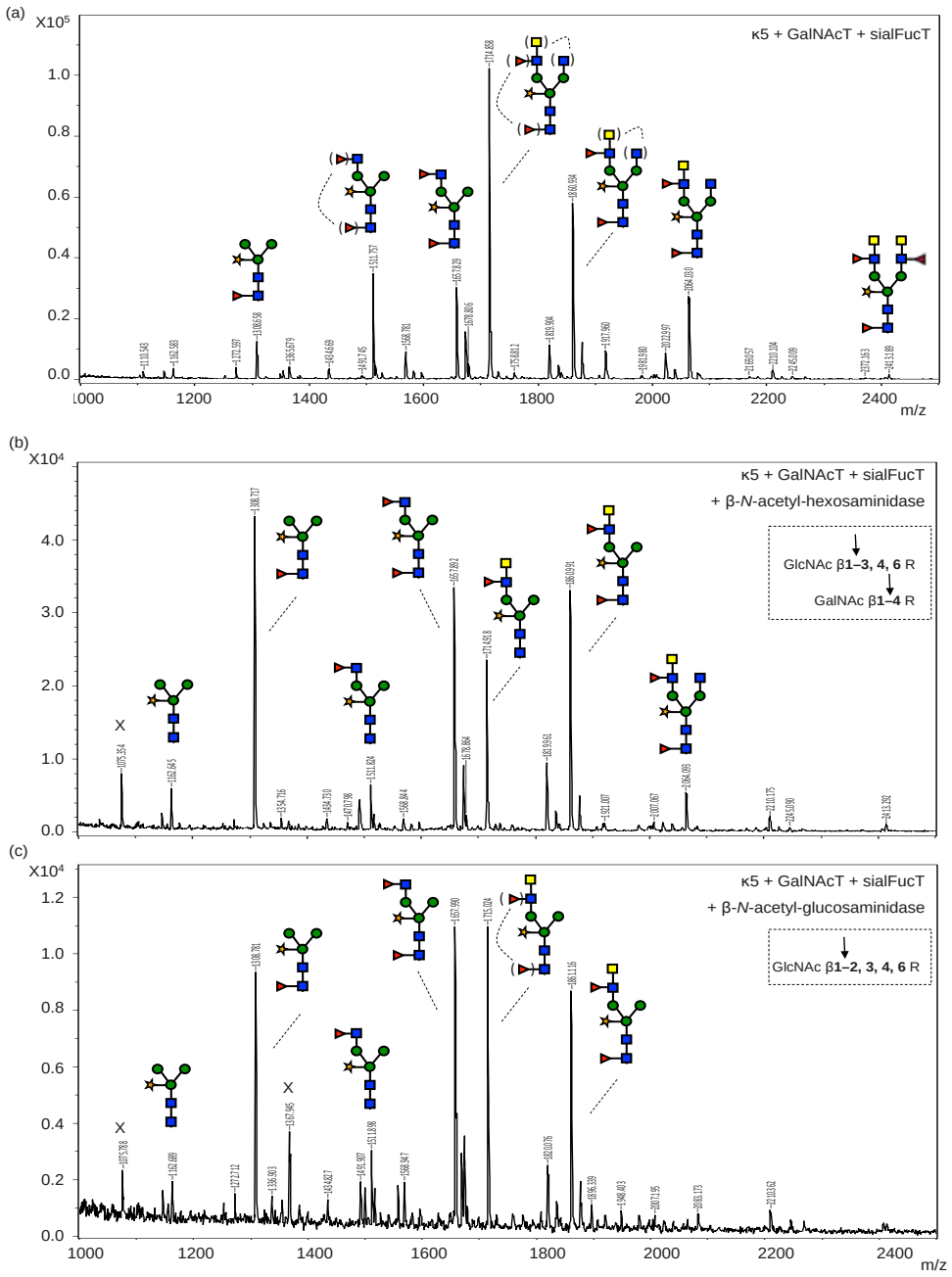

Figure S3 ◆ Confirmation of the presence of LDNF structures. N-glycans from purified kappa-5 were analysed by MALDI-TOF-MS upon tryptic digestion and PNGase A release of N-glycans. (a) N-glycan profile for kappa-5 from wild-type *N. benthamiana* plants upon co-expression of GalNAcT and sialFucT. Sugar residues for which the position is not completely clear are placed between brackets. (b) Profile of the same N-glycans upon treatment with β-*N*-acetyl-hexosaminidase from *Streptomyces plicatus*. (c) Profile of the same N-glycans upon treatment with β-*N*-acetyl-glucosaminidase from *Xanthomonas manihotis*. For both enzymatic digestions the substrate specificty is indicated in the dashed box.

References

1. Pearce EJ, Kane CM, Sun J, Taylor JJ, McKee AS, et al. (2004) Th2 response polarization during infection with the helminth parasite Schistosoma mansoni. Immunological Reviews 201: 117-126.
2. Pearce EJ and MacDonald AS (2002) The immunobiology of schistosomiasis. Nature Reviews Immunology 2: 499-511.
3. Elliott DE, Li J, Blum A, Metwali A, Qadir K, et al. (2003) Exposure to schistosome eggs protects mice from TNBS-induced colitis. American Journal of Physiology - Gastrointestinal and Liver Physiology 284: G385-391.
4. Mangan NE, van Rooijen N, McKenzie AN and Fallon PG (2006) Helminth-modified pulmonary immune response protects mice from allergen-induced airway hyperresponsiveness. Journal of Immunology 176: 138-147.
5. Sewell D, Qing Z, Reinke E, Elliot D, Weinstock J, et al. (2003) Immunomodulation of experimental autoimmune encephalomyelitis by helminth ova immunization. International Immunology 15: 59-69.
6. Cooke A, Tonks P, Jones FM, O'Shea H, Hutchings P, et al. (1999) Infection with Schistosoma mansoni prevents insulin dependent diabetes mellitus in non-obese diabetic mice. Parasite Immunology 21: 169-176.
7. Zaccone P, Fehervari Z, Jones FM, Sidobre S, Kronenberg M, et al. (2003) Schistosoma mansoni antigens modulate the activity of the innate immune response and prevent onset of type 1 diabetes. European Journal of Immunology 33: 1439-1449.
8. Allen JE and Maizels RM (2011) Diversity and dialogue in immunity to helminths. Nature Reviews Immunology 11: 375-388.
9. Cass CL, Johnson JR, Califf LL, Xu T, Hernandez HJ, et al. (2007) Proteomic analysis of Schistosoma mansoni egg secretions. Molecular & Biochemical Parasitology 155: 84-93.
10. Mathieson W and Wilson RA (2010) A comparative proteomic study of the undeveloped and developed Schistosoma mansoni egg and its contents: the miracidium, hatch fluid and secretions. International Journal for Parasitology 40: 617-628.
11. Fitzsimmons CM, Schramm G, Jones FM, Chalmers IW, Hoffmann KE, et al. (2005) Molecular characterization of omega-1: A hepatotoxic ribonuclease from Schistosoma mansoni eggs. Molecular & Biochemical Parasitology 144: 123-127.
12. Everts B, Perona-Wright G, Smits HH, Hokke CH, van der Ham AJ, et al. (2009) Omega-1, a glycoprotein secreted by Schistosoma mansoni eggs, drives Th2 responses. Journal of Experimental Medicine 206: 1673-1680.

13. Steinfelder S, Andersen JF, Cannons JL, Feng CG, Joshi M, et al. (2009) The major component in schistosome eggs responsible for conditioning dendritic cells for Th2 polarization is a T2 ribonuclease (omega-1). Journal of Experimental Medicine 206: 1681-1690.

14. Everts B, Hussaarts L, Driessen NN, Meevissen MHJ, Schramm G, et al. (2012) Schistosome-derived omega-1 drives Th2 polarization by suppressing protein synthesis following internalization by the mannose receptor. Journal of Experimental Medicine 209: 1753-1767.

15. Meevissen MHJ, Wuhrer M, Doenhoff MJ, Schramm G, Haas H, et al. (2010) Structural Characterization of Glycans on Omega-1, a Major Schistosoma mansoni Egg Glycoprotein That Drives Th2 Responses. Journal of Proteome Research 9: 2630-2642.

16. Meevissen MH, Balog CI, Koeleman CA, Doenhoff MJ, Schramm G, et al. (2011) Targeted glycoproteomic analysis reveals that kappa-5 is a major, uniquely glycosylated component of Schistosoma mansoni egg antigens. Molecular & Cellular Proteomics 10: M110 005710.

17. Schramm G, Hamilton JV, Balog CI, Wuhrer M, Gronow A, et al. (2009) Molecular characterisation of kappa-5, a major antigenic glycoprotein from Schistosoma mansoni eggs. Molecular & Biochemical Parasitology 166: 4-14.

18. Meevissen MHJ, Yazdanbakhsh M and Hokke CH (2012) Schistosoma mansoni egg glycoproteins and C-type lectins of host immune cells: Molecular partners that shape immune responses. Experimental Parasitology 132: 14-21.

19. Bosch D, Castilho A, Loos A, Schots A and Steinkellner H (2013) N-Glycosylation of Plant-produced Recombinant Proteins. Current Pharmaceutical Design 19: 5503-5512.

20. Strasser R, Stadlmann J, Schahs M, Stiegler G, Quendler H, et al. (2008) Generation of glyco-engineered Nicotiana benthamiana for the production of monoclonal antibodies with a homogeneous human-like N-glycan structure. Plant Biotechnology Journal 6: 392-402.

21. Castilho A, Bohorova N, Grass J, Bohorov O, Zeitlin L, et al. (2011) Rapid High Yield Production of Different Glycoforms of Ebola Virus Monoclonal Antibody. Plos One 6(10): e26040.

22. Rouwendal GJ, Florack DE, Hesselink T, Cordewener JH, Helsper JP, et al. (2009) Synthesis of Lewis X epitopes on plant N-glycans. Carbohydrate Research 344: 1487-1493.

23. Strasser R, Castilho A, Stadlmann J, Kunert R, Quendler H, et al. (2009) Improved virus neutralization by plant-produced anti-HIV antibodies with a homogeneous beta1,4-galactosylated N-glycan profile. Journal of Biological Chemistry 284: 20479-20485.

24. Castilho A, Neumann L, Daskalova S, Mason HS, Steinkellner H, et al. (2012) Engineering of sialylated mucin-type O-glycosylation in plants. Journal of Biological Chemistry 287: 36518-36526.

25. Daskalova SM, Radder JE, Cichacz ZA, Olsen SH, Tsaprailis G, et al. (2010) Engineering of N. benthamiana L. plants for production of N-acetylgalactosamine-glycosylated proteins--towards development of a plant-based platform for production of protein therapeutics with mucin type O-glycosylation. BMC Biotechnology 10: 62.

26. Yang Z, Drew DP, Jorgensen B, Mandel U, Bach SS, et al. (2012) Engineering mammalian mucin-type O-glycosylation in plants. Journal of Biological Chemistry 287: 11911-11923.

27. Wang L and Roossinck M (2006) Comparative analysis of expressed sequences reveals a conserved pattern of optimal codon usage in plants. Plant Molecular Biology 61: 699-710.

28. Palacpac NQ, Yoshida S, Sakai H, Kimura Y, Fujiyama K, et al. (1999) Stable expression of human β 1,4-galactosyltransferase in plant cells modifies N-linked glycosylation patterns. Proceedings of the National Academy of Sciences 96: 4692-4697.

29. Strasser R, Singh J, Bondili JS, Schoberer J, Svoboda B, et al. (2007) Enzymatic properties and subcellular localization of Arabidopsis beta-N-acetyl-hexosaminidases. Plant Physiology 145: 5-16.

30. Liebminger E, Veit C, Pabst M, Batoux M, Zipfel C, et al. (2011) beta-N-Acetylhexosaminidases HEXO1 and HEXO3 Are Responsible for the Formation of Paucimannosidic N-Glycans in Arabidopsis thaliana. Jounral of Biological Chemistry 286: 10793-10802.

31. Bakker H, Rouwendal GJ, Karnoup AS, Florack DE, Stoopen GM, et al. (2006) An antibody produced in tobacco expressing a hybrid beta-1,4-galactosyltransferase is essentially devoid of plant carbohydrate epitopes. Proceedings of the National Academy of Sciences of the United States of America 103: 7577-7582.

32. Zeng YC, Bannon G, Thomas VH, Rice K, Drake R, et al. (1997) Purification and specificity of beta 1,2-xylosyltransferase, an enzyme that contributes to the allergenicity of some plant proteins. Journal of Biological Chemistry 272: 31340-31347.

33. Kajiura H, Okamoto T, Misaki R, Matsuura Y and Fujiyama K (2012) Arabidopsis beta 1,2-xylosyltransferase: Substrate specificity and participation in the plant-specific N-glycosylation pathway. Journal of Bioscience & Bioengineering 113: 48-54.

34. Schoberer J, Liebminger E, Botchway SW, Strasser R and Hawes C (2013) Time-resolved fluorescence imaging reveals differential interactions of N-glycan processing enzymes across the Golgi stack in planta. Plant Physiology 161: 1737-1754.

35. Bencur P, Steinkellner H, Svoboda B, Mucha J, Strasser R, et al. (2005) Arabidopsis thaliana beta1,2-xylosyltransferase: an unusual glycosyltransferase with the potential to act at multiple stages of the plant N-glycosylation pathway. Biochemistry Journal 388: 515-525.

36. Niemann MC, Bartrina I, Ashikov A, Weber H, Novak O, et al. (2015) Arabidopsis ROCK1 transports UDP-GlcNAc/UDP-GalNAc and regulates ER protein quality control and cytokinin activity. Proceedings of the National Academy of Sciences of the United States of America 112: 291-296.

37. Westerhof LB, Wilbers RHP, Roosien J, van de Velde J, Goverse A, et al. (2012) 3D Domain Swapping Causes Extensive Multimerisation of Human Interleukin-10 When Expressed In Planta. Plos One 7(10): e46460.

38. Hesselink T, Rouwendal GJ, Henquet MG, Florack DE, Helsper JP, et al. (2014) Expression of natural human beta1,4-GalT1 variants and of non-mammalian homologues in plants leads to differences in galactosylation of N-glycans. Transgenic Research 23: 717-728.

39. van Engelen FA, Molthoff JW, Conner AJ, Nap JP, Pereira A, et al. (1995) pBINPLUS: an improved plant transformation vector based on pBIN19. Transgenic Research 4: 288-290.

40. Sacco MA, Koropacka K, Grenier E, Jaubert MJ, Blanchard A, et al. (2009) The cyst nematode SPRYSEC protein RBP-1 elicits Gpa2- and RanGAP2-dependent plant cell death. PLoS Pathogens 5: e1000564.

41. Voinnet O, Rivas S, Mestre P and Baulcombe D (2003) An enhanced transient expression system in plants based on suppression of gene silencing by the p19 protein of tomato bushy stunt virus. Plant Journal 33: 949-956.

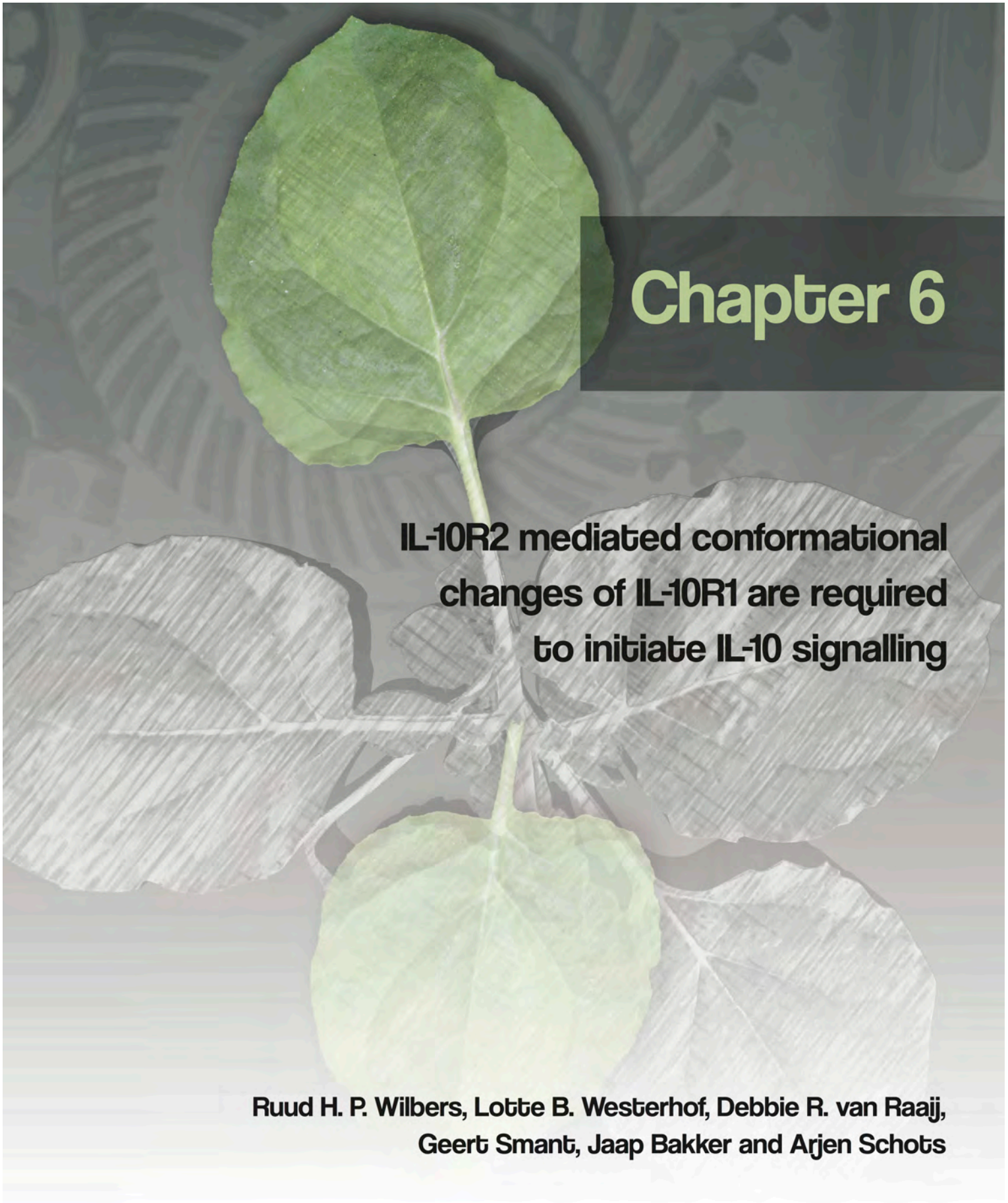

Chapter 6

IL-10R2 mediated conformational changes of IL-10R1 are required to initiate IL-10 signalling

Ruud H. P. Wilbers, Lotte B. Westerhof, Debbie R. van Raaij, Geert Smant, Jaap Bakker and Arjen Schots

Abstract

Interleukin-10 (IL-10) is an anti-inflammatory cytokine that plays a key role in maintaining immune homeostasis. IL-10-mediated responses are triggered upon binding to a heterodimeric receptor complex consisting of IL-10 receptor 1 (IL-10R1) and IL-10R2. Engagement of the IL-10R complex activates the intracellular kinases Jak1 and Tyk2, but to date the exact role of IL-10R2 and IL-10R2-associated signalling via Tyk2 remains unclear. In this study we re-evaluated IL-10-mediated responses, in particular on bone marrow-derived dendritic cells, macrophages and mast cells to elucidate the contribution of IL-10R2. Our results show that IL-10-mediated responses depend on both IL-10R1 and IL-10R2 in the investigated cell types, but IL-10R2 associated signalling via Tyk2 only plays a limited role. Tyk2 was shown to control the amplitude of signaling and up-regulation of expression of suppressor of cytokine signalling 3 (SOCS3). SOCS3 up-regulation was cell-type dependent, but correlated with early suppression of LPS-induced tumour necrosis factor α (TNF-α). Further investigation of the IL-10R complex revealed that both the extracellular and intracellular domain of IL-10R2 influences IL-10R1 conformation and that both domains were required for transducing IL-10 signals.

Introduction

Interleukin (IL)-10 is an essential regulator of the immune system, notably because of its anti-inflammatory properties and its role in re-establishing immune homeostasis. IL-10 is a strong suppressor of antigen presenting cells and lymphocytes [2, 3] and it was revealed that IL-10-deficient mice develop spontaneous inflammation in the intestine [4]. Besides its anti-inflammatory properties, IL-10 is also able to regulate proliferation of B cells, mast cells and NK cells [3, 5]. IL-10 signals through a heterodimeric receptor complex composed of IL-10 receptor (IL-10R)1 and IL-10R2 [6, 7]. Mice lacking either one of these two receptors develop spontaneous intestinal inflammation, like IL-10-deficient mice [8, 9]. Engagement of the IL-10 receptor complex activates the Janus kinases Jak1 and Tyk2 [10, 11], which are associated with IL-10R1 and IL-10R2, respectively [12]. IL-10's anti-inflammatory properties were shown to be dependent on the activation of Jak1 and the transcription factor STAT3 [13]. A role for the IL-10R2-associated kinase Tyk2 is more elusive. Karaghiosoff and co-workers showed that Tyk2-deficient mice develop normally and that the ability of IL-10 to suppress LPS-induced TNF-α expression in macrophages is not impaired [14]. However, Shaw and co-workers showed that IL-10 was not able to suppress nitric oxide production upon stimulation with a high dose of IFN-γ in macrophages lacking Tyk2 [15]. Therefore, the exact contribution of IL-10R2 or associated signalling via Tyk2 to IL-10-mediated responses is still largely unknown.

To assess the biological activity of IL-10 a variety of assays is used. In most assays cell lines are used and most common are those assays using mast cell or macrophage cell lines. The mast cell line MC/9 is routinely used to study the induction of proliferation by IL-10 [5, 16], whereas various macrophage cell lines are used to study IL-10's anti-inflammatory properties [17, 18]. In some cases cell lines are transfected with plasmids for the expression of the native IL-10R or using chimeric constructs that employ the intracellular domain of IFN-γR molecules instead of the intracellular domain of the IL-10 receptors [7, 16, 19]. However, one might question the appropriateness of the use of cell lines in research on the mechanisms of cellular responses of IL-10. It is doubtful whether cell lines respond similar to *in vivo* cells as many cell lines are already cultured for a long time in different labs under different culturing conditions. The only selection pressure that these cells have encountered is efficient growth, and in the meantime these cell lines might have acquired (epi)genetic changes [20]. Cell lines could therefore have lost the ability to respond identical to their *in vivo* counterparts.

Previously, we have reported that a stable monomeric form of human IL-10 (IL-10m) lacks the ability to suppress LPS-induced TNF-α in a macrophage cell line, whereas dimerization of this monomer via fusion to the Fc portion of IgA restored its activity [17]. In contrast, stable monomeric IL-10 was reported to have activity on a B cell line that was either stably transfected with human or murine IL-10R1 [19]. This addressed the question

whether cell lines are indeed a reliable model system as different assays can give different outcomes. Furthermore, the use of hybrid IL-10R constructs might also not reflect the natural signalling complex for IL-10. Re-evaluation of IL-10 activity on *ex vivo* cells could therefore give new insights on the molecular mechanisms of IL-10 mediated responses.

To re-evaluate IL-10 mediated responses and particularly the role of IL-10R2 we set-up biological activity assays for IL-10 using three different cell types that were differentiated from mouse bone marrow. We re-evaluated IL-10 mediated responses on these bone marrow-derived cells and investigated the role of IL-10R2. As expected, IL-10 activity depends on both IL-10R1 and IL-10R2, but the IL-10R2-associated Tyk2 kinase only played a limited role in IL-10 mediated responses. Yet, we do show that Tyk2 contributes to the amplitude and kinetics of IL-10-mediated responses. Further investigation of the IL-10 signalling complex revealed that IL-10R2 mediates conformational changes of the extracellular domain of IL-10R1. Our study demonstrates that interactions between IL-10R1 and IL-10R2 (both intracellular and extracellular) reduce cellular binding of IL-10, but are crucial to initiate IL-10 mediated signalling.

Results

Bone marrow-derived cells differentially respond to IL-10

To set up biological activity assays for IL-10 based on *ex vivo* cells as an alternative for commonly used cell lines, mouse bone marrow-derived cells were differentiated into different cell types. To investigate the anti-inflammatory properties of IL-10, as commonly done on macrophage cell lines, bone marrow cells were differentiated into macrophages as well as dendritic cells. Flow cytometric analysis shows that ≥95% pure $CD11b^+$ $F4/80^+$ macrophages and ≥90% $CD11c^+$ $MHC\text{-}II^+$ dendritic cells were obtained (Figure 1a and 1d, respectively). Macrophages and dendritic cells were pre-treated with IL-10 and subsequently challenged with lipopolysaccharide (LPS). IL-10 inhibits TNF-α expression in a dose-dependent matter in both macrophages and dendritic cells (Figure 1b and 1e, respectively). We also observed that dendritic cells produced significantly more TNF-α when compared to macrophages, which is in line with the findings of Fleetwood and co-workers [21]. Furthermore, our data show that the maximum percentage inhibition of TNF-α levels is higher in macrophages than in dendritic cells (80% versus 60% in macrophages and dendritic cells, respectively). Next, we analysed the activation of STAT transcription factors by IL-10 in macrophages and dendritic cells. As expected, we observed strong tyrosine phosphorylation of $STAT3^{Y705}$ in both cell types (Figure 1c and 1f). However, in contrast with existing literature we did not detect activation of STAT1

[15]. On the other hand, STAT5 was constitutively activated in dendritic cells, but no activation of STAT5 was observed in macrophages.

To investigate proliferative responses of IL-10, which is typically done in MC/9 cells or B cell lines, bone marrow cells were differentiated into mast cells. Flow cytometric analysis showed that ≥95% pure c-kit$^+$ FcεRI$^+$ mast cells were obtained after 4 weeks of culture (Figure 1h). To test proliferative effects of IL-10, mast cells were cultured for 48 hours in the presence of IL-10 only, where after cell viability was assessed. IL-10 maintained viability of mast cells in a dose-dependent manner (Figure 1i). We also observed that the amount of viable cells was lower when compared to an IL-3 control (data not shown). This could indicate that IL-10 by itself does not induce proliferation, but only induces a survival signal in bone marrow-derived mast cells. When analysing IL-10 signalling in mast cells, we again observed strong activation of STAT3 and to a reduced extent of STAT5 (Figure 1j, only higher doses of IL-10). STAT1 was not activated in mast cells as was also observed in macrophages and dendritic cells. Further investigation of STAT1 involvement using bone marrow-derived cells from STAT1$^{-/-}$ mice revealed that STAT1 is not required for IL-10 mediated responses on bone marrow-derived cells (Figure S1).

Altogether, these biological activity assays provide a solid basis for studying IL-10-mediated responses on *ex vivo* cells. We have previously reported contrasting results on the activity of a stable monomeric form of human IL-10 when using cell lines [17]. We therefore re-evaluated the activity of this stable monomeric form of human IL-10 (IL-10m) on bone marrow-derived cells. We transiently expressed and purified IL-10m as previously reported for human IL-22 (Chapter 4). No differences in activity were observed between recombinant human and mouse IL-10 (data not shown), but application of monomeric IL-10 to bone marrow-derived cells revealed that up to 100-1000 fold more IL-10m was required to obtain similar responses as recombinant human IL-10 (Figure S2). This reduction in activity of stable monomeric IL-10 was much stronger as reported by Josephson and co-workers, who only observed a 8-19-fold reduction in activity depending on which IL-10R was used to transfect a B cell line [19]. We therefore conclude that the activity of IL-10m is stronger impaired than previously reported. Furthermore, this reveals that *ex vivo* cells might also be a more reliable model to investigate cellular responses of IL-10.

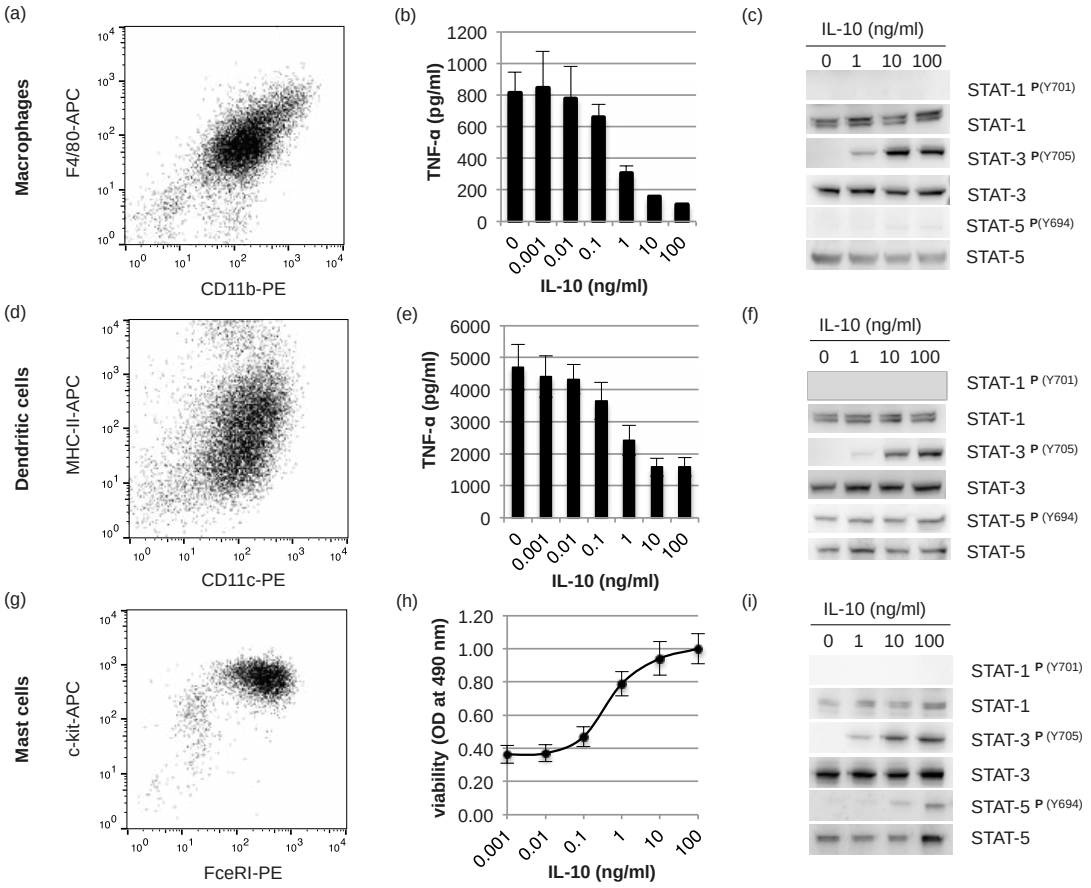

Figure 1 ◆ The differential response of bone marrow-derived cells to IL-10. Bone marrow-derived macrophages, dendritic cells and mast cells were analysed by flow cytometry for the expression of cellular markers CD11b & F4/80 (a), CD11c & MHC-II (d) and FcεRI & c-kit (g), respectively. Bone marrow-derived cells were tested for their response to IL-10 by measuring suppression of TNF-α expression by macrophages (b) and dendritic cells (e) or proliferative/anti-apoptotic ability in mast cells (h) (*n*=4, error bars indicate standard error). Dose dependent tyrosine phosphorylation of STAT transcription factors by IL-10 (0, 1, 10 or 100 ng/ml) was analysed by western blot in macrophages (c), dendritic cells (f) and mast cells (i).

IL-10 requires both IL-10R's for activity, but not signalling via Tyk2

To investigate the role of IL-10R2 in IL-10 mediated responses on bone marrow-derived cells, we cultured macrophages, dendritic cells and mast cells from bone marrow of IL-10R1$^{-/-}$and IL-10R2$^{-/-}$ mice and tested them for their response to IL-10. As expected, both IL-10R1 and IL-10R2 are required for IL-10's anti-inflammatory responses in macrophages and dendritic cells (Figure 2a and 2b, respectively). In the absence of either one of the two IL-10 receptors, IL-10 is not able to suppress LPS induced TNF-α expression. Similarly, bone marrow-derived mast cells also depend on both IL-10R1 and IL-10R2 for activity of IL-10 (Figure 2c). As IL-10R2 seems to be required for IL-10 activity, we further investigated whether IL-10R2 signalling via Tyk2 plays a role in our mast cell-based assay.

Tyk2 is a member of the janus kinase family of tyrosine kinases and to date is the only signalling molecule described to be associated with IL-10R2. We investigated the ability of IL-10 to maintain viability in mast cells in the absence of the Tyk2 kinase.

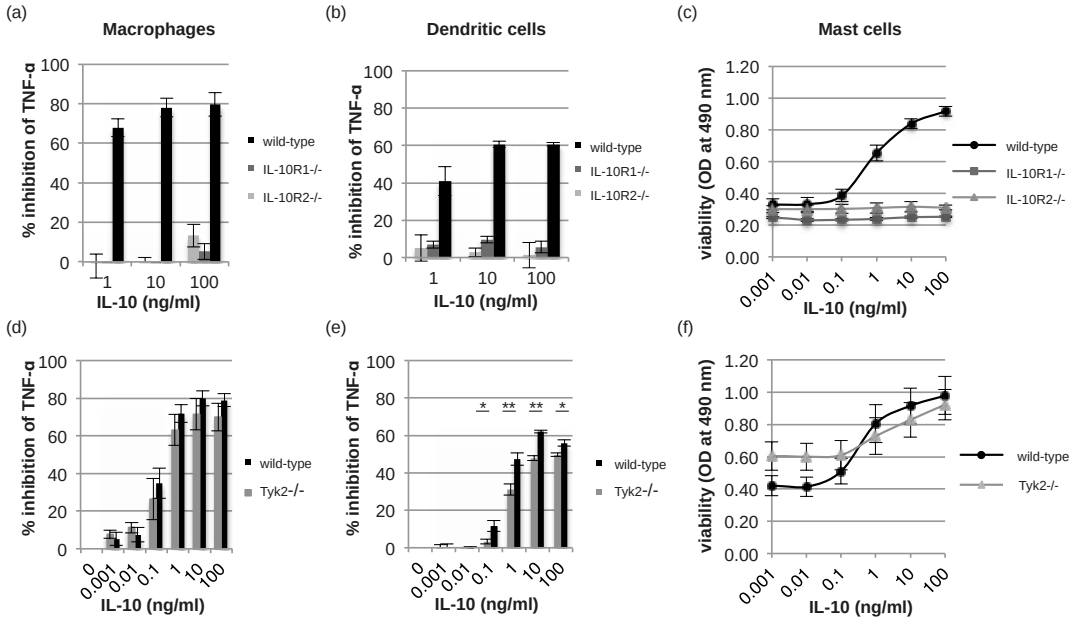

Figure 2 ◆ IL-10R2 mediated signalling via Tyk2 plays a limited role in IL-10 activity. Bone marrow-derived macrophages, dendritic cells and mast cells from wild-type, IL-10R1$^{-/-}$, IL-10R2$^{-/-}$ and Tyk2$^{-/-}$ mice were tested for their response to IL-10. Macrophages and dendritic cells from wild-type and IL-10R$^{-/-}$ mice were pre-treated with IL-10 and subsequently stimulated with 100 ng/ml LPS. The percentage of inhibition of TNF-α expression of macrophages and dendritic cells was determined after overnight incubation (a and b, respectively) (n=3, error bars indicate standard error). Similarly, macrophages and dendritic cells from Tyk2$^{-/-}$ mice were tested for their response to IL-10 (d and e, respectively) (n=4, error bars indicate standard error). Mast cells from wild-type and transgenic mice were cultured for 48 hours in the presence of IL-10 and cell viability was determined (c and f) (n=3 for IL-10R$^{-/-}$ mice and n=4 for Tyk2$^{-/-}$ mice, error bars indicate standard error). Asterisk(s) indicate significant differences as determined by a Welch's t-test (*P<0.05; **P<0.01).

Macrophages and dendritic cells were taken along, since literature is elusive on the role of Tyk2 in IL-10 anti-inflammatory responses. In the absence of IL-10R2-mediated signalling via Tyk2, IL-10 is perfectly capable to suppress TNF-α expression in macrophages and no significant differences were found between wild-type and Tyk2$^{-/-}$ mice (Figure 2d). The percentage of inhibition of TNF-α after LPS stimulation is approximately 8% lower in Tyk2$^{-/-}$ macrophages, but this is not significant. However, the percentages of inhibition of TNF-α of wild-type and Tyk2$^{-/-}$ dendritic cells were significantly different. Although a similar dose-response curve was observed for both dendritic cells, the level of TNF-α inhibition in Tyk2$^{-/-}$ dendritic cells was ~15% lower when compared to wild-type cells (Figure 2e). A similar reduction in IL-10 mediated

responses was also observed in the mast cell based assay. At high concentrations of IL-10, Tyk2$^{-/-}$ mast cells are slightly less viable than their wild-type counterparts, but this difference was not significant (Figure 2f). Altogether, we conclude that IL-10 requires both IL-10 receptors for activity, but there is only a minor role for the IL-10R2 associated Tyk2 kinase.

Tyk2 controls the amplitude and kinetics of IL-10-mediated responses

Deficiency of Tyk2 in bone marrow-derived cells only plays a limited role in IL-10-mediated responses and this is in line with a previous report by Karaghiosoff and co-workers [14]. They also showed that IL-10 is able to suppress LPS induced TNF-α expression in Tyk2$^{-/-}$ macrophages. However, Shaw and co-workers revealed that Tyk2$^{-/-}$ macrophages are unable to suppress IFN-γ-induced nitric oxide synthesis at a high dose of IFN-γ [15]. We therefore investigated IL-10 mediated responses in Tyk2$^{-/-}$ dendritic cells and macrophages in more detail to elucidate the contribution of Tyk2 in IL-10 mediated responses. First, we determined the dose-dependent phosphorylation of the transcription factor STAT3 (Y705) in both wild-type and Tyk2$^{-/-}$ macrophages and dendritic cells (Figure 3a and 3b, respectively). In both cell types we observed a ~10-fold reduction in STAT3 phosphorylation when cells are deficient in Tyk2. Furthermore, STAT3 phosphorylation in dendritic cells is rather poor when compared to macrophages, but IL-10 is perfectly capable to suppress TNF-α in those cells (even in the absence of Tyk2). We therefore conclude that Tyk2 is required for optimal IL-10-induced STAT3 tyrosine phosphorylation.

To investigate whether Tyk2 is required for optimal IL-10 induced gene expression we analysed the expression of suppressor of cytokine signalling 3 (SOCS3). SOCS3 is strongly up-regulated by IL-10 and is one of the major factors that mediate IL-10's anti-inflammatory functions [3]. In Figure 3c we show that SOCS3 is upregulated in a dose-dependent manner in both dendritic cells and macrophages and that Tyk2 deficiency significantly reduces the upregulation of SOCS3 in macrophages at a concentration of 100 ng/ml IL-10. Surprisingly, SOCS3 upregulation is significantly reduced in dendritic cells when compared to macrophages regardless of Tyk2 deficiency (P<0.05 at 10 and 100 ng/ml IL-10). No significant differences were observed for SOCS3 upregulation in wild-type versus Tyk2 deficient dendritic cells. Tyk2 therefore plays a role in regulating IL-10 induced gene expression, but its role is cell type dependent.

The role of SOCS3 in IL-10-mediated responses was previously investigated by Qasimi and co-workers (2006). In the case of TNF-α suppression SOCS3 seemed to play a role in early inhibition [18]. We therefore investigated whether Tyk2 deficiency would influence the suppression of TNF-α only 2 hours after LPS stimulation. In figure 3d we reveal that Tyk2 is indeed required for the early inhibition of LPS-induced TNF-α in macrophages. At

2 hours after stimulation IL-10 already supresses TNF-α by 80% in wild-type macrophages, but in Tyk2$^{-/-}$ macrophages this is significantly reduced to 50%. Furthermore, we show that IL-10 is unable to suppress TNF-α at an earlier time point in dendritic cells, which is in line with impaired SOCS3 upregulation in these cells. All together we conclude that Tyk2 optimizes STAT3 signalling and induction of SOCS3 expression and thereby controls the amplitude and kinetics of one the main anti-inflammatory signalling cascades Jak1-STAT3-SOCS3 in macrophages.

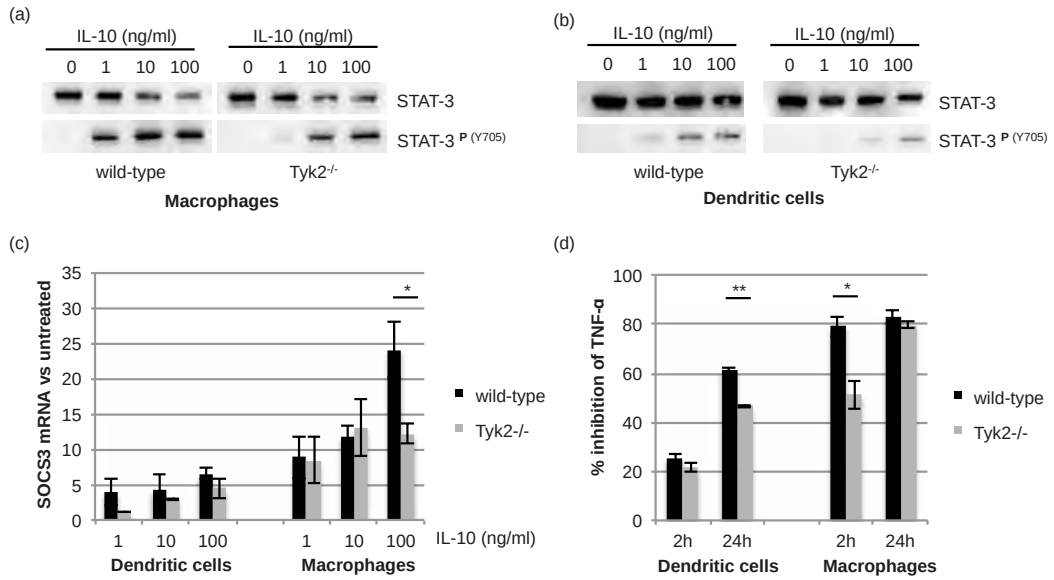

Figure 3 ◆ Tyk2 influences kinetics of IL-10 mediated responses. Bone marrow-derived macrophages and dendritic cells from Tyk2$^{-/-}$ mice were investigated in more detail for their signalling. Phosphorylation of tyrosine 705 (Y705) of STAT3 by IL-10 (0, 1, 10 and 100 ng/ml) was analysed in wild-type and Tyk2$^{-/-}$ macrophages and dendritic cells by western blot (a and b respectively). Relative up-regulation of SOCS3 mRNA expression by IL-10 was analysed by quantitative PCR in both macrophages and dendritic cells (c). Fold induction of SOCS3 expression was calculated using the $2^{\Delta Ct}$ method using HPRT as a reference gene. Macrophages and dendritic cells from wild-type and Tyk2$^{-/-}$ transgenic mice were pre-treated with IL-10 and were stimulated with 100 ng/ml LPS and the inhibition of TNF-α expression was determined at 2 and 24 hours (d). Asterisk(s) indicate significant differences as determined by a Welch's *t*-test (*P<0.05; **P<0.01).

The extracellular domain of IL-10R2 is not sufficient to maintain IL-10 activity

As IL-10R2 mediated signalling via Tyk2 only plays a limited role in IL-10 mediated responses, we hypothesised that the intracellular domain of IL-10R2 may be dispensable for activity. Krause and co-workers reported that IL-10R1 and IL-10R2 pre-assemble in the cell membrane prior to the binding of IL-10 [22]. We hypothesized that the extracellular domain of IL-10R2 might be sufficient to form a signalling complex with the high affinity IL-10R1. To investigate whether IL-10 mediated signalling could be triggered from a

receptor complex that lacks the intracellular domain of IL-10R2 we co-transfected CHO-K1 cells with expression vectors for IL-10R1 in combination with IL-10R2, IL-10R2$^{\Delta 230\text{-}330}$ (extracellular domain), IL-10R2$^{\Delta 1\text{-}190}$ (intracellular domain) or an empty vector control (mcs). Upon transfection, surface IL-10R expression was analysed by flow cytometry (Figure 4a). No significant differences were observed in surface IL-10R1 expression upon co-transfection with different IL-10R2 constructs. Furthermore, surface IL-10R2 expression was only detected for cells that were transfected with the complete or only the extracellular domain of IL-10R2 (IL-10R2$^{\Delta 230\text{-}330}$). Cells were also stained simultaneously for IL-10R1 and IL-10R2 to check for the efficiency of co-transfection (Figure S3a). The cytoplasmic domain of IL-10R2 was stained intracellular to confirm expression of IL-10R2$^{\Delta 1\text{-}190}$ (Figure S3b). Next we treated transfected CHO-K1 cells with 100 ng/ml IL-10 to induce STAT3 phosphorylation. Figure 4b reveals that STAT3 was only phosphorylated by IL-10 in CHO-K1 cells when IL-10R1 was co-transfected with the full IL-10R2. We therefore conclude that both the extracellular and intracellular domains of IL-10R2 are required to initiate IL-10-mediated signalling. But as signalling can occur in the absence of the IL-10R2-associated kinase Tyk2, the exact role of the intracellular part of IL-10R2 remains to be elucidated.

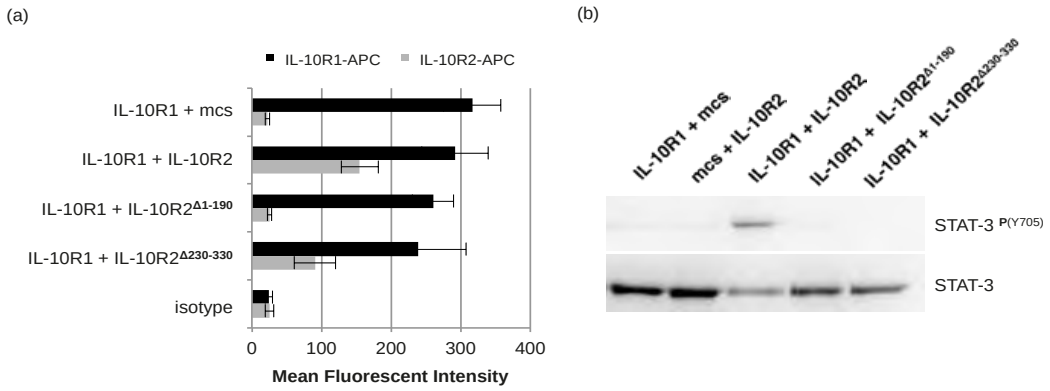

Figure 4 ◆ The extracellular domain of IL-10R2 is not sufficient to maintain IL-10 activity. CHO-K1 cells were co-transfected with combinations of the expression vectors for IL-10R1, IL-10R2, IL-10R2$^{\Delta 230\text{-}330}$ (extracellular domain), IL-10R2$^{\Delta 1\text{-}190}$ (intracellular domain) or an empty vector (mcs) and cultured for 24 hours. Surface expression of IL-10R1 or IL-10R2 was analysed by flow cytometry and mean fluorescent intensity is plotted (*n*=6, error bars represent standard error) (a). Phosphorylation of tyrosine 705 (Y705) of STAT3 by IL-10 (100 ng/ml) in CHO-K1 cells upon transient transfection with IL-10 receptors was analysed by western blot (b).

IL-10R2 mediates conformational changes of IL-10R1

A role for the intracellular domain of IL-10R2 may be found in the association with yet unidentified signalling components. In this manner, IL-10R2 could contribute to IL-10-mediated signalling independent of Tyk2. However, when staining transfected CHO-K1

cells with the monoclonal antibody 1B1.3a we made the striking observation that IL-10R1 detection was reduced by the co-expression of IL-10R2. We repeated the co-transfections and stained the cells with the 1B1.3a antibody (Figure 5a). Upon co-transfection of IL-10R1 and IL-10R2 we observed a significant reduction in maximum binding of the monoclonal 1B1.3a antibody ($P<0.05$ at all concentrations). As we show in figure 4a, staining with a polyclonal anti-IL-10R1 antibody did not differ significantly between co-transfections, which indicates that there are no differences in overall expression of IL-10R1. The reduction in binding of the 1B1.3a antibody could be explained by steric hindrance of the extracellular domain of IL-10R2 or by conformational changes that are induced by IL-10R2. Yet, upon co-expression of IL-10R2 lacking an extracellular domain (IL-10R2$^{\Delta 1\text{-}190}$) we observed an even stronger reduction of 1B1.3a binding ($P<0.01$ at all concentrations). We therefore conclude that the intracellular domain of IL-10R2 mediates conformational changes of the extracellular domain of IL-10R1 that influence the binding of the 1B1.3a antibody to its epitope on IL-10R1.

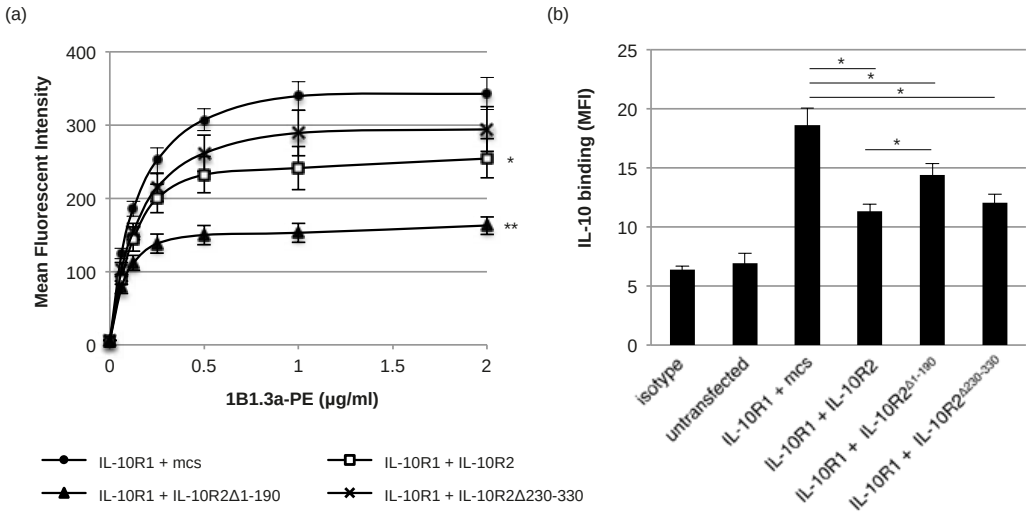

Figure 5 ◆ The intracellular domain of IL-10R2 mediates conformational changes in IL-10R1. CHO-K1 cells were co-transfected with combinations of the expression vectors for IL-10R1, IL-10R2, IL-10R2$^{\Delta 230\text{-}330}$, IL-10R2$^{\Delta 1\text{-}190}$ or an empty vector (mcs) and cultured for 24 hours. Cells were surface stained with the 1B1.3a anti-mouse IL-10R1 monoclonal antibody and analysed by flow cytometry (a). Mean fluorescent intensity for IL-10R1 binding is plotted in a dose-dependent manner ($n=6$, error bars represent standard error). IL-10 was cross-linked to the surface of transfected cells and surface-bound IL-10 was detected by flow cytometry (b). Mean fluorescent intensity for IL-10 binding is plotted ($n=3$, error bars represent standard error). Asterisk(s) indicate significant differences as determined by a Welch's *t*-test (*$P<0.05$; **$P<0.01$).

To investigate whether these conformational changes mediated by the intracellular domain of IL-10R2 also influence the binding of IL-10 to its receptors, we labelled

transfected CHO-K1 cells by cross-linking IL-10 onto the surface. Surface-bound IL-10 was then analysed by flow cytometry. Mean fluorescent intensity of surface-bound IL-10 is shown in Figure 5b. The maximum level of IL-10 binding was found for CHO-K1 cells transfected with only IL-10R1. Co-expression of all three IL-10R2 constructs significantly reduced the amount of surface-bound IL-10, but the reduction by the IL-10R2 lacking the extracellular domain (IL-10R2$^{\Delta 1\text{-}190}$) was less prominent. In fact, the full IL-10R2 construct significantly reduces the amount of surface-bound IL-10 compared to IL-10R1 alone and upon co-transfection of the intracellular domain of IL-10R2. Altogether we conclude that interactions between IL-10R1 and IL-10R2, and most strikingly the intracellular domain of IL-10R2, mediate conformational changes of the extracellular domain of IL-10R1. These interactions putatively reduce the affinity of IL-10 for its receptor, but are required for transducing IL-10 mediated signalling.

Discussion

Interleukin-10 (IL-10) plays a key role in maintaining immune homeostasis and mediates its activity by binding to a heterodimeric receptor complex consisting of IL-10R1 and IL-10R2. However, the exact contribution of IL-10R2, and in particular IL-10R2-associated signalling via Tyk2, to IL-10-mediated responses is still elusive. Therefore, we re-evaluated IL-10-mediated responses and investigated the contribution of IL-10R2. We developed cellular assays using mouse bone marrow-derived cells as commonly used cell lines might not be the most reliable model system. Our study shows that IL-10 is able to suppress LPS-induced TNF-α expression in bone marrow-derived macrophages and dendritic cells. However, subtle differences in the magnitude of TNF-α suppression were found between these two cell types. Next to IL-10's anti-inflammatory properties, we show that IL-10 is also able to maintain viability in mast cells in the absence of IL-3. As expected, IL-10 induces strong activation of the transcription factor STAT3 in all three cell types, but IL-10 did not activate STAT1 or STAT5. The lack of STAT1 activation is in contrast to previous reports [14, 15], but the use of bone marrow-derived cells from STAT1$^{-/-}$ mice in our study did not affect IL-10-mediated responses. We therefore conclude that STAT1 does not play a major role in the downstream signalling of IL-10.

Tyk2 signalling is investigated intensively and Tyk2-deficient mice mainly display impaired responses to interferons and IL-12 [14, 23]. However, the contribution of Tyk2 signalling to IL-10-mediated responses is more elusive. As previously reported by Karaghiosoff and co-workers IL-10 is not impaired in its ability to suppress LPS-induced TNF-α in macrophages from Tyk2$^{-/-}$ mice [14]. Yet, when activated with high doses of IFN-γ, IL-10 is no longer able to suppress nitric oxide production in macrophages [15]. In

our study we investigated the involvement of Tyk2 on three different cell types and our work demonstrates that Tyk2 only plays a limited role in IL-10-mediated responses. IL-10 activity on macrophages and mast cells was slightly reduced, but was not found to be significant. Like in macrophages, we observed a 8-16% reduction in maximum suppression of LPS-induced TNF-α in dendritic cells, but for dendritic cells this difference was significant. Tyk2 does play a role in suppressing TNF-α expression in macrophages upon LPS stimulation, but only early IL-10 responses are affected. Qasimi and co-workers showed that early IL-10-mediated suppression of LPS-induced TNF-α is controlled by SOCS3 [18]. Indeed, IL-10 enhances SOCS3 expression in a STAT3 dependent manner [3, 24] and we observed a ~10-fold reduction in tyrosine phosphorylation of STAT3 (Y705) in Tyk2-deficient macrophages and dendritic cells. Furthermore, Tyk2-deficient macrophages also showed reduced up-regulation of SOCS3 expression, which in turn explains the altered early response to IL-10 in macrophages. In addition to a role in early suppression of TNF-α, SOCS3 also plays a role in IL-10-mediated suppression of nitric oxide production in LPS-stimulated macrophages [18]. Furthermore, SOCS3 is able to suppress IFN signalling [3, 25]. Impaired up-regulation of SOCS3 could therefore also explain why IL-10 is not able to suppress nitric oxide in macrophages upon stimulation with IFN-γ [15]. Altogether, we conclude that IL-10R2-associated signalling via Tyk2 controls the amplitude and kinetics of one of the main anti-inflammatory signalling cascades Jak1-STAT3-SOCS3 in macrophages.

Previously we have reported that stable monomeric IL-10 is not able to suppress LPS-induced TNF-α expression in a macrophage cell line [17], but Josephson and co-workers showed that this monomer was able to induce proliferation in a B cell line transfected with either human or mouse IL-10R1 [19]. Monomeric IL-10 had an EC_{50} value that was approximately 9 or 18 fold higher compared to the activity of recombinant IL-10 depending on which IL-10R1 was used to transfect B cells. However, when we tested monomeric IL-10 on bone marrow-derived cells, we found that 100-1000-fold more monomeric IL-10 is required to obtain the same activity as recombinant IL-10. We cannot exclude that the N-terminal 6x histidine-FLAG tag of our monomeric IL-10 influences the activity, but we previously fused the Fc portion of human IgA to the N-terminus of IL-10 without affecting its activity [17]. IL-10R1 expression level has been reported to play a critical role in IL-10-mediated responses [16, 26]. For instance, neutrophils require enhanced IL-10R1 expression to respond to IL-10 [26]. The observed difference in activity for monomeric IL-10 in our study and the study of Josephson and co-workers likely arises from overexpression of IL-10R1 upon transfection in the latter study. Cellular assays based on *ex vivo* cells might therefore be more representative for the *in vivo* situation.

Monomeric IL-10 might be able to assemble the complete IL-10 receptor complex when IL-10R1 expression is high, but not under natural conditions when IL-10R expression is much lower. Crystallization studies of IL-10 with soluble (s)IL-10R1 revealed

that a complex is formed consisting of 2 IL-10 dimers and 4 IL-10R1 chains [27]. On the contrary, monomeric IL-10 forms a complex with sIL-10R1 in a 1:1 ratio [19]. This would indicate that the signalling complex formed by monomeric IL-10 differs from the receptor complex with dimeric IL-10. We have previously shown that dimerization of monomeric IL-10 restores its ability to suppress LPS-induced TNF-α expression in macrophages [17]. This could indicate that dimerization of IL-10 is required for the assembly of a signalling complex that consists of multiple IL-10R subunits.

Complex assembly requires the initial binding of IL-10 to the high affinity receptor IL-10R1. This interaction mediates conformational changes within IL-10 that increase the binding affinity of IL-10R2 to the IL-10/IL-10R1 complex [28]. This structural information on IL-10 receptor complex assembly based on soluble receptors has been valuable, but this cannot reveal the rearrangement of receptors induced by cytokine binding. Furthermore, receptor rearrangements that take place inside the cell cannot be investigated in this way due to the lack of transmembrane regions and intracellular domains. Therefore the exact mechanism by which IL-10 initiates the downstream activation of Jak1 and Tyk2 remains unknown. Our study now demonstrates that the conformation of the extracellular domain of IL-10R1 is influenced by interactions with IL-10R2 (both extracellular and intracellular). Co-expression of IL-10R2, or parts thereof, reduces the binding of IL-10 to IL-10R1 on the cell surface. The observation that the intracellular domain of IL-10R2 influences IL-10 binding to IL-10R1 might also explain why affinity of IL-10 towards IL-10R1 on intact cells is higher than for sIL-10R1 [29]. Although co-expression of both receptors results in reduced cellular binding of IL-10, the affinity for IL-10 to IL-10R1 on the surface might still be higher compared to the soluble extracellular domain of IL-10R1 used in crystallization studies. But above all, this observation highlights the importance of the intracellular domain in the molecular mechanism of IL-10R activation.

A common model for class I cytokine receptor activation has recently been proposed by Pang and co-workers [30]. This model of activation involves scissor-like rotation and self-rotation of the receptors. The intracellular domains of two receptor molecules are separated from each other by scissor-like rotation, allowing intracellular signalling components to bind. Self-rotation of the receptors arranges the Janus kinases in such an orientation that they can be *trans*-phosphorylated and initiate signalling. Although IL-10 belongs to class II cytokines, scissor-like rotation has been proposed as an activation mechanism [27]. However, Krause and co-workers demonstrated by confocal fluorescence spectroscopy that IL-10R1 and IL-10R2 are pre-assembled in the cellular membrane. Furthermore, they revealed that there are no major structural changes among the intracellular domains upon ligand binding [22]. It is therefore more likely that IL-10 receptors are activated by a different mechanism. In contrast, the receptor complex of IFN-γ undergoes major structural changes upon cytokine binding [31]. Binding of IFN-γ

induces rearrangement of the intracellular domains of both IFN-γR1 and IFN-γR2 thereby allowing more space for downstream signalling components to bind. The rearrangement of intracellular receptor domains seems to differ between the signalling complexes of IL-10 and IFN-γ. We therefore reason that cell-based assays using hybrid IL-10 receptors harbouring the intracellular domains of their respective IFN-γR's are not a reliable model to investigate IL-10 signalling.

In line with pre-assembly of IL-10R1 and IL-10R2 on the cellular surface, our study now reveals that co-expression of both receptor chains influences the conformation of the extracellular domain of IL-10R1. We also conclude that even though cellular binding of IL-10 is reduced by co-expressing IL-10R1 and IL-10R2, interactions between the extracellular and intracellular domains of both receptors are required to initiate signal transduction via Jak1 and Tyk2. Future investigation should now focus on how these interactions between IL-10R1 and IL-10R2 influence receptor rearrangements upon ligand binding. Confocal fluorescent spectroscopy studies would enable the investigation of intracellular receptor rearrangements among the components of the IL-10R complex as well as the Janus kinases Jak1 and Tyk2. This would ultimately give novel insights into the molecular mechanism of the IL-10R complex activation and activation of down-stream Janus kinases Jak1 and Tyk2.

Experimental procedures

Mice

Wild-type C57BL/6J mice were bred and maintained under specific pathogen-free conditions in the animal facilities at Wageningen University. IL-10R1$^{-/-}$ mice were kindly provided by dr. W. Muller (University of Manchester), IL-10R2$^{-/-}$ mice were obtained from Genentech (San Francisco, CA, USA) and bones from TYK2$^{-/-}$ and STAT1$^{-/-}$ mice were kindly provided by dr. B. Strobl (University of Veterinary Medicine Vienna).

Cell culture

Bone marrow was isolated from the femur and tibia of 6-12 week old mice. Bone marrow derived macrophages (BMMΦ's) were differentiated at 37°C/5% CO_2 in RPMI-1640 medium containing 4 mM L-glutamine, 25 mM HEPES and supplemented with 10% fetal calf serum, 50 µM β-mercaptoethanol, 50 U/ml penicillin and 50 µg/ml streptomycin and 20% spent medium from L929 cells (ATCC). Bone marrow cells were seeded at 1×10^6 cells/ml in 6- or 96-well tissue culture plates and cultured for 6 days, while refreshing medium at day 3. After 6 days of culture ≥95% of the cells expressed the macrophage markers F4/80 and CD11b.

Bone marrow derived dendritic cells (BMDC's) were differentiated for 10 days as described [32] using 10% spent medium from murine GM-CSF transfected X63 cells [33]. X63-GM-CSF cells were kindly provided by dr. M. Lutz (University of Erlangen-Nuremberg) with approval of dr. B. Stockinger (MRC National Institute for Medical Research). Briefly, bone marrow cells were plated at 2×10^5 cells/ml in bacteriological petri dishes and incubated at 37°C/5% CO_2. At day 3, 6 and 8 medium was refreshed and at day 10 both adherent and non-adherent cells were harvested. At this time typically ~90% of the cells expressed the dendritic cell markers CD11c and MHC class II.

Bone marrow-derived mast cells (BMMC) were differentiated at 37°C/5% CO_2 using 1 ng/ml IL-3 (R&D Systems). Bone marrow cells were plated at 4×10^5 cells/ml in bacteriological petri dishes and non-adherent cells were sub-cultured for at least 5 weeks, while refreshing growth medium twice a week. After 5 weeks of culture ≥95% of the cells expressed the mast cell markers FcεRI and c-kit.

Chinese hamster ovarian cells (CHO-K1; obtained from DSMZ) were maintained at 37°C with 5% CO_2 in RPMI-1640 medium containing 4 mM L-glutamine, 25 mM HEPES and supplemented with 10% fetal calf serum, 50 µM β-mercaptoethanol, 50 U/ml penicillin and 50 µg/ml streptomycin. Cells were sub-cultured three times a week by harvesting with trypsin.

Expression and purification of monomeric IL-10

The sequence encoding the mature protein of stable monomeric human IL-10 was digested from pHYG-hFcα-IL-10m [17] and was cloned in frame with the *Arabidopsis thaliana* chitinase signal peptide (cSP) followed by a 6x histidine and FLAG tag as previously reported for IL-22 (Chapter 4). Plant produced IL-10m was purified from fluids extracted from the leaf apoplast (intercellular space) using Ni-NTA Sepharose (IBA Life Sciences) as reported for IL-22 (Chapter 4).

LPS stimulation assays

BMMΦ's were differentiated in 96 well plates and BMDC's were seeded in 96 well plates at a density of $5x10^4$/well. Cells were pre-treated for 15 min. with IL-10 and subsequently stimulated with 100 ng/ml lipopolysaccharide (LPS). After 2 hours or overnight stimulation, supernatants were analysed for TNF-α using the Ready-Set-Go!® ELISA kit (eBioscience) according to the supplier's protocol.

Mast cell viability assay

BMMC's were seeded in 96 well plates at a density of 1.5×10^5 cells/well. Mast cells were then cultured in the presence of IL-10 or 1 ng/ml IL-3. After 48 hours cell viability was assessed by using the CellTiter 96® aqueous one solution (Promega) according to the supplier's protocol.

STAT activation

Bone marrow-derived cells were treated for 20 min. with IL-10 (0, 1, 10 or 100 ng/ml). Cells were lysed using 1x Cell Lysis Buffer (Cell Signaling Technology) and total soluble protein content in the lysates was determined by the BCA method (Pierce). Proteins were separated on 12% Bis-Tris gels followed by transfer to a PVDF membrane by a wet blotting procedure. Thereafter the membrane was blocked in PBS (containing 0.1% v/v Tween-20 and 5% w/v non-fat dry milk powder) for 1 hour at room temperature, followed by overnight incubation at 4°C with monoclonal antibodies specific for STAT1, phospho-STAT1^{Y701}, STAT3, phospho-STAT3^{Y705}, STAT5 or phospho-STAT5^{Y694} in PBS (containing 0.1% v/v Tween-20 and 1% w/v BSA). All STAT antibodies were obtained from Cell Signaling Technology. A HRP-conjugated donkey anti-rabbit IgG (Jackson ImmunoResearch) was used as a secondary antibody. Blots were visualised in the G:BOX Chemi System (Syngene) using the SuperSignal West Femto substrate (Pierce).

Construction of IL-10R expression vectors and transfections

The open reading frame of mouse IL-10R1, IL-10R2, IL-10R2$^{\Delta 230\text{-}330}$ and IL-10R2$^{\Delta 1\text{-}190}$ were amplified from mouse spleen cDNA using the Expand High Fidelity PCR System (Roche). The IL-10R2$^{\Delta 1\text{-}190}$ fragment was cloned in frame with the native signal peptide by means of overlap extension PCR. Sense and antisense primers included BamHI and NheI restriction sequences respectively for subsequent cloning into the pMAX expression vector (Lonza). CHO-K1 cells were co-transfected with 0.5 µg/plasmid using the jetPRIME® transfection reagent (PolyPlus Transfection) using the supplier's protocol. 24 hours after transfection, CHO-K1 cells were analysed for IL-10R expression by flow cytometry.

Flow cytometry

Bone marrow derived cells were stained in FACS buffer (PBS containing 0.1% BSA and 5mM EDTA) using the following monoclonal antibodies for cell surface markers (all obtained from eBioscience): PE-conjugated anti-CD11b, APC-conjugated anti-F4/80, PE-conjugated anti-CD11c, APC-conjugated MHC-II, PE-conjugated anti-FcεRI and APC-conjugated c-kit. Cells were first incubated with Fc receptor block (eBioscience) for 10 min to block any non-specific binding and subsequent staining steps were performed for 20 min. at 4°C, followed by washing with FACS buffer. An overview of the flow cytometric analysis of bone marrow-derived cells from all transgenic mice used in this study can be found in figure S4.

Upon CHO-K1 transfection, goat polyclonal anti-IL-10R1 and anti-IL-10R2 antibodies (R&D Systems) were used for detection of IL-10R expression followed by an APC-conjugated donkey anti-goat IgG secondary antibody (R&D Systems). Surface expression of IL-10R1 was also analysed by staining with a PE-conjugated monoclonal anti-IL-10R1 (1B1.3a; BioLegend). Intracellular staining of IL-10R2 was performed on methanol-permeabilized cells using a mouse monoclonal antibody that binds the cytoplasmic domain of IL-10R2 (clone F-6; Santa Cruz Biotechnology), followed by a PE-conjugated goat anti-mouse IgG secondary antibody (R&D Systems).

Surface labelling with IL-10 was performed by incubating 1.0 x10^6 cells with 40 ng of IL-10 for 1 hour at 4°C. Surface-bound IL-10 was then cross-linked for 2 hours at 4°C with 2.5 mM BS3 (Pierce). Surface IL-10 was then detected with a goat polyclonal anti-IL-10 antibody (R&D Systems) followed by a PE-conjugated donkey anti-goat IgG secondary antibody (Jackson ImmunoResearch). CHO-K1 cells without IL-10 cross-linked to their surface were used as a negative control and mean fluorescent intensity obtained for these cells were subtracted from IL-10 labelled cells.

Stained cells were acquired using a Cyan-ADP Analyzer (Beckman Coulter) and analysed with FlowJo software (Tree Star, Inc.).

Quantitative PCR

BMMΦ's were differentiated in 6 well plates and $3x10^6$ BMDC's were seeded in 6 well plates and were treated for 2 hours with IL-10 (0, 1, 10 or 100 ng/ml). Cells were then washed with PBS and mRNA was isolated with the RNeasy Mini kit (Qiagen) using the supplier's protocol. A Turbo DNase I (Ambion) treatment was included to remove any residual DNA. Then cDNA was synthesized using the SuperScript III First-Strand Synthesis System (Invitrogen) according to the supplier's protocol. Samples were analysed in triplicate for SOCS3 and HPRT (reference gene) expression by quantitative PCR using ABsolute SYBR Green Fluorescein mix (Thermo Scientific). Fold induction of SOCS3 expression was determined by the Pfaffl method [34].

Data analysis

All data shown in the figures indicate the average of at least three biological replicates (*n*) that were determined by three technical replicates. In the figure legends *n* is indicated and error bars indicate the standard error. Significant differences between samples were calculated using the student's t-test and regarded as significant when $P<0.05$. Significant differences are indicated in the figures by asterisks ($P<0.05$ (*) or $P<0.01$ (**)).

Acknowledgements

This study was financially supported in part by Synthon (Nijmegen, The Netherlands). We would like to thank Dr. Birgit Strobl at Vienna University for providing us with the bones of $STAT1^{-/-}$ and $Tyk2^{-/-}$ mice. We like to thank Dr. Werner Muller at Manchester University and Genentech for providing us with $IL\text{-}10R1^{-/-}$ and $IL\text{-}10R2^{-/-}$ mice, respectively. Finally we would like to thank all the people at the animal facilities of Wageningen University (CKP) for their care of all the animals used in this study.

Supplemental Figures

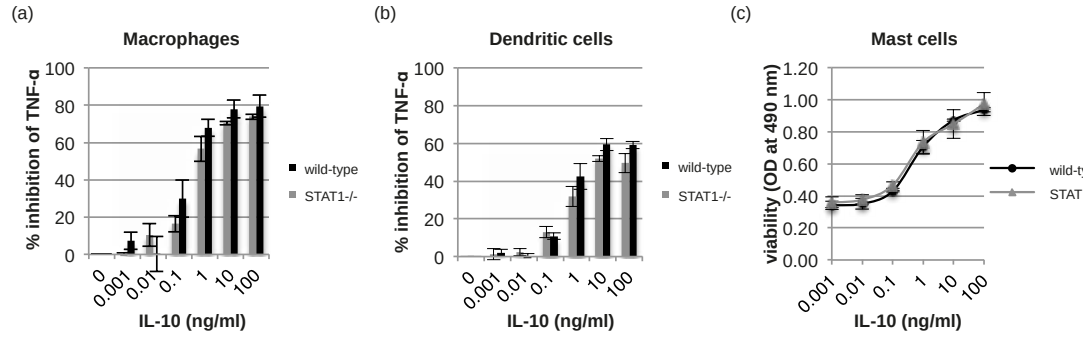

Figure S1 ◆ STAT1 is not required for IL-10 activity. Bone marrow-derived macrophages, dendritic cells and mast cells from wild-type and STAT1$^{-/-}$ mice were tested for their response to IL-10. Cells pre-treated with IL-10 were stimulated with 100 ng/ml LPS and TNF-α expression was determined to asses anti-inflammatory properties of IL-10 in macrophages (a) and dendritic cells (b) (*n*=3, error bars indicate standard error). Mast cells were cultured for 48 hours in the presence of IL-10, where after cell viability was determined (c) (*n*=3, error bars indicate standard error).

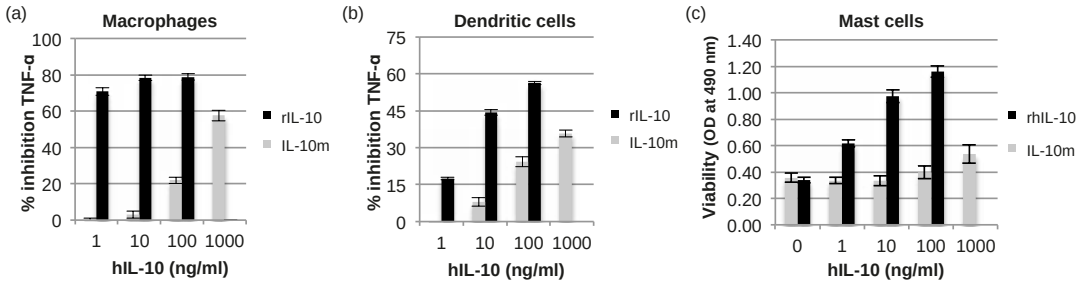

Figure S2 ◆ A stable monomeric form of human IL-10 has impaired activity. Bone marrow-derived macrophages, dendritic cells and mast cells from wild-type mice were tested for their response to human IL-10 and a stable monomeric form of IL-10 (IL-10m). Cells pre-treated with IL-10 were stimulated with 100 ng/ml LPS and TNF-α expression was determined to asses anti-inflammatory properties of IL-10 in macrophages (a) and dendritic cells (b) (*n*=3, error bars indicate standard error). Mast cells were cultured for 48 hours in the presence of IL-10, where after cell viability was determined (c) (*n*=3, error bars indicate standard error). $P<0.01$ at all concentrations in all three assays.

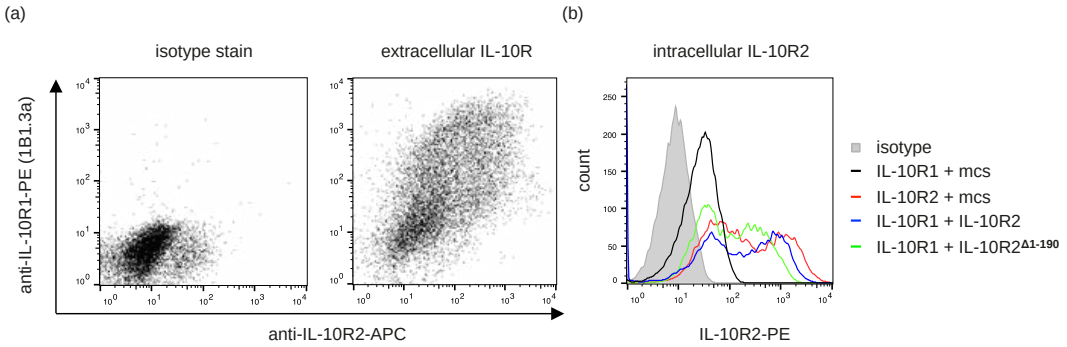

Figure S3 ◆ Flow cytometric analysis of transfected CHO-K1 cells. CHO-K1 cells were analysed by flow cytometry upon co-transfection of IL-10R1 and IL-10R2 constructs. (a) Dual staining for extracellular expression of IL-10R1 and IL-10R2. Pictures are given for the isotype and surface staining upon co-transfection of full IL-10R1 and IL-10R2 constructs and reveals the efficiency of co-transfection. (b) Histograms are given for the intracellular staining of IL-10R2 upon co-transfection of different combinations of IL-10R1 and IL-10R2 constructs.

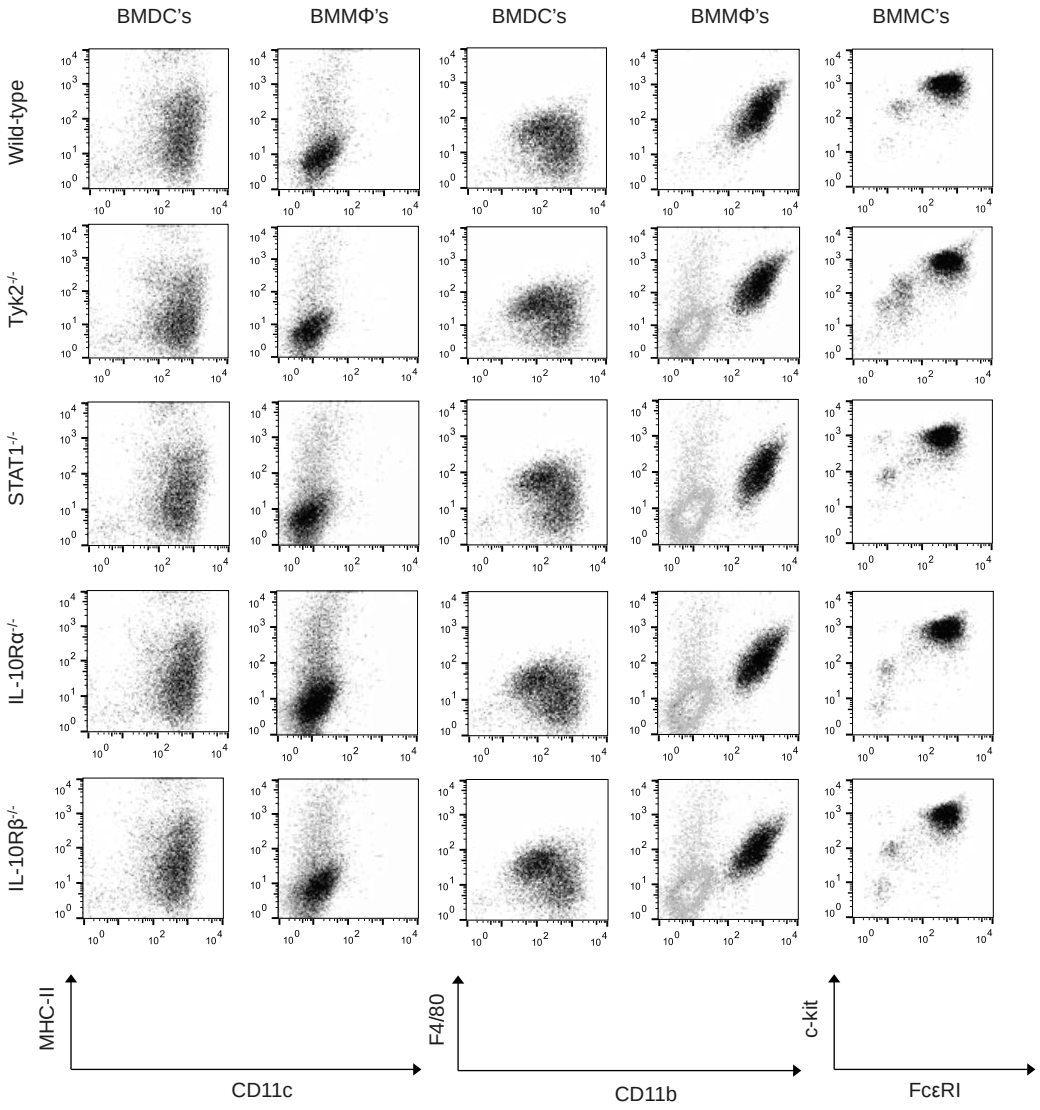

Figure S4 ◆ Flow cytometric analysis of bone marrow-derived cells. Bone marrow-derived macrophages, dendritic cells and mast cells were analysed by flow cytometry for the expression of cellular markers CD11b & F4/80 (macrophage markers), CD11c & MHC-II (dendritic cell markers) or FcεRI & c-kit (mast cell markers). Bone marrow-derived cells from all transgenic mice used in this study show identical phenotypes. Furthermore, macrophages and dendritic cells are distinct cell populations as they have different expression profiles for CD11b, CD11c, F4/80 and MHC-II.

References

1 Fiorentino DF, Bond MW and Mosmann TR (1989) Two types of mouse T helper cell. IV. Th2 clones secrete a factor that inhibits cytokine production by Th1 clones. Journal of Experimental Medicine 170: 2081-2095.

2 Fiorentino DF, Zlotnik A, Mosmann TR, Howard M and O'Garra A (1991) IL-10 inhibits cytokine production by activated macrophages. Journal of Immunology 147: 3815-3822.

3 Asadullah K, Sterry W and Volk HD (2003) Interleukin-10 therapy--review of a new approach. Pharmacological Reviews 55: 241-269.

4 Kuhn R, Lohler J, Rennick D, Rajewsky K and Muller W (1993) Interleukin-10-deficient mice develop chronic enterocolitis. Cell 75: 263-274.

5 Thompson-Snipes L, Dhar V, Bond MW, Mosmann TR, Moore KW, et al. (1991) Interleukin 10: a novel stimulatory factor for mast cells and their progenitors. Journal of Experimental Medicine 173: 507-510.

6 Ho AS, Liu Y, Khan TA, Hsu DH, Bazan JF, et al. (1993) A receptor for interleukin 10 is related to interferon receptors. Proceedings of the National Academy of Sciences of the United States of America 90: 11267-11271.

7 Kotenko SV, Krause CD, Izotova LS, Pollack BP, Wu W, et al. (1997) Identification and functional characterization of a second chain of the interleukin-10 receptor complex. EMBO Journal 16: 5894-5903.

8 Spencer SD, Di Marco F, Hooley J, Pitts-Meek S, Bauer M, et al. (1998) The orphan receptor CRF2-4 is an essential subunit of the interleukin 10 receptor. Journal of Experimental Medicine 187: 571-578.

9 Pils MC, Pisano F, Fasnacht N, Heinrich JM, Groebe L, et al. (2010) Monocytes/macrophages and/or neutrophils are the target of IL-10 in the LPS endotoxemia model. European Journal of Immunology 40: 443-448.

10 Ho AS, Wei SH, Mui AL, Miyajima A and Moore KW (1995) Functional regions of the mouse interleukin-10 receptor cytoplasmic domain. Molecular and cellular biology 15: 5043-5053.

11 Finbloom DS and Winestock KD (1995) IL-10 induces the tyrosine phosphorylation of tyk2 and Jak1 and the differential assembly of STAT1 alpha and STAT3 complexes in human T cells and monocytes. Journal of Immunology 155: 1079-1090.

12 Pestka S, Krause CD, Sarkar D, Walter MR, Shi Y, et al. (2004) Interleukin-10 and related cytokines and receptors. Annual Reviews Immunology 22: 929-979.

13 Riley JK, Takeda K, Akira S and Schreiber RD (1999) Interleukin-10 receptor signaling through the JAK-STAT pathway. Requirement for two distinct receptor-derived signals for anti-inflammatory action. Journal of Biological Chemistry 274: 16513-16521.

14 Karaghiosoff M, Neubauer H, Lassnig C, Kovarik P, Schindler H, et al. (2000) Partial impairment of cytokine responses in Tyk2-deficient mice. Immunity 13: 549-560.

15 Shaw MH, Freeman GJ, Scott MF, Fox BA, Bzik DJ, et al. (2006) Tyk2 negatively regulates adaptive Th1 immunity by mediating IL-10 signaling and promoting IFN-gamma-dependent IL-10 reactivation. Journal of Immunology 176: 7263-7271.

16 Ding Y, Qin L, Zamarin D, Kotenko SV, Pestka S, et al. (2001) Differential IL-10R1 expression plays a critical role in IL-10-mediated immune regulation. Journal of Immunology 167: 6884-6892.

17 Westerhof LB, Wilbers RHP, Roosien J, van de Velde J, Goverse A, et al. (2012) 3D Domain Swapping Causes Extensive Multimerisation of Human Interleukin-10 When Expressed In Planta. Plos One 7(10): e46460.

18 Qasimi P, Ming-Lum A, Ghanipour A, Ong CJ, Cox ME, et al. (2006) Divergent mechanisms utilized by SOCS3 to mediate interleukin-10 inhibition of tumor necrosis factor alpha and nitric oxide production by macrophages. Journal of Biological Chemistry 281: 6316-6324.

19 Josephson K, DiGiacomo R, Indelicato SR, Iyo AH, Nagabhushan TL, et al. (2000) Design and analysis of an engineered human interleukin-10 monomer. Journal of Biological Chemistry 275: 25054.

20 Masters JR and Stacey GN (2007) Changing medium and passaging cell lines. Nature Protocols 2: 2276-2284.

21 Fleetwood AJ, Dinh H, Cook AD, Hertzog PJ and Hamilton JA (2009) GM-CSF- and M-CSF-dependent macrophage phenotypes display differential dependence on Type I interferon signaling. Journal of Leukocyte Biology 86: 411-421.

22 Krause CD, Mei EW, Mirochnitchenko O, Lavnikova N, Xie JX, et al. (2006) Interactions among the components of the interleukin-10 receptor complex. Biochemical & Biophysical Research Communications 340: 377-385.

23 Vogl C, Flatt T, Fuhrmann B, Hofmann E, Wallner B, et al. (2010) Transcriptome analysis reveals a major impact of JAK protein tyrosine kinase 2 (Tyk2) on the expression of interferon-responsive and metabolic genes. BMC Genomics 11: 199.

24 Cassatella MA, Gasperini S, Bovolenta C, Calzetti F, Vollebregt M, et al. (1999) Interleukin-10 (IL-10) selectively enhances CIS3/SOCS3 mRNA expression in human neutrophils: evidence for an IL-10-induced pathway that is independent of STAT protein activation. Blood 94: 2880-2889.

25 Song MM and Shuai K (1998) The Suppressor of Cytokine Signaling (SOCS) 1 and SOCS3 but Not SOCS2 Proteins Inhibit Interferon-mediated Antiviral and Antiproliferative Activities. Journal of Biological Chemistry 273: 35056-35062.

26 Crepaldi L, Gasperini S, Lapinet JA, Calzetti F, Pinardi C, et al. (2001) Up-Regulation of IL-10R1 Expression Is Required to Render Human Neutrophils Fully Responsive to IL-10. Journal of Immunology 167: 2312-2322.

27 Josephson K, Logsdon NJ and Walter MR (2001) Crystal structure of the IL-10/IL-10R1 complex reveals a shared receptor binding site. Immunity 15: 35-46.

28 Yoon SI, Logsdon NJ, Sheikh F, Donnelly RP and Walter MR (2006) Conformational changes mediate interleukin-10 receptor 2 (IL-10R2) binding to IL-10 and assembly of the signaling complex. Journal of Biological Chemistry 281: 35088-35096.

29 Tan JC, Braun S, Rong H, DiGiacomo R, Dolphin E, et al. (1995) Characterization of recombinant extracellular domain of human interleukin-10 receptor. Journal of Biological Chemistry 270: 12906-12911.

30 Pang X and Zhou HX (2012) A common model for cytokine receptor activation: combined scissor-like rotation and self-rotation of receptor dimer induced by class I cytokine. PLoS Computational Biology 8: e1002427.

31 Krause CD, Mei E, Xie J, Jia Y, Bopp MA, et al. (2002) Seeing the light: preassembly and ligand-induced changes of the interferon gamma receptor complex in cells. Molecular & Cellular Proteomics 1: 805-815.

32 Lutz MB, Kukutsch N, Ogilvie ALJ, Rossner S, Koch F, et al. (1999) An advanced culture method for generating large quantities of highly pure dendritic cells from mouse bone marrow. Journal of Immunological Methods 223: 77-92.

33 Zal T, Volkmann A and Stockinger B (1994) Mechanisms of tolerance induction in major histocompatibility complex class II-restricted T cells specific for a blood-borne self-antigen. Journal of Experimental Medicine 180: 2089-2099.

34 Pfaffl MW (2001) A new mathematical model for relative quantification in real-time RT-PCR. Nucleic acids research 29: e45.

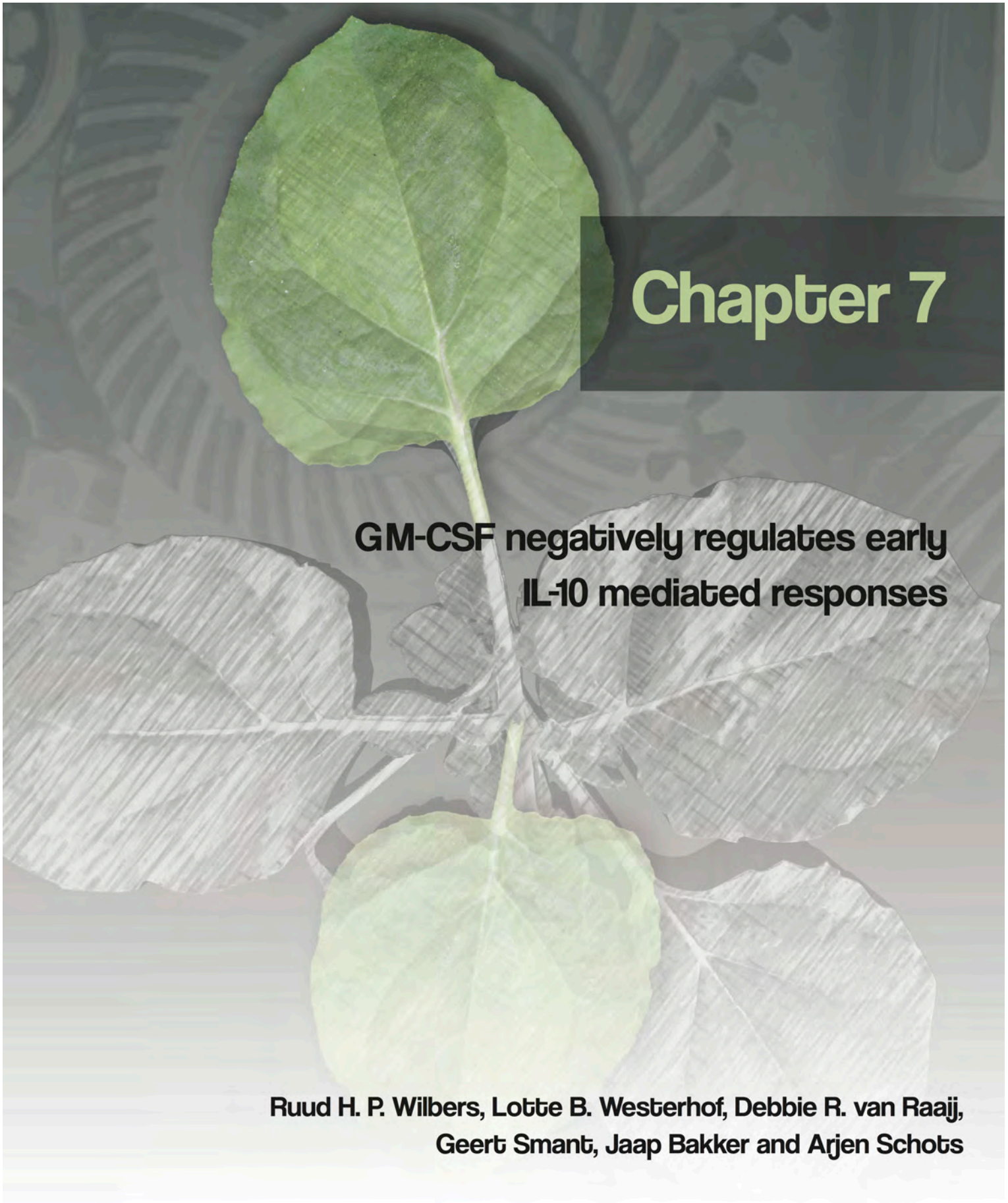

Chapter 7

GM-CSF negatively regulates early IL-10 mediated responses

Ruud H. P. Wilbers, Lotte B. Westerhof, Debbie R. van Raaij,
Geert Smant, Jaap Bakker and Arjen Schots

Abstract

Inflammatory disorders are becoming more prevalent in the Western world. Treatment of these diseases relies on the intervention in inflammatory responses thereby restoring immune homeostasis. One cytokine that has the potential to restore immune homeostasis is the anti-inflammatory cytokine interleukin-10 (IL-10). But until now IL-10 treatment has not been as successful as anticipated. A reason for this may be that IL-10 responsiveness depends on the environment of the inflamed tissue. In this study we describe that granulocyte-macrophage colony-stimulating factor (GM-CSF) is a key cytokine that negatively regulates IL-10-mediated responses. Dendritic cells differentiated from bone marrow with GM-CSF have a reduced ability to respond to IL-10. Dendritic cells are impaired in their up-regulation of IL-10-induced SOCS3 expression and are unable to suppress LPS-induced TNF-α expression at an early time point. Furthermore, GM-CSF treatment partially replicates this phenotype in macrophages. Surprisingly, GM-CSF seems to regulate IL-10 activity in macrophages without affecting STAT3 activation. Still, GM-CSF induces constitutive phosphorylation of glycogen synthase kinase 3β, a signalling component downstream of the PI3K/Akt pathway. Knowledge on the exact mechanism by which GM-CSF negatively regulates IL-10 activity could give novel insights on the integration of signal transduction pathways elicited by different cytokines. Ultimately this knowledge could provide us with new therapeutic strategies to treat inflammatory disorders.

Introduction

The prevalence of inflammatory disorders, like multiple sclerosis, rheumatoid arthritis, inflammatory bowel disease or allergies, has drastically increased over the last couple of decades. These inflammatory disorders are characterised by uncontrolled immune responses against harmless antigens or commensal bacteria. Treatment of these diseases relies on the intervention in inflammatory responses and thereby restoring immune homeostasis. Many inflammatory disorders are treated with immunosuppressive drugs or monoclonal antibodies that target key pro-inflammatory cytokines, such as tumour necrosis factor alpha (TNF-α). However, immune intervention can also be performed with anti-inflammatory cytokines. One such cytokine capable of restoring homeostasis is interleukin-10 (IL-10). IL-10 is an anti-inflammatory cytokine that suppresses the activity of both antigen presenting cells and lymphocytes and has been considered as a promising therapy for several inflammatory disorders [1]. However, until now IL-10 therapy has not been as successful as previously anticipated.

Systemic administration of recombinant human IL-10 produced in *Escherichia coli* has been studied in phase II clinical trials to treat patients with Crohn's disease. But, even though IL-10 treatment is well tolerated [2], patients seem to respond differently to IL-10 treatment [3]. Several explanations for why IL-10 treatment has not been a successful therapy for Crohn's disease have been postulated: (1) systemic administration does not result in an effective dose in the intestine; (2) disease phenotype/severity cause differences in response to IL-10; (3) IL-10 treatment is only successful as preventive therapy; (4) treatment with IL-10 alone is not sufficient; or (5) IL-10's immunostimulatory effects counterbalance its immunosuppressive effects [4]. To circumvent systemic administration of IL-10, *Lactococcus lactis* was engineered to secrete human IL-10 and used as an oral delivery system [5]. This local delivery system for IL-10 was shown to be successful in two mouse models of intestinal inflammation [5] and was proven to be safe in a small phase I human trial [6]. However, in 2009 a phase II human trial with engineered *L. lactis* in patients with ulcerative colitis was completed, but no significant difference in mucosal healing versus a placebo control was observed (ActoGeniX press release). Future research has to address whether local delivery of IL-10 is indeed a promising therapeutic approach.

Another explanation for IL-10's lack of efficacy as therapy could arise from differences between patients depending on disease phenotype or severity [4]. For instance, alveolar macrophages have the reduced ability to respond to IL-10 during chronic inflammation [7]. Pre-treatment of these macrophages with TNF-α reduced their ability to respond to IL-10 without affecting IL-10 receptor (IL-10R) expression. Similarly, agonists of Toll-like receptors (TLR) were able to reduce IL-10-mediated phosphorylation and nuclear translocation of the transcription factor STAT3 in macrophages and dendritic cells without lowering surface IL-10R expression [8, 9]. In contrast, IL-10R expression and subsequent

IL-10R signalling was reduced in macrophages upon recognition of zymosan [10] or ligation of Fc receptors [11]. Furthermore, cytokines, like IFN-γ, have also been shown to alter IL-10-mediated responses [12]. Altogether, there is quite some evidence that inflammatory mediators can influence IL-10 activity.

In Chapter 5 we have described that bone marrow-derived dendritic cells respond differently to IL-10 when compared to macrophages. Dendritic cells have a reduced capacity to suppress LPS-induced TNF-α, especially when evaluating early IL-10-mediated suppression. The lack of early TNF-α suppression coincided with the impaired ability of dendritic cells to up-regulate SOCS3 expression upon IL-10 treatment. We therefore continued to investigate the underlying mechanism that explains why dendritic cells respond differently to IL-10 than macrophages. In this study we describe that GM-CSF, the cytokine used to differentiate dendritic cells, is a key factor that negatively regulates IL-10 mediated responses. We also show that GM-CSF regulates IL-10 activity without strongly affecting STAT3 activation. In contrast, GM-CSF induces constitutive phosphorylation of GSK-3β, but whether this is the mechanism by which GM-CSF controls IL-10 activity needs further investigation.

Results

IL-10 mediated signalling in dendritic cells and macrophages

As described in Chapter 5 we observed cell-specific differences in the response to IL-10 in macrophages and dendritic cells. Dendritic cells are strongly impaired in their ability to suppress LPS-induced TNF-α after 2 hours of stimulation, whereas macrophages already inhibit TNF-α expression by ~75% (Figure 1a). We therefore investigated whether IL-10 signalling differs in these two cell types. First we focused on the activation of the transcription factor STAT3. As shown in figure 1b, IL-10 induces strong tyrosine phosphorylation of STAT3 (Y705) in a dose-dependent manner in both cell types. Upon quantification of relative STAT3 activation, we observed a stronger degree of $STAT3^{Y705}$ phosphorylation in macrophages than in dendritic cells (Figure 1c). However, this was only significantly higher at a dose of 1 ng/ml IL-10. On the other hand, the degree of serine phosphorylation (S727) in macrophages was only significantly higher at a dose of 10 ng/ml (Figure 1d). Yet, when comparing untreated cells with IL-10 treated cells we only observed dose-dependent $STAT3^{S727}$ phosphorylation in macrophages ($P<0.05$, for all concentrations). Untreated dendritic cells already have a higher degree of $STAT3^{S727}$ phosphorylation, which is not further enhanced by IL-10 treatment. Serine phosphorylation of STAT3 could therefore be cell-type specific.

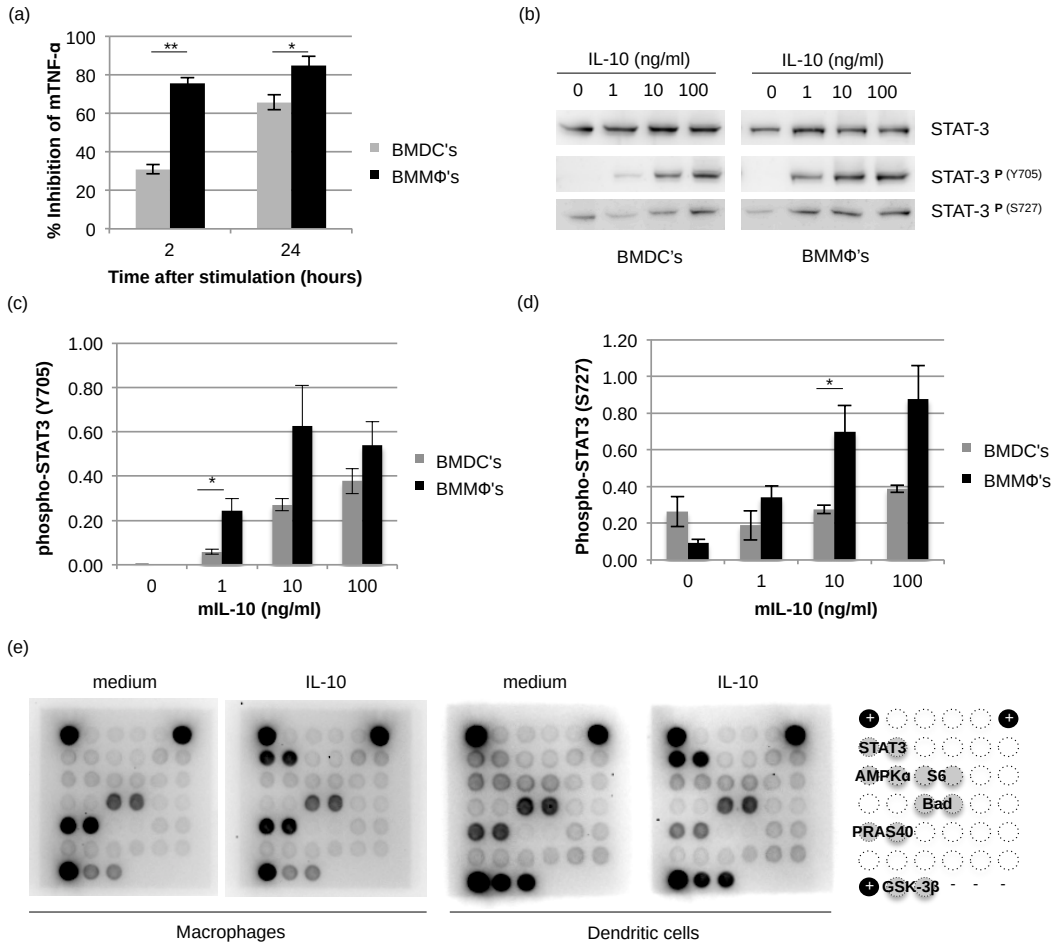

Figure 1 ◆ IL-10 mediated signalling in dendritic cells and macrophages. (a) Macrophages and dendritic cells were pre-treated with IL-10 and were stimulated with 100 ng/ml LPS and the inhibition of TNF-α expression was determined at 2 and 24 hours (*n*=3, error bars represent standard error). (b) Phosphorylation of tyrosine 705 (Y705) and serine 727 (S727) of STAT3 by IL-10 (0, 1, 10 and 100 ng/ml) was analysed in macrophages and dendritic cells using western blot. (c/d) Relative induction of STAT3 phosphorylation was quantified for Y705 (c) and S727 (d) upon western blot analysis (*n*=3 or 4 for Y705 and S727 respectively, error bars represent standard error). (e) Macrophages and dendritic cells were treated with 100 ng/ml IL-10 and the activation of intracellular signalling pathways was analysed with a PathScan Array. A representative figure is given for 2 independent experiments. Asterisk(s) indicate significant differences as determined by a Welch's *t*-test (**P*<0.05; ***P*<0.01).

Next, we assessed the activation of 18 well-characterized signalling molecules using the PathScan Intracellular Signalling Array kit. In Figure 1e representative arrays are given for macrophages and dendritic cells treated with 100 ng/ml IL-10 and their respective medium controls. The legend indicates which signalling molecules are differentially affected. Strikingly, we only detected phosphorylation of $STAT3^{Y705}$ upon treatment with IL-10. Interestingly, we did observe differences in the activation of other signalling molecules between untreated macrophages and dendritic cells. Untreated dendritic cells

seem to have a higher degree of phosphorylated AMPKα and the ribosomal protein S6, which are indicators for cell cycle progression and cellular growth. Furthermore, several signalling molecules downstream of the PI3K/Akt pathway (PRAS40, Bad and GSK-3β) are activated in untreated macrophages and dendritic cells, but the degree of GSK-3β phosphorylation (Ser9) is much stronger in dendritic cells. Phosphorylation of GSK-3β inhibits its activity and thereby promotes cell survival. Altogether we conclude that STAT3 is the major downstream signalling molecule for IL-10. Furthermore, macrophages and dendritic are differentially affected in signalling molecules that regulate cellular growth and survival.

GM-CSF negatively regulates IL-10 activity

Dendritic cells are differentiated from bone marrow cells by culturing them in the presence of the cytokine GM-CSF. In order to find out if GM-CSF could be responsible for the altered responses of dendritic cells to IL-10, we investigated whether GM-CSF could replicate this phenotype in macrophages. Macrophages and dendritic cells were differentiated from bone marrow, but now GM-CSF was added to macrophages or depleted from dendritic cells for the last 24 hours of culture. Cells were then pre-treated with IL-10 and subsequently challenged with lipopolysaccharide (LPS). Figures 2a-c reveals that GM-CSF is indeed able to alter the response of macrophages towards IL-10. IL-10 inhibits TNF-α expression in a dose-dependent matter in macrophages independent of GM-CSF treatment (Figure 2a), but GM-CSF treatment lowers the maximum percentage of TNF-α expression at a lower dose of IL-10. Furthermore, GM-CSF treatment of macrophages significantly reduced early IL-10-mediated suppression of TNF-α by ~25%. We also observed that macrophages treated with GM-CSF produced significantly more TNF-α than untreated macrophages (Figure 2c). These results indicate that GM-CSF is able to alter IL-10-mediated responses in macrophages as was observed for GM-CSF differentiated dendritic cells.

Similarly, depletion of dendritic cells from GM-CSF enhanced their response towards IL-10. No differences were observed in the suppression of TNF-α expression after 24 hour stimulation when dendritic cells were depleted from GM-CSF (Figure 2d). However, early IL-10-mediated suppression of TNF-α expression increased significantly with almost 25% when dendritic cells were depleted from GM-CSF. Also, production of TNF-α was significantly reduced when dendritic cells were cultured in the absence of GM-CSF. We therefore conclude that GM-CSF is a key factor that modulates early IL-10-mediated responses in both macrophages and dendritic cells.

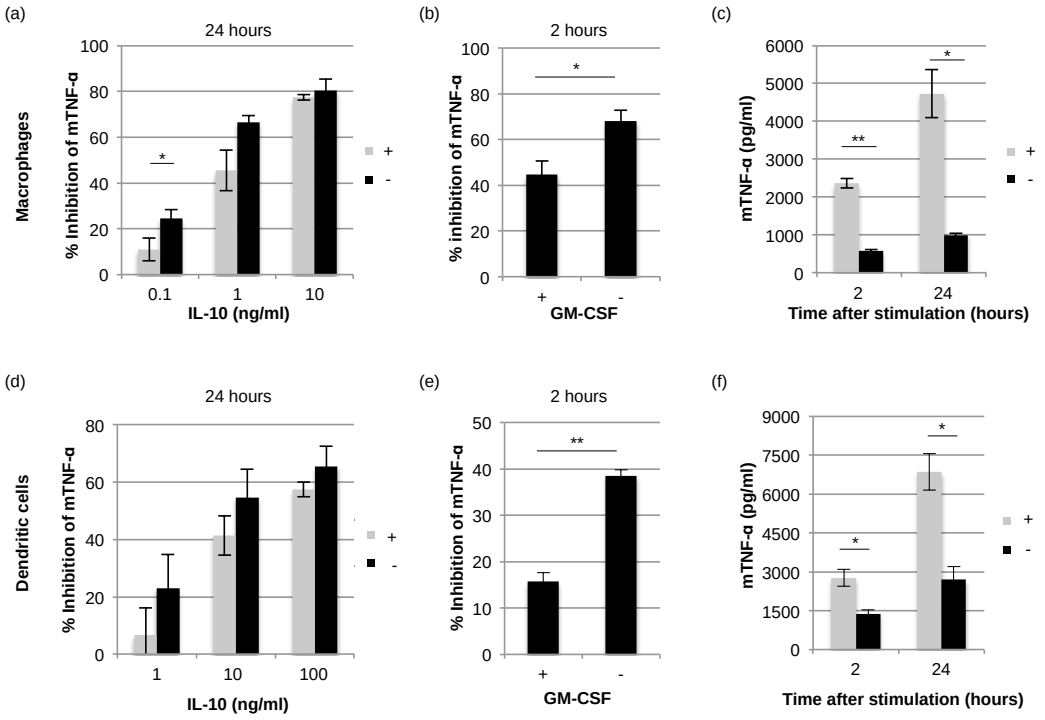

Figure 2 ◆ GM-CSF suppresses early IL-10-mediated responses. Macrophages (a-c) and dendritic cells (d-f) were cultured for the last 24 hours in the presence or absence (+/-) of GM-CSF. Cells were pre-treated for 20 min. with IL-10 followed by stimulation with 100 ng/ml LPS. The inhibition of TNF-α expression was determined after 24 hours of stimulation (a/d). Alternatively, cells were pre-treated for 20 min with 10 ng/ml IL-10 and then stimulated with 100 ng/ml LPS. The inhibition of TNF-α expression was determined after 2 hours of stimulation (b/e). Absolute expression levels of TNF-α for the abovementioned experiments are also given (c/f). All bars represent the average of 3-5 biological replicates (n=3-5, error bars indicate standard error) and asterisk(s) indicate significant differences as determined by a Welch's t-test (*P<0.05; **P<0.01).

GM-CSF regulates IL-10 activity without affecting STAT3 activation

As described in chapter 5, early IL-10 mediated responses seem to be controlled by the major anti-inflammatory pathway Jak1-STAT3-SOCS3. To investigate how GM-CSF influences early IL-10-mediated responses we first focused on the activation of STAT3. As shown in figure 3a, IL-10 induces strong $STAT3^{Y705}$ phosphorylation regardless of GM-CSF treatment. Phosphorylation of $STAT3^{S727}$ seemed also not to be affected by GM-CSF treatment. GM-CSF seems to regulate early IL-10-mediated responses without affecting STAT3 activation. However, early inhibition of TNF-α by IL-10 is completely abrogated in GM-CSF treated macrophages from LysMcre/Stat3flox mice that lack Stat 3 expression in macrophages (Figure S1). This indicates that STAT3 is required for early IL-10-mediated responses, but that GM-CSF negatively regulates this response in a STAT3 independent manner.

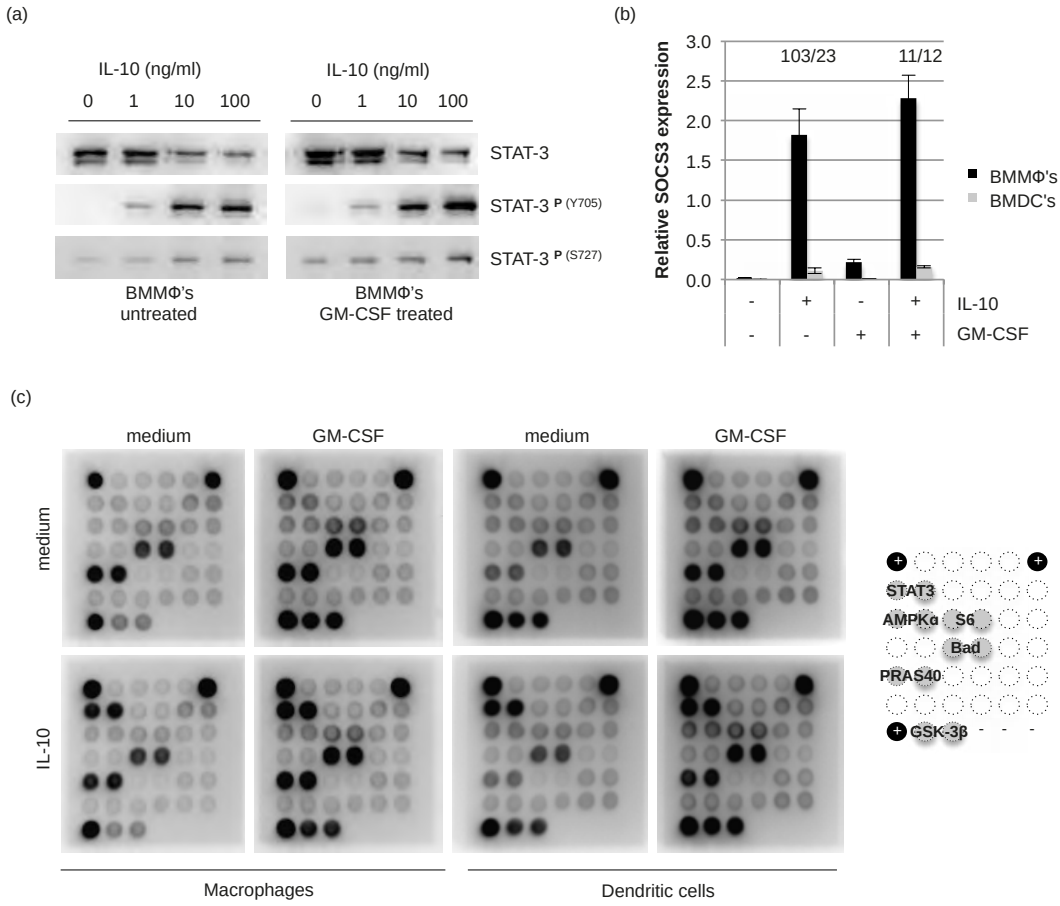

Figure 3 ◆ GM-CSF negatively influences IL-10 activity without affecting STAT3 activation. (a) Macrophages were treated for 24 hours with GM-CSF or left untreated. Cells were then activated with IL-10 (0, 1, 10 and 100 ng/ml) and phosphorylation of tyrosine 705 (Y705) and serine 727 (S727) of STAT3 was analysed by western blot. (b) Relative SOCS3 transcript levels were analysed by quantitative PCR in both macrophages and dendritic cells that were treated overnight by GM-CSF or were left untreated (n=3, error bars represent standard error). Fold induction of SOCS3 expression upon IL-10 treatment (100 ng/ml) was calculated using the $2^{\Delta Ct}$ method using HPRT as a reference gene and is depicted above the bars in the graph (macrophages/dendritic cells). (c) Macrophages and dendritic cells were treated overnight with GM-CSF or left untreated. Cells were then stimulated with 100 ng/ml IL-10 and the activation of intracellular signalling pathways was analysed by PathScan Array. A representative figure is given for 2 independent experiments. Asterisk(s) indicate significant differences as determined by a Welch's t-test (*P<0.05; **P<0.01).

As STAT3 phosphorylation was not affected by GM-CSF we continued to investigate the effect of GM-CSF on IL-10-induced SOCS3 expression. Relative SOCS3 transcript levels were determined by quantitative PCR in both macrophages and dendritic cells. As shown in figure 3b, IL-10 induces SOCS3 expression by ~100-fold in macrophages, whereas SOCS3 up-regulation is significantly lower in dendritic cells (12-fold, P=0.008). Unexpectedly, no significant differences were found for relative SOCS3 expression levels

upon IL-10 treatment of normal and GM-CSF treated macrophages. However, the IL-10 specific induction of SOCS3 was reduced ~10-fold. This is because GM-CSF itself already enhances SOCS3 expression in macrophages prior to IL-10 treatment. Depletion of GM-CSF from dendritic cells only resulted in a 2-fold increase in SOCS3 expression. Therefore GM-CSF seems to regulate early IL-10-mediated responses not only in a STAT3 independent manner, but also without affecting SOCS3 expression levels.

Next, we assessed whether GM-CSF treatment of macrophages alters IL-10-mediated signalling or other signalling pathways by using the PathScan Intracellular Signalling Array kit. As we observed previously, IL-10 only induces $STAT3^{Y705}$ phosphorylation in macrophages and dendritic cells, which is independent of GM-CSF pre-treatment. GM-CSF itself induces an activation state in macrophages that is indistinguishable from dendritic cells. GM-CSF treatment of macrophages enhances the phosphorylation of AMPKα and the ribosomal protein S6, but most strongly induces the phosphorylation of GSK-3β. Phosphorylation of other signalling molecules downstream of PI3K/Akt (PRAS40 and Bad) is also enhanced. On the other hand, depletion of dendritic cells from GM-CSF relieves PRAS40 from phosphorylation, whereas GSK-3β remains strongly phosphorylated. We therefore conclude that GM-CSF alters the activation status of signalling molecules that regulate cellular growth and survival in macrophages and dendritic cells.

Discussion

Interleukin-10 (IL-10) is an anti-inflammatory cytokine with promising therapeutic potential, but to date IL-10 therapy has not been as successful in the clinic as previously anticipated. A likely explanation for this phenomenon is that IL-10 activity is influenced by the cytokine milieu present in inflamed tissues [10-12]. In Chapter 5 we have already described the differential response of macrophages and dendritic cells towards IL-10. Dendritic cells are unable to respond rapidly to IL-10 as they are unable to suppress LPS-induced TNF-α at early stages. Furthermore, IL-10-induced SOCS3 expression was strongly reduced compared to macrophages. In this Chapter we further investigated the mechanism that controls this differential response between macrophages and dendritic cells. Our study demonstrates that the cytokine GM-CSF, the cytokine used to differentiate dendritic cells, is a key factor that negatively regulates IL-10 activity. GM-CSF pre-treatment of bone marrow-derived macrophages also reduced their ability to suppress LPS-induced TNF-α at 2 hours after stimulation. Vice versa, depletion of dendritic cells from GM-CSF partially restored their early response to IL-10. Furthermore, both macrophages and dendritic cells cultured in the presence of GM-CSF produced significantly higher

levels of TNF-α, which coincided with previous reports from Fleetwood and co-workers [13, 14]. Increased TNF-α expression levels upon LPS stimulation are caused by increased basal TNF-α mRNA transcript levels upon GM-CSF treatment [14]. In our study GM-CSF treated macrophages and dendritic cells do not produce significantly different levels of TNF-α, whereas both cell types respond significantly different towards IL-10. Differences in basal TNF-α expression levels cannot explain the observed differential response towards IL-10. Therefore, we continued to investigate IL-10-mediated signalling in macrophages and dendritic cells.

IL-10 receptor engagement results in the activation of downstream janus kinases Jak1 and Tyk2, which in turn phosphorylate the transcription factors STAT1, STAT3 and in some cell types STAT5 [15-17]. IL-10 is well known for its ability to activate the Jak-STAT pathway [18], but alternative signalling pathways have been described as well. Especially IL-10-mediated activation of the PI3K signalling pathway has been implicated in IL-10's survival promoting properties [19, 20]. Zhou and co-workers also revealed that IL-10 induced the activation of extracellular signal-related kinase (ERK)1/2 in a PI3K-dependent manner in promyeloid cells [20]. Furthermore, IL-10 has been shown to activate p38 MAPK signalling to induce the expression of heme oxygenase-1 [21]. In our study we could only detect IL-10-mediated activation of the transcription factor STAT3 in bone marrow-derived macrophages and dendritic cells. This indicates that STAT3 is the major transcription factor required for IL-10-mediated responses in bone marrow-derived cells. This is further supported by our observation that STAT3-deficient macrophages are unable to suppress LPS-induced TNF-α expression. However, we did observe subtle differences in the phosphorylation of $STAT3^{Y705}$ between regular macrophages and dendritic cells. More striking was the observation that IL-10 was not able to induce $STAT3^{S727}$ phosphorylation in a dose-dependent manner in dendritic cells. Serine phosphorylation of STAT3 has been reported previously for IL-6, IL-22, IFN-y and EGF [22-25] and enhances transcriptional activity of STAT3. The lack of $STAT3^{S727}$ phosphorylation might explain why IL-10-induced SOCS3 expression and early inhibition of TNF-α expression are impaired in dendritic cells.

Qasimi and co-workers previously described that SOCS3 is required by IL-10 to suppress TNF-α expression at early time points of stimulation [26]. We therefore investigated the role of SOCS3 in more detail. We observed a reduction in the ability of macrophages to respond rapidly to IL-10 upon GM-CSF treatment, but this seemed to be independent from upregulation of SOCS3 expression. Relative induction of SOCS3 expression by IL-10 was hardly affected by overnight treatment of macrophages with GM-CSF or depletion of dendritic cells from GM-CSF. This is in contrast to the difference in IL-10-induced SOCS3 expression between regular macrophages and dendritic cells. Furthermore, we also did not observe a difference in the phosphorylation of $STAT3^{Y705}$ and $STAT3^{S727}$ between regular macrophages or GM-CSF treated macrophages. Therefore,

GM-CSF seems to negatively regulate early IL-10-mediated responses in macrophages independent from STAT3-induced SOCS3 expression.

Interestingly, we did find major differences in the activation status of signalling molecules downstream of PI3K/Akt signalling in macrophages and dendritic cells. Furthermore, GM-CSF induced an activation state in macrophages that was indistinguishable from dendritic cells. Particularly the strong serine phosphorylation of GSK-3β^{S9} was a striking observation in GM-CSF cultured dendritic cells or GM-CSF treated macrophages. The degree of GSK-3β^{S9} phosphorylation also seems inversely correlated with early IL-10-mediated responses. A higher degree of GSK-3β^{S9} phosphorylation results in reduced suppression of LPS-induced TNF-α expression by IL-10. As IL-10 is also able to trigger the PI3K signalling pathway it is of great interest to investigate how these signalling pathways of IL-10 and GM-CSF are integrated and result in impaired IL-10-mediated responses.

Activation of STAT3 is regulated by a diverse set of post-translational modifications, including phosphorylation, acetylation and methylation [24, 25, 27-32]. Every modification plays its own role in regulating optimal STAT3 dimerization, DNA binding activity and transcriptional activity [33]. Involvement of the PI3K signalling pathway in the activation of STAT3 has also been reported previously. Spencer and co-workers revealed that the cytomegalovirus homologue of IL-10 was capable of inducing serine phosphorylation of STAT3^{S727} in a PI3K-dependent manner [34]. Furthermore, acetylation of STAT3^{L685} by IL-6 was also shown to depend on PI3K/Akt activation [35]. However, whether IL-10-induced STAT3 transcriptional activation requires acetylation and/or methylation and whether the PI3K pathway is involved, needs further investigation. Interestingly, Waitkus and co-workers recently reported on a novel mechanism of activation of STAT3, which was mediated by GSK-3α/β [33]. GSK-3α/β was shown to directly phosphorylate STAT3 at the residues S727 and T714. The requirement of GSK-3α/β in IL-10-induced STAT3 activation is therefore of great interest as this study shows that GM-CSF strongly inhibits GSK-3β by phosphorylation of serine residue 9. GSK-3α/β might therefore be a key signalling node that is able to control IL-10-mediated responses.

Previously, Hart and co-workers already reported that IL-10 was unable to suppress MHC-II expression in GM-CSF cultured monocytes [36]. Our study now also demonstrates that GM-CSF is able to alter IL-10-mediated suppression of TNF-α expression in both macrophages and dendritic cells. Furthermore, we and others show that GM-CSF cultured cells produce significantly higher levels of the pro-inflammatory cytokine TNF-α [14], but also the secretion of IL-12p70 and IL-23 is significantly enhanced by GM-CSF treated macrophages [14]. IL-23 has recently been identified as an important pro-inflammatory cytokine driving both innate and T cell-induced intestinal inflammation [37]. Therefore, GM-CSF seems to induce a cytokine environment favourable for chronic inflammation. Over the last couple of years GM-CSF has been identified as a key contributor to the

development of chronic inflammation in animal models of intestinal inflammation, multiple sclerosis and rheumatoid arthritis [38-40]. Taking together the key role of GM-CSF in the development of chronic inflammation with the results obtained in this study might explain why IL-10 therapy has not been as effective as previously anticipated. Our study demonstrates that the pro-inflammatory cytokine GM-CSF is able to negatively regulate IL-10-mediated responses in macrophages and dendritic cells. However, future research has to elucidate the exact mechanism on how GM-CSF and IL-10 signalling pathways are integrated and result in impaired cellular responses towards IL-10. Ultimately this knowledge could provide us with new therapeutic strategies to treat inflammatory disorders.

Experimental procedures

Bone marrow cultures

Bone marrow was isolated from the femur and tibia of 6-12 week old C57BL/6J mice. Bone marrow derived macrophages (BMMΦ's) were differentiated at 37°C/5% CO_2 in RPMI-1640 medium containing 4 mM L-glutamine, 25 mM HEPES and supplemented with 10% fetal calf serum, 50 µM β-mercaptoethanol, 50 U/ml penicillin and 50 µg/ml streptomycin and 20% spent medium from L929 cells (ATCC). Bone marrow cells were seeded at 1×10^6 cells/ml in 6- or 96-well tissue culture plates and cultured for 6 days, while refreshing medium at day 3. After 6 days of culture ≥95% of the cells expressed the macrophage markers F4/80 and CD11b.

Bone marrow derived dendritic cells (BMDC's) were differentiated for 10 days as described [41] using 10% spent medium from murine GM-CSF transfected X63 cells [42]. X63-GM-CSF cells were kindly provided by dr. M. Lutz (University of Erlangen-Nuremberg) with approval of dr. B. Stockinger (MRC National Institute for Medical Research). Briefly, bone marrow cells were plated at 2×10^5 cells/ml in bacteriological petri dishes and incubated at 37°C/5% CO_2. At day 3, 6 and 8 medium was refreshed and at day 10 both adherent and non-adherent cells were harvested. At this time typically ~90% of the cells expressed the dendritic cell markers CD11c and MHC class II.

Flow cytometry

Bone marrow derived cells were stained in FACS buffer (PBS containing 0.1% BSA and 5mM EDTA) using the following monoclonal antibodies for cell surface markers (all obtained from eBioscience): PE-conjugated anti-CD11b, APC-conjugated anti-F4/80, PE-conjugated anti-CD11c, APC-conjugated MHC-II. Cells were first incubated with Fc receptor block (eBioscience) for 10 min to block any non-specific binding and subsequent staining steps were performed for 20 min. at 4°C, followed by washing with FACS buffer. Stained cells were acquired using a Cyan-ADP Analyzer (Beckman Coulter) and analysed with FlowJo software (Tree Star, Inc.).

LPS stimulation assays

BMMΦ's were differentiated in 96 well plates and BMDC's were seeded in 96 well plates at a density of $5x10^4$/well. Cells were pre-treated for 15 min. with IL-10 and subsequently stimulated with 100 ng/ml lipopolysaccharide (LPS). After 2 hours or overnight stimulation, supernatants were analysed for TNF-α using the Ready-Set-Go!® ELISA kit (eBioscience) according to the supplier's protocol.

IL-10 induced signalling

Bone marrow-derived cells were treated for 20 min. with IL-10 (0, 1, 10 or 100 ng/ml). Cells were lysed using 1x Cell Lysis Buffer (Cell Signaling Technology) and total soluble protein content in the lysates was determined by the BCA method (Pierce). Proteins were separated on 12% Bis-Tris gels followed by transfer to a PVDF membrane by a wet blotting procedure. Thereafter the membrane was blocked in PBS (containing 0.1% v/v Tween-20 and 5% w/v non-fat dry milk powder) for 1 hour at room temperature, followed by overnight incubation at 4°C with monoclonal antibodies specific for STAT3, phospho-STAT3^{Y705} or phospho-STAT3^{S727} in PBS (containing 0.1% v/v Tween-20 and 1% w/v BSA). All STAT3 antibodies were obtained from Cell Signaling Technology. A HRP-conjugated donkey anti-rabbit IgG (Jackson ImmunoResearch) was used as a secondary antibody. Band intensities were analysed with Image J Software.

Cell lysates were also used to investigate the activation of 18 well-characterized signalling molecules using the PathScan Intracellular Signaling Array kit (Cell Signaling Technology) according to the manufacturer's protocol. Blots and arrays were visualised in the G:BOX Chemi System (Syngene).

Quantitative PCR

BMMΦ's were differentiated in 6 well plates and 3x10^6 BMDC's were seeded in 6 well plates and were treated for 2 hours with IL-10 (0, 1, 10 or 100 ng/ml). Cells were then washed with PBS and mRNA was isolated with the Maxwell® 16 Tissue LEV Total RNA Purification Kit and the Maxwell® 16 instrument (both from Promega). Then cDNA was synthesized using the GoScript™ Reverse Transcription System (Promega) according to the supplier's protocol. Samples were analysed in triplicate for SOCS3 and HPRT (reference gene) expression by quantitative PCR using ABsolute SYBR Green Fluorescein mix (Thermo Scientific). Fold induction of SOCS3 expression was determined by the Pfaffl method [43].

Data analysis

All data shown in the figures indicate the average of at least three biological replicates (*n*) that were determined by three technical replicates. In the figure legends *n* is indicated and error bars indicate the standard error. Significant differences between samples were calculated using the student's t-test and regarded as significant when $P<0.05$. Significant differences are indicated in the figures by asterisks ($P<0.05$ (*) or $P<0.01$ (**)).

Acknowledgements

We would like to thank Dr. Birgit Strobl at Vienna University for providing us with the bones of conditional Stat3 knockout mice (LysMcre/Stat3flox) and control mice. We would like to thank all the people at the animal facilities of Wageningen University (CKP) for their care of all the animals used in this study.

Supplemental figure

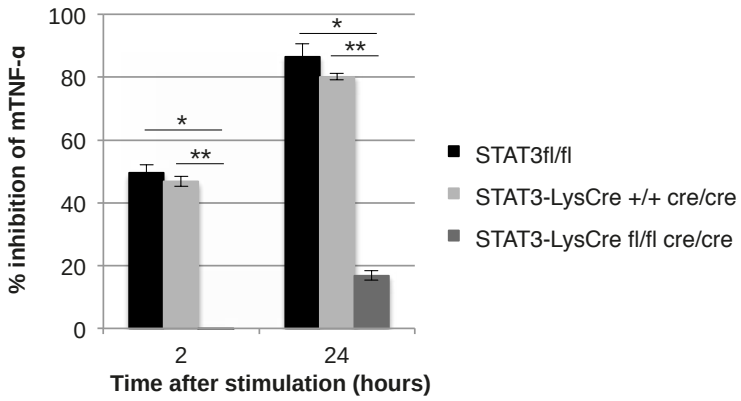

Figure S1 ◆ IL-10 mediated responses are STAT3 dependent. Macrophages from STAT3 transgenic mice were treated overnight with GM-CSF. Cells were then pre-treated with IL-10 and subsequently stimulated with 100 ng/ml LPS. The inhibition of TNF-α expression was determined at 2 and 24 hours (n=3, error bars represent standard error). Asterisk(s) indicate significant differences as determined by a Welch's t-test (*P<0.05; **P<0.01).

References

1. Asadullah K, Sterry W and Volk HD (2003) Interleukin-10 therapy--review of a new approach. Pharmacological Reviews 55: 241-269.
2. van Deventer SJ, Elson CO and Fedorak RN (1997) Multiple doses of intravenous interleukin 10 in steroid-refractory Crohn's disease. Crohn's Disease Study Group. Gastroenterology 113: 383-389.
3. Schreiber S, Fedorak RN, Nielsen OH, Wild G, Williams CN, et al. (2000) Safety and efficacy of recombinant human interleukin 10 in chronic active Crohn's disease. Crohn's Disease IL-10 Cooperative Study Group. Gastroenterology 119: 1461-1472.
4. Marlow GJ, van Gent D and Ferguson LR (2013) Why interleukin-10 supplementation does not work in Crohn's disease patients. World Journal of Gastroenterology : WJG 19: 3931-3941.
5. Steidler L, Hans W, Schotte L, Neirynck S, Obermeier F, et al. (2000) Treatment of murine colitis by Lactococcus lactis secreting interleukin-10. Science 289: 1352-1355.
6. Braat H, Rottiers P, Hommes DW, Huyghebaert N, Remaut E, et al. (2006) A phase I trial with transgenic bacteria expressing interleukin-10 in Crohn's disease. Clinical gastroenterology and hepatology : the official clinical practice journal of the American Gastroenterological Association 4: 754-759.
7. Avdiushko R, Hongo D, Lake-Bullock H, Kaplan A and Cohen D (2001) IL-10 receptor dysfunction in macrophages during chronic inflammation. Journal of Leukocyte Biology 70: 624-632.
8. Fernandez S, Jose P, Avdiushko MG, Kaplan AM and Cohen DA (2004) Inhibition of IL-10 receptor function in alveolar macrophages by Toll-like receptor agonists. Journal of Immunology 172: 2613-2620.
9. Jose P, Avdiushko MG, Akira S, Kaplan AM and Cohen DA (2009) Inhibition of interleukin-10 signaling in lung dendritic cells by toll-like receptor 4 ligands. Experimental Lung Research 35: 1-28.
10. Du Z, Kelly E, Mecklenbrauker I, Agle L, Herrero C, et al. (2006) Selective regulation of IL-10 signaling and function by zymosan. Journal of Immunology 176: 4785-4792.
11. Ji JD, Tassiulas I, Park-Min KH, Aydin A, Mecklenbrauker I, et al. (2003) Inhibition of interleukin 10 signaling after Fc receptor ligation and during rheumatoid arthritis. Journal of Experimental Medicine 197: 1573-1583.
12. Herrero C, Hu X, Li WP, Samuels S, Sharif MN, et al. (2003) Reprogramming of IL-10 activity and signaling by IFN-gamma. Journal of Immunology 171: 5034-5041.
13. Fleetwood AJ, Dinh H, Cook AD, Hertzog PJ and Hamilton JA (2009) GM-CSF- and M-CSF-dependent macrophage phenotypes display differential dependence on Type I interferon signaling. Journal of Leukocyte Biology 86: 411-421.

14. Fleetwood AJ, Lawrence T, Hamilton JA and Cook AD (2007) Granulocyte-macrophage colony-stimulating factor (CSF) and macrophage CSF-dependent macrophage phenotypes display differences in cytokine profiles and transcription factor activities: implications for CSF blockade in inflammation. Journal of Immunology 178: 5245-5252.

15. Finbloom DS and Winestock KD (1995) IL-10 induces the tyrosine phosphorylation of tyk2 and Jak1 and the differential assembly of STAT1 alpha and STAT3 complexes in human T cells and monocytes. Journal of Immunology 155: 1079-1090.

16. Wehinger J, Gouilleux F, Groner B, Finke J, Mertelsmann R, et al. IL-10 induces DNA binding activity of three STAT proteins (Stat1, Stat3, and Stat5) and their distinct combinatorial assembly in the promoters of selected genes. FEBS Letters 394: 365-370.

17. Weber-Nordt RM, Riley JK, Greenlund AC, Moore KW, Darnell JE, et al. (1996) Stat3 Recruitment by Two Distinct Ligand-induced, Tyrosine-phosphorylated Docking Sites in the Interleukin-10 Receptor Intracellular Domain. Journal of Biological Chemistry 271: 27954-27961.

18. Riley JK, Takeda K, Akira S and Schreiber RD (1999) Interleukin-10 receptor signaling through the JAK-STAT pathway. Requirement for two distinct receptor-derived signals for anti-inflammatory action. Journal of Biological Chemistry 274: 16513-16521.

19. Sharma S, Yang B, Xi X, Grotta JC, Aronowski J, et al. (2011) IL-10 directly protects cortical neurons by activating PI-3 kinase and STAT-3 pathways. Brain Research 1373: 189-194.

20. Zhou JH, Broussard SR, Strle K, Freund GG, Johnson RW, et al. (2001) IL-10 inhibits apoptosis of promyeloid cells by activating insulin receptor substrate-2 and phosphatidylinositol 3'-kinase. Journal of Immunology 167: 4436-4442.

21. Lee TS and Chau LY (2002) Heme oxygenase-1 mediates the anti-inflammatory effect of interleukin-10 in mice. Nature Medicine 8: 240-246.

22. Lejeune D, Dumoutier L, Constantinescu S, Kruijer W, Schuringa JJ, et al. (2002) Interleukin-22 (IL-22) activates the JAK/STAT, ERK, JNK, and p38 MAP kinase pathways in a rat hepatoma cell line - Pathways that are shared with and distinct from IL-10. Journal of Biological Chemistry 277: 33676-33682.

23. Schuringa JJ, Jonk LJ, Dokter WH, Vellenga E and Kruijer W (2000) Interleukin-6-induced STAT3 transactivation and Ser727 phosphorylation involves Vav, Rac-1 and the kinase SEK-1/MKK-4 as signal transduction components. Biochemistry Journal 347 Pt 1: 89-96.

24. Wen Z and Darnell JE, Jr. (1997) Mapping of Stat3 serine phosphorylation to a single residue (727) and evidence that serine phosphorylation has no influence on DNA binding of Stat1 and Stat3. Nucleic Acids Research 25: 2062-2067.

25. Wen Z, Zhong Z and Darnell JE, Jr. (1995) Maximal activation of transcription by Stat1 and Stat3 requires both tyrosine and serine phosphorylation. Cell 82: 241-250.

26. Qasimi P, Ming-Lum A, Ghanipour A, Ong CJ, Cox ME, et al. (2006) Divergent mechanisms utilized by SOCS3 to mediate interleukin-10 inhibition of tumor necrosis factor alpha and nitric oxide production by macrophages. Journal of Biological Chemistry 281: 6316-6324.

27. Iwasaki H, Kovacic JC, Olive M, Beers JK, Yoshimoto T, et al. (2010) Disruption of protein arginine N-methyltransferase 2 regulates leptin signaling and produces leanness in vivo through loss of STAT3 methylation. Circulation Research 107: 992-1001.

28. Nie Y, Erion DM, Yuan Z, Dietrich M, Shulman GI, et al. (2009) STAT3 inhibition of gluconeogenesis is downregulated by SirT1. Nature Cell Biology 11: 492-500.

29. Yuan ZL, Guan YJ, Chatterjee D and Chin YE (2005) Stat3 dimerization regulated by reversible acetylation of a single lysine residue. Science 307: 269-273.

30. Sestito R, Madonna S, Scarponi C, Cianfarani F, Failla CM, et al. (2011) STAT3-dependent effects of IL-22 in human keratinocytes are counterregulated by sirtuin 1 through a direct inhibition of STAT3 acetylation. FASEB journal 25: 916-927.

31. Yang J, Huang J, Dasgupta M, Sears N, Miyagi M, et al. (2010) Reversible methylation of promoter-bound STAT3 by histone-modifying enzymes. Proceedings of the National Academy of Sciences of the United States of America 107: 21499-21504.

32. Zhong Z, Wen Z and Darnell JE, Jr. (1994) Stat3: a STAT family member activated by tyrosine phosphorylation in response to epidermal growth factor and interleukin-6. Science 264: 95-98.

33. Waitkus MS, Chandrasekharan UM, Willard B, Tee TL, Hsieh JK, et al. (2014) Signal integration and gene induction by a functionally distinct STAT3 phosphoform. Molecular and Cellular Biology 34: 1800-1811.

34. Spencer JV (2007) The cytomegalovirus homolog of interleukin-10 requires phosphatidylinositol 3-kinase activity for inhibition of cytokine synthesis in monocytes. Journal of Virology 81: 2083-2086.

35. Ohbayashi N, Ikeda O, Taira N, Yamamoto Y, Muromoto R, et al. (2007) LIF- and IL-6-Induced Acetylation of STAT3 at Lys-685 through PI3K/Akt Activation. Biological and Pharmaceutical Bulletin 30: 1860-1864.

36. Hart PH, Jones CA and Finlay-Jones JJ (1995) Monocytes cultured in cytokine-defined environments differ from freshly isolated monocytes in their responses to IL-4 and IL-10. Journal of Leukocyte Biology 57: 909-918.

37. Hue S, Ahern P, Buonocore S, Kullberg MC, Cua DJ, et al. (2006) Interleukin-23 drives innate and T cell-mediated intestinal inflammation. Journal of Experimental Medicine 203: 2473-2483.

38. Sonderegger I, Iezzi G, Maier R, Schmitz N, Kurrer M, et al. (2008) GM-CSF mediates autoimmunity by enhancing IL-6-dependent Th17 cell development and survival. Journal of Experimental Medicine 205: 2281-2294.

39. Griseri T, McKenzie BS, Schiering C and Powrie F (2012) Dysregulated hematopoietic stem and progenitor cell activity promotes interleukin-23-driven chronic intestinal inflammation. Immunity 37: 1116-1129.

40. Hamilton JA (2008) Colony-stimulating factors in inflammation and autoimmunity. Nature Reviews Immunology 8: 533-544.

41. Lutz MB, Kukutsch N, Ogilvie ALJ, Rossner S, Koch F, et al. (1999) An advanced culture method for generating large quantities of highly pure dendritic cells from mouse bone marrow. Journal of Immunological Methods 223: 77-92.

42. Zal T, Volkmann A and Stockinger B (1994) Mechanisms of tolerance induction in major histocompatibility complex class II-restricted T cells specific for a blood-borne self-antigen. Journal of Experimental Medicine 180: 2089-2099.

43. Pfaffl MW (2001) A new mathematical model for relative quantification in real-time RT-PCR. Nucleic Acids Research 29: e45.

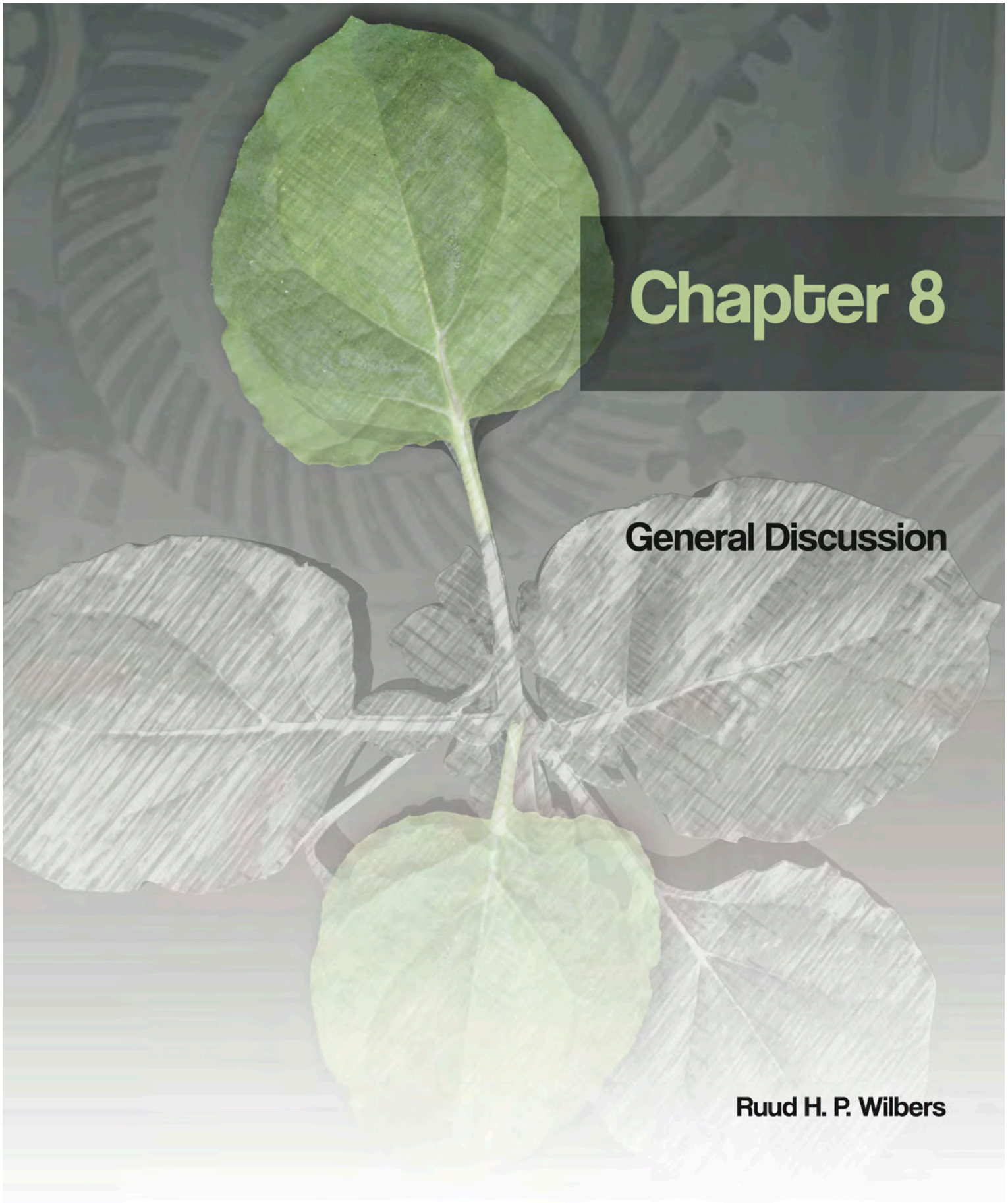

Chapter 8

General Discussion

Ruud H. P. Wilbers

The use of therapeutic proteins (or biopharmaceuticals) has become a common strategy to treat human diseases. Over a four-year period (2010-2014) a total of 147 novel pharmaceutical products have been approved by the Food and Drug Administration (FDA) in the United States of which ~26% constituted biopharmaceuticals [1]. The majority of these biopharmaceuticals are produced in the bacterium *Escherichia coli*, the yeast *Saccharomyces cerevisiae* or mammalian cell lines, like Chinese hamster ovarian (CHO) cells or murine myeloma (SP2/0) cells. A trend emerges that shows that mammalian expression systems are becoming more popular, whereas the use of *E. coli* as expression system is declining [1]. This trend is in line with the growing demand for biopharmaceuticals that harbour specific post-translational modifications, particularly N-glycans. A large group of biopharmaceuticals relies on appropriate N-glycosylation for optimal activity. For instance, N-glycosylation of antibodies (the fastest growing group of biopharmaceuticals) is essential for optimal binding to Fcγ-receptors and subsequent effector functions, like antibody-dependent cellular cytotoxicity (ADCC) [2]. Yet, typical mammalian core α1,6-fucose (for details see chapter 1, figure 3, page 21) was shown to strongly inhibit ADCC by reducing the binding to Fcγ-receptors by several orders of magnitude [2]. Hence, to circumvent this problem antibodies should be engineered that lack this fucose residue. N-glycans and their composition can therefore be crucial to obtain optimal efficacy of certain biopharmaceuticals.

N-glycosylation also formed the basis for the approval of the first plant-expressed biopharmaceutical in 2012, namely human glucocerebrosidase. Glucocerebrosidase is an enzyme used to treat the lysosomal storage disorder Gaucher disease. Recombinant human glucocerebrosidase is currently produced in CHO cells (trade name Cerezyme; Genzyme) or fibrosarcoma cells (trade name Velaglucerase alfa; Shire). Furthermore, the enzyme requires N-glycans that terminate in mannose residues to ensure uptake by macrophages via the mannose receptor. However, when produced in CHO cells the enzyme still requires *in vitro* deglycosylation steps to obtain terminal mannoses on its N-glycans [3]. For the same reason Velaglucerase alfa producing fibrosarcoma cells are cultured in the presence of a α-mannosidase I inhibitor [4]. Plants as an alternative expression system offer the possibility to produce human glucocerebrosidase with N-glycans that terminate in mannose residues *in vivo*. The company Protalix Biotherapeutics demonstrated this by producing human glucocerebrosidase with a vacuolar targeting signal in carrot root cells [5]. This plant-produced glucocerebrosidase (Taliglucerase alfa) performed better than its mammalian cell-produced counterpart. The approval of Taliglucerase alfa by the FDA was accelerated due to viral contamination of Genzyme's production facilities [6]. Another advantage of plants in this respect is that plants have a low risk for contamination with human pathogens. This example illustrates that plants have finally claimed their position within the pharmaceutical market.

Over the last decade plants have proven to be a good alternative production platform for biopharmaceuticals [7-10], especially in terms of speed, costs and scalability [11]. However, plant specific N-glycosylation has long been a major limitation for acceptance of plants as a production platform. But in fact, the relatively limited glycome of plants offers great advantages as it allows relative easy manipulation of the N-glycosylation pathway. Current plant-based expression systems have established themselves as a superior platform in terms of engineering post-translational modifications, like N-glycosylation [11]. This provides a unique niche within the therapeutic market for the production of pharmaceutical glycoproteins which function can be enhanced by appropriate post-translational modifications.

A part of this thesis describes the production of a variety of pharmaceutically interesting glycoproteins in *Nicotiana benthamiana* plants and focuses on the engineering of post-translational modifications to obtain optimal activity. In the first half of this chapter we will discuss our findings and experiences with regard to post-translational modifications in plants. Furthermore, we will elaborate on how protein intrinsic properties influence N-glycan composition of heterologously expressed glycoproteins. The second half of this chapter will continue to discuss our findings on our parallel research line on IL-10-mediated signalling. IL-10-mediated signalling was investigated to find clues on why IL-10 therapy is not as successful as previously anticipated. This will be briefly introduced after the first two sections.

Post-translational modifications in plants

Post-translational modifications are modifications of a protein that occur during or after translation. Post-translational modifications include protein folding, disulfide bond formation, proteolytic processing, glycosylation, lipidation, phosphorylation, γ-carboxylation, β-hydroxylation, amidation, and sulfation [12]. Such modifications have been shown to affect almost every aspect of protein function, including activitity, localisation, stability, and interactions with other molecules. In respect to recombinant protein production, post-translational modifications can enlarge protein heterogeneity. When a recombinant protein relies on post-translational modifications for proper functioning it may be a challenge to design a production system that produces recombinant proteins homogeneously.

Plants have emerged as an attractive expression system as they are capable of performing post-translational modifications, like proteolytic processing, N-glycosylation, O-glycosylation, proline hydroxylation and lipidation [12, 13]. Plant endogenous O-glycosylation has also been exploited to increase serum half-life of recombinant human IFN-α2b and growth hormone [14, 15]. Furthermore, the attachment of fatty acid chains on plant-produced recombinant proteins was demonstrated by the production of the

palmitoylated bacterial lipoprotein OspA [16] and the N-myristoylated HIV antigen Nef [17] in tobacco. However, plant-specific post-translational modifications can also lower the quality of heterologous expressed proteins. For instance, typical plant-specific N-glycans or O-glycans can become target of undesired immune responses [18, 19]. Furthermore, unintended processing of recombinant proteins by endogenous proteases within the plant secretory pathway can occur [20, 21]. Understanding the post-translational machinery in plants is therefore important to ensure that recombinant proteins can be produced with the highest quality possible. In the following sections we will discuss some of our experiences with post-translational modifications along the plant secretory pathway.

Signal peptide processing

Synthesis of secretory proteins occurs on ribosomes of the rough endoplasmic reticulum (ER). The first stretch of amino acids of a secretory protein is called the signal peptide. Upon recognition, the signal peptide is translocated into the lumen of the ER while translation continues. Inside the ER lumen the signal peptide is (in most cases) cleaved of by a serine protease called signal peptidase. This first post-translational modification results in the mature amino acid sequence of a secretory protein. For all the human cytokines that we have expressed transiently in *N. benthamiana* we confirmed translocation into the ER by confocal imaging when fused to GFP. Native signal peptides of human origin seem suitable for the use in plant-based expression systems. However, we also demonstrated that signal peptide cleavage was not complete when mature TGF-β1 was expressed in the absence of the latency-associated peptide (Chapter 2). For TGF-β1, IL-22 (Chapter 4) and the *Schistosoma mansoni* egg antigens omega-1 and kappa-5 (Chapter 5) we have employed the signal peptide of an *Arabidopsis* chitinase gene. This signal peptide in combination with our in-house codon optimization strategy enhanced the yield of TGF-β1, which is most likely explained by an increased efficiency of translation initiation (discussed in Chapter 2). The chitinase signal peptide also facilitated efficient secretion of IL-22 (~50%) and *S. mansoni* egg antigens (>90%). This was quite unexpected, as plants are generally believed to secrete proteins poorly as only few endogenous proteins reside in the extracellular space. The use of a plant specific signal peptide has previously been described to enhance secretion [22, 23]. In our lab we also observed that the protein itself has a strong influence on secretion efficiency. We have expressed up to 23 different recombinant proteins of which all mature protein sequences were preceded by the *Arabidopsis* chitinase signal peptide and N-terminal 6xhistidine and FLAG-tags. We observed a broad variety in secretion efficiency among this set of proteins (unpublished data), which can only be explained by intrinsic properties of these proteins. For three monoclonal IgG antibodies we demonstrated that secretion efficiency was

significantly reduced when the respective variable domains were grafted onto an IgA backbone, while using the same chitinase signal peptide [24]. It is of great interest to understand which factors determine secretion efficiency in plants as it enables efficient purification from the apoplast.

Proteolytic processing

Plants are rich in proteases and a wide variety of proteases reside within the secretory pathway of plants as well as in the apoplast [21, 25]. It is therefore inevitable that recombinant secretory proteins encounter proteases on their way out. Proteolytic processing is regarded as one of the largest bottlenecks of plant expression systems. A classic example is the unintended processing of antibodies when expressed in plants [20]. Strategies to circumvent proteolytic processing of recombinant proteins include: targeting of the protein to specific subcellular compartments [26], fusion to a stable partner [27], fusion to a protease inhibitor [28] or co-expression of protease inhibitors [21].

A common strategy to increase recombinant protein yield is retaining the protein in the ER by using a C-terminal KDEL targeting sequence [26]. The ER is regarded as a protein friendly environment due to the absence of many proteases. We have used ER-retention in order to increase the yield of TGF-β1 and IL-10 (Chapter 2 and 3, respectively), but for both cytokines this strategy did not result in significantly higher yields. As cytokines are inherently unstable we also attempted to increase the yield of IL-10 and TGF-β1 by fusing them to a stable partner. For this purpose we used the Fc portion of human IgA (Fcα). The yield only increased significantly for TGF-β1. In both cases we observed proteolytic degradation of the fusion proteins. For IL-10 we observed a degradation product of approximately 50 kDa, which could resemble the Fcα fragment (Chapter 3). The same degradation product was also observed for the Fcα-fusion of TGF-β1 (data not shown). This indicates that proteolytic cleavage most likely occurs between the Fcα portion and its fusion partner. For the Fcα-fusion of TGF-β1 we have pursued engineering of the linker sequence, unfortunately without success. We also attempted to co-express the protease inhibitors chicken ovocystatin (inhibiting cysteine proteases) and bovine aprotinin (inhibiting serine proteases). Co-expression of cystatin did enhance the overall yield of TGF-β1, but did not prevent proteolytic processing of the fusion protein (data not shown).

The activity of plant endogenous proteases is of course not always undesirable as some glycoproteins rely on proteolytic processing to become active. For example, proteolytic processing of human procollagen occurs by plant proteases on both the N-terminus and C-terminus upon expression in tobacco [29]. Another example is the processing of the Der p1 allergen from house dust mite [12]. Strikingly, the proteolytic processing of Der p1 only occurs in a plant-based expression system, but not in

mammalian or insect cells. Plants are therefore able to produce and process recombinant proproteins, although the cleavage sites might differ from the natural ones. In chapter 2 we describe the expression of the proprotein LAP-TGF-β1 and we demonstrated that proteolytic processing by a furin-like enzyme of this proprotein does not occur *in planta*. Biologically active TGF-β1 requires furin cleavage and this was accomplished by co-expressing human furin with LAP-TGF-β1. This engineering step is quite remarkable as furin itself is expressed as a complex membrane-bound proprotein. Furin undergoes autocatalytic processing of its N-terminus prior to transportation to the Golgi-system. Subsequently, furin is truncated at its C-terminus, which is dependent on the acidic environment of the *trans*-Golgi compartment [30]. Therefore, furin requires multiple proteolytic processing steps and correct localization within the secretory pathway to become active. Altogether, chapter 2 describes a novel engineering strategy for the production and proteolytic processing of complex proproteins in plants. This engineering strategy can further facilitate plant-based expression of other proproteins that rely on furin cleavage, like neural growth factor (NGF), bone-morphogenic proteins (BMP's) or even the Ebola Zaire envelope glycoprotein [31]. Furthermore, co-expression of other proteases can be explored as well to facilitate plant-based expression of a variety of complex proproteins.

Contribution of N-glycans to protein folding

N-glycosylation is the post-translational modification that has drawn most of the attention of plant biotechnologists, in particular engineering of the composition of N-glycans. One of the most conserved roles of N-glycosylation in eukaryotes is its contribution to protein folding, a feature independent of N-glycan composition. In chapter 3 we describe that extensive multimerisation is the major production bottleneck of human IL-10. Extensive multimerisation was shown to be caused by IL-10's intrinsic property to form dimers by a process called 3D domain swapping. When the concentration of a 3D domain swapping protein is high, swapping of domains does not have to be limited to two partners [32]. In the case of IL-10 this results in the formation of large intracellular aggregates, but this only occurs for human IL-10 and not mouse IL-10. We further demonstrated that N-glycosylation of the N-terminus (which only occurs in mouse IL-10) is crucial to limit extensive multimerisation of IL-10. Introduction of the mouse N-glycosylation signal in human IL-10 largely prevented aggregation, whereas deletion of the N-glycosylation signal in mouse IL-10 induced aggregation. This clearly states that N-glycosylation can play an important role in controlling protein folding properties.

Site-directed mutagenesis is a useful tool to study the role of N-glycans on protein folding. In chapter 4 we have also investigated the role of N-glycans on the folding of IL-22. We used both site-directed mutagenesis of a N-glycosylation site and co-expression of

ER-retained PNGase F. The addition of a N-glycan is completely abolished by mutagenesis of the N-glycosylation site and the glycan can no longer contribute to protein folding. In contrast, when co-expressing ER-retained PNGase F, N-glycans are initially attached to the glycoprotein and can assist the folding process before being removed by PNGase F. In the case of IL-22 we could not demonstrate that the N-glycan on Asn54 contributes to protein folding. However, in the case of plant-based expression of chicken ovalbumin we could find a role of N-glycosylation on protein folding (unpublished data). Chicken ovalbumin carries two potential N-glycosylation signals and both are occupied with a N-glycan upon transient expression in *N. benthamiana*. We observed multimerisation of ovalbumin on western blot when both N-glycosylation sites were mutated, which could be explained by inappropriate folding. However, upon co-expression of ER-retained PNGase F we did not observe these multimers, but instead we obtained monomeric ovalbumin without N-glycans. These results show that the combination of site-directed mutagenesis and *in vivo* deglycosylation with PNGase F is a powerful tool to study the role of N-glycans on protein folding.

Engineering of N-glycosylation

The N-glycan composition on biopharmaceuticals has to resemble the native composition as closely as possible and should not harbour immunogenic N-glycan structures. As most biopharmaceuticals are of human origin plant biotechnologists have done serious efforts and made great progress to engineer the N-glycosylation pathway of plants to synthesize human-like N-glycans. We exploited this to engineer the N-glycans of human IL-22 and investigated the contribution to the activity of IL-22 (Chapter 4).

Plants have shown to be highly tolerant to changes in their N-glycosylation pathways and are capable to synthesize human-like N-glycans with great homogeneity [18, 33]. Plants have in theory the ability to synthesize virtually any N-glycan structure and this also allows the synthesis of tailored N-glycans with immunogenic properties. Such immunogenic N-glycan structures could potentially be used to improve the efficacy of current vaccines by targeting them to the appropriate immune cells and receptors via their N-glycans. Furthermore, particular N-glycan structures can contribute to the biological activity of glycoproteins, like for example helminth secreted omega-1 (Chapter 5). Synthesis of helminth-like N-glycans would enable the functional characterization of helminth glycoproteins as well as investigation of the role that N-glycans play with regard to the immunomodulatory properties of these glycoproteins. For this reason we have explored the possibility to produce helminth glycoproteins and engineer the N-glycan structures naturally found on these glycoproteins (Chapter 5). A common N-glycan structure found on helminth glycoproteins is Lewis X. Lewis X has been synthesized before in *Nicotiana tabacum* by stably expressing a hybrid β1,4-galactosyltransferase and a

hybrid α1,3-fucosyltransferase IXa that were targeted to the medial-Golgi compartment by a CTS domain of *Arabidopsis* β1,2-xylosyltransferase [34]. The obtained N-glycans were of a hybrid type as they only contained one antenna with Lewis X, whereas the other antenna contained mannoses. The formation of hybrid N-glycans was attributed to the incorrect targeting of galactosyltransferase to the medial-Golgi. In this compartment β1,4-galactosyltransferase would interfere with the activity of plant endogenous glycosyltransferases, like α-mannosidase II. In contrast, targeting human β1,4-galactosyltransferase to the *trans*-Golgi compartment in ΔXT/FT plants allowed the synthesis of diantennary N-glycans containing two terminal galactose residues [35]. This illustrates that correct targeting of glycosyltransferases can be crucial in certain engineering strategies. Aberrant targeting of glycosyltransferases is commonly done by creating hybrid genes. In this approach the catalytic domain of a glycosyltransferase is genetically fused with the CTS domain (C, cytoplasmic tail; T, transmembrane domain; S, stem region) of another glycosyltransferase that has a different Golgi localization. In the case of human β1,4-galactosyltransferase the catalytic domain was fused with the CTS domain of rat α2,6-sialyltransferase for *trans*-Golgi targeting [35]. A drawback of using hybrid genes can be that the engineered glycosyltransferase looses its activity. We demonstrated the lack of activity of β1,4-*N*-acetylgalactosaminyltransferase from *C. elegans* when we fused it with the CTS domain of rat α2,6-sialyltransferase (Chapter 5). The native β1,4-*N*-acetylgalactosaminyltransferase on the other hand did work properly and was used to synthesize LDN and LDN-F structures in plants.

Another consideration for glyco-engineering approaches is whether stable or transient over-expression of glycosyltransferases is preferred. Generating stable transformants is time consuming and therefore we used the speed of transient expression in our study to engineer helminth-like N-glycans. To our surprise, we obtained hybrid Lewis X-type N-glycans upon transient expression of zebrafish β1,4-galactosyltransferase even though a *trans*-Golgi targeting CTS domain sequence was used (sialGalT). Over-expression of sialGalT under control of a dual 35S promoter (*d35S*:sialGalT) might result in incorrect targeting of the enzyme, whereby leakage into the medial-Golgi could explain the formation of these Lewis X-hybrid N-glycans. This was confirmed when the expression of GalT was lowered by using a weak constitutive promoter (Gpa2:sialGalT). This also indicates that not only a proper CTS domain, but also controlled expression levels are required for optimal glyco-engineering. In transient expression systems controlling expression levels of glycosyltransferases is more challenging than in stable tranformants. In stable transformation only one transformant with the desired expression level of your glycosyltransferase has to be selected. Nevertheless, during our work on transient glyco-engineering of Lewis X we have repeatedly obtained homogeneous N-glycan profiles. This indicates that efficient glyco-engineering is possible in a transient fashion, which was also

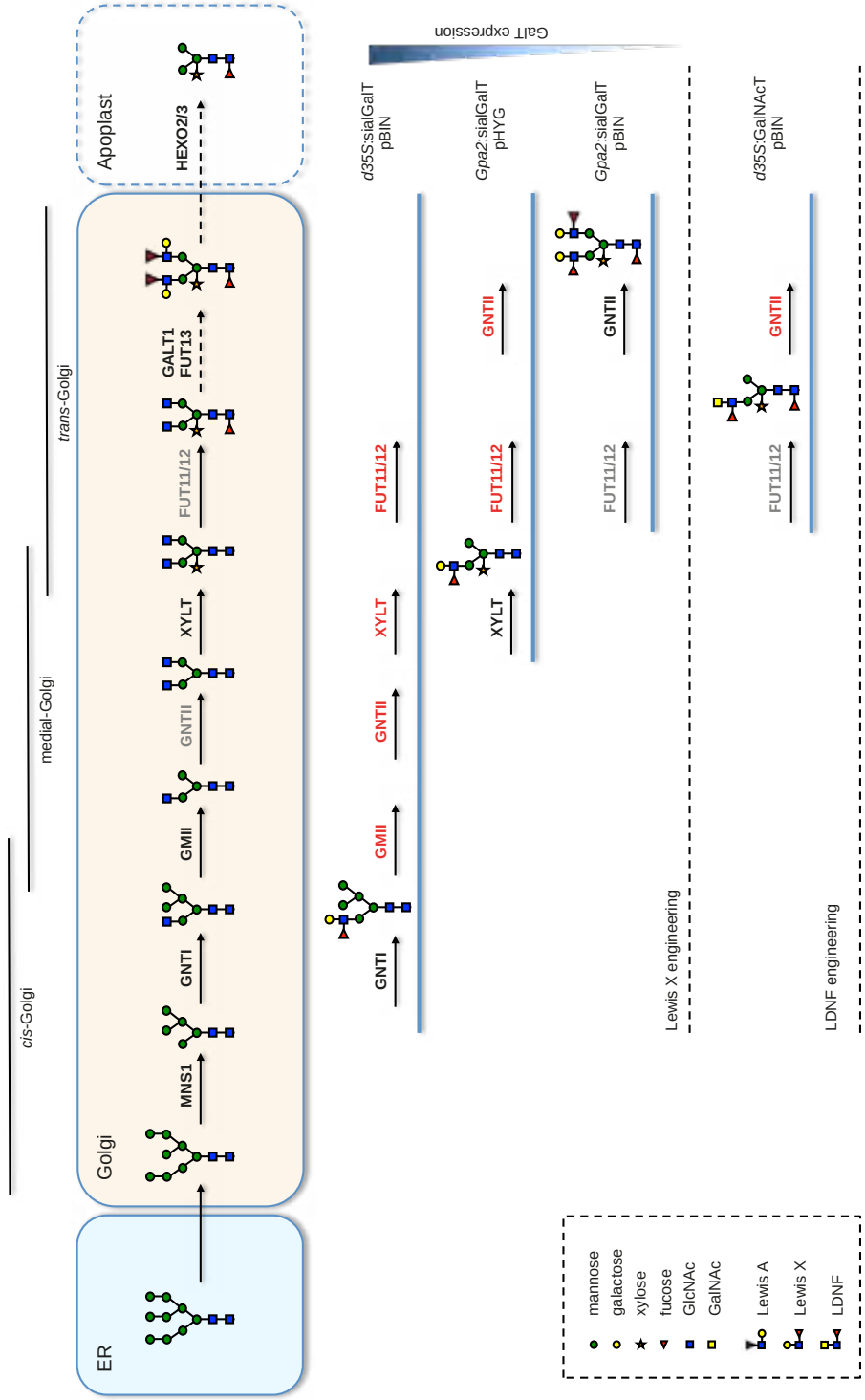

Figure 1 ◆ An overview of the successive N-glycan modifying steps in the plant Golgi-system. Underneath we provide novel insights on the putative localization of plant endogenous GnTII based on the transient engineering of helminth N-glycans. Enzymes are indicated in red when the activity of the enzyme is blocked by the respective engineering approach. MNSI: Golgi-α-mannosidase I; GnTI: *N*-acetylglucosaminyltransferase I; GMII: Golgi-α-mannosidase II; GnTII: *N*-acetylglucosaminyltransferase II; XYLT: β1,2-xylosyltransferase; FUT11/12: core α1,3-fucosyltransferase; FUT13: α1,4-fucosyltransferase; GALT1: α 1,3-galactosyltransferase; HEXO: β-*N*-acetylhexosaminidase.

demonstrated by the introduction of the entire mammalian sialic acid pathway in *N. benthamiana* using transient expression [36]. The speed of the transient expression system also allows to pinpoint bottlenecks of certain glyco-engineering approaches, which can then be solved quickly.

While engineering Lewis X and LDN(-F) in a transient fashion in wild-type plants we also obtained more insights on the plant endogenous N-glycosylation pathways. Several pathways for N-glycosylation in plants have been suggested, but the exact localization of certain plant endogenous enzymes, like β-*N*-acetylglucosaminyltransferase II (GnTII), is still unclear [37, 38]. In the situation described above, zebrafish GalT leaks into the medial-Golgi compartment where it inhibits the activity of α-mannosidase II (GMII in Figure 1). Furthermore, the addition of β1,2-xylose and core α1,3-fucose are blocked completely with this engineering strategy. By placing GalT under the control of a weak constitutive promoter (*Gpa2*:sialGalT) we were able to control the expression level of GalT to such an extent that we obtained homogeneous non-hybrid Lewis X-type N-glycans (Chapter 5). With two engineering strategies (*Gpa2*:sialGalT in either pBIN or pHYG) we obtained full activity of GMII as the additional mannoses on the α1,6-mannosyl branch were trimmed down completely. As all these non-hybrid N-glycans also carried β1,2-xylose it is most likely that β1,2-xylosyltransferase (XylT) acts downstream of GMII and is probably not directly inhibited by the presence of zebrafish GalT. However, our engineered N-glycans still lacked core α1,3-fucose and a second terminal *N*-acetylglucosamine (GlcNAc) when using the pHYG-based expression of the *Gpa2*:sialGalT cassette. These results suggest that GnTII acts later along the secretory pathway and supports a novel N-glycosylation pathway postulated by Kajiura and co-workers [37]. In this pathway GnTII acts on N-glycans that have already been modified by GMII and XylT, which positions GnTII to the end of the medial-Golgi or *trans*-Golgi compartment. Yet, the early addition of galactose or *N*-acetylgalactosamine (GalNAc) on the α1,3-mannosyl branch seems to block the activity of plant endogenous GnTII. When using pBIN-based expression of the *Gpa2*:sialGalT cassette we lowered the expression of GalT even more, which allowed the synthesis of diantennary N-glycans carrying two Lewis X motifs and core α1,3-fucose. The activity of α1,3-fucosyltransferase (FucT11/12), on the other hand, is probably directly inhibited by the presence of zebrafish GalT as core fucosylation does occur efficiently when the α1,3-mannosyl branch carries GalNAc instead of galactose. Our zebrafish GalT seems to interfere with quite some endogenous glycosyltransferases, but there are subtle differences when compared to human GalT. For instance, core α1,3-fucosylation was not strongly inhibited by transient over-expression of *trans*-Golgi targeted human GalT in wild-type *N. benthamiana* plants [35].

Transient expression has allowed us to efficiently engineer non-hybrid Lewis X-type N-glycans and brings us one step closer to synthesize diantennary N-glycans carrying two Lewis X structures. Remarkably, the plant protein synthesis machinery is able to produce

large quantities of recombinant helminth glycoproteins carrying helminth N-glycans. We are able to isolate up to 0.5 mg of omega-1 from a single agroinfiltrated plant and demonstrate that the N-glycans are up to 95% homogeneous and carry a single Lewis X motif. Furthermore, engineering of Lewis X as well as LDN(-F) demonstrates that the activity of endogenous GnTII is the major bottleneck for synthesizing diantennary N-glycans with helminth-like glycan structures. Re-localizing GnTII to earlier Golgi compartments or co-expression of a GnTII of animal origin might therefore enable the synthesis of N-glycans carrying two Lewis X or LDN(-F) structures in wild-type plants in the future.

N-glycan composition is strongly influenced by protein intrinsic properties

More detailed knowledge on how the plant N-glycosylation machinery operates is still required. This is further supported by the fact that N-glycan composition can strongly differ between recombinant proteins, even when the expression strategy is identical. We have expressed a variety of recombinant proteins in *N. benthamiana* and we have observed strong differences in N-glycan composition of these proteins. Recently, we have published that the N-glycan composition of monoclonal antibodies is strongly influenced by the antibody isotype [24]. In this study we expressed three monoclonal antibodies on either an IgG1 or IgA1 backbone and compared their expression profile and N-glycan composition. IgG1-based antibodies carried typical plant complex N-glycans with terminal GlcNAc residues, β1,2-xylose and core α1,3-fucose ($GnGnXF^3$). In contrast, the majority of the N-glycans found on IgA1-based antibodies lacked one terminal GlcNAc residue and core α1,3-fucose (GnMX or MGnX). The lack of core α1,3-fucose was also observed for the N-glycans of IL-22 (Chapter 4) and chicken ovalbumin (unpublished data). In the case of antibodies, the lack of core fucosylation might arise from differences in cellular localization as it is reported that the IgA tailpiece contains a cryptic vacuolar sorting signal [39, 40]. However, we also demonstrated that IgA isolated from the apoplast also lacked core α1,3-fucose [24]. Similarly, IL-22 isolated from the apoplast hardly contained core fucosylated N-glycans.

A more plausible explanation is that protein intrinsic properties have an influence on N-glycan composition. Petrescu and co-workers analyzed the protein environment of N-glycosylation sites and demonstrated that many N-glycan sites are poorly accessible [41]. As a result, N-glycans lacking one or more sugar residues are found, because the core of a N-glycan cannot always be reached by core altering glycosyltransferases. This would also explain why less than half of the N-glycans of human serum IgA harbor core α1,6-fucose [42, 43], whereas 80-98% of human serum IgG is core-fucosylated [44]. Besides accessibility it could also be that specific amino acids surrounding the N-glycosylation site may interfere with efficient core fucosylation. We have previously suggested that

hydrophobic amino acids within the N-X-S/T N-glycosylation signal might interfere with core altering enzymes as we found the amino acids leucine and valine on position X of the N-glycosylation signals in IgA and ovalbumin, but not in IgG [24]. More recently, we also identified the amino acid phenylalanine in one of the N-glycosylation sites of IL-22, which may explain the lack of core α1,3-fucose on this cytokine (Chapter 4).

Besides differences in core fucosylation, we also found differences in terminal sugar residues between IgG and IgA. Accessibility of N-glycans is probably one of the major properties that influence their composition. For instance, the N-glycans of the IgG constant domains are less exposed as they are within the dimer interface of two γ heavy chains [45]. For IgA antibodies the N-glycans are overall more exposed than the N-glycans of IgG [46] and are therefore more accessible for processing by glycosyltransferases. This can explain why the N-glycans on human serum IgA have increased levels of sialylation and galactosylation compared to the N-glycans of serum IgG [43]. Yet, efficient galactosylation of the N-glycans of IgG can be achieved upon engineering in plants [35, 47]. On the other hand, sialylation of the Fcγ constant domain seems not to be efficient. Co-expression of an EPO-Fc fusion protein in plants together with all the enzymes required for the synthesis of sialylated N-glycans results in sialylated N-glycans on EPO, but hardly on the N-glycans of the Fc-fragment [48]. Further engineering strategies to synthesize bi-secting and branched N-glycans have been successful for human EPO and transferrin, but again not for IgG antibodies [49]. Accessibility of the N-glycans of IgG can therefore to a large extent explain differences in N-glycan composition between IgG and IgA. However, overall higher accessibility of IgA N-glycans cannot explain why plant-produced IgA antibodies lack one terminal GlcNAc residue.

The lack of terminal GlcNAc residues on the N-glycans of plant-produced IgA can be due to differences in substrate specificity of N-glycan modifying enzymes. For instance, the addition of one of the terminal GlcNAc residues could be inefficient. In this case, GlcNAc is most likely absent from the α1,6-branched mannose. Kajiura and co-workers showed that the terminal GlcNAc on the α1,3-branched mannose is required for the activity of β1,2-xylosyltransferase [37] and all the N-glycans of IgA carry β1,2-xylose. Protein intrinsic properties of IgA could therefore influence the efficiency by which GnTII transfers terminal GlcNAc to the α1,6-branch of its N-glycans. Alternatively, removal of terminal GlcNAc residues by β-hexosaminidases could also explain the lack of one terminal GlcNAc residue. The N-glycans of IgA could be modified by enzymes homologues to *Arabidopsis* HEXO-1 or HEXO-2/HEXO-3 depending on whether IgA resides within the vacuole or apoplast [50]. However, in both cases substrate specificity would play a role, as β-hexosaminidases are known to remove both terminal GlcNAc residues.

Substrate specificity of β-hexosaminidases was again illustrated upon production of IL-22 and the *S. mansoni* secreted egg antigens omega-1 and kappa-5. All three proteins were expressed using the same expression strategy and all were purified from the apoplastic space. However, even though they were isolated from the same subcellular compartment they all carried different types of N-glycans. The majority of the N-glycans on omega-1 were predominantly of the paucimannosidic type ($MMXF^3$) whereas the majority of the N-glycans on kappa-5 did carry terminal GlcNAc ($GnGnXF^3$). This indicates that the N-glycans of omega-1 are sensitive to β-hexosaminidase activity, but not the N-glycans of kappa-5. IL-22 on the other hand is a more peculiar example. A large proportion of the N-glycans found on IL-22 are of the $GnGnF^6$-type upon expression in ΔXT/FT plants together with mouse fucosyltransferase 8. Yet, significant proportions of $GnMF^6$ and MMF^6 type N-glycans were also found. This would indicate that there is N-glycan site-specific sensitivity towards β-hexosaminidase activity among the N-glycans of IL-22. As both Asn54 and Asn68 of IL-22 carry a surface exposed N-glycan it is most likely that the N-glycan on Asn97, which is less surface exposed, is not affected by β-hexosaminidases. In contrast, the N-glycans of omega-1 are required for internalization by dendritic cells and are therefore likely to be surface exposed. This could then explain why omega-1 carries predominantly paucimannosidic N-glycans. Conclusions on the reduced sensitivity of kappa-5 towards β-hexosaminidase activity cannot be drawn as detailed structural and functional information on this protein is still lacking.

Another interesting observation made for plant-produced IL-22 was the presence of high proportions (~50%) of Lewis A carrying N-glycans when isolated from wild-type plants. Lewis A harbouring glycoproteins are widely distributed among plant species and mainly localize at the surface of the plant cell [51, 52]. The synthesis of Lewis A in plants is still poorly understood and the factors that determine whether a N-glycan is extended with Lewis A remain largely unknown. Lewis A was previously detected on a murine monoclonal antibody expressed in *Nicotiana tabacum* and on human erythropoietin expressed in either *Nicotiana benthamiana* or moss [48, 53, 54]. However, the presence of Lewis A on the majority of N-glycans of a heterologously produced glycoprotein is to our knowledge a rare observation. In addition, the N-glycans of omega-1 and kappa-5, which are known for their extended complex N-glycans with either Lewis X or LDN(-F), did hardly carry the Lewis A structure. We did, however, show that the presence of Lewis A on the N-glycans of IL-22 is to a large extent dependent on the presence of a N-glycan on Asn54. The N-glycan on Asn54 therefore most likely carries the majority of Lewis A. Furthermore, the presence of a N-glycan on Asn54 also influenced the addition of α1,3-fucose to the core of another N-glycan. Apparently the position and presence of a N-glycans can affect the composition of other N-glycans.

Altogether, our work describes a variety of glycoproteins with remarkable differences in N-glycan composition. These differences are partly explained by differences in cellular

localization. However, the majority can only be explained by intrinsic properties of the different glycoproteins. Characteristics that influence N-glycan composition can be accessibility of the N-glycan, amino acids surrounding the N-glycosylation site or structural features that influence substrate specificity of N-glycan modifying enzymes. On top of that, we show that N-glycans are able to influence each other's composition. Further knowledge on how protein intrinsic properties influence N-glycan composition can further aid in the synthesis of tailored N-glycans.

Within the second half of this chapter the focus will be on the immunological chapters in this thesis. For many inflammatory disorders therapy most likely relies on personalized medicine in the future. Each patient has unique genetic variations that predispose him or her to develop certain inflammatory disorders. Therefore more in-depth knowledge on the diagnosis and underlying cause within patients is required to develop personalized medicine. However, knowledge on why certain therapeutic approaches have not been successful in the past might also contribute to the development of novel approaches. For this reason, we dedicated two chapters in this thesis to the biological activity of IL-10, a cytokine with great therapeutic potential. We used bone marrow-derived cells to investigate IL-10-mediated signalling to possibly obtain clues on why IL-10 therapy has not been as effective as previously anticipated. In the following section we will discuss our findings on the contribution of IL-10R2 to cytokine signalling, but also how IL-10-mediated responses might be negatively influenced by the cytokine GM-CSF.

Effectiveness of IL-10 therapy

IL-10 is an anti-inflammatory cytokine that suppresses the activity of both antigen presenting cells and lymphocytes and thereby plays a crucial role in establishing immune homeostasis. For this reason IL-10 has long been considered as a promising therapy for several inflammatory disorders [55]. Systemic administration of recombinant human IL-10 produced in *Escherichia coli* (trade name Tenovil) has been investigated in phase II clinical trials to treat patients with Crohn's disease. In a first trial, IL-10 treatment was shown to be safe and well tolerated [56], but patients seem to respond differently to IL-10 treatment [57]. Overall, IL-10 therapy does not seem to provide treatment for Crohn's disease patients as there is no significant clinical improvement when compared to placebo control patients. Furthermore, the number of patients withdrawing from trials due to

adverse side effects was higher for IL-10 treated patients [58]. These adverse side effects are considered to be caused by IL-10's immunostimulatory properties (proliferative effects on B cells and mast cells) upon systemic administration. To circumvent systemic administration of IL-10, *Lactococcus lactis* was engineered to secrete human IL-10 and used as an oral delivery system [59]. This local delivery system for IL-10 was shown to be successful in two mouse models of intestinal inflammation [59] and was proven to be safe in a small phase I human trial [60]. However, in 2009 a phase II human trial with engineered *L. lactis* in patients with ulcerative colitis was completed, but no significant difference in mucosal healing versus a placebo control was observed (ActoGeniX press release). Alternative approaches for local delivery of IL-10 include gene therapy using replication-deficient adenoviral vectors or gelatin microspheres containing recombinant IL-10. Both methods have shown to be successful in murine models of intestinal inflammation [61-63]. However, future research has to address whether local delivery of IL-10 is indeed a promising therapeutic approach.

Local delivery of recombinant IL-10 ensures that an appropriate dose of active IL-10 is obtained at the site of inflammation, but the question remains whether IL-10 is provided in the correct form. IL-10 is believed to be active as a non-covalently bound homodimer [64]. However, there is no expression platform that is able to produce IL-10 efficiently in its dimeric form. Heterologous expression of IL-10 in *E. coli* leads to inclusion bodies and requires solubilisation and chemical refolding to obtain a monomeric molecule [65]. When expressed in *L. lactis* IL-10 is secreted in the culture medium as a monomer [59]. We have demonstrated in chapter 3 that human IL-10 forms large aggregates upon expression in *Nicotiana benthamiana* plants [27]. Nevertheless, IL-10 from all these expression platforms is biologically active.

In chapter 3 we also expressed a stable monomeric form of IL-10. Stable monomeric IL-10 was not able to suppress LPS-induced TNF-α expression in a macrophage cell line, whereas forced dimerization of monomeric IL-10 restored its ability to suppress TNF-α expression. This also indicates that IL-10 is indeed active as a dimer. However, stable monomeric IL-10 was shown to be able to induce proliferation in a B cell line transfected with either human or mouse IL-10R1 [66]. We therefore questioned whether cell lines are still a reliable model system to study cellular responses mediated by IL-10. Many cell lines have been cultured for a long time in different labs under different culturing conditions. Meanwhile, these cell lines might have acquired (epi)genetic changes [67] and have lost the ability to respond as *in vivo* cells would. Therefore we have set-up biological activity assays for IL-10 using bone marrow-derived cells and used them to re-evaluate IL-10-mediated responses.

Novel insights into the biology of IL-10R2-mediated responses

In this thesis we have investigated the IL-10 cytokine family members IL-10 and IL-22, which both use IL-10R2 for their signalling. IL-10R2 forms a heterodimeric receptor complex with high affinity receptors, like IL-10R1 or IL-22R1. Engagement of these receptor complexes activates the intracellular kinases Jak1 and Tyk2 [68-70], but to date the exact role of IL-10R2 and IL-10R2-associated signalling via Tyk2 remains unclear. In chapter 6 we investigated the involvement of IL-10R2 and Tyk2 in IL-10-mediated responses using dendritic cells, macrophages and mast cells that were differentiated from mouse bone marrow. We were able to show that IL-10-mediated responses depend on the presence of both IL-10R1 and IL-10R2, but IL-10R2-associated Tyk2 kinase only played a limited role. Yet, we do show that Tyk2 contributes to the amplitude and kinetics of IL-10-mediated responses. Tyk2 was required for optimal phosphorylation of the transcription factor STAT3 at tyrosine residue 705 ($STAT3^{Y705}$) and subsequent upregulation of SOCS3 gene expression. Furthermore, lack of Tyk2 reduced the ability of macrophages to quickly suppress TNF-α expression upon LPS stimulation. Therefore, IL-10R2-mediated signalling via Tyk2 can be crucial to obtain optimal signalling, but its contribution to activity was shown to be cell type dependent.

For IL-22 it has been reported that binding to IL-10R2 is crucial for its activity. Logsdon and co-workers revealed that the N-glycan on Asn54 of IL-22, and in particular the core α1,6-fucose residue on this N-glycan, is required for binding to IL-10R2 [71]. In chapter 4 we described the plant-based expression of IL-22 with engineered N-glycans harbouring human-like α1,6-fucose residue on its N-glycans. But in contrast to the work of Logsdon and co-workers we could not confirm that the core α1,6-fucose on the N-glycan of Asn54 plays a role in the activity of IL-22. Instead we showed that the amino acid that is used to mutate asparagine residue 54 plays a larger role in IL-22 activity. We do not dismiss the possibility that core α1,6-fucose may contribute to the binding of IL-22 to IL-10R2. Core α1,6-fucose-mediated binding to IL-10R2 might be required for some responses of IL-22 and as we demonstrated for IL-10, this might even be cell type dependent.

The cells used in the study by Logsdon and co-workers were stably transfected with human IL-10R2 and a chimeric receptor bearing the extracellular domain of IL-22R1 and the intracellular domain of IFN-γR1 [71]. Activity of IL-22 was then measured by transient transfection with a luciferase reporter gene. The use of hybrid IL-10 receptors harbouring the intracellular domains of their respective IFN-γR's has also been used to investigate IL-10 signalling [66, 72, 73]. Unfortunately, this might not reflect the *in vivo* situation. In chapter 6 we also discuss that the mechanism of receptor activation is likely different between the receptor complexes of IFN-γ and IL-10. Krause and co-workers demonstrated that binding of IFN-γ induces rearrangement of the intracellular domains of both IFN-γR1 and IFN-γR2 thereby allowing more space for downstream signalling components to bind [74]. In contrast, there are no major structural changes of the IL-10 receptor complex

upon binding of IL-10 [75]. For this reason we believe that cell-based assays using hybrid IL-10/IL-22 receptors harbouring the intracellular domains of their respective IFN-γR's are not a reliable model to investigate IL-10 signalling.

Further investigation of the IL-10 signalling complex revealed that both the extracellular and intracellular domain of IL-10R2 are required by IL-10 to induce STAT3 activation in transfected CHO cells (Chapter 6). Interestingly, we also demonstrated that both the extracellular and intracellular domain of IL-10R2 mediate conformational changes of the extracellular domain of IL-10R1 that reduce cellular binding of IL-10. We therefore reason that interactions between IL-10R1 and IL-10R2 (both intracellular and extracellular) are crucial to initiate IL-10-mediated signalling. Yet, the mechanism by which the downstream kinases Jak1 and Tyk2 are activated remains to be elucidated.

Remarkably, Syto and co-workers demonstrated that IL-10 is dimeric at concentrations above 3 µg/ml (at neutral pH and 4°C) [64], which is several orders of magnitude higher as physiological concentrations. When IL-10 would be monomeric under physiological conditions it needs to dimerize on the cell surface. This could be a potential mechanism by which IL-10 assembles a signalling complex that consists of multiple IL-10R subunits and induces signalling. Stable monomeric IL-10 is able to assemble the complete IL-10 receptor complex when IL-10R1 expression is high upon transfection [66], but is less efficient under natural conditions when IL-10R expression is much lower (Chapter 6). Crystallization studies of IL-10 with soluble (s)IL-10R1 revealed that a complex is formed consisting of 2 IL-10 dimers and 4 IL-10R1 chains [76]. On the contrary, monomeric IL-10 forms a complex with sIL-10R1 in a 1:1 ratio [66]. This would indicate that the signalling complex formed by monomeric IL-10 differs from the receptor complex with dimeric IL-10. In chapter 3 and 6 we have shown that stable monomeric IL-10 has impaired activity when compared to recombinant IL-10 from *E.* coli. However, forced dimerization of monomeric IL-10 restored its anti-inflammatory properties (Chapter 3). This again indicates that dimerization of IL-10 is required for the assembly of a signalling complex.

Mechanisms by which GM-CSF might influence IL-10 activity

In chapter 6 we describe that dendritic cells respond differently to IL-10 when compared to macrophages. Dendritic cells treated with IL-10 were not able to rapidly suppress TNF-α expression upon LPS stimulation, whereas IL-10 inhibited TNF-α expression by 80% in macrophages after 2 hours of stimulation. This correlated with the impaired ability of IL-10 to upregulate SOCS3 expression in dendritic cells. Qasimi and co-workers previously described that SOCS3 is required by IL-10 to suppress TNF-α expression at early time points of stimulation [77]. This reduction in IL-10-induced SOCS3 expression can therefore explain the differential response of dendritic cells and macrophages to IL-10. In chapter 7 we continued to investigate the underlying mechanism that explains the

differential response of dendritic cells to IL-10. We demonstrated that GM-CSF, the cytokine used to differentiate dendritic cells, is the key factor that negatively influences IL-10-mediated responses. GM-CSF treatment of macrophages reduces their ability to suppress TNF-α expression at early time points. Vice versa, depletion of GM-CSF from dendritic cells partly restores early suppression of TNF-α expression upon LPS stimulation.

When we investigated STAT3 activation in dendritic cells and macrophages we only found subtle differences in relative amounts of phosphorylated $STAT3^{Y705}$. However, we did observe that IL-10 was not able to induce significantly higher levels of phosphorylated STAT3 at serine 727 ($STAT3^{S727}$) in dendritic cells when compared to untreated cells. On the other hand, IL-10 induced $STAT3^{S727}$ phosphorylation in macrophages in a dose-dependent manner. Phosphorylation of $STAT3^{S727}$ could therefore be required for optimal induction of SOCS3 expression by IL-10. Alternatively, there might be a role for STAT5 in inhibiting IL-10-mediated responses in dendritic cells. In chapter 6 we describe that STAT5 is constitutively phosphorylated at tyrosine residue 694 ($STAT5^{Y694}$) and this was not observed in macrophages. Yang and co-workers revealed that STAT5 was shown to directly suppress STAT3-induced IL-17 expression in Th17 cells without influencing STAT3 phosphorylation [78]. However, the same study showed that STAT5 did not influence SOCS3 expression in Th17 cells. Still, Yang and co-workers revealed that STAT3 and STAT5 have opposing roles in regulating the transcription of at least 300 genes. Constitutive active STAT5 could therefore contribute to the differential response of dendritic cells to IL-10 (Figure 2a).

STAT5 could also contribute to the suppression of IL-10-mediated signalling by upregulating the expression of cytokine-inducible SH2-containing protein/suppressor of cytokine signalling (CIS/SOCS) molecules (Figure 2a). GM-CSF induces the expression of CIS1, SOCS1, SOCS2 and SOCS3 [79-81] of which SOCS1 has been reported to negatively influence IL-10 signalling [82]. Upregulated levels of CIS/SOCS molecules could therefore explain why IL-10-induced transcription of SOCS3 is largely blocked in dendritic cells. However, relative induction of SOCS3 expression by IL-10 was hardly affected by overnight treatment of macrophages with GM-CSF or depletion of dendritic cells from GM-CSF (Chapter 7). This is in contrast to the difference in IL-10-induced SOCS3 expression between macrophages and dendritic cells. Furthermore, we also did not observe a difference in the phosphorylation of $STAT3^{Y705}$ and $STAT3^{S727}$ between regular macrophages or GM-CSF treated macrophages. Therefore, GM-CSF seems to negatively regulate early IL-10-mediated responses in macrophages independent from STAT3-induced SOCS3 expression.

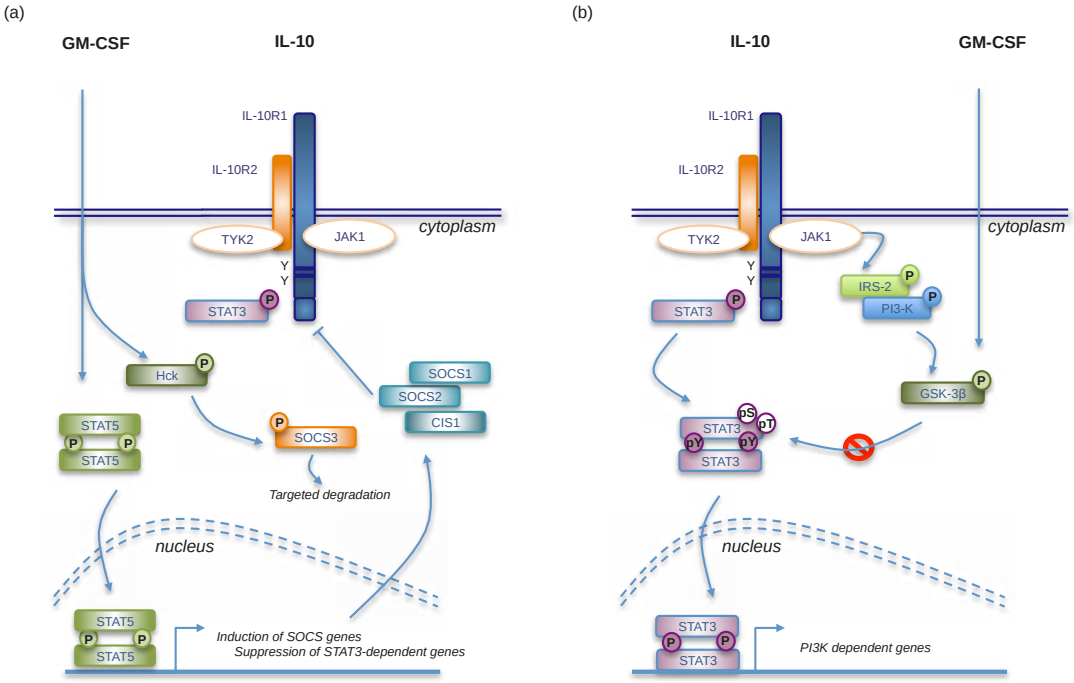

Figure 2 ◆ Mechanisms by which GM-CSF potentially influences IL-10-mediated responses. (a) A schematic overview of potential mechanisms by which GM-CSF can inhibit IL-10-mediated responses as described in the main text. (b) A schematic overview on how GM-CSF-mediated inactivation of GSK-3β can inhibit IL-10-induced signalling.

As SOCS3 is a key player in mediating IL-10's anti-inflammatory responses at early time points [77] it might also be possible that GM-CSF not only regulates SOCS3 expression, but also influences the activity of SOCS3. Tyrosine phosphorylation of SOCS3 at residues Y204 and Y221 has been shown to accelerate SOCS3 degradation [83]. The mechanism by which cytokines induce SOCS3 phosphorylation is not well understood, but a role for Janus kinases and Src kinases has been suggested [84]. GM-CSF activates the Janus kinase Jak2 and Src kinase hematopoietic cell kinase (Hck) [85] and both might contribute to the phosphorylation and subsequent degradation of SOCS3. Strikingly, Hck activation is also correlated with increased TNF-α expression in a macrophage cell line upon LPS stimulation [86]. Enhanced Hck activity could therefore also explain why GM-CSF differentiated dendritic cells and GM-CSF treated macrophages secrete significantly higher levels of TNF-α (Chapter 6 and 7).

Inhibition of early IL-10-mediated responses by GM-CSF might also be independent of altered expression or activity of CIS/SOCS molecules. In chapter 7 we describe that both GM-CSF differentiated dendritic cells and GM-CSF treated macrophages have high levels of phosphorylated GSK-3β at serine residue 9 (GSK-3β^{S9}). GSK-3β is a signalling component downstream of the PI3K/Akt pathway and GSK-3β^{S9} phosphorylation leads to

its inactivation. Interestingly, Waitkus and co-workers recently reported on a novel mechanism of activation of STAT3, which was mediated by GSK-3α/β [87]. GSK-3α/β was shown to directly phosphorylate STAT3 at the residues S727 and T714 (Figure 2b). The requirement of GSK-3α/β in IL-10-induced STAT3 activation is therefore of great interest as we have shown that GM-CSF strongly inhibits GSK-3β by phosphorylation of serine residue 9. Furthermore, GSK-3β was shown to selectively modulate IL-10-induced gene expression. GSK-3β was required for the upregulation of IL-10-induced genes that are dependent on the activation of the PI3K pathway, like autotaxin and caspase 5 [88]. In contrast, SOCS3 expression was shown to be independent of the activation of PI3K/GSK-3β. This coincides with our observation that IL-10-induced SOCS3 expression is not affected in GM-CSF treated macrophages, which have high levels of phosphorylated GSK-3β^{S9}.

Over the last couple of years GM-CSF has been identified as a key contributor to the development of chronic inflammation in animal models of intestinal inflammation, multiple sclerosis and rheumatoid arthritis [89-91]. Taking together the key role of GM-CSF in the development of chronic inflammation with the results obtained in this thesis might explain why IL-10 therapy has not been as effective as previously anticipated. Our study demonstrates that the pro-inflammatory cytokine GM-CSF is able to negatively regulate IL-10-mediated responses in macrophages and dendritic cells. However, future research has to elucidate the exact mechanism on how GM-CSF and IL-10 signalling pathways are integrated and result in impaired cellular responses towards IL-10. Ultimately this knowledge could provide us with new therapeutic strategies to treat inflammatory disorders.

References

1. Walsh G (2014) Biopharmaceutical benchmarks 2014. Nature Biotechnology 32: 992-1000.
2. Jefferis R (2009) Recombinant antibody therapeutics: the impact of glycosylation on mechanisms of action. Trends in Pharmacological Sciences 30: 356-362.
3. Grabowski GA, Barton NW, Pastores G, Dambrosia JM, Banerjee TK, et al. (1995) Enzyme therapy in type 1 Gaucher disease: comparative efficacy of mannose-terminated glucocerebrosidase from natural and recombinant sources. Annals of Internal Medicine 122: 33-39.
4. Burrow TA and Grabowski GA (2011) Velaglucerase alfa in the treatment of Gaucher disease type 1. Clinical Investigation (London) 1: 285-293.
5. Shaaltiel Y, Bartfeld D, Hashmueli S, Baum G, Brill-Almon E, et al. (2007) Production of glucocerebrosidase with terminal mannose glycans for enzyme replacement therapy of Gaucher's disease using a plant cell system. Plant Biotechnology Journal 5: 579-590.
6. Bethencourt V (2009) Virus stalls Genzyme plant. Nature Biotechnology 27: 681-681.
7. Daniell H, Streatfield SJ and Wycoff K (2001) Medical molecular farming: production of antibodies, biopharmaceuticals and edible vaccines in plants. Trends in Plant Science 6: 219-226.
8. Giddings G, Allison G, Brooks D and Carter A (2000) Transgenic plants as factories for biopharmaceuticals. Nature Biotechnology 18: 1151-1155.
9. Goldstein DA and Thomas JA (2004) Biopharmaceuticals derived from genetically modified plants. QJM : monthly journal of the Association of Physicians 97: 705-716.
10. Warzecha H (2008) Biopharmaceuticals from plants: a multitude of options for posttranslational modifications. Biotechnology & Genetic Engineering Reviews 25: 315-330.
11. Stoger E, Fischer R, Moloney M and Ma JK (2014) Plant molecular pharming for the treatment of chronic and infectious diseases. Annual Reviews Plant Biology 65: 743-768.
12. Gomord V and Faye L (2004) Posttranslational modification of therapeutic proteins in plants. Current Opinion Plant Biology 7: 171-181.
13. Webster DE and Thomas MC (2012) Post-translational modification of plant-made foreign proteins; glycosylation and beyond. Biotechnology Advances 30: 410-418.
14. Xu J, Okada S, Tan L, Goodrum KJ, Kopchick JJ, et al. (2010) Human growth hormone expressed in tobacco cells as an arabinogalactan-protein fusion glycoprotein has a prolonged serum life. Transgenic Research 19: 849-867.

15. Xu J, Tan L, Goodrum KJ and Kieliszewski MJ (2007) High-yields and extended serum half-life of human interferon alpha2b expressed in tobacco cells as arabinogalactan-protein fusions. Biotechnology & Bioengineering 97: 997-1008.

16. Hennig A, Reinders Y, Giritsch A, Reinders J and Warzecha H (2008) Assessment of Different Expression Strategies for the Production of a Recombinant Lipoprotein Vaccine in Plants.The Open Biotechnology Journal 2: 51-55.

17. Zhou F, Badillo-Corona JA, Karcher D, Gonzalez-Rabade N, Piepenburg K, et al. (2008) High-level expression of human immunodeficiency virus antigens from the tobacco and tomato plastid genomes. Plant Biotechnology Journal 6: 897-913.

18. Bosch D and Schots A (2010) Plant glycans: friend or foe in vaccine development? Expert Reviews Vaccines 9: 835-842.

19. Showalter AM (2001) Arabinogalactan-proteins: structure, expression and function. Cellular and Molecular Life Sciences 58: 1399-1417.

20. De Muynck B, Navarre C and Boutry M (2010) Production of antibodies in plants: status after twenty years. Plant Biotechnology Journal 8: 529-563.

21. Goulet C, Khalf M, Sainsbury F, D'Aoust MA and Michaud D (2012) A protease activity-depleted environment for heterologous proteins migrating towards the leaf cell apoplast. Plant Biotechnology Journal 10: 83-94.

22. Lund P and Dunsmuir P (1992) A plant signal sequence enhances the secretion of bacterial ChiA in transgenic tobacco. Plant Mol Biol 18: 47-53.

23. Schaaf A, Tintelnot S, Baur A, Reski R, Gorr G, et al. (2005) Use of endogenous signal sequences for transient production and efficient secretion by moss (Physcomitrella patens) cells. BMC Biotechnology 5: 30.

24. Westerhof LB, Wilbers RH, van Raaij DR, Nguyen DL, Goverse A, et al. (2014) Monomeric IgA can be produced in planta as efficient as IgG, yet receives different N-glycans. Plant Biotechnology Journal 12(9):1333-1342.

25. van der Hoorn RA (2008) Plant proteases: from phenotypes to molecular mechanisms. Annual Reviews Plant Biology 59: 191-223.

26. Schouten A, Roosien J, van Engelen FA, de Jong GA, Borst-Vrenssen AW, et al. (1996) The C-terminal KDEL sequence increases the expression level of a single-chain antibody designed to be targeted to both the cytosol and the secretory pathway in transgenic tobacco. Plant Molecular Biology 30: 781-793.

27. Westerhof LB, Wilbers RHP, Roosien J, van de Velde J, Goverse A, et al. (2012) 3D Domain Swapping Causes Extensive Multimerisation of Human Interleukin-10 When Expressed In Planta. Plos One 7(10): e46460.

28. Redkiewicz P, Więsyk A, Góra-Sochacka A and Sirko A (2012) Transgenic tobacco plants as production platform for biologically active human interleukin 2 and its fusion with proteinase inhibitors. Plant Biotechnology Journal 10: 806-814.

29. Ruggiero F, Exposito JY, Bournat P, Gruber V, Perret S, et al. (2000) Triple helix assembly and processing of human collagen produced in transgenic tobacco plants. FEBS Letters 469: 132-136.

30. Vey M, Schafer W, Berghofer S, Klenk HD and Garten W (1994) Maturation of the trans-Golgi network protease furin: compartmentalization of propeptide removal, substrate cleavage, and COOH-terminal truncation. Journal of Cell Biology 127: 1829-1842.

31. Thomas G (2002) FURIN AT THE CUTTING EDGE: FROM PROTEIN TRAFFIC TO EMBRYOGENESIS AND DISEASE. Nature Reviews Molecular Cell Biology 3: 753-766.

32. Yang S, Levine H and Onuchic JN (2005) Protein oligomerization through domain swapping: role of inter-molecular interactions and protein concentration. Journal of Molecular Biology 352: 202-211.

33. Bosch D, Castilho A, Loos A, Schots A and Steinkellner H (2013) N-Glycosylation of Plant-produced Recombinant Proteins. Current Pharmaceutical Design 19: 5503-5512.

34. Rouwendal GJ, Florack DE, Hesselink T, Cordewener JH, Helsper JP, et al. (2009) Synthesis of Lewis X epitopes on plant N-glycans. Carbohydrate Research 344: 1487-1493.

35. Strasser R, Castilho A, Stadlmann J, Kunert R, Quendler H, et al. (2009) Improved virus neutralization by plant-produced anti-HIV antibodies with a homogeneous beta1,4-galactosylated N-glycan profile. Journal of Biological Chemistry 284: 20479-20485.

36. Castilho A, Strasser R, Stadlmann J, Grass J, Jez J, et al. (2010) In planta protein sialylation through overexpression of the respective mammalian pathway. Journal of Biological Chemistry 285: 15923-15930.

37. Kajiura H, Okamoto T, Misaki R, Matsuura Y and Fujiyama K (2012) Arabidopsis beta 1,2-xylosyltransferase: Substrate specificity and participation in the plant-specific N-glycosylation pathway. Journal of Bioscience & Bioengineering 113: 48-54.

38. Bencur P, Steinkellner H, Svoboda B, Mucha J, Strasser R, et al. (2005) Arabidopsis thaliana beta1,2-xylosyltransferase: an unusual glycosyltransferase with the potential to act at multiple stages of the plant N-glycosylation pathway. Biochemistry Journal 388: 515-525.

39. Frigerio L, Vine ND, Pedrazzini E, Hein MB, Wang F, et al. (2000) Assembly, secretion, and vacuolar delivery of a hybrid immunoglobulin in plants. Plant Physiology 123: 1483-1494.

40. Hadlington JL, Santoro A, Nuttall J, Denecke J, Ma JK, et al. (2003) The C-terminal extension of a hybrid immunoglobulin A/G heavy chain is responsible for its Golgi-mediated sorting to the vacuole. Molecular Biology of the Cell 14: 2592-2602.

41. Petrescu AJ, Milac AL, Petrescu SM, Dwek RA and Wormald MR (2004) Statistical analysis of the protein environment of N-glycosylation sites: implications for occupancy, structure, and folding. Glycobiology 14: 103-114.

42. Field MC, Amatayakul-Chantler S, Rademacher TW, Rudd PM and Dwek RA (1994) Structural analysis of the N-glycans from human immunoglobulin A1: comparison of normal human serum immunoglobulin A1 with that isolated from patients with rheumatoid arthritis. Biochemistry Journal 299 (Pt 1): 261-275.

43. Mattu TS, Pleass RJ, Willis AC, Kilian M, Wormald MR, et al. (1998) The glycosylation and structure of human serum IgA1, Fab, and Fc regions and the role of N-glycosylation on Fcalpha receptor interactions. Journal of Biological Chemistry 273: 2260-2272.

44. Pucic M, Knezevic A, Vidic J, Adamczyk B, Novokmet M, et al. (2011) High throughput isolation and glycosylation analysis of IgG-variability and heritability of the IgG glycome in three isolated human populations. Molecular & Cellular Proteomics 10: M111 010090.

45. Herr AB, Ballister ER and Bjorkman PJ (2003) Insights into IgA-mediated immune responses from the crystal structures of human FcalphaRI and its complex with IgA1-Fc. Nature 423: 614-620.

46. Yoo EM, Yu LJ, Wims LA, Goldberg D and Morrison SL (2010) Differences in N-glycan structures found on recombinant IgA1 and IgA2 produced in murine myeloma and CHO cell lines. MAbs 2: 320-334.

47. Castilho A, Bohorova N, Grass J, Bohorov O, Zeitlin L, et al. (2011) Rapid High Yield Production of Different Glycoforms of Ebola Virus Monoclonal Antibody. Plos One 6(10): e26040.

48. Castilho A, Neumann L, Gattinger P, Strasser R, Vorauer-Uhl K, et al. (2013) Generation of biologically active multi-sialylated recombinant human EPOFc in plants. Plos One 8(1): e54836.

49. Castilho A, Gattinger P, Grass J, Jez J, Pabst M, et al. (2011) N-glycosylation engineering of plants for the biosynthesis of glycoproteins with bisected and branched complex N-glycans. Glycobiology 21: 813-823.

50. Liebminger E, Veit C, Pabst M, Batoux M, Zipfel C, et al. (2011) beta-N-Acetylhexosaminidases HEXO1 and HEXO3 Are Responsible for the Formation of Paucimannosidic N-Glycans in Arabidopsis thaliana. Journal of Biological Chemistry 286: 10793-10802.

51. Fitchette-Laine AC, Gomord V, Cabanes M, Michalski JC, Saint Macary M, et al. (1997) N-glycans harboring the Lewis a epitope are expressed at the surface of plant cells. Plant Journal 12: 1411-1417.

52. Wilson IB, Zeleny R, Kolarich D, Staudacher E, Stroop CJ, et al. (2001) Analysis of Asn-linked glycans from vegetable foodstuffs: widespread occurrence of Lewis a, core alpha1,3-linked fucose and xylose substitutions. Glycobiology 11: 261-274.

53. Petruccelli S, Otegui MS, Lareu F, Tran Dinh O, Fitchette AC, et al. (2006) A KDEL-tagged monoclonal antibody is efficiently retained in the endoplasmic reticulum in leaves, but is both partially secreted and sorted to protein storage vacuoles in seeds. Plant Biotechnology Journal 4: 511-527.

54. Parsons J, Altmann F, Arrenberg CK, Koprivova A, Beike AK, et al. (2012) Moss-based production of asialo-erythropoietin devoid of Lewis A and other plant-typical carbohydrate determinants. Plant Biotechnology Journal 10: 851-861.

55. Asadullah K, Sterry W and Volk HD (2003) Interleukin-10 therapy--review of a new approach. Pharmacological Reviews 55: 241-269.

56. van Deventer SJ, Elson CO and Fedorak RN (1997) Multiple doses of intravenous interleukin 10 in steroid-refractory Crohn's disease. Crohn's Disease Study Group. Gastroenterology 113: 383-389.

57. Schreiber S, Fedorak RN, Nielsen OH, Wild G, Williams CN, et al. (2000) Safety and efficacy of recombinant human interleukin 10 in chronic active Crohn's disease. Crohn's Disease IL-10 Cooperative Study Group. Gastroenterology 119: 1461-1472.

58. Buruiana FE, Sola I and Alonso-Coello P (2010) Recombinant human interleukin 10 for induction of remission in Crohn's disease. Cochrane Database of Systematic Reviews: CD005109.

59. Steidler L, Hans W, Schotte L, Neirynck S, Obermeier F, et al. (2000) Treatment of murine colitis by Lactococcus lactis secreting interleukin-10. Science 289: 1352-1355.

60. Braat H, Rottiers P, Hommes DW, Huyghebaert N, Remaut E, et al. (2006) A phase I trial with transgenic bacteria expressing interleukin-10 in Crohn's disease. Clinical gastroenterology and hepatology : the official clinical practice journal of the American Gastroenterological Association 4: 754-759.

61. Lindsay JO, Ciesielski CJ, Scheinin T, Brennan FM and Hodgson HJ (2003) Local delivery of adenoviral vectors encoding murine interleukin 10 induces colonic interleukin 10 production and is therapeutic for murine colitis. Gut 52: 363-369.

62. Barbara G, Xing Z, Hogaboam CM, Gauldie J and Collins SM (2000) Interleukin 10 gene transfer prevents experimental colitis in rats. Gut 46: 344-349.

63. Nakase H, Okazaki K, Tabata Y, Ozeki M, Watanabe N, et al. (2002) New cytokine delivery system using gelatin microspheres containing interleukin-10 for experimental inflammatory bowel disease. Journal of Pharmacology & Experimental Therapeutics 301: 59-65.

64. Syto R, Murgolo NJ, Braswell EH, Mui P, Huang E, et al. (1998) Structural and biological stability of the human interleukin 10 homodimer. Biochemistry 37: 16943-16951.

65. Sun J, Li BA, Qi Y, Zhou JW, Zhu L, et al. (2007) [Cloning, expression and identification of human interleukin-10 gene]. Xi Bao Yu Fen Zi Mian Yi Xue Za Zhi 23: 220-222.

66. Josephson K, DiGiacomo R, Indelicato SR, Iyo AH, Nagabhushan TL, et al. (2000) Design and analysis of an engineered human interleukin-10 monomer. Journal of Biological Chemistry 275: 25054.

67. Masters JR and Stacey GN (2007) Changing medium and passaging cell lines. Nature Protocols 2: 2276-2284.

68. Lejeune D, Dumoutier L, Constantinescu S, Kruijer W, Schuringa JJ, et al. (2002) Interleukin-22 (IL-22) activates the JAK/STAT, ERK, JNK, and p38 MAP kinase pathways in a rat hepatoma cell line - Pathways that are shared with and distinct from IL-10. Journal of Biological Chemistry 277: 33676-33682.

69. Ho AS, Wei SH, Mui AL, Miyajima A and Moore KW (1995) Functional regions of the mouse interleukin-10 receptor cytoplasmic domain. Molecular and Cellular Biology 15: 5043-5053.

70. Finbloom DS and Winestock KD (1995) IL-10 induces the tyrosine phosphorylation of tyk2 and Jak1 and the differential assembly of STAT1 alpha and STAT3 complexes in human T cells and monocytes. Journal of Immunology 155: 1079-1090.

71. Logsdon NJ, Jones BC, Allman JC, Izotova L, Schwartz B, et al. (2004) The IL-10R2 binding hot spot on IL-22 is located on the n-terminal helix and is dependent on N-linked glycosylation. Journal of Molecular Biology 342: 503-514.

72. Ding Y, Qin L, Zamarin D, Kotenko SV, Pestka S, et al. (2001) Differential IL-10R1 expression plays a critical role in IL-10-mediated immune regulation. Journal of Immunology 167: 6884-6892.

73. Kotenko SV, Krause CD, Izotova LS, Pollack BP, Wu W, et al. (1997) Identification and functional characterization of a second chain of the interleukin-10 receptor complex. EMBO Journal 16: 5894-5903.

74. Krause CD, Mei E, Xie J, Jia Y, Bopp MA, et al. (2002) Seeing the light: preassembly and ligand-induced changes of the interferon gamma receptor complex in cells. Molecular & Cellular Proteomics 1: 805-815.

75. Krause CD, Mei EW, Mirochnitchenko O, Lavnikova N, Xie JX, et al. (2006) Interactions among the components of the interleukin-10 receptor complex. Biochemical & Biophysical Research Communications 340: 377-385.

76. Josephson K, Logsdon NJ and Walter MR (2001) Crystal structure of the IL-10/IL-10R1 complex reveals a shared receptor binding site. Immunity 15: 35-46.

77. Qasimi P, Ming-Lum A, Ghanipour A, Ong CJ, Cox ME, et al. (2006) Divergent mechanisms utilized by SOCS3 to mediate interleukin-10 inhibition of tumor necrosis factor alpha and nitric oxide production by macrophages. Journal of Biological Chemistry 281: 6316-6324.

78. Yang XP, Ghoreschi K, Steward-Tharp SM, Rodriguez-Canales J, Zhu J, et al. (2011) Opposing regulation of the locus encoding IL-17 through direct, reciprocal actions of STAT3 and STAT5. Nature Immunology 12: 247-254.

79. Kasper S, Kindler T, Sonnenschein S, Breitenbuecher F, Bohmer FD, et al. (2007) Cross-inhibition of interferon-induced signals by GM-CSF through a block in Stat1 activation. Journal of interferon & cytokine research : the official journal of the International Society for Interferon and Cytokine Research 27: 947-959.

80. Trengove MC and Ward AC (2013) SOCS proteins in development and disease. American Journal of Clinical and Experimental Immunology 2: 1-29.

81. Fujimoto M and Naka T (2003) Regulation of cytokine signaling by SOCS family molecules. Trends in Immunology 24: 659-666.

82. Ding Y, Chen D, Tarcsafalvi A, Su R, Qin L, et al. (2003) Suppressor of cytokine signaling 1 inhibits IL-10-mediated immune responses. Journal of Immunology 170: 1383-1391.

83. Haan S, Ferguson P, Sommer U, Hiremath M, McVicar DW, et al. (2003) Tyrosine phosphorylation disrupts elongin interaction and accelerates SOCS3 degradation. Journal of Biological Chemistry 278: 31972-31979.

84. Sommer U, Schmid C, Sobota RM, Lehmann U, Stevenson NJ, et al. (2005) Mechanisms of SOCS3 phosphorylation upon interleukin-6 stimulation. Contributions of Src- and receptor-tyrosine kinases. Journal of Biological Chemistry 280: 31478-31488.

85. Suh HS, Kim MO and Lee SC (2005) Inhibition of granulocyte-macrophage colony-stimulating factor signaling and microglial proliferation by anti-CD45RO: role of Hck tyrosine kinase and phosphatidylinositol 3-kinase/Akt. Journal of Immunology 174: 2712-2719.

86. English BK, Ihle JN, Myracle A and Yi T (1993) Hck tyrosine kinase activity modulates tumor necrosis factor production by murine macrophages. Journal of Experimental Medicine 178: 1017-1022.

87. Waitkus MS, Chandrasekharan UM, Willard B, Tee TL, Hsieh JK, et al. (2014) Signal integration and gene induction by a functionally distinct STAT3 phosphoform. Molecular and Cellular Biology 34: 1800-1811.

88. Antoniv TT and Ivashkiv LB (2011) Interleukin-10-induced gene expression and suppressive function are selectively modulated by the PI3K-Akt-GSK3 pathway. Immunology 132: 567-577.

89. Sonderegger I, Iezzi G, Maier R, Schmitz N, Kurrer M, et al. (2008) GM-CSF mediates autoimmunity by enhancing IL-6-dependent Th17 cell development and survival. Journal of Experimental Medicine 205: 2281-2294.

90. Griseri T, McKenzie BS, Schiering C and Powrie F (2012) Dysregulated hematopoietic stem and progenitor cell activity promotes interleukin-23-driven chronic intestinal inflammation. Immunity 37: 1116-1129.

91. Hamilton JA (2008) Colony-stimulating factors in inflammation and autoimmunity. Nature Reviews Immunology 8: 533-544.

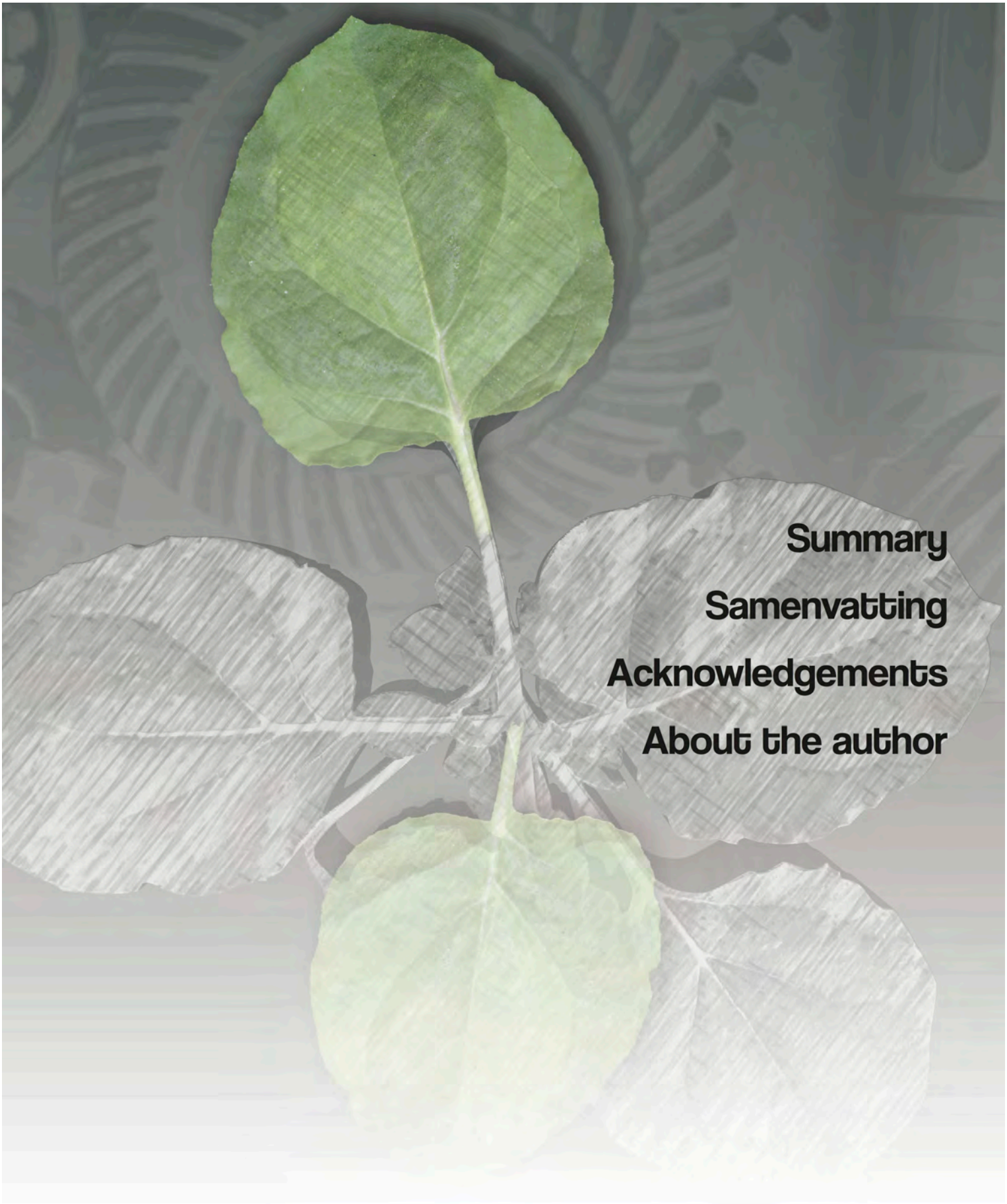

Summary

The incidence of inflammatory disorders in industrialized countries has dramatically increased over the last decennia, which is believed to result from a change in life-style. Treatment of these inflammatory disorders relies on the intervention in immune responses thereby restoring homeostasis. For now, many inflammatory disorders are treated with broad-acting immunosuppressive drugs or monoclonal antibodies that specifically target pro-inflammatory molecules of the immune system. An alternative therapeutic approach would be to use immunomodulatory proteins that are naturally involved in re-establishing immune homeostasis. This thesis describes the plant-based expression of a variety of immunomodulatory cytokines that may be used as biopharmaceutical proteins in the future. Furthermore, this thesis contains a pioneering chapter on the plant-based expression of immunomodulatory helminth-secreted glycoproteins. Additionally, we put some emphasis on the biological activity of the cytokine interleukin-10 to elucidate why IL-10 is not as effective in the clinic as previously anticipated.

In Chapter 2 we describe the transient expression of the immunoregulatory cytokine human transforming growth factor β1 (TGF-β1) in *Nicotiana benthamiana* leaves. TGF-β1 plays a key role in the differentiation of regulatory T cells (Tregs) and might be used to restore immune homeostasis in patients suffering from inflammatory disorders. The homologous isoform TGF-β3 has been produced in tobacco plants before, but this expression strategy required chemical refolding upon purification. We want to avoid chemical refolding because in this case plants would loose their economical advantage over bacterial expression. Production of human TGF-β1 is a complex process as the protein is synthesized as a latent complex whereby the latency-associated peptide (LAP) keeps mature TGF-β1 in an inactive form. Activation of TGF-β1 requires proteolytic cleavage between LAP and TGF-β1, which is mediated by the serine protease furin. We demonstrated that LAP is required for the production of biologically active TGF, but that a furin-like cleavage between LAP and TGF-β1 does not occur *in planta*. When LAP-TGF-β1 was co-expressed with human furin the proteolytic processing of latent TGF-β1 occured *in planta* and enabled the production of biologically active TGF-β1.

In Chapter 3 we describe the expression of the anti-inflammatory cytokine interleukin-10 (IL-10), which has been considered as a promising therapy for inflammatory bowel disease. Like many other plant-produced cytokines, the initial yield of heterologous expressed IL-10 was low. Cytokines are considered inherently unstable as they have short *in vivo* half-lives and this is generally believed to be the major bottleneck for heterologous expression. However, we demonstrate that the major expression bottleneck for the natural IL-10 dimer was its tendency to form large multimers by swapping protein domains. This extensive multimerisation was visualised in leaves as intracellular aggregates of organelle

size. By protein engineering we were able to prevent multimerisation and increase yield 30-fold, however, this strategy also rendered the protein inactive. Yet, forced dimerization of this engineered IL-10 by fusion to the Fc portion of IgA restored its ability to suppress LPS-induced TNF-α expression in a macrophage cell line.

In Chapter 4 we investigate the plant-based expression of the IL-10 related cytokine IL-22. IL-22 is an unusual cytokine as it does not act directly on immune cells, but is involved in maintaining epithelial barrier function. Only recently, IL-22 has been considered for treatment of inflammatory bowel disease and inflammation of liver and pancreas. We demonstrate that IL-22 does not form aggregates *in planta* and its yield was ~10-fold higher compared to native IL-10. The biological activity of IL-22 has been reported to depend on core α1,6-fucosylation of its N-glycan on asparagine 54 (Asn54). Therefore, we exploited a glyco-engineering strategy to obtain tailored human-like N-glycans. By co-expressing fucosyltransferase 8 we were able to add core α1,6-fucose to the N-glycans of IL-22, but this did not affect activity. We also investigated the role of N-glycosylation on folding of IL-22 by combining site-directed mutagenesis of N-glycosylation sites and co-expression of the deglycosylating enzyme PNGase F. Altogether we concluded that neither the presence of a N-glycan on Asn54 nor the composition of this N-glycan influenced the biological activity of IL-22. However, we revealed that the presence of a N-glycan on Asn54 influences the composition of another N-glycan. That the presence of an N-glycan can influence the composition of another has, to our knowledge, not been demonstrated before.

In Chapter 5 we continued to investigate the potential of glyco-engineering in plants, but now focusing on engineering helminth-like N-glycans. Helminths are complex multicellular organisms that upon infection are master regulators of their host's immune system. Helminths employ a range of secreted glycoproteins for immunomodulation. And these proteins, are potential drugs for the treatment of various inflammatory disorders. Several of these glycoproteins rely on specific N-glycan structures for their function. We expressed omega-1 and kappa-5, two major antigens that are secreted by the eggs of *Schistosoma mansoni*. Omega-1 is a T2 RNase and carries N-glycans with terminal Lewis X structures, which are required for uptake by dendritic cells and subsequent polarization into a type 2 T cell response. The function of kappa-5 is still unknown, but in contrast to omega-1, kappa-5 carries complex N-glycans with terminal LDN or LDNF. This chapter describes the production of large quantities of these helminth glycoproteins and the successful engineering of the helminth-like N-glycan structures Lewis X, LDN and LDN-F. This enables the functional characterization of helminth-secreted glycoproteins and subsequently investigation on the contribution of the N-glycan structures to the immunomodulatory properties of these glycoproteins. Our results demonstrate that plants are an excellent expression platform for helminth glycoproteins with tailored helminth-like N-glycans. This enables further research in host-parasite interactions, which may lead to the development of vaccines and/or discovery of new therapeutic proteins for inflammatory disorders.

Altogether, the results presented in the first four chapters reveal the remarkable flexibility of plants as a production platform for recombinant proteins. It showcases the potential of engineering proteins as well as post-translational modifications in plants, but it especially highlights the engineering of tailor made N-glycans in plants. This, combined with the speed of transient expression by means of agroinfiltration, makes transient expression in *Nicotiana benthamiana* a powerful tool to study the role of N-glycans on glycoprotein function. In parallel to these plant biotechnological research lines, we also developed an *in vitro* model system based on mouse bone marrow-derived cells to study immunological responses. We used this model to obtain clues on why IL-10 therapy has not been as successful as previously anticipated.

In Chapter 6 we utilised bone marrow-derived cells to investigate the biological activity of interleukin-10. Until now IL-10 therapy has not been as successful as previously anticipated and especially the role of IL-10R2 in IL-10-mediated responses is still elusive. We have set-up biological activity assays with bone marrow-derived dendritic cells, macrophages and mast cells to re-evaluate IL-10-mediated responses. We demonstrate that IL-10-mediated responses depend on both IL-10R1 and IL-10R2 in the investigated cell types, but IL-10R2-associated signalling via Tyk2 only plays a limited role. Further investigation of the IL-10R complex revealed that both the extracellular and intracellular domain of IL-10R2 influence IL-10R1 conformation. Our results highlight the importance of the intracellular domain of IL-10R2 on cellular binding of IL-10 as well as initiation of signal transduction.

In Chapter 7 we continued to investigate an interesting observation made in Chapter 6. We revealed that dendritic cells have an impaired ability to respond to IL-10 whereby especially early IL-10-mediated responses are affected. Upon IL-10 treatment dendritic cells were unable to suppress LPS-induced TNF-α secretion at an early time point after stimulation. We also demonstrate in this chapter that GM-CSF is a key factor that negatively regulates IL-10 activity. GM-CSF influences IL-10-mediated responses without strongly affecting the activation of the transcription factor STAT3. Instead, GM-CSF induces strong constitutive phosphorylation of GSK-3β, a signalling component downstream of the PI3K/Akt pathway. Future research on the exact mechanism by which GM-CSF negatively regulates IL-10 activity could give novel insights on the integration of signal transduction pathways elicited by different cytokines. Ultimately this knowledge could provide us with insights to design new therapeutic strategies to treat inflammatory disorders.

Samenvatting

De incidentie van immunologische aandoeningen (zoals allergieën, de ziekte van Crohn en multipele sclerose) in geïndustrialiseerde landen is sterk toegenomen in de afgelopen decennia. Deze toename wordt toegeschreven aan een veranderende levensstijl die leidt tot een onbalans van het immuunsysteem. De behandeling van deze ziekten richt zich daarom op het opnieuw in balans brengen van het immuunsysteem. Tot nog toe vindt behandeling doorgaans plaats met breed werkende chemische ontstekingsremmers of met monoklonale antilichamen die specifieke componenten van ons immuunsysteem neutraliseren. Een mogelijke alternatieve behandelwijze is het gebruiken van lichaamseigen componenten die er voor zorgen dat het evenwicht in ons immuunsysteem terugkeert. Dit zijn bijvoorbeeld ontstekingsremmende eiwitten van ons immuunsysteem (zoals sommige cytokines). Echter, om humane eiwitten te gebruiken als medicijn dienen deze door andere levende cellen geproduceerd te worden. Dit proefschrift beschrijft het produceren van dergelijke potentieel medische eiwitten in planten. Daarnaast beschrijft dit proefschrift het onderzoek naar de biologische activiteit van het cytokine interleukine-10 (IL-10). Met dit onderzoek proberen we te verklaren waarom IL-10, als ontstekingsremmer, in de kliniek tot dusver nog niet zo effectief is gebleken als verwacht.

In hoofdstuk 2 beschrijven we de expressie van het immuun-regulerend cytokine “transforming growth factor β1” (TGF-β1) in de bladeren van tabaksplanten. Dit cytokine speelt een belangrijke rol bij de ontwikkeling van een bepaald type immuuncellen (zogenaamde regulatoire T cellen) die in staat zijn om ons immuunsysteem te onderdrukken. Deze eigenschap van TGF-β1 zou mogelijk gebruikt kunnen worden om het immuunsysteem van patiënten met ontstekingsziekten weer in evenwicht te brengen. Productie van TGF-β1 is een complex proces, omdat TGF-β1 van nature wordt aangemaakt als een inactief (latent) eiwit. Het TGF-β1 eiwit bestaat uit twee delen waarbij het actieve deel van TGF-β1 als het ware wordt afgeschermd door een ander eiwitdomein. Om actief TGF-β1 te kunnen produceren, moet er een scheiding plaatsvinden tussen de twee eiwitdomeinen. Deze scheiding wordt bewerkstelligd door een ander eiwit, een enzym genaamd furine. In dit onderzoek laten wij zien dat de scheiding door furine normaalgesproken niet plaatsvindt in planten. Pas als we humaan furine samen met TGF-β1 tot expressie brengen in de plant gebeurt dit wel. Dit maakt het produceren van biologisch actief TGF-β1 mogelijk in planten.

In hoofdstuk 3 doen we vervolgens onderzoek naar de productie van het ontstekingsremmende cytokine IL-10. Dit cytokine wordt gezien als veelbelovend voor de behandeling van diverse ontstekingsziekten, zoals bijvoorbeeld de ziekte van Crohn. IL-10 is al meerdere malen succesvol geproduceerd in planten, maar tot nu blijft het

productieniveau laag. Uit ons onderzoek blijkt dat er een eiwit-intrinsiek probleem is voor de productie van IL-10. Het vermogen van IL-10 om dimeren te vormen (binding van twee dezelfde eiwitten aan elkaar) blijft namelijk niet beperkt tot twee eiwitten, maar zorgt voor de vorming van grote 'klompen' van IL-10 eiwitten (granulen). Door te voorkomen dat IL-10 dimeren vormt, slaagden we erin het productieniveau met een factor 30 te verhogen. Echter bleek deze monomere variant van IL-10 niet actief. Activiteit kon worden hersteld door deze monomeer weer te dimeriseren, maar nu via een ander eiwit domein (het constante domein van een antilichaam) dat aan IL-10 gefuseerd werd.

In hoofdstuk 4 bestuderen we de productie van IL-22, een cytokine dat qua structuur gerelateerd is aan IL-10, in planten. IL-22 speelt een rol bij het handhaven van de barrièrefunctie van epitheelweefsel, bijvoorbeeld in de darm. Recentelijk is de aandacht voor IL-22 sterk toegenomen en het wordt gezien als een veelbelovend medicijn voor de behandeling van ontstekingen van de darm, lever en alvleesklier. Met ons onderzoek laten we zien dat humaan IL-22 geen granules vormt in de plant en dat ook het productieniveau 10 keer hoger ligt in vergelijking met IL-10. Voor IL-22 is verder beschreven dat activiteit afhankelijk is van de samenstelling van de suikers die het draagt (zogenaamde N-glycanen). In ons onderzoek maken we daarom ook gebruik van de mogelijkheid om planten aan te passen zodat er verschillende suikers gekoppeld worden aan eiwitten die uitgescheiden worden. Door manipulatie van de plant konden we typische dierlijke suikers verkrijgen die nodig zijn voor activiteit van IL-22. Maar in tegenstelling tot voorgaande studies concluderen wij dat de activiteit van IL-22 niet afhankelijk is van de aanwezigheid van N-glycanen of hun samenstelling. Daarnaast laten we wel zien dat een N-glycaan op een specifieke plek de compositie van N-glycanen op ander plekken kan beïnvloeden. Dit was opvallend aangezien deze waarneming niet eerder is beschreven.

In hoofdstuk 5 zetten we het onderzoek naar het aanpassen van N-glycanen voort, maar focussen op het synthetiseren van typische N-glycanen van parasitaire wormen. Parasitaire wormen zijn complexe organismen die meester zijn in het manipuleren van het immuunsysteem van hun gastheer. Parasitaire wormen doen dit met behulp van een breed scala aan eiwitten die ze uitscheiden. Deze eiwitten hebben de potentie om gebruikt te worden voor de behandeling van meerdere ontstekingsziekten, maar veel van deze eiwitten zijn nog niet functioneel gekarakteriseerd en er is, daarom, nog geen geschikt productieplatform ontwikkeld. Daarnaast is een aantal van deze eiwitten afhankelijk van de samenstelling van hun specifieke N-glycanen. In dit hoofdstuk beschrijven we de productie van twee eiwitten die worden uitgescheiden door de eieren van de parasitaire worm *Schistosoma mansoni* genaamd omega-1 en kappa-5. We beschrijven de eerste succesvolle stappen naar de synthese van typische worm-achtige N-glycaan motieven in planten (Lewis X voor omega-1 en LDN(-F) voor kappa-5). Onze resultaten laten zien dat planten uitermate geschikt zijn voor de productie van immunomodulerende eiwitten van parasitaire wormen. Daarnaast zijn planten ook in

staat om deze eiwitten te produceren met hun natuurlijke N-glycanen. Dit maakt onderzoek naar parasiet-gastheer interacties mogelijk en zou uiteindelijk kunnen leiden tot de ontwikkeling van nieuwe therapeutische eiwitten voor het bestrijden van ontstekingsziekten.

De resultaten beschreven in deze vier hoofdstukken laten zien dat planten uitermate geschikt zijn als productieplatform voor recombinante eiwitten. Daarnaast is het een mooie showcase voor de mogelijkheden om eiwitten en post-translationele modificaties van eiwitten aan te passen in planten. Daarnaast laat ons expressiesysteem zien dat het mogelijk is om 'op maat gemaakte' N-glycanen te construeren. De snelheid waarmee recombinante eiwitten gemaakt kunnen worden in tabak maakt het een krachtig hulpmiddel om de rol van N-glycanen en de biologische functies van eiwitten te bestuderen. Parallel aan deze plantbiotechnologische onderzoekslijn hebben we ook gewerkt aan een onderzoekslijn waarbij een *in vitro* model op basis van beenmergcellen van muizen is opgezet ten behoeve van immunologische studies. Met dit model hebben we geprobeerd te achterhalen waarom IL-10 therapie niet zo succesvol is gebleken als men eerder had verwacht.

In hoofdstuk 6 hebben we gebruik gemaakt van immuuncellen die we gedifferentieerd hebben uit beenmerg om de biologische activiteit van IL-10 te bestuderen. IL-10 bewerkstelligt zijn activiteit door te binden aan twee receptoren, namelijk IL-10 receptor 1 en 2 (IL-10R1 en IL-10R2). Maar met name de bijdrage van IL-10R2 aan IL-10 activiteit is nog onduidelijk. Met behulp van uit beenmerg gedifferentieerde dendritische cellen, macrofagen en mestcellen laten wij zien dat IL-10 activiteit afhankelijk is van beide receptoren. Daarentegen is de rol van signaaltransductie van IL-10R2 via Tyk2 beperkt. Verder onderzoek naar het IL-10 receptor complex laat zien dat IL-10R2 invloed heeft op de conformatie van IL-10R1 en daarmee IL-10 binding beïnvloedt. Verassend was dat het intracellulaire deel van IL-10R2 hieraan bijdraagt.

In hoofdstuk 7 zetten we het onderzoek naar een interessante waarneming uit hoofdstuk 6 voort. In hoofdstuk 6 zagen we dat dendritische cellen anders reageren op IL-10 dan macrofagen. IL-10 is niet in staat om in een vroeg stadium na stimulatie de productie van het pro-inflammatoire cytokine TNF-α in dendritische cellen te onderdrukken. Wij tonen aan dat GM-CSF (het cytokine waarmee dendritische cellen gedifferentieerd worden uit beenmerg) hierbij een belangrijke rol speelt. GM-CSF doet dit echter zonder een effect te hebben op de activatie van de transcriptie factor STAT3 door IL-10. Het bleek dat GM-CSF een ander signaaltransductie-eiwit genaamd GSK-3β sterk activeert. Toekomstig onderzoek moet het exacte mechanisme waarmee GM-CSF IL-10 activiteit onderdrukt blootleggen. Dit zou nieuwe inzichten kunnen geven in de interacties tussen verschillende signaaltransductieroutes na activatie door verschillende cytokines. Uiteindelijk kan deze kennis bijdragen aan de ontwikkeling van nieuwe therapeutische strategieën om ontstekingsziekten te behandelen.

Acknowledgements

Like science, cooking is an art. Some will love it, others will hate it. For most of you it is no surprise: 'I love both'. I have even considered opening a restaurant (or British pub) as a career switch if I don't make it in science. But is this really an alternative career? Is being a cook so different to being a molecular scientist? And how different is a restaurant from a laboratory? Come to think of it.… Let's take Noma as an example, one of the best restaurants in the world and awarded with 2 Michelin stars since 2008. Change one letter and you get Nema, a laboratory that investigates microscopic worms, and is awarded with '4 gold medals' for excellence in research since 2009. These gold medals we owe to our 'head-chef' Jaap Bakker. Thank you Jaap for managing our metaphorical 'kitchen' so well. You have a gift of assembling the right mix of people, which creates an inspiring working environment.

The first step in a cook's road to success starts with the creation of a great recipe, the first step in a scientist career starts with a PhD degree. It can be tough at times (for instance when you have to find the perfect recipe to win the yearly Christmas lunch). Luckily I had a good mentor or 'sous-chef'. Thank you Arjen for your guidance, always tasting my concoctions and giving me all the freedom to try new recipes. You always saw the potential and you were able to keep me motivated when it was needed. And, even though you bear some resemblance to Gordon Ramsay, it was never Hell's Kitchen for me.

Secondly, cooks learn form each other, and not from a recipe book.… I had the privilege to observe and learn from an inspiring expert, my Heston Blumenthal. Without his guidance in the beginning of my PhD journey I would not have gotten this far. Thank you Jan Roosien for introducing me to your world of molecular biology (or molecular gastronomy for that matter) and teaching me all the tricks and trades of this profession. Furthermore, I would like to thank all Nema's experts, Joost, Sven, Paul, Hein, Rikus, Casper S. and of course Debbie for their role in keeping our 'kitchen' running. Your combined effort makes it possible to run all our experiments with ease; all our recipes are always at hand, we hardly ever run out off supplies and our 'kitchen' is always spotless. Also, Debbie, I have teased you on quite some occasions that your contribution to my thesis is limited (you probably know what I refer to). But without your help and your enthusiasm for cellular biology I would have never finished chapter 6. Furthermore, your marriage to Phytopathology was always very convenient (thank you also DJ!). Also Koen, Lizeth and Octavina, even though it wasn't your job, thank you for for being experts for my students at the end of my PhD journey when I was stuck in front of my computer.

As a dish is only as good as its ingredients, cooks rely on high quality produce. During my PhD thesis I have used many high quality tobacco plants. For this I would like to thank Bertus van der Laan, Henk Smid and Bert Essenstam from Unifarm. Thanks to your dedication our laboratory is provided with tobacco plants (and other plants) for weekly experimentation. Special thanks go to Bert for always being available for discussion when things in the greenhouse were not running optimal. Besides tobacco plants, I also relied on animal cells for some of my experiments. Therefore, I would like to thank the entire crew of the CKP. Thank you Rene Bakker, Bert Weijers, Wilma Blauw, Judith Hulsman and Lisette van Druten.

A cook in training also has the responsibility to teach the new potato peelers how to peel potatoes. During the six and a half years of my PhD track I have (co)-supervised many BSc and MSc students. And as with herbs and spices, they came in all kinds of different flavours. Amazingly all of you have shown great enthusiasm and I thank you all for your efforts in progressing our research and seasoning my journey. Although not all your work has found its place in this thesis, thanks go to (in alphabetical order): Mohamed Abdi Hassan, Yemisrach Abebaw, Marloes van Adrichem, Jose Bakker, Mariska van den Berg, Winnie van den Boogaard, Eva Capuder, Ira Chestakova, Che Chong, Marieke de Cock, Maarten Costerus, Etienne van Dalen, Annieck Diks, Natalia Domeradzka, Kevin van der Eijken, Bob Engelen, Josue Fonseca, Bas van Gestel, Anne Glasbergen, Sophie van Gorkom, Raul Guerreiro Covita, Simone Hayen, Kelly Heckman, Jorrit Heijkamp, Tram Hong, Myrte Huijskens, Kirstin Jansen, Sandra de Jongh, Eline Jongsma, Kassiani Kytidou, Amber van ‘t Land, Francisco Marques, Lizeth Meza Guzman, Renée Moerkens, Tam Nguyen, Bart Nijland, Kim van Noort, Simone Oostindie, Silvi Paskov, Alexandra Pelgrom, Donny Prakasa, Joyce Quist, Debbie van Raaij, Lauri Reuter, Carina Rietema, Eva van Rijsingen, Diecke de Ronde, Thomas Roodsant, Bram de Rooij, Huldah Sang, Xandra Schrama, Alja van der Schuren, Allard Stellingwerf, Jorik Swier, Aleksandra Syta, Eva Thijssen, Eveline Ultee, Koen Varossieau, Leroy Versteeg, Ziwei Wang, Tim Warbroek, Sonja Warmerdam, Marloes van Wijk, Edgar Wils, Nicole van ‘t Wout Hofland, Tomasz Wypich, Michelle Yang and Levine Zinger. I also wish you the best of luck for your future careers.

For a cook it is of vital importance to check out other kitchens. Sometimes this results in great fusion cooking. In science, collaborations are of equal importance and research excels where different disciplines merge. Dear Geert and Jose, our quest to find parallels in plant and animal immunity has been a blast and I trust we will get the soufflé right in the near future. Thank you for a great collaboration. Thank you also Dirk, Maurice and Thamara at PRI for introducing our group into the world of sugars ;). Last but not least, I would also like to thank Ron Hokke and Linh Nguyen at LUMC for their sweet tooth and always willing to analyse more sugars for us. I really enjoy our fruitful collaboration.

The resemblance between a laboratory and a restaurant is not complete by only looking at the kitchen. Every good restaurant also has an outstanding host or hostess; someone who welcomes new customers, making sure they get nice seats and that there is a nice atmosphere. Within the laboratory of Nematology we even have the luxury of having more than one 'hostess'. Lisette and Christel, thank you for dealing with all organisational aspects of our chair group, welcoming all of our new customers (a.k.a. students and guest workers), keeping our website up to date and your endless patience with your 'kitchen crew'. At this point I would also like to thank all my other colleagues (and former colleagues). The aforementioned inspiring working environment is because of you. Thank you for being great colleagues in both work-related and social aspects. Special thanks go to Jet for organizing the thesis rings so well. I believe it is a great addition to the supervision of thesis students and brings our chair group even closer together. And last but not least, Jan van de Velde for always being the cherry on top.

A good chef also knows how to enjoy food and what better way to do this than to enjoy it together with family and friends. From the beginning of my PhD journey I was part of our so-called 'Wageningen family'. We regularly got together for drinks and/or bites. This was a crucial relieve from the daily stress accompanied with our PhD/MSc tracks and gave ample opportunity to complain (Yes yes) about the number of thesis students, our boss or other situations (at work), reasonable or not. So thank you Annemarie, Ana, Kamila, Tomek and Tineke for all the good times and our friendship. Also Femke and Ronald, thank your for all the comic relief, your interest in 'zapping' bacteria and 'pregnant proteins' and for annually cooking up a storm together on New Years Eve. Furthermore, I would like to thank my parents for always giving me the freedom to pursue my own career and providing me with the means to do so. Also, thanks go to my parents-in-law for providing a listening ear when needed.

Than finally, there is one person that will complete this chapter. Dear Lotte, the entire PhD journey you have been by my side. We have always been (and still are) involved in each other's work at every single step. We have co-supervised a record number of thesis students at Nema and you played a crucial role in getting some of the manuscripts in this thesis ready for publication. Furthermore, on more than one occasion you have mediated between me and Gordon Ramsay ;). I believe we make an excellent team and this extends also to our non-professional life. Our friendship, relationship, marriage and the birth of our son Flip have made me a better person. I gained more self-confidence and I realised that there is more in life than just 'work'. Dear Lotte, there are not enough words to describe my gratitude to you, so I will end this chapter by saying the one thing that brought us together: "You're one of a kind".

Curriculum vitae

Ruud Hendrikus Petrus Wilbers was born on the 11th of October 1983 in Tegelen, The Netherlands. He graduated from the high school Valuas College In Venlo in 2002. Thereafter he joined the BSc program Biology at Wageningen University (Wageningen, The Netherlands) and specialised himself in animal biology. After obtaining his BSc degree in 2005 he continued his studies at Wageningen University with the MSc program Biology. During his MSc program he studied the development of T-cells in common carp under the supervision of Dr. ir. Jan Rombout of the Laboratory of Cell Biology and Immunology at Wageningen University. He spent half a year at the Sir William Dunn School of Pathology (Oxford, United Kingdom) working on 'the role of cytolethal distending toxin in *Helicobacter hepaticus* mediated intestinal inflammation in mice' under the supervision of Dr. Kevin Maloy. At the Laboratory of Nematology at Wageningen University he investigated the plant-based expression of human interleukin-10 under the supervision of Dr. ir. Arjen Schots and worked on the role of venom allergen-like proteins in plant-nematode interactions under the supervision of Dr. ir. Geert Smant. In 2008 he obtained his MSc degree in Biology with the specialization in 'animal biology' and his MSc degree in Plant Biotechnology with a specialization in 'plants for human and animal health'. Within the Laboratory of Nematology he joined the group of Dr. ir. Arjen Schots as a PhD and continued to do research on plant-based production of (potential) biopharmaceuticals and other immunologically interesting proteins. On the 23rd of October 2015 he will be given the opportunity to defend his PhD thesis. Since September 2014 he holds a Postdoc position at Wageningen University and lives in Wageningen with his wife Lotte Westerhof and their son Flip.

Publications

R.H.P. Wilbers, L.B. Westerhof, L.J. Reuter, A. Castilho, D.R. van Raaij, D-L. Nguyen, J.L. Lozano-Torres, G. Smant, C.H. Hokke, J. Bakker and A. Schots (2015). The N-glycan on Asn54 affects the atypical N-glycan composition of plant-produced interleukin-22, but does not influence its activity. *Plant Biotechnology Journal* (online first).

J. van de Velde, R.H.P. Wilbers, L.B. Westerhof, D.R. van Raaij, I. Stavrakaki, A.S.M. Sonnenberg, J. Bakker and A. Schots (2015). Assessing the immunomodulatory potential of high-molecular-weight extracts from mushrooms; an assay based on THP-1 macrophages. *Journal of the Science of Food and Agriculture* 95: 344–350.

J.L. Lozano-Torres, R.H.P. Wilbers, S. Warmerdam, A.M. Finkers-Tomczak, A. Diaz-Granados, C.C. van Schaik, J. Helder, J. Bakker, A. Goverse, A. Schots and G. Smant (2014). Apoplastic Venom Allergen-like Proteins of Cyst Nematodes Modulate the Activation of Basal Plant Innate Immunity by Cell Surface Receptors. *Plos Pathogens* 10 (12): e1004569.

L.B. Westerhof, R.H.P. Wilbers, D.R. van Raaij, D-L. Nguyen, A. Goverse, M.G.L. Henquet, C.H. Hokke, D. Bosch, J. Bakker and A. Schots (2014). Monomeric IgA can be produced *in planta* as efficient as IgG, yet receives different N-glycans. *Plant Biotechnology Journal* 12 (9): 1333-1342.

E.J. Slootweg, L.N. Spiridon, J. Roosien, P.B.E. Butterbach, H. Pomp, L.B. Westerhof, R.H.P. Wilbers, E.H. Bakker, J. Bakker, A.J. Petrescu, G. Smant and A. Goverse (2013). Structural Determinants at the Interface of the ARC2 and LRR Domains Control the Activation of the NB-LRR Plant Immune Receptors Rx1 and Gpa2. *Plant Physiology* 162 (3): 1510 - 1528.

L.B. Westerhof, R.H.P. Wilbers, J. Roosien, J. van de Velde, A. Goverse, J. Bakker and A. Schots (2012). 3D Domain Swapping Causes Extensive Multimerisation of Human Interleukin-10 When Expressed *In Planta*. *PLoS One* 7 (10): e46460.

J.L. Lozano,-Torres, R.H.P. Wilbers, P. Gawronski, J.C. Boshoven, A.M. Finkers-Tomczak, J.H.G. Cordewener, A.H.P. America, H.A. Overmars, J.W. van t Klooster, L. Baranowski, M. Sobczak, M. Ilyas, R.A.L. van der Hoorn, A. Schots, P.J.G.M. de Wit, J. Bakker, A. Goverse, and G. Smant (2012). Dual disease resistance mediated by the immune receptor Cf-2 in tomato requires a common virulence target of a fungus and a nematode. *Proceedings of the National Academy of Sciences of the United States of America* 109 (25): 10119 - 10124.

Education Statement of the Graduate School

Experimental Plant Sciences

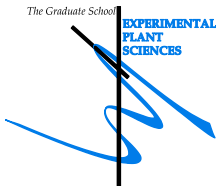

Issued to: Ruud Wilbers
Date: 23 October 2015
Group: Laboratory of Nematology
University: Wageningen University & Research Centre

1) Start-up phase	date
► **First presentation of your project**	
Biological activity of in planta produced cytokine traps	Jan 2008
► **Writing or rewriting a project proposal**	
► **Writing a review or book chapter**	
► **MSc courses**	
► **Laboratory use of isotopes**	
Subtotal Start-up Phase	*1.5 credits**

2) Scientific Exposure	date
► **EPS PhD student days**	
EPS PhD student day, Leiden University	Feb 26, 2009
EPS PhD student day, Utrecht University	Jun 01, 2010
► **EPS theme symposia**	
EPS theme 3 symposium 'Developmental Biology of Plants', Leiden University	Jan 20, 2011
EPS theme 3 symposium 'Metabolism and Adaptation', Wageningen University	Feb 10, 2011
► **NWO Lunteren days and other National Platforms**	
► **Seminars (series), workshops and symposia**	
Science from an Editor's view, by Dr. Paula J. Hines	Nov 06, 2008
The Immune System in Darwinian Time, by Dr. P. de Wit & Dr. ir. H. Savelkoul	May 19, 2009
Pre-Congres Workshop (ICMI 2009): Microbes and Mucosal Immunology	Jul 04, 2009
Plantbiotechnology workshop, with G. Rouwendal, J. Ma and D. Orzáez	Jul 31, 2009
Scientific Publishing (WGS Workshop)	Nov 19, 2009
COST workshop on molecular farming - Focus on Downstream processing and Facilities	Jan 25-26, 2010
EPS symposium 'On the Endomembrane System of Plants', Vrije University Amsterdam	Jul 02, 2010
COST workshop on molecular farming - Plants as a Production Platform for High Value Proteins	Oct 07-08, 2010
Immunogy Workshop within PSG - organized by A. Schots & D. Bosch	Aug 29, 2011
► **Seminar plus**	
► **International symposia and congresses**	
2008 Advances in Inflammatory Bowel Disease, Hollywood (Florida, USA)	Dec 04-07, 2008
European Congres of Immunology, Berlin (Germany): "Immunity for Life – Immunology for Health"	Sep14-16, 2009
Cell Signaling Technology Symposium "Innovative Technologies for Signal Transduction Research"	Oct 12, 2010
Plant-Based Vaccines and Antibodies Meeting (PBVA), Porto (Portugal)	Jun 08-10, 2011
► **Presentations**	
Oral presentations Synthon (progress reports)	2008-2012
In vitro and in vivo analysis of biopharmaceuticals (Talk - Plantbiotechnology workshop at Synthon)	Jul 31, 2009
Aggregation as a bottleneck for IL-10 expression in Nicotiana benthamiana (Poster - COST meeting)	Oct 08, 2010
Aggregation as a bottleneck for IL-10 expression in Nicotiana benthamiana (Poster - PBVA 2011 - Porto)	Jun 08, 2011
Immunogy Workshop within Plant Sciene Group (Talk)	Aug 29, 2011
Comparative study of plant-produced antibodies on an IgG and IgA backbone (Talk - PBVA 2013 - Verona)	Jun 07, 2013
Biological activity of human interleukin-22 expressed in Nicotiana benthamiana (Poster - ISPMF - Berlin)	Jun 18, 2014
Expression of Omega-1 with diantennary N-glycans carrying Lewis X motifs (Poster - HYDRA meeting)	Sep 05, 2014
► **IAB interview**	
Meeting with a member of the International Advisory Board of EPS	Feb 17, 2011
► **Excursions**	
EPS PhD company excursion - KeyGene	Jan 26, 2012
Subtotal Scientific Exposure	*25.4 credits**

3) In-Depth Studies	date
► **EPS courses or other PhD courses**	
Flow Cytometry Hands-On Course (York University, UK)	Jun 15-18, 2010
14th International Congress of Mucosal Immunology, Boston (Massachusetts, USA): "Reconciling Immunity, Tolerance and Inflammation at the Mucosal Surface"	Jul 05-09, 2009
European Mucosal Immunology Meeting 2008, Milan (Italy)	Oct 08-10, 2008
► **Journal club**	
Member of literature discussion group at Laboratory of Nematology	2008-2012
► **Individual research training**	
Subtotal In-Depth Studies	*6.6 credits**

4) Personal development	date
► **Skill training courses**	
Advanced course Guide to scientific artwork	Feb 16-17, 2009
PhD competence assessment	Aug 25, 2009
Scientific writing	Apr-May 2009
Scientific writing for high impact journals like Science and Nature	Feb-Mar 2013
► **Organisation of PhD students day, course or conference**	
► **Membership of Board, Committee or PhD council**	
Subtotal Personal Development	*3.3 credits**

TOTAL NUMBER OF CREDIT POINTS*	**36,8**

Herewith the Graduate School declares that the PhD candidate has complied with the educational requirements set by the Educational Committee of EPS which comprises of a minimum total of 30 ECTS credits

** A credit represents a normative study load of 28 hours of study.*

This research was conducted at the Laboratory of Nematology, Wageningen University, (Wageningen, The Netherlands) and financially supported in part by Synthon (Nijmegen, The Netherlands).

Cover design: Agilecolor Design Studio/Atelier
Printed by: Ridderprint BV, the Netherlands